

https://dspace.org/

The design and synthesis of A54556 acyldepsipeptide derivatives and nanomaterials targeting the mycobacterium tuberculosis caseinolytic protease

Cobongela, Sinazo Zezethu Zongeziwe

2024

https://hdl.handle.net/10539/37510

Downloaded from a DSpace repository. https://dspace.org/



UNIVERSITY OF THE
WITWATERSRAND,
JOHANNESBURG

THE DESIGN AND SYNTHESIS OF A54556 ACYLDEPSIPEPTIDE DERIVATIVES AND NANOMATERIALS TARGETING THE MYCOBACTERIUM TUBERCULOSIS CASEINOLYTIC PROTEASE

Sinazo Zezethu Zongeziwe Cobongela

Supervisor: Dr Maya Makatini

Co-supervisor: Dr Zikhona Njengele-Tetyana

DECLARATION

I, **Sinazo Zezethu Zongeziwe Cobongela** declare that:

- The research reported in this thesis, except where otherwise indicated, is my original research.
- This thesis has not been submitted for any degree or examination at any other university.
- This thesis does not contain other persons' data, pictures, graphs or other information, unless specifically acknowledged as being sourced from other persons.
- This thesis does not contain other persons' writing, unless specifically acknowledged as being sourced from other researchers. Where other written sources have been quoted, then:
    - Their words have been re-written but the general information attributed to them has been referenced.
    - Where their exact words have been used, then their writing has been placed in italics and inside quotation marks, and referenced.

  This thesis does not contain text, graphics or tables copied and pasted from the internet, unless specifically acknowledged, and the source being detailed in the thesis and in the references sections. This entire work was conducted by me under the supervision of Dr Maya Makatini and Dr Zikhona Njengele-Tetyana. It is submitted for examination for the degree of Doctor of Philosophy at the University of Witwatersrand.

Signed  Date: 30 May 2023

ACKNOWLEDGEMENTS

My sincere gratitude and appreciation to:

- To my supervisor, Dr. Maya Makatini, for her direction, encouragement, and support throughout the study: I am incredibly appreciative of your belief in my potential as a young researcher and for giving me the freedom to experiment and express myself. You have supported me through difficult times and rejoiced with me when things are about to get better. I'll always be appreciative.
- Dr. Zikhona Njengele-Tetyana, my co-supervisor, for your willingness to share your in-depth expertise and help me develop my research skills: I appreciate the motivation and help, both emotionally and technically. At first, selecting you appeared to be a "by the way, a *haha* matter," but you changed the situation for the benefit of this project. You helped me realize every goal I had and brought it to reality. "The sky is the limit" with you. I can't thank you enough; without you, I wouldn't have been able to accomplish this. I'm grateful.
- Dr. Nicole Sibuyi for supporting me when I had a hard time having faith in myself. You literally kept me going during my darkest days, when I wanted to give up. We appreciate your time and emotional support; your dedication made our late nights worthwhile.
- Dr. Thompho Rashamuse, who agreed to assist with the NMR analysis.
- The soon-to-be Dr. Bambesiwe May, who provided the quantum dots and assisted with an analysis of the nanomaterials.
- Dr. Lucky Sikhwivhilu, thank you for your kindness, patience, and support. I appreciate you standing up for me and making sure there are no obstacles in my way.
- To my mother, Nomasango Cobongela, I sincerely thank you for your support. I would want to thank you for continuing to help me as I pursue my education. I'm grateful, mom.
- Alunamda Cobongela, my niece, and my sisters Amahle and Milani Cobongela have kept me sane throughout. I appreciate you providing the light in what felt like gloomy days. You genuinely make my world shine.

- I would want to express my gratitude to my entire family for their unwavering love and support. PS. Despite this, they are sick of me and my studying. This might be the final one, I swear.
- Ntombi Ngqinayo, Priscilla Nyembe, Thandokuhle Ntombela, Khanani Machumela, Lesotho Ntlamo, Refilwe Moepa, Pious Shuro, and Thapelo Mbhele are my Wits colleagues who deserve praise for all of our joint successes.
- My coworkers at DSI/Mintek NIC, Health Platform, and Biomed for their helpful suggestions and assistance.
- Mintek and DSI/Mintek NIC for providing me with financial assistance while I was a student.
- Mintek/AMD/Biomed group, University of South Africa, University of Witwatersrand, and DSI/Mintek NIC for providing the necessary infrastructure for the project.
- All of my companions, Fezile Nkomo-Lebina, Thulaganyo Domfe, Zikhona Njengele-Tetyana (again☺), Zikhona Magaxeni, Lufuno Matlawa, Nikiwe Mhlanga, Ketshepile Moropa, and a host of others for their support and efforts to ensure my overall well-being. I appreciate your emotional support and your constant reminders of the value of looking after my mental health. I'm sure you're all eager to celebrate this success. We did it guys, we did it!
- Lastly, to my late grandfather: I know wherever you are you continue to boast about every little thing I do. I am certain your face is beaming with joy now that I got the red gown we have been both waiting for.

Above all, praise be to the Most High God! I sensed your hand holding mine as I traveled this journey. Your promises and your word gave me the courage to go through to the finish line.

LIST OF PUBLICATIONS

Cobongela SZZ, Makatini MM, Mdluli PS, Sibuyi NRS. Acyldepsipeptide Analogues: A Future Generation Antibiotics for Tuberculosis Treatment. Pharmaceutics. 2022; 14(9):1956. https://doi.org/10.3390/pharmaceutics14091956

Cobongela SZZ, Makatini MM, Njengele-Tetyana Z, Sikhwivhilu LM, Sibuyi NRS. Design and synthesis of Acyldepsipeptide-1 analogues: Antibacterial activity and cytotoxicity screening. Arabian Journal of Chemistry. 2023; 16(8):105000. https://doi.org/10.1016/j.arabjc.2023.105000

ABSTRACT

Antibiotics have saved many lives since their discovery in the 1920s, and continue as a first line of defence against microbial infections to date. Unfortunately, their misuse gave rise to the multi-drug resistant (MDR) bacteria that require intensive therapy. *Mycobacterium tuberculosis* (*M. tb*) is one of the top pathogens rapidly gaining resistance to current treatment regimens. Over 480 000 cases of MDR tuberculosis (TB) occur every year globally, 9% are caused by the extensively drug-resistant (XDR) *M. tb* strains. The treatment of MDR/XDR-TB is long, toxic and expensive, and the success rate is largely unsatisfactory. Hence, there is an urgent need for new and effective anti-TB drugs. Over the years, peptide based therapeutics have been used and were successful in treatment of various diseases such as TB, cancer, cardiovascular diseases, diabetes and others. Due to the instability, poor solubility and toxicity of natural antimicrobial peptides (AMPs), great attention is now focussed towards synthetic analogues of the AMPs to improve their pharmacokinetics. One of the new antibacterial targets that have gained traction over the years is the proteolytic regulating protease called Caseinolytic protease (ClpP). ClpP degrades misfolded and aggregated proteins and peptides that have potential to induce toxicity within the bacterial cell. ClpP can be indirectly targeted by dysregulating ClpP-ATPases such as ClpC1 and ClpX, which are responsible for activation of the ClpP proteolytic activity. Acyldepsipeptides (ADEPs) function by mimicking the binding of ClpP-ATPases to ClpP, thereby inducing nonselective proteolysis, which ultimately leads to bacterial death. Due to the essential role played by ClpP in the biology of the *M. tb*, thus ADEPs are regarded as potential antibiotics with a novel mechanism to combat the bacterial resistance problem. However, ADEPs also have limitations such as poor membrane permeability and high cytotoxicity. Therefore, the aim of this study was to design and synthesise biocompatible ADEP1 analogues as potent antibacterial agents, and to improve their membrane permeability and efficacy by conjugating the analogues to Silver/Indium/Sulphide ($AgInS_2$) quantum dots (QDs) as nano-carriers.

Twenty cyclic ADEP1 analogues were designed and synthesised using the solid phase peptide synthesis (SPPS) strategy. Four of the ADEP1 analogues were conjugated to the $AgInS_2$ QDs, and characterised with UV-Vis, Spectro Xepos05 energy-dispersive X-ray fluorescence, high-resolution transmission electron microscope, and spectrofluorophotometer. The antibacterial activity of the ADEP1 analogues and $AgInS_2$ QDs-ADEP1 analogue conjugates was tested against two Gram-negative bacteria, *Escherichia coli* (*E. coli*) and *Pseudomonas aeruginosa*

(*P. aeruginosa*), and three Gram-positive bacteria, *Bacillus subtilis* (*B. subtilis*) and *Staphylococcus aureus* (*S. aureus*), including Methicillin-resistant *Staphylococcus aureus* (MRSA). The biocompatibility and cytotoxicity effects of the ADEP1 analogues and $AgInS_2$ QDs-ADEP1 analogue conjugates was evaluated on HEK-293 and Caco-2 cells using the MTS viability assay. The effect of the ADEP1 analogues on the peptidase activity of the *M. tb* ClpP1P2 was investigated. The aqueous solubility and membrane permeability of the ADEP1 analogues was investigated using the MultiScreen aqueous solubility assay and the Parallel Artificial Membrane Permeability Assay (PAMPA), respectively.

Four of the ADEP1 analogues were successfully synthesized by SPPS with >96% purity and >36% yield. Both the ADEP1 analogues and $AgInS_2$ QDs-ADEP1 analogue conjugates showed potency against Gram-positive and Gram-negative bacteria, however, the efficacy of the ADEP1 analogues was significantly enhanced when conjugated to the $AgInS_2$ QDs. In Gram-positive bacteria, the ADEP1 analogues exhibited a minimum inhibition concentration (MIC) ranging from 63-125 µM while the $AgInS_2$ QDs-ADEP1 analogue conjugates had lower MIC values (9.38-18.75 µM). The MIC values of ADEP1 analogues against Gram-negative bacteria were between 125 and 500 µM while the $AgInS_2$ QDs-ADEP1 analogue conjugates had MICs between 2.34 and 37.5 µM. Both the unconjugated peptides and conjugates showed minimum bactericidal concentrations (MBC) twice their MIC. In addition, the ADEP1 analogues and $AgInS_2$ QDs-ADEP1 proved to be biocompatible as they were non-toxic to the cells. The ADEP1 analogues further showed moderate aqueous solubility and gastrointestinal membrane permeability. Furthermore, the effect of the ADEP1 analogues on the peptidase activity of the *M. tb* ClpP1P2 protease was investigated. All the analogues enhanced *M. tb* ClpP1P2 activity. Of the four ADEP1 analogues that were tested, SC008 and SC005 showed activation percentages that were 32% and 14% higher than benzoyl-leucyl-leucine (Bz-LL), a known ClpP1P2 activator, respectively. These results suggested the potential use of these novel ADEP1 analogues as leads in the development of broad spectrum anti-bacterial agents. The ADEP1 analogues also demonstrated potential anti-mycobacterium activity by activating *M.tb* ClpP1P2. The mode of action followed by the ADEP1 analogues is an interesting finding that can be explored to develop new and effective antibacterial drugs with potential to eradicate drug resistance. Therefore, future studies warrants investigation of the anti-TB effects and molecular mechanism of the ADEP1 analogues and conjugates in *in vitro* and *in vivo* models of *M.tb*.

OUTLINE

Chapter one

Chapter 1 is introducing the infectious bacteria causing TB on how it is affecting South Africa and the rest of the world.

Chapter two

Chapter 2 is divulging into the literature of the topic, from addressing TB to current TB treatment. It also discusses in detailed review the mechanism of ADEPs on ClpP, advantages and limitations of ADEPs. The chapter further discusses the potential strategies to improve ADEPs to be more drug-like compounds.

Chapter three

Chapter 3 addresses the design of all twenty ADEP1 analogues and its limitation in successfully synthesising ADEP1 analogues containing ester bond cyclisation and some of the inactive ADEP1 analogues containing disulphide cyclisation.

Chapter four

This chapter outlines the material and methods used in the synthesis, purification and characterization of ADEP1 analogues. It discusses in detail the solid phase peptide synthesis (SPPS) and characterisation of peptoid moieties used in synthesis of some ADEP1 analogues. The chapter also details the synthesis, purification, and characterization of N-benzoyl-Leucyl-Leucine (Bz-LL) used as ClpP positive control

Chapter five

Chapter 5 is written in a manuscript format tittled "Design and synthesis of AcyldepsipeptideADEP1 analogues: Antibacterial activity and cytotoxicity screening". It discusses briefly the design and synthesis, purification, and characterization of four disulphide bond containing ADEP1 analogues (SC005-8). The chapter also contains antimicrobial activity against five bacterial strain and cytotoxicity screening on two different cell lines.

Chapter six

Chapter 6 is also written in a manuscript format tittled "Antibacterial activity and cytotoxicity screening of Silver/Indium/Sulphide quantum dots conjugated ADEP1 analogues". Antibacterial activity and cytotoxicity screening of quantum dots conjugates are discussed in

this Chapter. The chapter further outlines the synthesis of silver/indium/sulphur ($AgIS_2$) gelatin-capped quantum dots, conjugation of ADEP1 analogues (SC005-8) to the $AgIS_2$ quantum dots followed by the antibacterial and cytotoxicity screening.

Chapter seven

Chapter 7 is focusing on the CpP protease proteolytic subunits ClpP1 (21.8 kDa) and ClpP2 (23.5 kDa) genes cloned into pET-15b plasmids were transformed into E. coli T7 cells. The chapter further discusses expression, purification, and characterisation of recombinant M. tb ClpP1/ClpP2 domains and possible binding to SC005-8. M. tb ClpP1P2 activity assay was also perfumed to screen the influence of SC005-8 and the known activator (Bz-LL) on the activity of this protease. This chapter also discusses the importance of clinical pharmacokinetic properties of ADEP1 analogues. This chapter further details the methods used to determine the aqueous solubility and membrane permeability of SC005-8.

Chapter eight

Chapter 8 is a collective conclusion of all the chapters and future prospects of this project.

TABLE OF CONTENTS

Declaration i
Acknowledgements ii
List of publications iv
Abstract v
Outline vii
Table of Contents ix
LIST OF ABBREVIATIONS xiii
List of Figures xvi
List of Schemes xx
List of Tables 1
Chapter 1. 2
INTRODUCTION 2
1.1. Background 2
1.2. Aim and objectives 4
1.2.1. Aim 4
1.2.2. Objectives 4
1.3. Hypothesis and question 5
1.3.1. Hypothesis 5
1.3.2. Question 5
1.4. References 1
Chapter 2. 2
1. Introduction 3
2. Tuberculosis 3
2.1. M. tb Epidemiology and Pathophysiology 3
2.2. Treatment of TB 5
2.2.1 Bacterial Resistance as a Main Limitation for TB Drugs 6
3. AMPs as Future Antibiotics 7
3.1 AMP Mode of Action 7
4. ClpP as a Putative Bacterial Therapeutic Target 8
4.1. ADEPs Competes with Clp-ATPases to Deactivate ClpP 10
4.2. ADEP1 Analogues 11
4.3. ADEPs Activity on M. tb ClpP1P2 14
4.4. Limitation of ADEPs 15

4.4.1. Strategies to Improve on ADEP's Pharmacokinetics and Pharmacodynamics 15
Chemical Modification 15
Amino Acid Substitution 15
Lipophilic Molecules 16
Nano-Carriers 16
5. Conclusions 16
References 17
Chapter 3. 27
Design OF ADEP1 peptide analogues 27
3.1. ADEP1 analogues 27
3.1.1. Lipophilic molecules. 27
3.1.2. Cyclisation 28
3.2. Design of ester bond cyclised ADEP1 analogues 28
3.2.1. Design and limitations encountered during the synthesis of ADEP1 analogues 29
3.2.2. Esterification techniques for cyclisation of ester ADEP1 analogues 30
3.3. Design of disulphide bond cyclised ADEP1 analogues 34
3.4. Design of disulphide bond cyclised ADEP1 analogues containing Lysine 36
3.5. Design of disulphide bond cyclised ADEP1 analogues containing peptoid moieties 39
3.6. Summary of all designed ADEP1 analogues 40
3.7. Synthesis of Bz-LL 41
3.8. Conclusion 42
3.9. References 43
Chapter 4. 45
Materials and methods 45
4.1. Chemicals 45
4.2. Instrumentation for data collection and analysis 45
4.2.1. Resin loading capacity 45
4.2.2. Purification 45
4.2.3. Analytical analysis of the synthesised peptide 46
4.2.4. Structural characterisation 46
4.2.5. Peptoid synthesis analysis 46
4.3. General peptide synthesis 47
4.3.1. Resin loading test 47
4.3.2. Cleaving of peptides from the resin 48
4.4. Cyclisation 48

4.4.1. Iodine mediated oxidation 48
4.4.2. DMSO mediated oxidation 48
4.5. Purification and analysis 49
4.6. Synthesis of N-benzoyl-Leucyl-Leucine (Bz-LL) 49
4.7. Synthesis, Characterisation, and structural elucidation of Fmoc-N-methylated alanine and Fmoc-peptoid alanine (Fmoc-sarcosine) 49
4.7.1. General procedure for the synthesis of Fmoc-N-methylated amino acids 49
4.7.2. Synthesis of Fmoc-Alanine peptoid 51
4.8. Characterisation of peptoids and Bz-LL 53
4.8.1. Fmoc-N-Methyl Alanine 53
4.8.2. Fmoc-Sarcosine 53
4.8.3. N-benzoyl-Leucyl-Leucine (Bz-LL) 54
4.9. References 54
Chapter 5. 55
Abstract 55
1. Introduction 57
2. Materials and methods 57
2.1. Materials 57
2.2. Solid phase synthesis of ADEP1 analogues 57
2.2.1. Loading capacity and yield of ADEP1 analogues 58
2.3. Cyclization of ADEP1 analogues 58
2.3.1. Iodine-mediated oxidation 58
2.3.2. DMSO-mediated oxidation 59
2.4. ADEP1 analogues purification by HPLC 59
2.5. Antibacterial activity tests of the ADEP1 analogues 59
2.5.1. Agar well diffusion method 59
2.5.2. Minimum inhibitory concentration and minimum bactericidal concentration 59
2.6. Cell viability studies 59
2.7. Statistical analysis 60
3. Results and discussion 60
3.1. Synthesis and characterization of ADEP1 analogues 60
3.2. Antibacterial activity of the ADEP analogues 61
3..3 Cytotoxicity 64
4. Conclusion 66
References 66

Chapter 6. 71
Abstract 71
6.1. INTRODUCTION 72
6.2. Materials and methods 73
6.2.1. Material 73
6.2.2. Synthesis of QD 74
6.2.3. Conjugation of $AgInS_2$ quantum dots to ADEP1 analogues 74
6.2.4. Characterization of QD, QD-peptide conjugates and peptides 74
6.2.5. Minimum inhibitory concentration and minimum bactericidal concentration 75
6.2.6. Cytotoxicity assay 75
6.3. Results and discussion 76
6.4. conclusion and future perspectives 84
6.5. References 85
Chapter 7. 87
Design OF ADEP1 peptide analogues 87
7.1. Introduction 87
7.2. Materials and Methods 88
7.2.1. Recombinant expression of ClpP1 and ClpP2 in E. coli 88
7.2.2. Solubilisation of the ClpP1 and ClpP2 recombinant proteins 89
7.2.3. Purification of ClpP1 and ClpP2 89
7.2.4. Characterisation of the purified recombinant proteins 90
7.2.5. M. tb ClpP1P2 Peptidase activity assay 91
7.2.6. Aqueous solubility test of the ADEP1 analogues 92
7.3. Results and Discussion 94
7.3.1. ClpP1 and ClpP2 expression, solubilisation and purification 94
7.3.2. Characterisation of the purified recombinant proteins 97
7.4. Conclusion and future perspectives 104
7.5. References 106
Chapter 8. 109
8.1. Concluding remarks and future work 109
Appendix 111

LIST OF ABBREVIATIONS

Abbreviations/ symbols	Full names
δ	chemical shift
Ada	adamantane
ADEP	acyldepsipeptides
$AgInS_2$	silver/indium/sulphide
Ala (A)	alanine
AMP	antimicrobial peptides
Boc	Tert-Butyl-Oxycarbonyl
CD	circular dichroism
Cys (C)	cysteine
DCM	dichloromethane
DIPEA	N,N-diisopropylethylamine
DMF	N,N-dimethylformamide
DMSO	dimethyl sulfoxide
EDT	1,2-Ethanedithiol
ESI	electrospray Ionisation
EtOAc	ethyl acetate
Fmoc	9-Fluorenylmethoxycarbonyl
HATU	1-[Bis(dimethylamino)methylene]-1H-1,2,3-triazolo[4,5-b]pyridinium 3-oxide hexaflourophosphate
HBTU	(2-(1H-benzotrial-1-yl-1,1,3,3-tetramethyluronium hexafluorophosphate
HPLC	high performance liquid chromatography
HOBt	hydroxybenzotriazole
HRMS	high resolution mass spectrometry
h (hr)	hour

LC-MS	liquid chromatography-mass spectrometry
LSPR	localised surface plasmon resonance
Lys (K)	lysine
m	multiplet
mA	methyl alanine
MBHA	rink Amide 4-methylbenzhydrylamine
MeCN	acetonitrile
MeOH	methanol
mg	milligram
MBC	minimum bactericidal concentration
MIC	minimum inhibitory concentration
min	minute
mL	milliliter
mM	millimolar
MS	mass spectrometry
MTS	3-(4,5-Dimethylthiazol-2-yl)-5-(3-carboxymethoxyphenyl)-2-(4-sulfophenyl)-2H-tetrazolium
m/z	mass charge
NMR	nuclear magnetic resonance
nm	nanometer
NPs	nanoparticles
Pal	palmitic acid
PBS	phosphate buffer saline
PDB	protein data bank
Phe (F)	phenylalanine
Pro (P)	proline
QD	quantum dots

SPPS	solid phase peptide synthesis
Ser (S)	serine
TEA	triethylamine
TEM	transmission electron microscopy
TFA	trifluoroacetic acid
TLC	thin layer chromatography
TIS	triisopropyl silane
TMS	tetramethylsilane

LIST OF FIGURES

Chapter 2

Figure 1. Antibacterial mechanism of AMPS. 8

Figure 2. Schematic representation of the mechanism involved in regulated degradation of proteins by the ClpP complex.. 9

Figure 3. X-ray structure of inactive and active ClpP. 11

Figure 4. Structures of ADEP analogues modified from a core structure of ADEP1.. 12

Figure 5. Structures of ADEP analogues modified from a core structure with pipecolic acid. 13

Figure 6. Structures of ADEP analogues modified from a core structure by Thr. 13

Figure 7. Structures of ADEP analogues modified from a core structure with 3-methoxypropylamine and ADEP fragments. 14

Chapter 3

Figure 3. 1: Parent structure of ADEP1. 27

Figure 3. 3: ADEP1 ester cyclised analogues. 32

Figure 3. 4: Schematic representation of Fischer esterification. 33

Figure 3. 5: Schematic representation of Steglich esterification. 33

Figure 3. 6: Cyclisation of the peptides through forming an ester bond. 33

Figure 3. 7: Disulphide bond cyclised ADEP1 analogues. 35

Figure 3. 8: Disulphide bond cyclised ADEP1 analogues with Lys 37

Chapter 4

Figure 4. 1: Synthesis of the 5-oxazolidinones from Fmoc alanine 50

Figure 4. 2: Synthesis of Fmoc-N-methyl alanine from the oxazolidinone precursors. 51

Figure 4. 3: Synthesis of Fmoc-sarcosine. 52

Chapter 5

Fig. 1 Effect of ADEP analogues on the viability of HEK-293 (A) Caco-2 (B) cells, and Auranofin treatment on HEK-293 and Cac-2 (C). Cell viability was assessed by MTS assay, where $p < 0.05$ was considered statistically significant. *=$p < 0.05$, **=$p < 0.01$, and***=$p < 0.001$.....65

Chapter 6

Figure 6. 1: Disulphide bond cyclized ADEP1 analogues.....73

Figure 6. 2: TEM images gelatin-capped $AgInS_2$ QDs.....77

Figure 6. 3: Chemical structure of gelatin. 77

Figure 6. 4: Conjugation of ADEP1 analogues to gelatin-capped $AgInS_2$ QDs.....78

Figure 6. 5: TEM images gelatin-capped $AgInS_2$ QDs/ ADEP1 analogues conjugates……79

Figure 6. 6: PL properties of $AgInS_2$ QDs and ADEP1 analogues conjugates.....79

Figure 6. 7: Cell viability assay of QD-ADEP1 analogues and auranofin on HEK-293.....83

Chapter 7

Figure 7. 1: Three steps in solubility assay protocol. 93

Figure 7. 2: Disulphide bond cyclised ADEP1 analogues.....94

Figure 7. 3: SDS-PAGE analysis of recombinant ClpP1 and ClpP2 proteins.....95

Figure 7. 4: Elution profiles ClpP1 and ClpP from the Ni-NTA columns 97

Figure 7. 5: Qualitative ELISA analysis of the purified recombinant proteins 98

Figure 7. 6: Far-UV CD spectrum of the purified recombinant ClpP1 subunit.....99

Figure 7. 7: Far-UV CD spectrum of the purified recombinant ClpP2 subunit.....99

Figure 7. 8: M.*tb* ClpP1P2 activity of free AMC by fluorescence spectrophotometer 100

Figure 7. 9: Solubility test of ADEP1 analogues.....101

Figure 7. 10: PAMPA assay for ADEP1 analogues 103

Appendix

Figure A. 1: Results of linear SC001 obtained from MS.....111

Figure A. 2: Results of linear SC009 obtained from MS.....111

Figure A. 3: Results of linear SC0010 obtained from MS.....112

Figure A. 4: Results of linear SC011 obtained from MS.....112

Figure A. 5: Results of linear SC0012 obtained from MS.....113

Figure A. 6: Results of SC009 treated with 1% H_2SO_4 obtained from MS. 113

Figure A. 7: Results of SC009 treated with 95% TFA obtained from MS. 114

Figure A. 8: Results of SC009 treated with DIC and DMAP obtained from MS. 114
Figure A. 9: Results of SC009 treated with EDC and DMAP obtained from MS. 115
Figure A. 10: Results of SC009 treated with CDI and DMAP obtained from MS.....115
Figure A. 11: Results of SC010 treated with 1% H_2SO_4 obtained from MS. 116
Figure A. 12: Results of SC010 treated with 95% TFA obtained from MS. 116
Figure A. 13: Results of SC010 treated with DIC and DMAP obtained from MS.....117
Figure A. 14:Results of SC010 treated with EDC and DMAP obtained from MS. 117
Figure A. 15: Results of SC010 treated with CDI and DMAP obtained from MS.....118
Figure A. 16: MS results of linear SC013.....118
Figure A. 17: MS results of linear SC014.....119
Figure A. 18: LCMS results of cyclized and purified SC016.....120
Figure A. 19: LCMS results of cyclized and purified SC016.....121
Figure A. 20: Linear SC017.....122
Figure A. 21: Linear SC018.....122
Figure A. 22: Linear SC019.....123
Figure A. 23: Linear SC020.....124
Figure A. 24: LCMS spectrum of Fmoc-N-Methyl Alanine. 125
Figure A. 25: LCMS spectrum of Fmoc-Alanine peptoid. 126
Figure A. 26: LCMS spectra of Bz-LL, N-terminal blocked dipeptide agonist comprised of two Leu residues and benzoic acid on the N-terminal. 127
Figure A. 27: ^{1}H NMR spectrum of Fmoc-N-Methyl Alanine in DMSO-d_6.....128
Figure A. 28: ^{13}C NMR spectrum of Fmoc-N-Methyl Alanine in DMSO-d_6. 128
Figure A. 29: DEPT45 spectrum of Fmoc-N-Methyl Alanine in DMSO-d_6.....129
Figure A. 30: DEPT90 spectrum of Fmoc-N-Methyl Alanine in DMSO-d_6.....129
Figure A. 31: DEPT135 sepctrum of Fmoc-N-Methyl Alanine in DMSO-d_6 130
Figure A. 32: NOESYPHSW spectrum of Fmoc-N-Methyl Alanine in DMSO-d_6. 130
Figure A. 33: ^{1}H NMR spectrum of Fmoc-Sarcosine in DMSO-d_6. 131
Figure A. 34: ^{13}C NMR spectrum of Fmoc-Sarcosine in DMSO-d_6.. 131
Figure A. 35: DEPT45 spectrum of Fmoc-Sarcosine in DMSO-d_6.....132
Figure A. 36: DEPT90 spectrum of Fmoc-Sarcosine in DMSO-d_6.....132
Figure A. 37: DEPT135 spectrum of Fmoc-Sarcosine in DMSO-d_6.....133
Figure A. 38: NOESYPHSW spectrum of Fmoc-Sarcosine in DMSO-d_6. 133
Figure A. 39: ^{1}H NMR spectrum of Bz-LL in DMSO-d_6.....134
Figure A. 40: ^{13}C NMR spectrum of Bz-LL in DMSO-d_6.....134
Figure A. 41: DEPT45 spectrum of Bz-LL in DMSO-d_6. 135

Figure A. 42: DEPT135 spectrum of Bz-LL in DMSO-d_6. 135
Figure A. 43: NOESYPHSW spectrum of Bz-LL in DMSO-d_6.....136

LIST OF SCHEMES

Chapter 5

Scheme 1 Schematic representation of a solid phase peptide synthesis of ADEP1 analogues 58

Scheme 2 ADEP1 analogues in relation to ADEP1 parent structure (A). The ADEP analogues were modified with either Ada (SC006 and SC007) (B) or Pal (SC005 and SC008) (C).....61

LIST OF TABLES

Chapter 2

Table 1: List of TB drugs and their mode of action....5

Chapter 3

Table 3. 1: ADEP1 analogues with linear and cyclised calculated MM. 31

Table 3. 2: ADEP1 analogues with linear and cyclised calculated MM. 34

Table 3. 3: List ADEP1 analogues with linear and cyclised calculated MM containing Cys residues. 36

Table 3. 4: List ADEP1 analogues with linear and cyclised calculated MM containing Cys residues and Lys.....38

Table 3. 5: List ADEP1 analogues with linear and cyclised calculated MM containing Cys residues and peptoid moieties. 40

Table 3. 6: Summary of ADEP1 peptide analogues library....40

Chapter 5

Table 1: Peptide sequences, stereochemistry, and net charge 58

Table 2: Peptide analysis by HR-LCMS and Zetasizer 63

Table 3: Diameter of zones of inhibition of CC ADEP analogues. 63

Table 4: MIC and MBC of the ADEP analogues on bacteria....64

Chapter 6

Table 6. 1: Elemental analysis of gelatin-capped $AgInS_2$ QDs....76

Table 6. 2: Zeta potential values of the ADEP1 analogues before and after conjugation the gelatin-capped $AgInS_2$ QDs 80

Table 6. 3: MIC and MBC values of the QD-ADEP1 analogue conjugates focusing on peptide concentration....82

Table 6. 4: MIC and MBC values of the QD-ADEP1 analogue conjugates focusing on QD concentration.....82

Chapter 7

Table 7. 1: *M.tb* ClpP1P2 peptidase activity percentage 100

CHAPTER 1.

INTRODUCTION

1.1. Background

Mycobacterium is a genus of species belonging to the *Mycobacteriaceae* family, *Actinomycetales* order and *Actinobacteria* domain of bacteria that was discovered in the late 1800s by Lehmann and Neumann. This genus has over 150 species of strict and opportunistic pathogens that causes diseases in animals [1]. These species are generally differentiated according to the rate of growth on a solid media. For fast-growing mycobacteria, colonies usually appear in less than 7 days while the slow growing mycobacteria takes longer than 7 days [2]. However, both these groups are causative agents of pulmonary, dissemination and cutaneous diseases especially in immunocompromised individuals [3], [4]. Out of about 40 species of fast growing, sometimes referred to as nontubular mycobacteria [1], only, a few which are associated with human and animal diseases. These species include *Mycobacterium* (*M*) *favescens*, *M. goodii*, *M. mucogenicum* and *M. neoaurum* [2], [5]. The slow-growing mycobacteria are more pathogenic than the fast-growing ones [6]. Some of the slow-growing mycobacteria are *M. leprae*, *M. Avium* complex and *M. tuberculosis* (*M. tb*). *M. tb* was first identifies in 1882 by a German scientist Robert Koch as a pathogenic bacteria causing tuberculosis (TB).

TB has long incubation time thus taking time to develop into an active disease with symptoms, as the *M. tb* is a slow growing bacterium [7]. Early symptoms are often mistaken with common cold, flu, pneumonia, etc. This makes it hard to administer the relevant treatment in time thus rendering the treatment ineffective for some patients with advanced TB. This also gives a chance for bacterial mutations leading to TB drug resistance [8]. Bacterial resistance occurs when the *M. tb* is resistant to at least one of the first line anti-TB drug. *M. tb* has become resistant to both the first and second line anti-TB drugs leading to a rise in resistant *M. tb* strains. Resistance of *M. tb* to treatment is mainly caused by defaulting on the prescribed treatment [9]. Defaulting is often caused by a number of social, health, and economic issues [10]. This ranges from people failing to collect their treatment to people who cannot sustain the nutritional demand of TB. With other bacterial infections, antibiotic treatment is usually not more than seven days. However, with TB, the minimum treatment is six months. The longer treatment periods with intense side effects associated with TB treatment further contributes to noncompliance to the treatment thus perpetuating the TB resistance. There are several resistant

strains, which are classified as multidrug-Resistant (MDR), rifampicin-resistant (RR), isoniazid-resistant, and extensively drug-resistant (XDR) TB [11]. South Africa is amongst the top ten countries that account to about 70% of global MDR/RR cases each year.

Unfortunately, TB is a community disease that does not only affect individuals but families, communities, and the economy. South Africa, especially the lower socio-economic strata, is largely affected by the poverty associated with TB [10]. Although South Africa is currently classified as an upper-middle income country, the unemployment rate is high especially for TB patients [12]. South Africa is also ranked amongst the top 30 countries with high-burden tuberculosis and has one of the highest incident rates. It is counted amongst the five countries with more than 500 cases per 100 000 population [13]. In 2021 alone, an estimated 10.6 million people fell ill and about 1.6 million people died from TB, globally. To this day, TB is still listed amongst the biggest killer ranking 13th on the causes of death and second leading infectious killer, worldwide [13].

Overall, TB and TB drug-resistance remains a global public health burden and a health threat to humans. Hence, the urgent need for new and effective anti-TB drugs. This study is focusing on developing a novel peptide based pharmaceutical active ingredients (ADEP1 analogues) that will have a different mode of action compared to the conventional TB treatment. The ADEPs bind and dysregulated bacterial caseinolytic protease (ClpP) which is responsible for the overall bacterial cell protein homeostasis [14]. The subsequent chapters address the limitations of conventional TB drugs and limitations of acyldepsipeptides (ADEPs). They also discuss the possible improvements that can be made in the ADEP1 thus subsequently leading to design, synthesis and characterisation of the ADEP1 analogues. The ADEP1 analogues were then tested for their antimicrobial activity in various bacterial strains. In silico and in vitro interactions between ADEP1 analogues and ClpP1P2 protease. The analogues were further screened for their pharmacokinetic properties. The study also demonstrates the inclusion of nanomaterial into drug-like compounds to improve the intended function. Finding a more effective TB drug will not only lift the burden on the public health but also improve livelihoods.

1.2. **Aim and objectives**

1.2.1. *Aim*

The aim is to design, synthesise and characterise ADEP1 analogues with improved pharmacokinetics such as less toxicity, increased solubility, decreased enzyme susceptibility, and increased therapeutic activity.

1.2.2. *Objectives*

The objectives of the project include:

- To synthesise and characterise the designed ADEP1 derivatives using the solid phase peptide synthesis strategy and liquid chromatography mass spectrometry, respectively.
- To synthesise peptides with D-amino acids N-methylated and peptoids amino acids moieties with increased selectivity and decreased enzyme susceptibility, respectively.
- To synthesise peptides with lipophilic molecules (palmitic acid and adamantane) for improved membrane permeability
- To investigate the effect of enlarging the cyclic ring of ADEP1by the addition of two cysteine amino acids on the activity
- To cyclise ADEP1 analogues through a disulphide bridge between two cysteine amino acids residues.
- To express and purify *M. tb* ClpP1/P2 domains and further screen interaction with ADEP1 analogues.
- To investigate the influence of ADEP1 analogues on *M. tb* ClpP1P2 activity.
- To screen the ADEP1 analogues for their cytoxicity, solubility, and membrane permeability.
- To conjugate ADEP1 analogues to gelatine capped Silver/Indium/Sulphide ($AgInS_2$) quantum dots via an amide bond for drug loading and delivery.

1.3. **Hypothesis and question**

1.3.1. *Hypothesis*

ADEPs have a unique mechanism of antibacterial action, acting as activators of ClpP by mimicking the binding action of Clp-ATPases to the ClpP hydrophobic pockets. This mechanism is a great strategy to trick bacteria to go under uncontrolled proteolysis, which will then lead to bacterial cell death. Unfortunately, these peptides still suffer from poor drug-like properties such as cytoxicity to mammalian cells. Structural changes on ADEP1 analogues such as peptoids, D amino acids might result in increased selectivity, decrease enzyme susceptibility as these moieties are not recognised by the mammalian cells. Substitution of the aliphatic chain to more membrane permeable compounds such as adamantane (Ada) and palmitic acid (Pal) will not only increase membrane permeability and subsequently increase therapeutic activity; they will also lessen cytoxicity, which is the current bottleneck for ADEPs.

1.3.2. *Question*

Can anionic or cationic amino acids, D-amino acids, N-methylation, Lipophilic molecules, cyclisation with disulphide bridge, incorporation of peptoids moieties and conjugation to nanomaterial improve synthesis yield, toxicity, and activity of ADEP1 analogues?

1.4. References

[1] N. Rastogi, E. Legrand, and C. Sola, “The mycobacteria: an introduction to nomenclature and pathogenesis,” *Rev. Sci. Tech. Int. Off. Epizoot.*, vol. 20, no. 1, pp. 21–54, Apr. 2001.

[2] T. M. Shinnick and R. C. Good, “Mycobacterial taxonomy,” *Eur. J. Clin. Microbiol. Infect. Dis. Off. Publ. Eur. Soc. Clin. Microbiol.*, vol. 13, no. 11, pp. 884–901, Nov. 1994.

[3] S. T. Howard and T. F. Byrd, “The rapidly growing mycobacteria: saprophytes and parasites,” *Microbes Infect.*, vol. 2, no. 15, pp. 1845–1853, Dec. 2000, doi: 10.1016/S1286-4579(00)01338-1.

[4] J. L. Cook, “Nontuberculous mycobacteria: opportunistic environmental pathogens for predisposed hosts,” *Br. Med. Bull.*, vol. 96, no. 1, pp. 45–59, Dec. 2010, doi: 10.1093/bmb/ldq035.

[5] R. J. Wallace *et al.*, “Diversity and sources of rapidly growing mycobacteria associated with infections following cardiac surgery,” *J. Infect. Dis.*, vol. 159, no. 4, pp. 708–716, Apr. 1989, doi: 10.1093/infdis/159.4.708.

[6] M. C. Leclerc, F. Thomas, and J. F. Guégan, “Evidence for phylogenetic inheritance in pathogenicity of Mycobacterium,” *Antonie Van Leeuwenhoek*, vol. 83, no. 3, pp. 265–274, 2003.

[7] M. O. Babalola, “The Strengths, Weaknesses, Opportunities and Threats (SWOT) Analysis of *Mycobacterium tuberculosis*: A Systematic Review,” *J. Tuberc. Res.*, vol. 03, no. 04, Art. no. 04, 2015, doi: 10.4236/jtr.2015.34025.

[8] S. K. Parida *et al.*, “Totally drug-resistant tuberculosis and adjunct therapies,” *J. Intern. Med.*, vol. 277, no. 4, pp. 388–405, 2015, doi: 10.1111/joim.12264.

[9] R. Loddenkemper, D. Sagebiel, and A. Brendel, “Strategies against multidrug-resistant tuberculosis,” *Eur. Respir. J.*, vol. 20, no. 36 suppl, pp. 66s–77s, Jul. 2002, doi: 10.1183/09031936.02.00401302.

[10] L. Vanleeuw, W. Zembe-Mkabile, and S. Atkins, “‘I’m suffering for food’: Food insecurity and access to social protection for TB patients and their households in Cape Town, South Africa,” *PLOS ONE*, vol. 17, no. 4, p. e0266356, Apr. 2022, doi: 10.1371/journal.pone.0266356.

[11] R. Prasad, N. Gupta, and A. Banka, “Multidrug-resistant tuberculosis/rifampicin-resistant tuberculosis: Principles of management,” *Lung India Off. Organ Indian Chest Soc.*, vol. 35, no. 1, pp. 78–81, 2018, doi: 10.4103/lungindia.lungindia_98_17.

[12] N. Foster, A. Vassall, S. Cleary, L. Cunnama, G. Churchyard, and E. Sinanovic, “The economic burden of TB diagnosis and treatment in South Africa,” *Soc. Sci. Med. 1982*, vol. 130, pp. 42–50, Apr. 2015, doi: 10.1016/j.socscimed.2015.01.046.

[13] WHO, “Global Tuberculosis Report 2022,” 2022.

[14] H. Brötz-Oesterhelt *et al.*, “Dysregulation of bacterial proteolytic machinery by a new class of antibiotics.,” *Nat Med*, vol. 11, pp. 1082–1087, 2005.

CHAPTER 2.

Literature Review: Published

Reference: Cobongela SZZ, Makatini MM, Mdluli PS, Sibuyi NRS. Acyldepsipeptide Analogues: A Future Generation Antibiotics for Tuberculosis Treatment. Pharmaceutics. 2022; 14(9):1956. https://doi.org/10.3390/pharmaceutics14091956

Copyright Permission: No special permission is required to reuse all or part of article published by MDPI, including figures and tables. For articles published under an open access Creative Common CC BY license, any part of the article may be reused without permission provided that the original article is clearly cited. Reuse of an article does not imply endorsement by the authors or MDPI.

Review

Acyldepsipeptide Analogues: A Future Generation Antibiotics for Tuberculosis Treatment

Citation: Cobongela, S.Z.Z.; Makatini, M.M.; Mdluli, P.S.; Sibuyi, N.R.S. Acyldepsipeptide Analogues: A Future Generation Antibiotics for Tuberculosis Treatment. *Pharmaceutics* **2022**, *14*, x. https://doi.org/10.3390/xxxxx

Academic Editor(s): Gene L. Bidwell, III

Received:15 August 2022
Accepted: 12 September 2022
Published: date

Publisher's Note: MDPI stays neutral with regard to jurisdictional claims in published maps and institutional affiliations.



Copyright: © 2022 by the authors. Submitted for possible open access publication under the terms and conditions of the Creative Commons Attribution (CC BY) license (https://creativecommons.org/licenses/by/4.0/).

Sinazo Z. Z. Cobongela [1,2,*], Maya M. Makatini [2], Phumlane S. Mdluli [1,3] and Nicole R. S. Sibuyi [1,4,*]

[1] Nanotechnology Innovation Centre (NIC), Health Platform, Advanced Materials Division, Mintek, Randburg, 2194, South Africa; phumlanem@mintek.co.za
[2] Molecular Sciences Institute, School of Chemistry, University of the Witwatersrand, Johannesburg, 2050, South Africa; maya.makatini@wits.ac.za
[3] Department of Chemistry, Durban University of Technology, P.O. Box 1334, Durban 4000, South Africa
[4] DSI/Mintek NIC, Biolabels Research Node, Department of Biotechnology, University of the Western Cape, Bellville, 7535, South Africa
* Correspondence: sinazoc@mintek.co.za (S.Z.Z.C.); nicoles@mintek.co.za (N.R.S.S.); Tel.: +27-117094303 (S.Z.Z.C.); +27-117094280 (N.R.S.S.)

Abstract: Acyldepsipeptides (ADEPs) are a new class of emerging antimicrobial peptides (AMPs), which are currently explored for treatment of pathogenic infections, including tuberculosis (TB). These cyclic hydrophobic peptides have a unique bacterial target to the conventional anti-TB drugs, and present a therapeutic window to overcome *Mycobacterium Tuberculosis* (*M. tb*) drug resistance. ADEPs exerts their antibacterial activity on *M. tb* strains through activation of the protein homeostatic regulatory protease, the caseinolytic protease (ClpP1P2). ClpP1P2 is normally regulated and activated by the ClpP-ATPases to degrade misfolded and toxic peptides and/or short proteins. ADEPs bind and dysregulate all the homeostatic capabilities of ClpP1P2 while inducing non-selective proteolysis. The uncontrolled proteolysis leads to *M. tb* cell death within the host. ADEPs analogues that have been tested possess cytotoxicity and poor pharmacokinetic and pharmacodynamic properties. However, these can be improved by drug design techniques. Moreover, the use of nanomaterial in conjunction with ADEPs would yield effective synergistic effect.

This new mode of action has potential to combat and eradicate the extensive multi-drug resistance (MDR) problem that is currently faced by the public health pertaining bacterial infections, especially TB.

Keywords: acyldepsipeptides; antimicrobial peptides; caseinolytic protease; *Mycobacterium tuberculosis*; antimicrobial; tuberculosis; multi-drug resistance bacteria; antibiotics; proteolytic core; nanomaterials

1. Introduction

Tuberculosis (TB) has been terrorizing the world for millennia [1], yet the disease continue to thrive with none of the current therapy effective against the *Mycobacterium Tuberculosis* (*M. tb*) drug-resistant strains [2]. Efforts have been made to develop novel and effective anti-TB strategies with the goal to eradicate TB. Among others, natural products have played a significant role in drug discovery for decades and continue to make a significant contribution toward novel drug development [3]. Acyldepsipeptides (ADEPs) are emerging as potential anti-TB agents that are explored against *M. tb* strains, this is encouraged by the fact that they target different mechanism that are unique to the ones targeted by the conventional TB agents. As such, they might succeed where the TB agents are ineffective [4]. ADEPs were shown to have broad spectrum antimicrobial activity, including in drug-resistant *M. tb* strains [5]. However, none of the ADEPs are used clinically as TB treatment due to various challenges which include toxicity, solubility, metabolic instability, non-specificity, and membrane permeability. Safety and target specificity are the main aspects of drug development, and strategies have been put into place to improve on the pharmacokinetics of various drugs in order to improve patient compliance. To increase the bioavailability and therapeutic index of drugs, strategies such as chemical modification of the drugs, substitution of amino acids [6–9], and use of drug carriers were employed. Therefore, the same strategies can be used for modification and modulation of ADEPs to improve their targeting and overall pharmacokinetic properties. This review article presents an overview of TB and its impact on human health and economy; the conventional TB drugs, their mode of actions, and their limitations. ADEPs are presented herein as the upcoming and potential anti-TB agents; and lastly, the strategies that can improve their bioavailability and efficacy following strategies used for other drugs are also highlighted.

2. Tuberculosis

TB is a highly infectious disease and still one of the biggest killer, ranked among the top ten causes of death globally [10]. It is one of the oldest bacterial diseases as confirmed by the *M. tb* strain found in human remains dating back to at least 5000 BC [11]. TB has been a crisis to humans for millennia, and its emergence and causative agent was not understood until later in history [1]. At first it was suggested to be transmitted to human by *M. bovis* from cattle causing bovine TB and later believed that it was caused by inhalation of an infectious agent [12]. The TB causative agent was confirmed in 1882 by a German scientist Robert Koch who discovered that TB in humans was caused by a pathogenic *M. tb*. His postulates enabled the study of TB transmission and encouraged the essential discovery of acid-fast bacilli technique that is still widely used to date for the diagnosis of TB [13].

2.1. M. tb Epidemiology and Pathophysiology

TB was not considered an epidemic before the 17th century because of less infected population. However, due to urbanization in the early 17th century, the rate of human to human transmission of this airborne pathogen increased resulting in TB being declared an epidemic [14]. The mechanism of *M. tb* transmission in humans was detailed in 1930. Wells and colleagues made a conclusion that this bacterium is expelled from a person with an active pulmonary TB when coughing as 1-micron sized droplet nuclei that gets suspended in air. These droplet nuclei remain in the air and be inhaled by the next person [15]. Once inhaled into the lungs (alveolar) of the susceptible person, it has a potential to grow, causing new infection [16]. The infection can develop from inhalation of a single tubercle bacilli. These findings led to TB being declared as an airborne transmitted disease [17,18].

The progression of the infection varies in part due to the immune system of the host. There are four possible outcomes post inhalation of the tubercle bacillus. Developing the infection being the worst outcome and this usually occur to individuals with pre-existing immune compromising conditions such as human immune deficiency virus (HIV) [19,20]. Otherwise, the immune system has an ability to completely eradicate the bacterium before it launches an infection. In cases where the bacterium is not successfully eradicated, it can exist in a dormant stage known as latent TB infection [21]. This stage is asymptomatic and infection cannot be transmitted. However, at any given time ranging from immediate to decades, approximately 10% of latent TB-infected individuals can progress to active TB triggered by the deterioration of their immune system. Sometimes, latent TB can be activated when the *M. tb* escapes from the lungs to manifest in extrapulmonary sites such as the central nervous system, lymph node, bones, etc., [22].

Alternately, the bacterium can either come into contact with the resident macrophages or be ingested by the alveolar epithelial type II pneumocytes which lines the alveoli in the lungs. Pneumocytes are found in abundance than the macrophages in the lungs, and it is where the infection manifests [23]. Phagocytosis is activated by the bacteria encountering the macrophage mannose receptor [24]. This process triggers a glycoprotein (surfactant protein A) found in the surface of the alveolar to upregulate mannose receptor activity to promote phagocytosis of the bacteria [25]. Inside the macrophage, the *M. tb* is contained in a phagosome, an endocytic vacuole. Under normal phagosomal maturity cycle, the phagosome fuses with lysosome which introduces a hostile environment for the bacteria to survive. These include acidic pH, reactive oxygen intermediates, lysosomal enzymes, and some toxic peptides, with reactive nitrogen intermediates acting as the major elements in the antimicrobial activity of the macrophages [26]. With little knowledge on how and when in the stage of infection, polyclonal antibodies against *M. tb* bind and neutralize the active *M. tb*. The opsonized cells are also engulfed by the macrophages. Concurrently, the production of chemokines by infected macrophages recruits other immune cells such as monocytes, lymphocytes, and neutrophils. These help in formation of granuloma which increases cellular immunity to kill the bacilli-loaded macrophages to contain the spread of *M. tb*. However, the mycobacterium can survive the granuloma stage and continue multiplying and spreading in the alveolar or remain dormant for decades resulting in latent TB [27,28].

TB prevails in Africa as it is the poorest continent, facing most of the socio-economic problems such as unemployment, access to land, poor healthcare systems, etc. In the poor socio-economic class, people are obliged to reside in densely populated areas resulting in intense exposure and increased transmission rate. While TB is prevalent among the poor, it however has an effect across geographic boarders and social strata. Economically active age group, between the ages of 14 and 54 years old, accounts for three quarters of all TB cases with a death rate of 17%. This leads to loss and/or decreased income in affected households [29].

The World Health Organization (WHO) declared TB as a global public health emergency due to the epidemic proportions in some parts of the world and the rapid rise of MDR strains of *M. tb*. Before 2019, TB has previously been counted amongst the top 10 causes of death worldwide and a leading cause of death than HIV/AIDS. It was estimated that in 2020 TB caused about 1.3 million deaths, majority were HIV-negative cases and around 214,000 were HIV-positive people [30]. Even though there was a decline in TB diagnosis in 2020, it was estimated that about 10 million people developed TB. Out of the 10 million, 5.6 of those were men, 3.3 million were women, and about 1.1 million were children. The severity of this epidemic varies among countries; however, Africa and South-East Asia are still counted amongst the most prevalent continents [30].

In addition, 132,222 and 25,681 cases of rifampicin-resistant TB (RR-TB) and pre-XDR-TB global cases, respectively, for 2019 were reported by the WHO [30]. This shows an exponential growth of RR-TB and an alarming public health crisis as rifampicin is the most effective first-line TB drug. It was estimated that 82% of the RR-TB cases have MDR-TB. About 23% of the world's population (1.7 billion) are estimated to have latent TB and are at a greater risk of developing the active TB disease later in their lives. The diagnosis and treatment of TB-infected people have helped to effectively avert millions of TB-related deaths.

2.2. Treatment of TB

The discovery of antibiotics is one of the most successful therapies to ever happen in the history of medicine. Antibiotics are antimicrobial agents produced by microorganisms in response to infections to inhibit growth or induce cell death upon interaction with microbial cells. Most TB antibiotics target the cell wall of the *M. tb* which is made up of peptidoglycan, polysaccharides, arabinogalactan, and mycolic acids [31]. To this day, the majority of the antibiotics currently used are mainly secondary metabolites produced by a number of microorganisms isolated from the soil. Antimicrobial agents are classified and named according to their mode of action by which they kill microorganisms [32]. Aminoglycosides, macrolides, etc., are known to inhibit the biosynthesis of proteins that are essential for bacterial cell homeostasis, thus causing cell death. Other antibiotics focus on disruption of the bacterial cell membranes, inhibition of folic acid metabolism, and inhibition of DNA replication and RNA synthesis. The conventional mode of action for most antibiotics, such as glycopeptides, is to target the bacterial cell wall biosynthesis. Penicillin is an example of β-lactam antibiotics that kill bacteria by specifically inhibiting the transpeptidase that catalyzes the final step in cell wall biosynthesis and the cross-linking of peptidoglycan [33].

It is widely known that penicillin was the first antibiotic discovered in 1928 by Sir Alexander Flemings [34], and it was only introduced into clinical practice in the 1930s [32,35]. Actually, in 1899, Emmerich and Low discovered pyocyanase [36], what we now call an antibiotic. Pyocyanase, extracted from *Pseudomonas aeruginosa,* was active against several pathogenic bacteria. It was the first antibiotic drug to be used clinically to treat various diseases. Unfortunately, pyocyanase was abandoned due to inconsistent treatment and its preparation was quite toxic to humans [37].

After a series of trials for compounds that were promising anti-mycobacterium by a soil microbiologist Selman Waksman, streptomycin was the very first successful TB drug introduced in 1947 [38]. Several active TB drugs were thereafter discovered and classified into two classes, the list of currently used anti-TB drugs and their mode of action is summarized in Table 1. The first-line drugs form a core treatment regimen, these include isoniazid, rifampicin, ethambutol, and pyrazinamide. Isoniazid is a prodrug which is activated by catalase peroxidase. Isoniazid inhibits an important enzyme (enoyl-acyl carrier protein reductase) component of fatty acid synthase II complex which is involved in the synthesis of mycolic acid and essential structure of the *M. tb* cell wall [39].

Second-line drugs are introduced to the regimen when dealing with resistant *M. tb* strains and these include but not limited to levofloxacin, moxifloxacin, bedaquiline, linezolid, and delamanid. In a case of XDR-TB, patients are given a combination of some of the first-line and second-line TB drugs with an addition of newly introduced drugs such as bedaquiline and delamanid [40–42].

Table 1. List of TB drugs and their mode of action.

TB Dugs			
Class	**Drugs**	**Mode of Action**	**References**
Thioamides	Ethionamide Prothionamide	Inhibit cell wall synthesis	[43,44]
Nitroimidazoles	Delamanid	Inhibit mycolic acid synthesis	[45]
Ethambutol		Inhibits cell wall synthesis	[46]
Cycloserine		Inhibits cell wall synthesis	[47,48]
Pyrazinamide		Exact target is unclear: Disrupts plasma membrane Disrupts energy metabolism	[49,50]
Diarylquinoline	Bedaquiline	Inhibits ATP synthesis	[51]
Aminoglycosides	Kanamycin Streptomycin	Inhibits protein synthesis	[52,53]
Cyclic peptides	Capreomycin	Inhibits protein synthesis	[54]
Fluoroquinolones	Moxifloxacin Levofloxacin	Inhibits DNA gyrase	[55,56]

Para-aminosalicyclic acid		Inhibit folate metabolism	[57,58]
Recent TB Drugs			
Nitroimidazoles	PA-24	Inhibits mycolic acid	[59]
SQ-109		Inhibits cell wall synthesis	[60]
Meropenem		Inhibits peptidoglycan synthesis	[61]
Benzothiazinones	PBTZ169 PBTZ043	Inhibits cells wall synthesis	[62–64]
Imidazopyridine amide		Inhibits cytochrome oxidase	[65,66]
Macrolides		Inhibits protein synthesis	[67,68]
Oxazolidinones	Linezolid Sutezolid	Inhibits protein synthesis	[69–71]

2.2.1 Bacterial Resistance as a Main Limitation for TB Drugs

The extensive use and prolonged courses of antibiotics to treat bacterial infections is causing an alarming increase in antibiotic resistance among Gram-negative and Gram-positive bacterial strains [72,73]. Most of the clinically relevant microorganisms have developed resistance toward almost all antibiotics known to man, including the first discovered antibiotic (penicillin). Among the β-lactam sensitive strains, a rapid increase in penicillin-resistance was reported against *Streptococcus pneumoniae* [74]. The mortality rate of penicillin-resistant *S. pneumoniae* infections is higher than that of penicillin-susceptible *S. pneumoniae* [75,76]. *M. tb* has been rapidly acquiring resistance toward most anti-TB drugs. This is mainly due to their hydrophobic thick cell wall composed of mycolic acid and other hydrophobic lipids such as phthiocerol dimycocerosates [2]. The cell wall components lead to difficulty in permeation of antibiotics to the bacterial cytoplasm [77]. The ability of the *M. tb* to be in a dormant state also increases their resistance to antibiotic treatment in their active state [78]. Hydrophilic TB antibiotics such as β-lactam use porin channels to penetrate *M. tb* cell wall [79]. However, *M. tb* modifies these porin channels to resist hydrophilic antibiotic uptake [80]. Additionally, *M. tb* possess efflux pump that help in expelling drugs that managed to infiltrate the bacterium [81]. *M. tb* also expresses anti-mycobacterium modifying and/or degrading enzymes [82,83].

M. tb strains that are resistant to various TB treatment, for instance rifampicin, isoniazid, pyrazinamide, ethambutol, and streptomycin have been reported. Rifampicin acts by binding to the bacterial DNA-dependent RNA polymerase *rpoB*-encoded β-subunit thereby inhibiting transcription. Rifampicin-resistance is caused by the mutation of 11 out of 12 amino acids within the *rpoB* gene that surrounds the rifampicin binding pocket [84]. MDR-TB is caused by *M. tb* that is resistant to at least rifampicin and isoniazid [42]. In the past two decades there has been an increase in the number of MDR cases [85–87] followed by XDR *M. tb* that is resistant to at least four of the core anti-TB drugs, mainly isoniazid, rifampicin, fluoroquinolone drugs, and at least one of the second-line injectables [88]. Recently, there has been *M. tb* strains that are resistant to all commercially available anti-TB drugs [89,90]. In low income countries, 8 out of 19 patients with XDR had *M. tb* that was resistant to all the anti-TB drugs leaving patients with no effective treatment [91].

Over 20 novel antibiotic classes were produced between 1930 and 1962 [92] and very few novel antibiotics have been marketed since then [93–95]. Despite the numerous numbers of novel antibiotics and their analogues, bacterial resistance is still a major clinical problem throughout the world. The emerging resistance of most pathogens to currently available antibiotics is raising an urgent need for new and effective antibiotic drugs. Exploring non-pharmaceutical compounds might give a wide range of chemical compounds utilized as effective antimicrobials. Over the years, peptides have been promising therapeutic agents for various diseases such as cancer [96], cardiovascular [97], diabetes [98], and others. There is an escalating attention toward synthetic analogues of natural antimicrobial peptides (AMPs) as potential and effective antimicrobial agents with novel mechanisms to combat the bacterial resistance problem [99,100].

3. AMPs as Future Antibiotics

AMPs, are host defense peptides that are endogenously produced by organisms for protection against pathogens [101]. AMPs are generally cationic with less than 50 amino acid residues [102]. They are part of innate immune response produced by eukaryotes and prokaryotes [103]. Cationic peptides exhibit diverse antimicrobial activities by enhancing bacterial agglutination, metal ion chelators, peroxidase activity, proteolytic inhibitors and impair cell wall activity [104]. These peptides have been proven to be active in vivo [105,106], effective against broad spectrum microbes [107–109] with reduced bacterial resistance [110] and side effects [111]. The antimicrobial activity of various AMPs have been reported against Gram-positive bacteria [9,112], Gram-negative bacteria [113,114], and fungi [115]. In addition, synthetic analogues of these peptides have demonstrated similar or enhanced activities compared to the natural AMPs. The synthetic peptides also have low minimum inhibitory concentration (MIC) [107], neutralizes the outer membrane lipopolysaccharides of Gram-negative bacteria [116], promote wound healing [117], and show synergistic activity with conventional antibiotics [118].

One of the first AMPs, named gramicidins, were isolated from *Bacillus brevis* in 1939 [119] . Gramicidins exhibited a bactericidal effect against a wide range of Gram-positive bacteria both in vitro and in vivo, and later was successfully used to treat bacteria-infected wounds in guinea-pigs skin [120]. As of August 2022, 3425 AMPs have been recorded in the Antimicrobial Peptide Database (APD3) isolated from microorganisms, plants, and animals as well as synthetic analogues. Examples include, magainins that were isolated from the skin of an African clawed frog (*Xenopus laevis*) [121] and purothionin from a common wheat plant *Triticumaestivum* [122]. The concentration of magainins that was found to be effective against pathogens was soluble in water and did not induce hemolytic effects. Magainins were proven to inhibit the growth of numerous bacterial species such as *Escherichia coli*, *Staphylococcus epidermidis* etc., and a known pathogenic fungi, *Candida albicans* [121,123]. Purothionin was found to be active against some pathogenic bacteria such as *Pseudomonas solanacearum* and *Xanthomonas campestris*, and fungi such as *Corynebacterium michiganense* [124]. These findings showed a promising future for AMPs as lead drug candidates against MDR microorganisms and possibly for effective TB treatment [7].

3.1 AMP Mode of Action

When AMPs are introduced to living microorganisms, they trigger anatomical/ functional changes at cellular and molecular levels. So far, disruption of membrane integrity and inhibition of intracellular activity have been identified as the two main mechanisms of action for AMPs [102]. In order to achieve this, AMPs must gain access to the cell by penetrating or interacting with the cell wall and/or cell membrane. Most of the AMPs have a cationic net charge due to their high content of the positively charged amino acid residues such as arginine, lysine, and histidine [125]. Due to the presence of lipopolysaccharides or teichoic acid, prokaryotes have a negative charge on their outer layer. In Gram-negative and Gram-positive bacteria, the cationic charge facilitates the accumulation of the AMP on the negatively charged surface of their outer membrane and cell wall, respectively [126]. The amphiphilic interaction between the AMPs and phospholipid bilayer of the bacterial cell wall/membrane is favorable in prokaryotes, this interaction encourages transmembrane pores which in turn disrupts the phospholipid bilayer and thus causing rapid cell lysis and eventually cell death [125]. Bacterial death by AMPs occur through similar mode of actions to those of antibiotics, by inhibition of DNA, RNA, and protein synthesis. AMP internalization can occur following one of the four mechanisms shown in Figure 1, i.e., aggregation, Barrel-Stave, Toroidal or Carpet models. All of these mechanisms are thoroughly explained elsewhere [127,128].

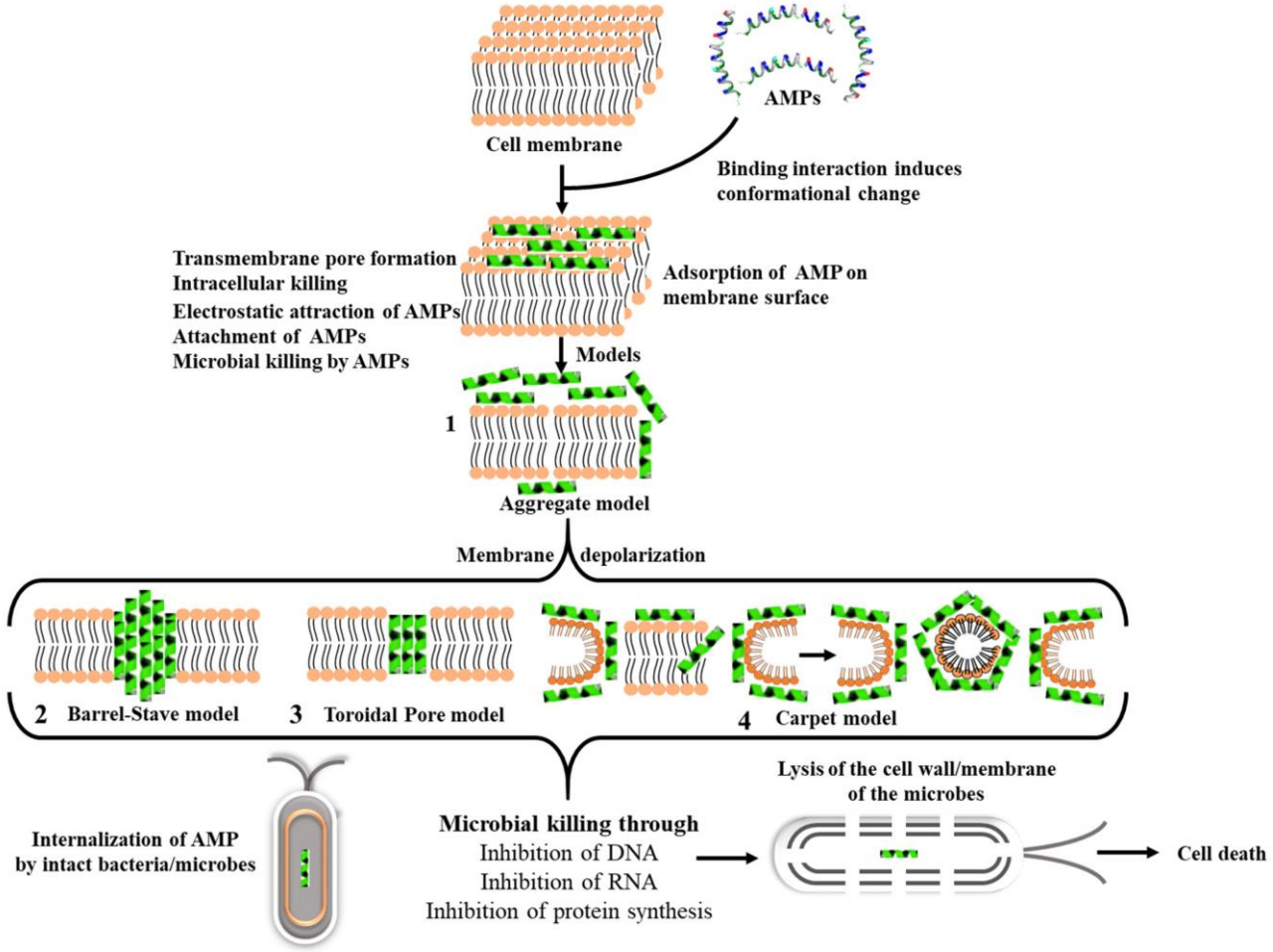


Figure 1. Antibacterial mechanism of AMPS. AMPs interact with bacteria and induce cell death following either aggregation (1), Barrel–Stave model (2), Toroidal Pore model (3) or Carpet model (4). Reprinted with permission from [127] published by MDPI, 2021.

It is vital that AMPs gain access to the intracellular targets through the cell wall and/or cell membrane. The cell wall of Gram-positive bacteria embodies a porous (40–80 nm) thick mash where AMPs can pass through to the cell cytoplasm [129]. Alternatively, the cationic AMPs can also manipulate the charge exchange mechanism for transmembrane on Gram-negative bacteria where it competes with the Ca^{2+} and Mg^{2+} bound to lipopolysaccharide of the outer membrane [6]. Proline-rich peptides are one of the AMPs that target the intracellular processes to inhibit bacterial growth [8]. Once inside the cell, the AMPs may inhibit vital biological processes such as enzyme activity, nucleic acid synthesis, and protein folding or synthesis [126,130,131].

One of the examples of the AMPs that uses these properties to translocate to the cytoplasm is indocilin [132], investigations showed that it inhibits DNA synthesis thus inhibiting bacterial growth [133]. There are some AMPs that bind to both RNA and DNA such as buforin II causing rapid cell death [134]. PR-39 is a proline-arginine-rich peptide that was found to inhibit the growth of MDR *M. tb* by binding to DNA and inhibiting intracellular protein synthesis [135,136]. Though there are a number of intracellular AMP targets, bacterial proteases are one of the underexploited for new AMPs. There is a number of bacterial proteases such as ATP-dependent zinc metalloprotease complex such as caseinolytic protease (ClpP) complex that can be targeted as therapeutic targets [137].

4. ClpP as a Putative Bacterial Therapeutic Target

ClpP is a serine peptidase that plays a crucial role in general protein quality control by degrading misfolded or aggregated proteins [138]. The ClpP belongs to a family of AAA+ ATPases and it is important for protein turnover and homeostasis in order to maintain vital cellular functions particularly under stress conditions. This protease is ATP dependent and referred to as proteolytic core [139,140]. It

is made up of fourteen ClpP protomers that form a tetradecameric barrel-shape with two heptameric rings [141]. The catalytic residues are embedded within the barrel with seven hydrophobic pockets for interaction with the Clp-ATPase [142]. Clp-ATPase supports the refolding of proteins independent of ClpP, failure to achieve this, Clp-ATPase directs the misfolded or aggregated proteins to the proteolytic core where it is unfolded and degraded [143]. The misfolded proteins have a degron tag following the post-translation modifications [144]. The degron tag then binds to the adaptor protein which activates AAA+ ATPases to bind to the inactive ClpP [145]. Figure 2 illustrates the Clp proteolytic degradation cycle of the misfolded or aggregated protein. ClpP conformation plays a huge role in its catalytic activity, such that the compressed conformation is inactive with the increase in distance between the active site side chains of Ser 98, His 123, and Asp 172 while the extended conformation has these side chains at close proximity to allow interaction, thus it is active [141,146].

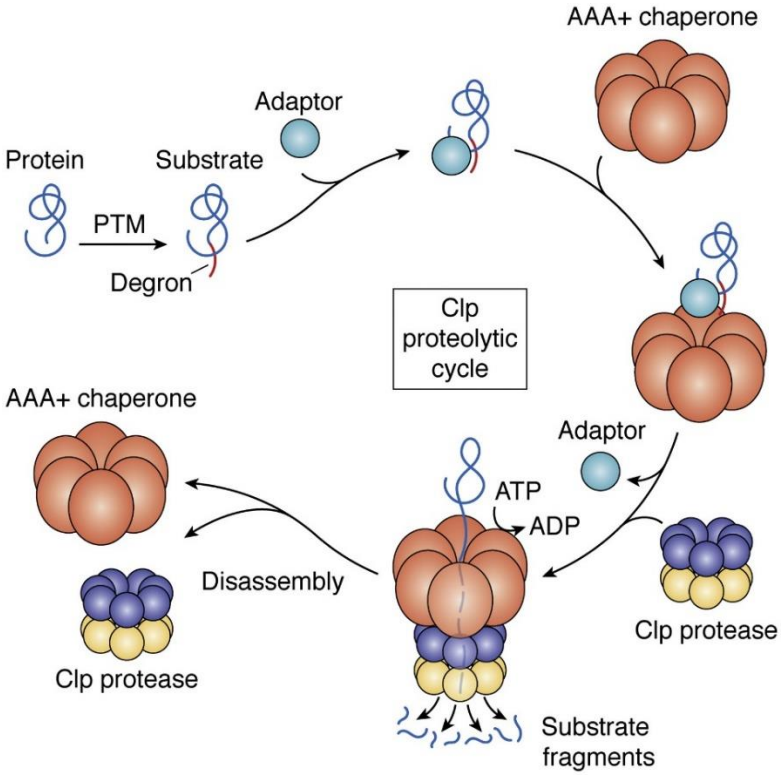


Figure 2. Schematic representation of the mechanism involved in regulated degradation of proteins by the ClpP complex. ClpP proteolytic activity is modulated by a series of events triggered by binding of misfolded/aggregated proteins to AAA+ chaperones. Reprinted with permission from [147] published by Elsevier, 2021.

The role and importance of ClpP on the bacterial cell viability can then be explored as a target for antibacterial abilities. Currently, there are three mechanisms to deregulate ClpP i.e., disruption of the AAA+ ATPases coupling to the ClpP, the inhibition, and activation of the ClpP proteolysis chamber [137]. As mentioned above, ClpP is dependent on ATPases to select and unfold aggregated or misfolded proteins, disruption of this partnership deregulates the proteolytic activity of ClpP. Similarly, lassomycin and ecumicin have been proven to bind to the Clp-ATPase N-terminal domain and activate ATPase activity [148,149].

Lassomycin is a sixteen amino acid lasso-peptide produced by *Lentzea kentuckeyensis* [150]. It binds to the N-terminal domain of ClpC1 one of Clp-ATPase causing functional abnormalities in the ClpP [151,152] by increasing ATP hydrolysis. In theory, increase in ATP hydrolysis by ClpC1 is associated with increase in protein degradation. Lassomycin prevents translocation of proteins which further inhibits the proteolysis by ClpP [151]. Lassomycin binds to the N-terminus domain of ClpC1, a highly acidic region encouraged by its four positively charged amino acids [153,154]. The binding site on the ClpC1 has arginine21 and proline79; however, the most critical binding site was glutamine17 which forms a hydrogen bonding with lassomycin. The bactericidal activity of lassomycin is assumed to be its

ability to increase ATP hydrolysis by ClpC1 thus leading to ATP depletion in the cell and/or excessive protein unfolding [151].

Ecumicin is a cyclic tridecapeptide extracted from *Nonomuraea* sp., like lassomycin, it binds to the N-terminal domain (glycine1-tyrosine145) of ClpC1 [150,151]. It also increases ATP hydrolysis by ClpC1 by blocking substrate/protein recognition by ClpC1 therefore inhibiting proteolysis [155]. It is assumed that there are hydrophobic interactions between ecumicin and ClpC1, furthermore, ecumicin forms two hydrogen bonds with the N-terminal domain of ClpC1 [155] [151]. It was suggested that arginine83 of ClpC1 is important for interaction with ecumicin [155]. Ecumicin was found to act in a similar manner to MecA, an adaptor protein that enhances the hexamerization of ClpC, thus increases the ATPase activity [149,155].

Other molecules such as β-lactone, focus on inhibiting the proteolytic core of the ClpP, where they covalently bind to Serine98 thus irreversibly inhibiting the proteolytic activity [156]. Interestingly, this mechanism was also shown to inhibit the growth of *M. tb*, suggesting that the ClpP could be an important target for the TB therapeutic intervention. For instance, cyclomarine A, a natural cyclic heptapeptide produced by *Streptomyces* sp., was shown to have high affinity and specificity for ClpC1 ATPase of *M. tb* by binding to the N-terminal domain of ClpC1 [149,151]. Most importantly, activation of the ClpP protease is distinctly an option that is exploited for development of therapeutic AMPs for various infectious diseases, including TB. Exploring this option of activation rather than inhibition of the ClpP may be effective against dormant or drug resistant bacteria. Since ADEPs have been reported to be using this antimicrobial mechanism, they can be explored as TB therapy [137].

4.1. ADEPs Competes with Clp-ATPases to Deactivate ClpP

ADEPs, also known as cyclic ADEPs, are a class of AMPs that bind and deregulates bacterial ClpP [4]. They are naturally produced by *Strepomyces hawaiiensis* [157] and are most active against Gram-positive bacteria [137]. ADEPs bind to the cavities formed by two of ClpP monomers. ClpP/ADEP complex adopts a proteolytic active conformation in the absence of Clp-ATPase [4,158]. ADEPs mimic the Clp-ATPases activity and competitively binds to the hydrophobic pockets. This event inhibits interaction between ClpP and Clp-ATPases, and therefore eliminates all natural functions of the Clp-protease that require Clp-ATPase-mediated degradation [159–161]. Figure 3 displays the X-ray structure of unbound ClpP N-terminal region and ADEP ClpP complex. Upon binding of the ADEP or Clp-ATPase, ClpP let loose of its N-terminal of the β-loop which on an intact state prevents ClpP from randomly going through degradation [159,160]. ADEPs or Clp-ATPase increases the proteolytic activity of ClpP thus degrading proteins (both essential and nonessential) around the target cells leading to cell death.

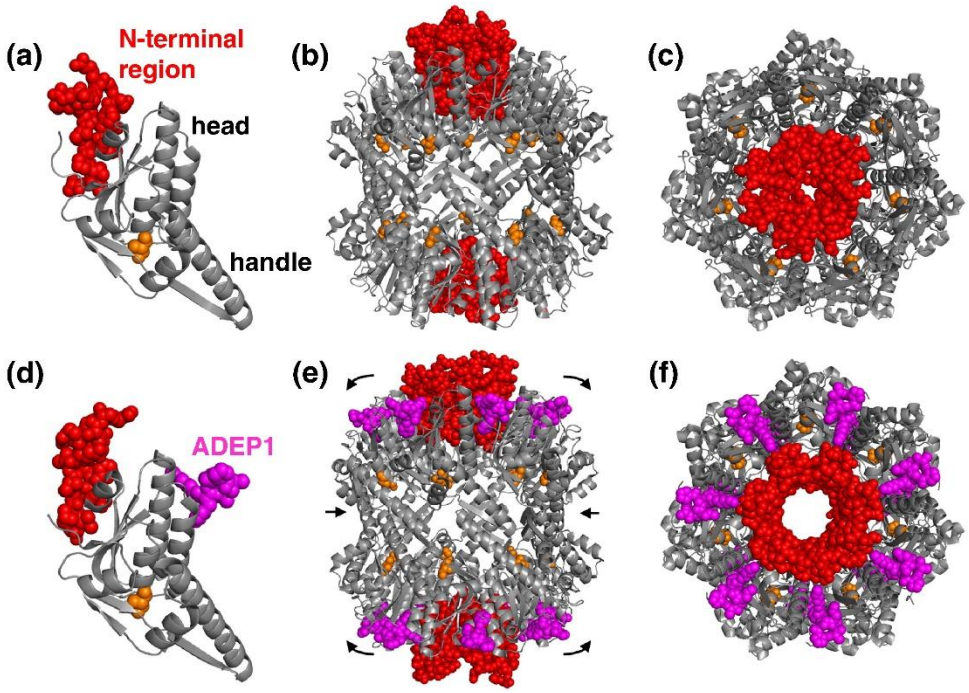


Figure 3. X-ray structure of inactive and active ClpP. (**a**) Inactive ClpP N-terminal domain (red). N-terminal residues from 1-18 are highlighted in red and the nucleophile active site is highlighted in orange. (**b**) Equatorial view of the inactive ClpP. (**c**) Axial view of the inactive ClpP. (**d**) ADEP1 (purple) bound active ClpP N-terminal domain. (**e**) Equatorial view of the ADEP1 activated ClpP. (**f**) Axial view of the ADEP1 activated ClpP. Reprinted with permission from [162], published by Elsevier, 2013.

The catalytic core of the ClpP has three amino acid residues, Serine98, Histidine123, and Aspartic acid172, that form a catalytic triad [163]. On the active conformation of ClpP, Serine98 undergoes a nucleophilic attack on the electron deficient carbonyl group of the peptide bond. The imidazole ring on Histidine123 abstracts a proton from the serine hydroxyl group and the resultant positively charged histidine imidazole ring is stabilized by the carboxyl function of the aspartic acid172. The aspartate acyl-ester undergoes hydrolysis regenerating the serine for the next catalytic cycle [141].

The aspartic acid and threonine side chains create a polar environment whereas the aliphatic side chain and benzene ring of the phenylalanine are buried deep into the hydrophobic pocket of ClpP [159]. The aliphatic side chain and N-acylphenylalanine moiety closely resembles the isoleucine/leucine-glycine-phenylalanine structure of one of Clp-ATPase (ClpX) hence this is a minimum structural requirement for ADEP activity [164]. Moreover, Tyrosine62 residue form two hydrogen bonds with N-group of phenylalanine e and a carboxylic group of alanine thus increasing rigidity between ADEP and ClpP [159]. The ADEP1 Factor A (A54556) is one of the ADEPs to be discovered [4], and has been reported to have antibacterial activity against Gram-positive bacteria [5] and Gram-negative bacteria [165]. ADEP1 was also reported to be bactericidal against a number of antibiotic-resistant Gram-positive bacteria such as penicillin-resistant *S. pneumoniae*, vancomycin-resistant *Enterococcus faecium,* and methicillin-resistant *Staphylococcus aureus* [5].

4.2. ADEP1 Analogues

There is a number of modification that have been done on the original ADEPs to yield better pharmacokinetics and pharmacodynamics. Figures 4–7 show some of the synthesized and tested ADEP analogue structures and fragments. ADEP1 Factor A (Figure 4) is cyclic peptide composed of four natural amino acids (proline, alanine, serine, and phenylalanine), two methylated amino acids (4-methyl proline and N-methylated alanine) and octa-2,4,6-trienoic acid. ADEP1 Factor A is active against various microorganisms including *Bacillus subtilis*, *S. pneumoniae*, *Streptococcus pyogenes*, *Enterococcus faecalis*, *E. faecium*, *S. aureus* [4,165], etc. The very first modification was the removal of the methyl group from proline (ADEP1 Factor B) which is active against *S. aureus*, *E. faecalis,* and *S. pneumoniae* [165,166]. The removal of the methyl proline in Factor B led to a decrease in antibacterial activity in *S. aureus* [165,166].

Other ADEP1 analogues have been used in different types of enoic acids (ADEP1 Factor D) to reduce the number of double bonds in octa-2,4,6-trienoic acid for thermal stability [165]. This analogue was active against a number of Gram-positive (Methicillin-resistant *S. Aureus*, vancomycin-resistant *enterococcus*, and penicillin-resistant *S. pneumoniae*) and Gram-negative pathogenic bacteria (*Neisseria meningitidis* and *Neisseria gonorrheae*) [5,167]. The use of fluorinated *bis*-fluorophenylalanine side chain in a place of phenylalanine has shown enhanced antibacterial activity of ADEP2, ADEP4, and ADEP5 on *S. aureus* [4]. Modifications have also aimed in rigidifying the macrolactone core. This was achieved by replacing the N-methyl alanine on the macrolactone core with pipecolic acid to yield ADEP2, ADEP4, ADEP14 as shown in Figure 5 [4,168,169], etc. The rigidified ADEP4 and its analogues still maintained the antimicrobial activity against *S. aureus*, *S. pneumoniae*, and *E. faecalis* [169]. ADEP14, ADEP28, and ADEP41 (Figure 6) were achieved by replacing serine with threonine. Fragments of the ADEPs (Figure 7) have also been tested for the ClpP activation and antimicrobial activity. Two fragments still maintained the antimicrobial activity against *B. subtilis* [170].

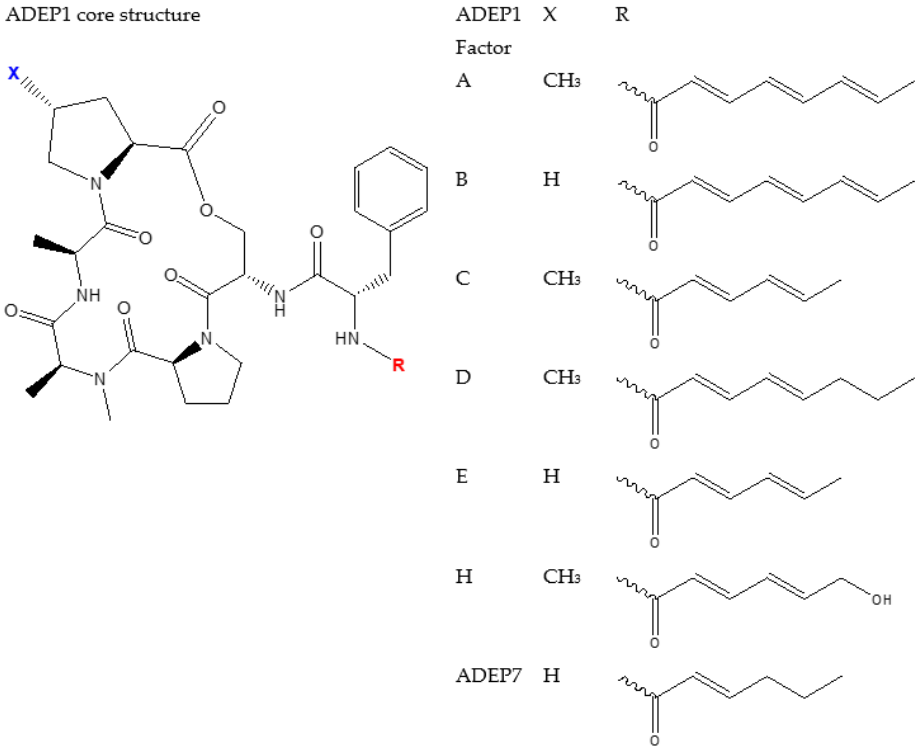


Figure 4. Structures of ADEP analogues modified from a core structure of ADEP1.

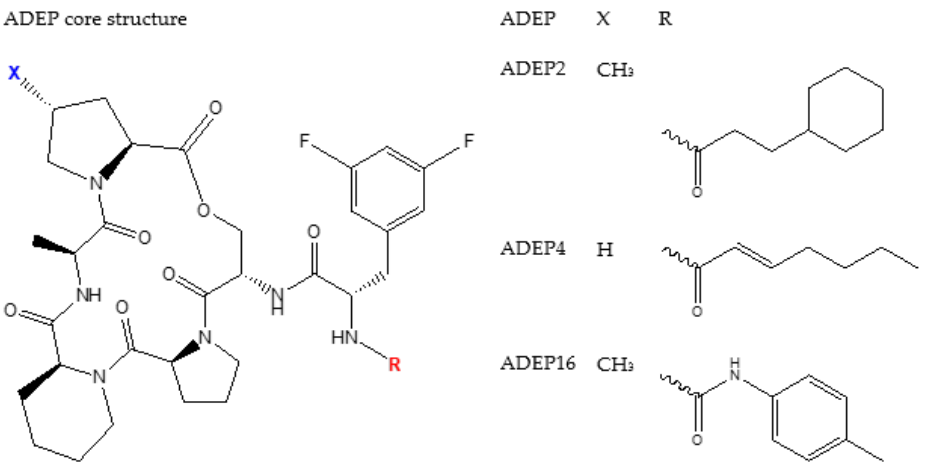


Figure 5. Structures of ADEP analogues modified from a core structure with pipecolic acid.

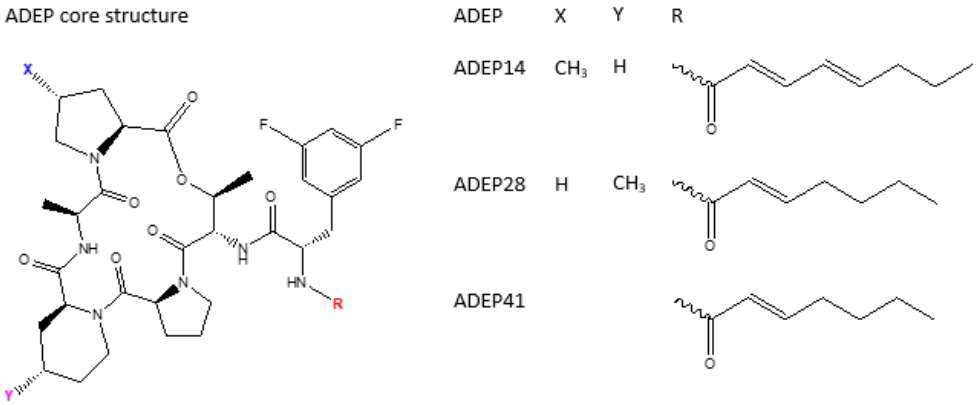
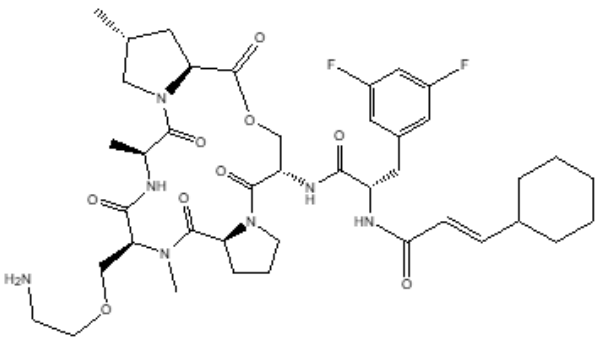
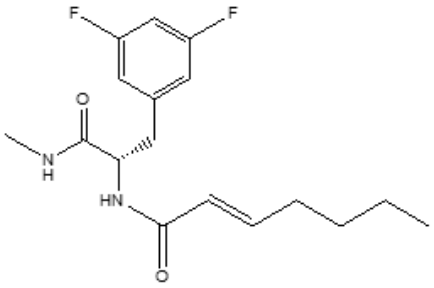


Figure 6. Structures of ADEP analogues modified from a core structure with Ser replaced by Thr.

ADEP5



Fragment 14



Fragment 2a

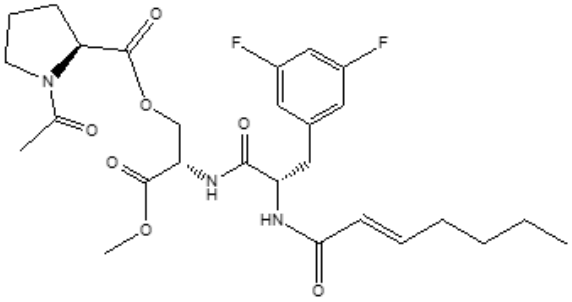


Figure 7. Structures of ADEP analogues modified from a core structure with 3-methoxypropylamine and ADEP fragments.

4.3. ADEPs Activity on M. tb ClpP1P2

ADEPs have particularly been of interest in *M. tb* targeting due to its distinct mode of action on ClpP [4]. The *M. tb* ClpP not only maintains intracellular protein homeostasis, it also contributes to the mycobacterium virulence and helps with the dormancy of the *M. tb* within the host [171–173]. Unlike other bacteria with a single gene for ClpP, *M. tb* has two genes encoding for ClpP1 and ClpP2 proteolytic subunits [174]. Like other ClpP, ClpP1 and ClpP2 heptamer rings are inactive until they associate to form a 300 kDa ClpP1P2 tetradecamer [152,171]. Upon binding together, both these rings influence each other's conformation [152,175]. In vitro, ADEPs exclusively bind to the *M. tb* ClpP2 which in turn changes the whole ClpP1P2 tetradecamer conformation to open both heptamer axial pores thus activating the ClpP1P2 [175]. This phenomenon is naturally controlled by ATPases in response to increased concentration of substrates. In low concentrations of substrates, ATPase-bound ClpP1P2 remains inactive. However, ClpP1P2 activation by ADEPs is independent of the amount of substrate present. The anti-mycobacterium activity of ADEPs and the exact mechanism of how they bind thus causing bacterial growth inhibition through ClpP1P2 is poorly understood.

It has been previously reported that the anti-mycobacterium activity of ADEPs is through nonselective protein degradation by *M. tb* ClpP1P2, and/or allosterically binding to ClpP1P2 to prevent physiological activity of the ATPase [175]. Anti-mycobacterium activity of ADEPs is also through ClpP1P2 inability to degrade and eliminate toxic proteins [176]. The ADEPs and analogues bind to leucine-glycine-phenylalanine hydrophobic pockets on the ClpP2 which is the same binding site for the ATPases [177,178]. A list of ADEP analogues (ADEP2, ADEP3, ADEP4, IDR-10001, and IDR-10011) were

found to be active against *M. tb* with an MIC range between 25 and 100 μg/mL [179]. Although the ADEP binding to the ClpP1P2 is similar to other bacterial ClpP complexes, the maximum effect of ADEPs on ClpP1P2 require activators such as dipeptide benzyloxycarbonyl-leucyl-leucine [176]. ADEPs were also shown to have improved activity with addition of efflux pump inhibitors which prevents export of intracellular ADEPs [81,179] and therefore, have potential to be effective where the current anti-TB drugs have failed.

4.4. Limitation of ADEPs

The problems mainly associated with novel therapeutic AMPs, including ADEPs are their poor pharmacokinetic properties such as susceptibility to enzyme degradation, short plasma half-life (leading to frequent invasive administration), lack of oral availability, difficulty in membrane permeability, lack of selectivity thus causing toxicity to normal cells [180,181]. These complications raise a need to improve the natural peptides in drug like molecules with less toxicity, high selectivity, good solubility, increased proteolytic stability, and membrane permeability. This in turn will increase drug bioavailability and consequently increasing their therapeutic activity. Therefore, modification and modulation of conformational dynamics of these AMPs and designing of similar systems that mimic the potential therapeutic peptides will be the first step toward improving the pharmacokinetic properties of the AMPs. There are several ways that can be employed to improve the pharmacokinetic properties of novel peptides. Peptide modification and use of drug carriers are some of the strategies that have been successful in enhancing the bioactivity of AMPs and their analogues [6–9].

4.4.1. Potential Strategies to Improve on ADEP's Pharmacokinetics and Pharmacodynamics

ADEPs are produced by natural sources such as plants and microorganisms, often in minute quantities and majority of them are less soluble, which presents a huge challenge for their application in therapeutics. Drug modifications has been successful in improving the membrane permeability, drug stability, and controlled delivery at the target site. Some of the strategies that can be employed to prevent ADEPs biodegradation or interaction with biomolecules include chemical modification of the drugs, substitution of amino acids [6–9], and use of drug delivery agents.

Chemical Modification

Chemical modification and amino acid substitution in lead drugs, no matter how small it is, have significant impact on their bioactivity; a lesson learnt from nature, where a slight change in a structure can completely alter its function, target, mode of action and improve drug selectivity [182]. Changing the drug structure conformation through cyclization is another way of increasing their metabolic stability compared to linear analogues. Cyclization can be formed through chemically stable bonds such as ether, disulphide, lactone etc., and the most common technique used in peptide chemistry [183].

Amino Acid Substitution

Protease stability is also vital in the development of peptide-based drugs, the incorporation of unnatural amino acids is one of the approaches used to increase their stability and bioavailability. There is quite a number of processes to achieve these unnatural amino acid analogues such as, substitution with either cationic [184], D-amino acids or N-methylated amino acids [185], can help improve on the metabolic stability and potency of peptide-based therapies. For instance, cationic peptides exhibit more bactericidal effects than their anionic counterparts. Therefore, replacing negatively charged amino acids (aspartic acid and glutamic acid) with positively charged ones (lysine and arginine) increases the positive net charge of the peptides. Moreover, lysine and/or arginine rich peptides easily interact with the negatively charged cell membrane and are used to shuttle biomolecules across the cell membrane [184]. The cationic peptides will therefore serve dual functions as cell-penetrating peptides and antimicrobial agents [186,187]. Additionally, substituting the natural L-amino acids with D-amino acids may be used to increase proteolytic stability of the peptide drugs. The L-amino are easily metabolized by the body and are susceptible to protease degradation. D-amino acids on the other hand, have similar activity to L-amino acids but are not susceptible to degradation, thus improving their bioavailability and drug activity [188,189]. N-methylation and fluorination of the amino acids also improve pharmacokinetic

characteristics, activity, selectivity, and delivery of peptides [185]. N-methylation also improved metabolic stability and intestinal permeability of peptides that were highly active but with poor bioavailability [190]. Nature has also employed N-methylation of peptides on the ADEP1 to improve its biological functions and mode of survival by inhibiting enzymatic degradation [165]. Multiple N-methylation also increased selectivity of a cyclic hexapeptide integrin antagonist toward different integrin subtypes [185,191]. Attention has also been given to fluorination to modulate physicochemical properties of proteins, especially of hydrophobic amino acids (phenylalanine, isoleucine and others), to increase peptide stability and prevent proteolytic degradation [192].

Lipophilic Molecules

Lipophilic molecules were also used to improve and facilitate the cellular uptake of AMPs or ADEPs as their mode of action is targeted on intracellular proteins. Lipophilic molecules such as linoleic, oleic, and palmitic acids are often conjugated to the drugs to increase membrane permeability of peptide-based drugs. They are mostly used in pharmaceuticals to enhance uptake of chemicals [193]. The conjugation of lipids to drugs increases their lipophilicity which enhances their interaction with the cell membrane thus increasing cellular uptake. Amongst other advantages of lipid-drug conjugates, they also improve the oral bioavailability and decrease toxicity of the drug molecule [194].

Nano-Carriers

The urgent need for development of new drug delivery systems with improved properties to achieve desirable therapeutic efficacy is driven by the toxicity and side effects of drugs. Nanomaterials have a wide range of applications in various fields. In the pharmaceutical industry, they are receiving significant interest and are being investigated for drug formulation and delivery (nanomedicine) [195]. Nanomaterials are very small in size, usually ranging from 1 to 100 nm, and yet have a larger surface area that can be easily manipulated by conjugating compounds of interest [196]. Because these particles are too small, they easily diffuse through cell membrane pores and ion channels, and their target specificity can be further improved when the targeting ligands are attached to nanomaterials [197]. Nanomaterials as drug carriers can also help in increasing drug solubility therefore increasing bioavailability of drugs [198]. Additionally, they can reduce toxicity and side effects by increasing selectivity and can improve transfer across membranes including the blood–brain barrier [199] without the aid of targeting moieties. These conjugates also decrease enzyme susceptibility of unstable drugs at physiological conditions [200]. There are several organic and inorganic nanomaterials that are promising drug delivery agents. Inorganic or metal nanoparticles such as zinc, copper, and iron oxides nanoparticles have been explored for this application, mostly due to their antibacterial activity.

The nanomaterials have been shown to exhibit antimicrobial properties against a wide range of pathogens including drug-resistant strains. For example, copper oxide (CuO) nanoparticles were effective against methicillin-resistant *S. aureus* and *E. coli* [201,202]. When loaded with drugs, they can translocate their cargoes across the cell membrane. Iron oxide (FeO) nanoparticles loaded with doxorubicin could transport doxorubicin across cellular membranes without any targeting moiety and accumulate in the nucleus [203]. The nanoparticles increased the selectivity and bioavailability of the drugs to the target cells and at the same time reduce the side effects. Nanomaterials such as zinc oxide (ZnO) nanoparticles were also shown to possess anti-TB activities, and could be used as both antimicrobial as well as drug delivery agents. Interestingly, bimetallic NPs, in this case mixing ZnO with silver nanoparticles improved their biocompatibility and reduced the toxicity resulting from individual metal nanoparticles in *M. tb* [204]. Thus, NPs alone or in combination with targeting molecules such as antibodies or targeting ligands can help improve the potency and bioavailability of ADEPs.

5. Conclusions

ADEPs bind and dysregulate bacterial ClpP complex leading to uncontrolled proteolysis of proteins that are essential for bacterial survival. They have proven to be effective antimicrobial and/or bactericidal agents in a number of bacterial strains including the drug-resistant mycobacterium. Even though ADEPs are highly potent antimicrobial agents, they have poor pharmacokinetics and pharmacodynamics properties to be used as active pharmaceutical agents. Since their discovery about 15 years ago, much

work has been carried out to modify these peptides to yield better results. Some modifications were successful, while others diminished their antimicrobial effect. There is still more to be done regarding these antimicrobial peptides. Especially the modification of ADEPs to increase the binding ability to the ClpP1P2 without the help of activators. This includes changing the cyclization bond and using enantiomers, lipophilic molecules, and drug carriers. Moreover, the strategic use of cationic amino acids would increase the interaction with the highly negative bacterial cell wall/cell membrane. This in turn would increase the solubility and cell penetrative ability of ADEPs. Another approach to overcome this tailback is the conjugation of ADEPs to nanomaterials. This approach will not only increase the drug delivery, but it will also increase drug availability and effectiveness of the ADEPs. Nanomaterials have been used as effective antimicrobials, thus can synergistically work with the cargoes toward eradicating TB.

Author Contributions: Writing—original draft preparation, project administration, S.Z.Z.C. Conceptualization, supervision, resources, writing—review and editing, S.Z.Z.C., M.M.M., P.S.M. and N.R.S.S. All authors have read and agreed to the published version of the manuscript.

Funding: The study was financially supported by Mintek Science Vote, Project No. ADR 42304.

Institutional Review Board Statement: Not applicable

Informed Consent Statement: Not applicable

Data Availability Statement: Not applicable

Conflicts of Interest: The authors declare no conflict of interest

References

1. Doetsch, R.N. Benjamin Marten and His "New Theory of Consumptions". *Microbiol. Rev.* **1978**, *42*, 521–528.
2. Augenstreich, J.; Haanappel, E.; Sayes, F.; Simeone, R.; Guillet, V.; Mazeres, S.; Chalut, C.; Mourey, L.; Brosch, R.; Guilhot, C.; et al. Phthiocerol Dimycocerosates from *Mycobacterium Tuberculosis* Increase the Membrane Activity of Bacterial Effectors and Host Receptors. *Front. Cell Infect. Microbiol.* **2020**, *10*, 420. https://doi.org/10.3389/fcimb.2020.00420.
3. Atanasov, A.G.; Zotchev, S.B.; Dirsch, V.M.; Supuran, C.T. Natural Products in Drug Discovery: Advances and Opportunities. *Nat. Rev. Drug Discov.* **2021**, *20*, 200–216. https://doi.org/10.1038/s41573-020-00114-z.
4. Brötz-Oesterhelt, H.; Beyer, D.; Endermann, R.; Ladel, C.; Schroeder, W.; Hinzen, B.; Raddatz, S.; Paulsen, H.; Henninger, K.; Bandow, J.E.; et al. Dysregulation of Bacterial Proteolytic Machinery by a New Class of Antibiotics. *Nat. Med.* **2005**, *11*, 1082–1087.
5. Goodreid, J.D.; Janetzko, J.; Santa Maria, J.P.; Wong, K.S.; Leung, E.; Eger, B.T.; Bryson, S.; Pai, E.F.; Gray-Owen, S.D.; Walker, S.; et al. Development and Characterization of Potent Cyclic Acyldepsipeptide Analogues with Increased Antimicrobial Activity. *J. Med. Chem.* **2016**, *59*, 624–646. https://doi.org/10.1021/acs.jmedchem.5b01451.
6. Anunthawan, T.; de la Fuente-Núñez, C.; Hancock, R.E.W.; Klaynongsruang, S. Cationic Amphipathic Peptides KT2 and RT2 Are Taken up into Bacterial Cells and Kill Planktonic and Biofilm Bacteria. *Biochim. Biophys. Acta (BBA) Biomembr.* **2015**, *1848*, 1352–1358. https://doi.org/10.1016/j.bbamem.2015.02.021.
7. Hollmann, A.; Martinez, M.; Maturana, P.; Semorile, L.C.; Maffia, P.C. Antimicrobial Peptides: Interaction with Model and Biological Membranes and Synergism with Chemical Antibiotics. *Front. Chem.* **2018**, *6*. https://doi.org/10.3389/fchem.2018.00204.
8. Hansen, A.; Schäfer, I.; Knappe, D.; Seibel, P.; Hoffmann, R. Intracellular Toxicity of Proline-Rich Antimicrobial Peptides Shuttled into Mammalian Cells by the Cell-Penetrating Peptide Penetratin. *Antimicrob. Agents Chemother.* **2012**, *56*, 5194–5201. https://doi.org/10.1128/AAC.00585-12.
9. Malanovic, N.; Lohner, K. Antimicrobial Peptides Targeting Gram-Positive Bacteria. *Pharmaceuticals* **2016**, *9*, 59. https://doi.org/10.3390/ph9030059.
10. World Health Organization. *The Top 10 Causes of Death*; World Health Organization: Geneva, Switzerland, 2018.
11. Gerszten, P.C.; Gerszten, E.; Allison, M.J. Diseases of the Spine in South American Mummies. *Neurosurgery* **2001**, *48*, 208–213. https://doi.org/10.1097/00006123-200101000-00039.
12. Riley, R.L.; O'Grady, F. Airborne Infection Transmission and Control. In *Molecular Medical Microbiology*; Elsevier: Amsterdam, The Netherlands, 1961; pp. 1–180.
13. Sakula, A. Robert Koch: Centenary of the Discovery of the Tubercle Bacillus, 1882. *Thorax* **1982**, *37*, 246–251.

14. Rubin, S.A. Tuberculosis. Captain of All These Men of Death. *Radiol. Clin. N. Am.* **1995**, *33*, 619–639.
15. Wells, W.F. On Air-Borne Infection Study ii. Droplets and Droplet Nuclei. *Am. J. Epidemiol.* **1934**, *20*, 611–618. https://doi.org/10.1093/oxfordjournals.aje.a118097.
16. Wells, W.F.; Ratcliffe, H.L.; Grumb, C. On the Mechanics of Droplet Nuclei Infection; Quantitative Experimental Air-Borne Tuberculosis in Rabbits. *Am. J. Hyg.* **1948**, *47*, 11–28. https://doi.org/10.1093/oxfordjournals.aje.a119179.
17. Riley, R.L.; Mills, C.C.; Nyka, W.; Weinstock, N.; Storey, P.B.; Sultan, L.U.; Riley, M.C.; Wells, W.F. Aerial Dissemination of Pulmonary Tuberculosis. A Two-Year Study of Contagion in a Tuberculosis Ward. 1959. *Am. J. Epidemiol.* **1995**, *142*, 3–14. https://doi.org/10.1093/oxfordjournals.aje.a117542.
18. Fennelly, K.P. Variability of Airborne Transmission of *Mycobacterium Tuberculosis*: Implications for Control of Tuberculosis in the HIV Era. *Clin. Infect. Dis.* **2007**, *44*, 1358–1360. https://doi.org/10.1086/516617.
19. Duggal, S.; Chugh, T.D.; Duggal, A.K. HIV and Malnutrition: Effects on Immune System. *Clin. Dev. Immunol.* **2012**, *2012*, 784740. https://doi.org/10.1155/2012/784740.
20. Trehan, I.; O'Hare, B.A.; Phiri, A.; Heikens, G.T. Challenges in the Management of HIV-Infected Malnourished Children in Sub-Saharan Africa. *AIDS Res. Treat.* **2012**, *2012*, 790786. https://doi.org/10.1155/2012/790786.
21. Jeong, Y.H.; Hur, Y.-G.; Lee, H.; Kim, S.; Cho, J.-E.; Chang, J.; Shin, S.J.; Lee, H.; Kang, Y.A.; Cho, S.-N.; et al. Discrimination between Active and Latent Tuberculosis Based on Ratio of Antigen-Specific to Mitogen-Induced IP-10 Production. *J. Clin. Microbiol.* **2015**, *53*, 504–510. https://doi.org/10.1128/JCM.02758-14.
22. Zumla, A.; Raviglione, M.; Hafner, R.; Fordham von Reyn, C. Tuberculosis. *N. Engl. J. Med.* **2013**, *368*, 745–755. https://doi.org/10.1056/NEJMra1200894.
23. Bermudez, L.E.; Sangari, F.J. Mycobacterial Invasion of Epithelial Cells. In *Bacterial Invasion into Eukaryotic Cells: Subcellular Biochemistry*; Oelschlaeger, T.A., Hacker, J., Eds.; Subcellular Biochemistry; Springer: Boston, MA, USA, 2000; pp. 231–249; ISBN 978-1-4757-4580-1.
24. Schlesinger, L.S. Macrophage Phagocytosis of Virulent but Not Attenuated Strains of *Mycobacterium Tuberculosis* Is Mediated by Mannose Receptors in Addition to Complement Receptors. *J. Immunol.* **1993**, *150*, 2920–2930.
25. Gaynor, C.D.; McCormack, F.X.; Voelker, D.R.; McGowan, S.E.; Schlesinger, L.S. Pulmonary Surfactant Protein a Mediates Enhanced Phagocytosis of *Mycobacterium Tuberculosis* by a Direct Interaction with Human Macrophages. *J. Immunol.* **1995**, *155*, 5343–5351.
26. Nathan, C.F.; Hibbs, J.B. Role of Nitric Oxide Synthesis in Macrophage Antimicrobial Activity. *Curr. Opin. Immunol.* **1991**, *3*, 65–70. https://doi.org/10.1016/0952-7915(91)90079-G.
27. Silva Miranda, M.; Breiman, A.; Allain, S.; Deknuydt, F.; Altare, F. The Tuberculous Granuloma: An Unsuccessful Host Defence Mechanism Providing a Safety Shelter for the Bacteria? *Clin. Dev. Immunol.* **2012**, *2012*, 139127. https://doi.org/10.1155/2012/139127.
28. Peddireddy, V.; Doddam, S.N.; Ahmed, N. Mycobacterial Dormancy Systems and Host Responses in Tuberculosis. *Front. Immunol.* **2017**, *8*, 1-8.
29. Zumla, A.; Grange, J.M. Is the Eradication of Tuberculosis 'yesterday's Ambition' or 'tomorrow's Triumph'? *Clin. Med.* **2010**, *10*, 450–453. https://doi.org/10.7861/clinmedicine.10-5-450.
30. WHO. *Global Tuberculosis Report 2021*; WHO: Geneva, Switzerland, 2021.
31. Jankute, M.; Cox, J.A.G.; Harrison, J.; Besra, G.S. Assembly of the Mycobacterial Cell Wall. *Annu. Rev. Microbiol.* **2015**, *69*, 405–423. https://doi.org/10.1146/annurev-micro-091014-104121.
32. Rolain, J.-M.; Abat, C.; Jimeno, M.-T.; Fournier, P.-E.; Raoult, D. Do We Need New Antibiotics? *Clin. Microbiol. Infect.* **2016**, *22*, 408–415. https://doi.org/10.1016/j.cmi.2016.03.012.
33. Yocum, R.R.; Rasmussen, J.R.; Strominger, J.L. The Mechanism of Action of Penicillin. Penicillin Acylates the Active Site of Bacillus Stearothermophilus D-Alanine Carboxypeptidase. *J. Biol. Chem.* **1980**, *255*, 3977–3986.
34. Fleming, A. On the Antibacterial Action of Cultures of a Penicillium, with Special Reference to Their Use in the Isolation of B. Influenzæ. *Br. J. Exp. Pathol.* **1929**, *10*, 226–236.
35. Tan, S.Y.; Tatsumura, Y. Alexander Fleming (1881–1955): Discoverer of Penicillin. *Singap. Med. J.* **2015**, *56*, 366–367. https://doi.org/10.11622/smedj.2015105.
36. Caltrider, P.G. Pyocyanine. In *Antibiotics: Volume I Mechanism of Action*; Gottlieb, D., Shaw, P.D., Eds.; Springer: Berlin/Heidelberg, Germany, 1967; pp. 117–121; ISBN 978-3-662-38439-8.
37. Aminov, R.I. A Brief History of the Antibiotic Era: Lessons Learned and Challenges for the Future. *Front. Microbiol.* **2010**, *1*, 1-7. https://doi.org/10.3389/fmicb.2010.00134.
38. History of TB Drugs—Which Was the First Drug? *TBFacts*.
39. Takayama, K.; Wang, C.; Besra, G.S. Pathway to Synthesis and Processing of Mycolic Acids in *Mycobacterium Tuberculosis*. *Clin. Microbiol. Rev.* **2005**, *18*, 81–101. https://doi.org/10.1128/CMR.18.1.81-101.2005.

40. Kim, C.T.; Kim, T.-O.; Shin, H.-J.; Ko, Y.C.; Hun Choe, Y.; Kim, H.-R.; Kwon, Y.-S. Bedaquiline and Delamanid for the Treatment of Multidrug-Resistant Tuberculosis: A Multicentre Cohort Study in Korea. *Eur. Respir. J.* **2018**, *51*, 1-44 https://doi.org/10.1183/13993003.02467-2017.
41. Seung, K.J.; Keshavjee, S.; Rich, M.L. Multidrug-Resistant Tuberculosis and Extensively Drug-Resistant Tuberculosis. *Cold Spring Harb. Perspect. Med.* **2015**, *5*, a017863. https://doi.org/10.1101/cshperspect.a017863.
42. Gandhi, N.R.; Nunn, P.; Dheda, K.; Schaaf, H.S.; Zignol, M.; van Soolingen, D.; Jensen, P.; Bayona, J. Multidrug-Resistant and Extensively Drug-Resistant Tuberculosis: A Threat to Global Control of Tuberculosis. *Lancet* **2010**, *375*, 1830–1843. https://doi.org/10.1016/S0140-6736(10)60410-2.
43. Nishida, C.R.; Ortiz de Montellano, P.R. Bioactivation of Anti-Tuberculosis Thioamide and Thiourea Prodrugs by Bacterial and Mammalian Flavin Monooxygenases. *Chem. Biol. Interact.* **2011**, *192*, 21–25. https://doi.org/10.1016/j.cbi.2010.09.015.
44. Shetty, A.; Dick, T. Mycobacterial Cell Wall Synthesis Inhibitors Cause Lethal ATP Burst. *Front. Microbiol.* **2018**, *9*, 1898. https://doi.org/10.3389/fmicb.2018.01898.
45. Thakare, R.; Soni, I.; Dasgupta, A.; Chopra, S. Delamanid for the Treatment of Pulmonary Multidrug-Resistant Tuberculosis. *Drugs Today* **2015**, *51*, 117–123. https://doi.org/10.1358/dot.2015.51.2.2245645.
46. Schubert, K.; Sieger, B.; Meyer, F.; Giacomelli, G.; Böhm, K.; Rieblinger, A.; Lindenthal, L.; Sachs, N.; Wanner, G.; Bramkamp, M. The Antituberculosis Drug Ethambutol Selectively Blocks Apical Growth in CMN Group Bacteria. *mBio* **2017**, *8*, e02213–16. https://doi.org/10.1128/mBio.02213-16.
47. Batson, S.; de Chiara, C.; Majce, V.; Lloyd, A.J.; Gobec, S.; Rea, D.; Fülöp, V.; Thoroughgood, C.W.; Simmons, K.J.; Dowson, C.G.; et al. Inhibition of D-Ala:D-Ala Ligase through a Phosphorylated Form of the Antibiotic D-Cycloserine. *Nat. Commun.* **2017**, *8*, 1939. https://doi.org/10.1038/s41467-017-02118-7.
48. Alghamdi, W.A.; Alsultan, A.; Al-Shaer, M.H.; An, G.; Ahmed, S.; Alkabab, Y.; Banu, S.; Barbakadze, K.; Houpt, E.; Kipiani, M.; et al. Cycloserine Population Pharmacokinetics and Pharmacodynamics in Patients with Tuberculosis. *Antimicrob. Agents Chemother.* **2019**, *63*, e00055-19. https://doi.org/10.1128/AAC.00055-19.
49. Zhang, Y.; Wade, M.M.; Scorpio, A.; Zhang, H.; Sun, Z. Mode of Action of Pyrazinamide: Disruption of *Mycobacterium Tuberculosis* Membrane Transport and Energetics by Pyrazinoic Acid. *J. Antimicrob. Chemother.* **2003**, *52*, 790–795. https://doi.org/10.1093/jac/dkg446.
50. Black, P.A.; Warren, R.M.; Louw, G.E.; van Helden, P.D.; Victor, T.C.; Kana, B.D. Energy Metabolism and Drug Efflux in *Mycobacterium Tuberculosis*. *Antimicrob. Agents Chemother.* **2014**, *58*, 2491–2503. https://doi.org/10.1128/AAC.02293-13.
51. Sarathy, J.P.; Gruber, G.; Dick, T. Re-Understanding the Mechanisms of Action of the Anti-Mycobacterial Drug Bedaquiline. *Antibiotics* **2019**, *8*, 261. https://doi.org/10.3390/antibiotics8040261.
52. Ruiz, P.; Rodríguez-Cano, F.; Zerolo, F.J.; Casal, M. Investigation of the in Vitro Activity of Streptomycin against *Mycobacterium Tuberculosis*. *Microb. Drug Resist.* **2002**, *8*, 147–149. https://doi.org/10.1089/107662902760190707.
53. Chulluncuy, R.; Espiche, C.; Nakamoto, J.A.; Fabbretti, A.; Milón, P. Conformational Response of 30S-Bound IF3 to A-Site Binders Streptomycin and Kanamycin. *Antibiotics* **2016**, *5*, 38. https://doi.org/10.3390/antibiotics5040038.
54. Lin, Y.; Li, Y.; Zhu, N.; Han, Y.; Jiang, W.; Wang, Y.; Si, S.; Jiang, J. The Antituberculosis Antibiotic Capreomycin Inhibits Protein Synthesis by Disrupting Interaction between Ribosomal Proteins L12 and L10. *Antimicrob. Agents Chemother.* **2014**, *58*, 2038–2044. https://doi.org/10.1128/AAC.02394-13.
55. Tunitskaya, V.L.; Khomutov, A.R.; Kochetkov, S.N.; Kotovskaya, S.K.; Charushin, V.N. Inhibition of DNA Gyrase by Levofloxacin and Related Fluorine-Containing Heterocyclic Compounds. *Acta Nat.* **2011**, *3*, 94–99.
56. Chopra, S.; Matsuyama, K.; Tran, T.; Malerich, J.P.; Wan, B.; Franzblau, S.G.; Lun, S.; Guo, H.; Maiga, M.C.; Bishai, W.R.; et al. Evaluation of Gyrase B as a Drug Target in *Mycobacterium Tuberculosis*. *J. Antimicrob. Chemother.* **2012**, *67*, 415–421. https://doi.org/10.1093/jac/dkr449.
57. Chakraborty, S.; Gruber, T.; Barry, C.E.; Boshoff, H.I.; Rhee, K.Y. Para-Aminosalicylic Acid Acts as an Alternative Substrate of Folate Metabolism in *Mycobacterium Tuberculosis*. *Science* **2013**, *339*, 88–91. https://doi.org/10.1126/science.1228980.
58. Howe, M.D.; Kordus, S.L.; Cole, M.S.; Bauman, A.A.; Aldrich, C.C.; Baughn, A.D.; Minato, Y. Methionine Antagonizes Para-Aminosalicylic Acid Activity via Affecting Folate Precursor Biosynthesis in *Mycobacterium Tuberculosis*. *Front. Cell. Infect. Microbiol.* **2018**, *8*, 1-12
59. Manjunatha, U.; Boshoff, H.I.; Barry, C.E. The Mechanism of Action of PA-824. *Commun. Integr. Biol.* **2009**, *2*, 215–218.
60. Tahlan, K.; Wilson, R.; Kastrinsky, D.B.; Arora, K.; Nair, V.; Fischer, E.; Barnes, S.W.; Walker, J.R.; Alland, D.; Barry, C.E.; et al. SQ109 Targets MmpL3, a Membrane Transporter of Trehalose Monomycolate Involved in Mycolic Acid Donation to the Cell Wall Core of *Mycobacterium Tuberculosis*. *Antimicrob. Agents Chemother.* **2012**, *56*, 1797–1809. https://doi.org/10.1128/AAC.05708-11.

61. Catalão, M.J.; Filipe, S.R.; Pimentel, M. Revisiting Anti-Tuberculosis Therapeutic Strategies That Target the Peptidoglycan Structure and Synthesis. *Front. Microbiol.* **2019**, *10*, 1-11. https://doi.org/10.3389/fmicb.2019.00190.
62. Vilchèze, C. Mycobacterial Cell Wall: A Source of Successful Targets for Old and New Drugs. *Appl. Sci.* **2020**, *10*, 2278. https://doi.org/10.3390/app10072278.
63. Makarov, V.; Lechartier, B.; Zhang, M.; Neres, J.; Sar, A.M.V.D.; Raadsen, S.A.; Hartkoorn, R.C.; Ryabova, O.B.; Vocat, A.; Decosterd, L.A.; et al. Towards a New Combination Therapy for Tuberculosis with next Generation Benzothiazinones. *EMBO Mol. Med.* **2014**, *6*, 372–383. https://doi.org/10.1002/emmm.201303575
64. Makarov, V.; Manina, G.; Mikusova, K.; Möllmann, U.; Ryabova, O.; Saint-Joanis, B.; Dhar, N.; Pasca, M.R.; Buroni, S.; Lucarelli, A.P.; et al. Benzothiazinones Kill *Mycobacterium Tuberculosis* by Blocking Arabinan Synthesis. *Science* **2009**, *324*, 801–804. https://doi.org/10.1126/science.1171583.
65. O'Malley, T.; Alling, T.; Early, J.V.; Wescott, H.A.; Kumar, A.; Moraski, G.C.; Miller, M.J.; Masquelin, T.; Hipskind, P.A.; Parish, T. Imidazopyridine Compounds Inhibit Mycobacterial Growth by Depleting ATP Levels. *Antimicrob. Agents Chemother.* **2018**, *62*, e02439–17. https://doi.org/10.1128/AAC.02439-17.
66. Lu, P.; Asseri, A.H.; Kremer, M.; Maaskant, J.; Ummels, R.; Lill, H.; Bald, D. The Anti-Mycobacterial Activity of the Cytochrome Bcc Inhibitor Q203 Can Be Enhanced by Small-Molecule Inhibition of Cytochrome Bd. *Sci. Rep.* **2018**, *8*, 2625. https://doi.org/10.1038/s41598-018-20989-8.
67. Zhu, Z.J.; Krasnykh, O.; Pan, D.; Petukhova, V.; Yu, G.; Liu, Y.; Liu, H.; Hong, S.; Wang, Y.; Wan, B.; et al. Structure-Activity Relationships of Macrolides against *Mycobacterium Tuberculosis*. *Tuberculosis* **2008**, *88*, S49–S63. https://doi.org/10.1016/S1472-9792(08)70036-2.
68. Van der Paardt, A.-F.; Wilffert, B.; Akkerman, O.W.; Lange, W.C.M. de; Soolingen, D. van; Sinha, B.; Werf, T.S. van der; Kosterink, J.G.W.; Alffenaar, J.-W.C. Evaluation of Macrolides for Possible Use against Multidrug-Resistant *Mycobacterium Tuberculosis*. *Eur. Respir. J.* **2015**, *46*, 444–455. https://doi.org/10.1183/09031936.00147014.
69. Zhang, M.; Sala, C.; Dhar, N.; Vocat, A.; Sambandamurthy, V.K.; Sharma, S.; Marriner, G.; Balasubramanian, V.; Cole, S.T. In Vitro and In Vivo Activities of Three Oxazolidinones against Nonreplicating *Mycobacterium Tuberculosis*. *Antimicrob. Agents Chemother.* **2014**, *58*, 3217–3223. https://doi.org/10.1128/AAC.02410-14.
70. Alcalá, L.; Ruiz-Serrano, M.J.; Pérez-Fernández Turégano, C.; García de Viedma, D.; Díaz-Infantes, M.; Marín-Arriaza, M.; Bouza, E. In Vitro Activities of Linezolid against Clinical Isolates of *Mycobacterium Tuberculosis* That Are Susceptible or Resistant to First-Line Antituberculous Drugs. *Antimicrob. Agents Chemother.* **2003**, *47*, 416–417. https://doi.org/10.1128/AAC.47.1.416-417.2003.
71. Wallis, R.S.; Dawson, R.; Friedrich, S.O.; Venter, A.; Paige, D.; Zhu, T.; Silvia, A.; Gobey, J.; Ellery, C.; Zhang, Y.; et al. Mycobactericidal Activity of Sutezolid (PNU-100480) in Sputum (EBA) and Blood (WBA) of Patients with Pulmonary Tuberculosis. *PLoS ONE* **2014**, *9*, e94462. https://doi.org/10.1371/journal.pone.0094462.
72. Gaynes, R.; Monnet, D. The Contribution of Antibiotic Use on the Frequency of Antibiotic Resistance in Hospitals. In *Ciba Foundation Symposium 207—Antibiotic Resistance: Origins, Evolution, Selection and Spread: Antibiotic Resistance: Origins, Evolution, Selection and Spread: Ciba Foundation Symposium 207*; John Wiley & Sons, Ltd.: Chichester, UK, 2007; pp. 47–56.
73. Coates, A.; Hu, Y.; Bax, R.; Page, C. The Future Challenges Facing the Development of New Antimicrobial Drugs. *Nat. Rev. Drug Discov.* **2002**, *1*, 895–910. https://doi.org/10.1038/nrd940.
74. Tang, Y.-W.; Li, H.; Griffin, J.P.; Haas, D.W.; D'Agata, E.M.C. Rapidly Increasing Prevalence of Penicillin-Resistant Streptococcus Pneumoniae in Middle Tennessee: A 10-Year Clinical and Molecular Analysis. *J. Clin. Microbiol.* **2002**, *40*, 395–399. https://doi.org/10.1128/JCM.40.2.395-399.2002.
75. Feikin, D.R.; Schuchat, A.; Kolczak, M.; Barrett, N.L.; Harrison, L.H.; Lefkowitz, L.; McGeer, A.; Farley, M.M.; Vugia, D.J.; Lexau, C.; et al. Mortality from Invasive Pneumococcal Pneumonia in the Era of Antibiotic Resistance, 1995-1997. *Am. J. Public Health* **2000**, *90*, 223–229.
76. Mamishi, S.; Moradkhani, S.; Mahmoudi, S.; Hosseinpour-Sadeghi, R.; Pourakbari, B. Penicillin-Resistant Trend of Streptococcus Pneumoniae in Asia: A Systematic Review. *Iran. J. Microbiol.* **2014**, *6*, 198–210.
77. Brennan, P.J. Structure, Function, and Biogenesis of the Cell Wall of *Mycobacterium Tuberculosis*. *Tuberculosis* **2003**, *83*, 91–97. https://doi.org/10.1016/s1472-9792(02)00089-6.
78. Chao, M.C.; Rubin, E.J. Letting Sleeping Dos Lie: Does Dormancy Play a Role in Tuberculosis? *Annu. Rev. Microbiol.* **2010**, *64*, 293–311. https://doi.org/10.1146/annurev.micro.112408.134043.
79. Danilchanka, O.; Pavlenok, M.; Niederweis, M. Role of Porins for Uptake of Antibiotics by Mycobacterium Smegmatis. *Antimicrob. Agents Chemother.* **2008**, *52*, 3127–3134. https://doi.org/10.1128/AAC.00239-08.
80. Stephan, J.; Mailaender, C.; Etienne, G.; Daffé, M.; Niederweis, M. Multidrug Resistance of a Porin Deletion Mutant of Mycobacterium Smegmatis. *Antimicrob. Agents Chemother.* **2004**, *48*, 4163–4170. https://doi.org/10.1128/AAC.48.11.4163-4170.2004.

81. Kardan Yamchi, J.; Haeili, M.; Gizaw Feyisa, S.; Kazemian, H.; Hashemi Shahraki, A.; Zahednamazi, F.; Imani Fooladi, A.A.; Feizabadi, M.M. Evaluation of Efflux Pump Gene Expression among Drug Susceptible and Drug Resistant Strains of *Mycobacterium Tuberculosis* from Iran. *Infect. Genet. Evol.* **2015**, *36*, 23–26. https://doi.org/10.1016/j.meegid.2015.08.036.
82. Wivagg, C.N.; Bhattacharyya, R.P.; Hung, D.T. Mechanisms of β-Lactam Killing and Resistance in the Context of *Mycobacterium Tuberculosis*. *J. Antibiot.* **2014**, *67*, 645–654. https://doi.org/10.1038/ja.2014.94.
83. Almeida Da Silva, P.E.A.; Palomino, J.C. Molecular Basis and Mechanisms of Drug Resistance in *Mycobacterium Tuberculosis*: Classical and New Drugs. *J. Antimicrob. Chemother.* **2011**, *66*, 1417–1430. https://doi.org/10.1093/jac/dkr173.
84. Campbell, E.A.; Korzheva, N.; Mustaev, A.; Murakami, K.; Nair, S.; Goldfarb, A.; Darst, S.A. Structural Mechanism for Rifampicin Inhibition of Bacterial RNA Polymerase. *Cell* **2001**, *104*, 901–912. https://doi.org/10.1016/S0092-8674(01)00286-0.
85. Centers for Disease Control (CDC) Nosocomial Transmission of Multidrug-Resistant Tuberculosis among HIV-Infected Persons—Florida and New York, 1988–1991. *MMWR Morb. Mortal. Wkly. Rep.* **1991**, *40*, 585–591.
86. Frieden, T.R.; Sterling, T.; Pablos-Mendez, A.; Kilburn, J.O.; Cauthen, G.M.; Dooley, S.W. The Emergence of Drug-Resistant Tuberculosis in New York City. *N. Engl. J. Med.* **1993**, *328*, 521–526. https://doi.org/10.1056/NEJM199302253280801.
87. Rullán, J.V.; Herrera, D.; Cano, R.; Moreno, V.; Godoy, P.; Peiró, E.F.; Castell, J.; Ibañez, C.; Ortega, A.; Agudo, L.S.; et al. Nosocomial Transmission of Multidrug-Resistant *Mycobacterium Tuberculosis* in Spain. *Emerg. Infect. Dis.* **1996**, *2*, 125–129.
88. Shah, N.S.; Wright, A.; Bai, G.-H.; Barrera, L.; Boulahbal, F.; Martín-Casabona, N.; Drobniewski, F.; Gilpin, C.; Havelková, M.; Lepe, R.; et al. Worldwide Emergence of Extensively Drug-Resistant Tuberculosis. *Emerg. Infect. Dis.* **2007**, *13*, 380–387. https://doi.org/10.3201/eid1303.061400.
89. Migliori, G.B.; Ortmann, J.; Girardi, E.; Besozzi, G.; Lange, C.; Cirillo, D.M.; Ferrarese, M.; De Iaco, G.; Gori, A.; Raviglione, M.C. Extensively Drug-Resistant Tuberculosis, Italy and Germany. *Emerg. Infect. Dis.* **2007**, *13*, 780–782. https://doi.org/10.3201/eid1305.060200.
90. Velayati, A.A.; Masjedi, M.R.; Farnia, P.; Tabarsi, P.; Ghanavi, J.; ZiaZarifi, A.H.; Hoffner, S.E. Emergence of New Forms of Totally Drug-Resistant Tuberculosis Bacilli: Super Extensively Drug-Resistant Tuberculosis or Totally Drug-Resistant Strains in Iran. *Chest* **2009**, *136*, 420–425. https://doi.org/10.1378/chest.08-2427.
91. Shah, N.S.; Richardson, J.; Moodley, P.; Moodley, S.; Babaria, P.; Ramtahal, M.; Heysell, S.K.; Li, X.; Moll, A.P.; Friedland, G.; et al. Increasing Drug Resistance in Extensively Drug-Resistant Tuberculosis, South Africa. *Emerg. Infect. Dis.* **2011**, *17*, 510–513. https://doi.org/10.3201/eid1703.101363.
92. Powers, J.H. Antimicrobial Drug Development—The Past, the Present, and the Future. *Clin. Microbiol. Infect.* **2004**, *10 Suppl 4*, 23–31. https://doi.org/10.1111/j.1465-0691.2004.1007.x.
93. Butler, M.S.; Buss, A.D. Natural Products—the Future Scaffolds for Novel Antibiotics? *Biochem. Pharmacol.* **2006**, *71*, 919–929. https://doi.org/10.1016/j.bcp.2005.10.012.
94. Hair, P.I.; Keam, S.J. Daptomycin: A Review of Its Use in the Management of Complicated Skin and Soft-Tissue Infections and Staphylococcus Aureus Bacteraemia. *Drugs* **2007**, *67*, 1483–1512.
95. Zappia, G.; Menendez, P.; Monache, G.D.; Misiti, D.; Nevola, L.; Botta, B. The Contribution of Oxazolidinone Frame to the Biological Activity of Pharmaceutical Drugs and Natural Products. *Mini Rev. Med. Chem* **2007**, *7*, 389–409.
96. Xie, M.; Liu, D.; Yang, Y. Anti-Cancer Peptides: Classification, Mechanism of Action, Reconstruction and Modification. *Open Biol.* **2020**, *10*, 200004. https://doi.org/10.1098/rsob.200004.
97. Rubattu, S.; Volpe, M. Natriuretic Peptides in the Cardiovascular System: Multifaceted Roles in Physiology, Pathology and Therapeutics. *Int. J. Mol. Sci.* **2019**, *20*, 3991. https://doi.org/10.3390/ijms20163991.
98. Wang, R.; Zhao, H.; Pan, X.; Orfila, C.; Lu, W.; Ma, Y. Preparation of Bioactive Peptides with Antidiabetic, Antihypertensive, and Antioxidant Activities and Identification of A-glucosidase Inhibitory Peptides from Soy Protein. *Food Sci. Nutr.* **2019**, *7*, 1848–1856. https://doi.org/10.1002/fsn3.1038.
99. Gordon, Y.J.; Romanowski, E.G.; McDermott, A.M. A Review of Antimicrobial Peptides and Their Therapeutic Potential as Anti-Infective Drugs. *Curr. Eye Res.* **2005**, *30*, 505–515.
100. Wang, S.; Zeng, X.; Yang, Q.; Qiao, S. Antimicrobial Peptides as Potential Alternatives to Antibiotics in Food Animal Industry. *Int. J. Mol. Sci.* **2016**, *17*, 603. https://doi.org/10.3390/ijms17050603.
101. Nguyen, L.T.; Haney, E.F.; Vogel, H.J. The Expanding Scope of Antimicrobial Peptide Structures and Their Modes of Action. *Trends Biotechnol.* **2011**, *29*, 464–472. https://doi.org/10.1016/j.tibtech.2011.05.001.
102. Ho, Y.-H.; Shah, P.; Chen, Y.-W.; Chen, C.-S. Systematic Analysis of Intracellular-Targeting Antimicrobial Peptides, Bactenecin 7, Hybrid of Pleurocidin and Dermaseptin, Proline–Arginine-Rich Peptide, and Lactoferricin B, by Using Escherichia Coli Proteome Microarrays. *Mol. Cell Proteom.* **2016**, *15*, 1837–1847. https://doi.org/10.1074/mcp.M115.054999.

103. Yount, N.Y.; Yeaman, M.R. Structural Congruence among Membrane-Active Host Defense Polypeptides of Diverse Phylogeny. *Biochim. Biophys. Acta (BBA) Biomembr.* **2006**, *1758*, 1373–1386. https://doi.org/10.1016/j.bbamem.2006.03.027.
104. Gorr, S.-U.; Abdolhosseini, M. Antimicrobial Peptides and Periodontal Disease. *J. Clin. Periodontol.* **2011**, *38* (Suppl. S11), 126–141. https://doi.org/10.1111/j.1600-051X.2010.01664.x.
105. Wu, X.; Wang, Z.; Li, X.; Fan, Y.; He, G.; Wan, Y.; Yu, C.; Tang, J.; Li, M.; Zhang, X.; et al. In Vitro and In Vivo Activities of Antimicrobial Peptides Developed Using an Amino Acid-Based Activity Prediction Method. *Antimicrob. Agents Chemother.* **2014**, *58*, 5342–5349. https://doi.org/10.1128/AAC.02823-14.
106. Forde, É.; Schütte, A.; Reeves, E.; Greene, C.; Humphreys, H.; Mall, M.; Fitzgerald-Hughes, D.; Devocelle, M. Differential In Vitro and In Vivo Toxicities of Antimicrobial Peptide Prodrugs for Potential Use in Cystic Fibrosis. *Antimicrob. Agents Chemother.* **2016**, *60*, 2813–2821. https://doi.org/10.1128/AAC.00157-16.
107. Travis, S.M.; Anderson, N.N.; Forsyth, W.R.; Espiritu, C.; Conway, B.D.; Greenberg, E.P.; McCray, P.B.; Lehrer, R.I.; Welsh, M.J.; Tack, B.F. Bactericidal Activity of Mammalian Cathelicidin-Derived Peptides. *Infect. Immun.* **2000**, *68*, 2748–2755.
108. Hancock, R.E.W.; Falla, T.J. Antimicrobial Peptides: Broad-Spectrum Antibiotics from Nature. *Clin. Microbiol. Infect.* **1996**, *1*, 226–229.
109. Rathinakumar, R.; Walkenhorst, W.F.; Wimley, W.C. Broad-Spectrum Antimicrobial Peptides by Rational Combinatorial Design and High-Throughput Screening: The Importance of Interfacial Activity. *J. Am. Chem. Soc.* **2009**, *131*, 7609–7617. https://doi.org/10.1021/ja8093247.
110. Li, Z.; Hu, Y.; Yang, Y.; Lu, Z.; Wang, Y. Antimicrobial Resistance in Livestock: Antimicrobial Peptides Provide a New Solution for a Growing Challenge. *Anim. Front.* **2018**, *8*, 21–29. https://doi.org/10.1093/af/vfy005.
111. Mahlapuu, M.; Håkansson, J.; Ringstad, L.; Björn, C. Antimicrobial Peptides: An Emerging Category of Therapeutic Agents. *Front. Cell Infect. Microbiol.* **2016**, *6*, 1-2 https://doi.org/10.3389/fcimb.2016.00194.
112. Omardien, S.; Brul, S.; Zaat, S.A.J. Antimicrobial Activity of Cationic Antimicrobial Peptides against Gram-Positives: Current Progress Made in Understanding the Mode of Action and the Response of Bacteria. *Front. Cell Dev. Biol.* **2016**, *4*, 1-16 https://doi.org/10.3389/fcell.2016.00111.
113. Volzing, K.; Borrero, J.; Sadowsky, M.J.; Kaznessis, Y.N. Antimicrobial Peptides Targeting Gram-Negative Pathogens, Produced and Delivered by Lactic Acid Bacteria. *ACS Synth. Biol.* **2013**, *2*, 643–650. https://doi.org/10.1021/sb4000367.
114. Gruenheid, S.; Moual, H. Resistance to Antimicrobial Peptides in Gram-Negative Bacteria. *FEMS Microbiol. Lett.* **2012**, *330*, 81–89. https://doi.org/10.1111/j.1574-6968.2012.02528.x.
115. Bondaryk, M.; Staniszewska, M.; Zielińska, P.; Urbańczyk-Lipkowska, Z. Natural Antimicrobial Peptides as Inspiration for Design of a New Generation Antifungal Compounds. *J. Fungi* **2017**, *3*, 46. https://doi.org/10.3390/jof3030046.
116. Sun, Y.; Shang, D. Inhibitory Effects of Antimicrobial Peptides on Lipopolysaccharide-Induced Inflammation. *Mediat. Inflamm.* **2015**, *2015*, 1-8. https://doi.org/10.1155/2015/167572.
117. Mangoni, M.L.; McDermott, A.M.; Zasloff, M. Antimicrobial Peptides and Wound Healing: Biological and Therapeutic Considerations. *Exp. Dermatol.* **2016**, *25*, 167–173. https://doi.org/10.1111/exd.12929.
118. Yu, G.; Baeder, D.Y.; Regoes, R.R.; Rolff, J. Combination Effects of Antimicrobial Peptides. *Antimicrob. Agents Chemother.* **2016**, *60*, 1717–1724. https://doi.org/10.1128/AAC.02434-15.
119. Dubos, R.J. Studies on a bactericidal agent extracted from a soil bacillus. *J. Exp. Med.* **1939**, *70*, 1–10.
120. Nakatsuji, T.; Gallo R.L. Antimicrobial Peptides: Old Molecules with New Ideas. *J. Invest Dermatol*. **2012**, *132*, 887-895. doi:10.1038/jid.2011.387.
121. Zasloff, M. Magainins, a Class of Antimicrobial Peptides from Xenopus Skin: Isolation, Characterization of Two Active Forms, and Partial CDNA Sequence of a Precursor. *Proc. Natl. Acad. Sci. USA* **1987**, *84*, 5449–5453.
122. Balls, A.K.; Hale, W.S.; Harris, T.H. A Crystalline Protein Obtained from a Lipoprotein of Wheat Flour. *Cereal Chem.* **1942**, *19*, 279–288.
123. Coll, P.; Garrigó, M.; Moreno, C.; Martí, N. Routine Use of Gen-Probe Amplified *Mycobacterium Tuberculosis* Direct (MTD) Test for Detection of *Mycobacterium Tuberculosis* with Smear-Positive and Smear-Negative Specimens. *Int. J. Tuberc. Lung Dis.* **2003**, *7*, 886–891.
124. De Caleya, R.F.; Gonzalez-Pascual, B.; García-Olmedo, F.; Carbonero, P. Susceptibility of Phytopathogenic Bacteria to Wheat Purothionins in Vitro. *Appl. Microbiol.* **1972**, *23*. https://doi.org/10.1128/am.23.5.998-1000.1972.
125. Wilson, D.N.; Guichard, G.; Innis, C.A. Antimicrobial Peptides Target Ribosomes. *Oncotarget* **2015**, *6*, 16826–16827.
126. Bechinger, B.; Gorr, S.-U. Antimicrobial Peptides. *J. Dent. Res.* **2017**, *96*, 254–260. https://doi.org/10.1177/0022034516679973.

127. Fadaka, A.O.; Sibuyi, N.R.S.; Madiehe, A.M.; Meyer, M. Nanotechnology-Based Delivery Systems for Antimicrobial Peptides. *Pharmaceutics* **2021**, *13*, 1795. https://doi.org/10.3390/pharmaceutics13111795.
128. Raheem, N.; Straus, S.K. Mechanisms of Action for Antimicrobial Peptides with Antibacterial and Antibiofilm Functions. *Front. Microbiol.* **2019**, *10*, 1-14.
129. Malanovic, N.; Lohner, K. Gram-Positive Bacterial Cell Envelopes: The Impact on the Activity of Antimicrobial Peptides. *Biochim. Biophys. Acta (BBA) Biomembr.* **2016**, *1858*, 936–946. https://doi.org/10.1016/j.bbamem.2015.11.004.
130. Zhang, Q.-Y.; Yan, Z.-B.; Meng, Y.-M.; Hong, X.-Y.; Shao, G.; Ma, J.-J.; Cheng, X.-R.; Liu, J.; Kang, J.; Fu, C.-Y. Antimicrobial Peptides: Mechanism of Action, Activity and Clinical Potential. *Mil. Med. Res.* **2021**, *8*, 48. https://doi.org/10.1186/s40779-021-00343-2.
131. Benfield, A.H.; Henriques, S.T. Mode-of-Action of Antimicrobial Peptides: Membrane Disruption vs. Intracellular Mechanisms. *Front. Med. Technol.* **2020**, *2*, 1-10.
132. Hsu, C.-H. Structural and DNA-Binding Studies on the Bovine Antimicrobial Peptide, Indolicidin: Evidence for Multiple Conformations Involved in Binding to Membranes and DNA. *Nucleic Acids Res.* **2005**, *33*, 4053–4064. https://doi.org/10.1093/nar/gki725.
133. Subbalakshmi, C.; Sitaram, N. Mechanism of Antimicrobial Action of Indolicidin. *FEMS Microbiol. Lett.* **1998**, *160*, 91–96. https://doi.org/10.1111/j.1574-6968.1998.tb12896.x.
134. Park, C.B.; Kim, H.S.; Kim, S.C. Mechanism of Action of the Antimicrobial Peptide Buforin II: Buforin II Kills Microorganisms by Penetrating the Cell Membrane and Inhibiting Cellular Functions. *Biochem. Biophys. Res. Commun.* **1998**, *244*, 253–257. https://doi.org/10.1006/bbrc.1998.8159.
135. Linde, C.M.A.; Hoffner, S.E.; Refai, E.; Andersson, M. In Vitro Activity of PR-39, a Proline-Arginine-Rich Peptide, against Susceptible and Multi-Drug-Resistant *Mycobacterium Tuberculosis*. *J. Antimicrob. Chemother.* **2001**, *47*, 575–580. https://doi.org/10.1093/jac/47.5.575.
136. Boman, H.G.; Agerberth, B.; Boman, A. Mechanisms of Action on Escherichia Coli of Cecropin P1 and PR-39, Two Antibacterial Peptides from Pig Intestine. *Infect. Immun.* **1993**, *61*, 2978–2984.
137. Culp, E.; Wright, G.D. Bacterial Proteases, Untapped Antimicrobial Drug Targets. *J. Antibiot.* **2017**, *70*, 366–377. https://doi.org/10.1038/ja.2016.138.
138. Yu, A.Y.H.; Houry, W.A. ClpP: A Distinctive Family of Cylindrical Energy-dependent Serine Proteases. *FEBS Lett.* **2007**, *581*, 3749–3757. https://doi.org/10.1016/j.febslet.2007.04.076.
139. Brötz-Oesterhelt, H.; Sass, P. Bacterial Caseinolytic Proteases as Novel Targets for Antibacterial Treatment. *Int. J. Med. Microbiol.* **2014**, *304*, 23–30. https://doi.org/10.1016/j.ijmm.2013.09.001.
140. Elsholz, A.K.W.; Birk, M.S.; Charpentier, E.; Turgay, K. Functional Diversity of AAA+ Protease Complexes in *Bacillus Subtilis*. *Front. Mol. Biosci.* **2017**, *4*, 44. https://doi.org/10.3389/fmolb.2017.00044.
141. Malik, I.T.; Brötz-Oesterhelt, H. Conformational Control of the Bacterial Clp Protease by Natural Product Antibiotics. *Nat. Prod. Rep.* **2017**, *34*, 815–831. https://doi.org/10.1039/C6NP00125D.
142. Frees, D.; Gerth, U.; Ingmer, H. Clp Chaperones and Proteases Are Central in Stress Survival, Virulence and Antibiotic Resistance of Staphylococcus Aureus. *Int. J. Med. Microbiol.* **2014**, *304*, 142–149. https://doi.org/10.1016/j.ijmm.2013.11.009.
143. Frees, D.; Savijoki, K.; Varmanen, P.; Ingmer, H. Clp ATPases and ClpP Proteolytic Complexes Regulate Vital Biological Processes in Low GC, Gram-positive Bacteria. *Mol. Microbiol.* **2007**, *63*, 1285–1295. https://doi.org/10.1111/j.1365-2958.2007.05598.x.
144. Dohmen, R.J.; Wu, P.; Varshavsky, A. Heat-Inducible Degron: A Method for Constructing Temperature-Sensitive Mutants. *Science* **1994**, *263*, 1273–1276. https://doi.org/10.1126/science.8122109.
145. Montandon, C.; Friso, G.; Liao, J.-Y.R.; Choi, J.; van Wijk, K.J. In Vivo Trapping of Proteins Interacting with the Chloroplast CLPC1 Chaperone: Potential Substrates and Adaptors. *J. Proteome Res.* **2019**, *18*, 2585–2600. https://doi.org/10.1021/acs.jproteome.9b00112.
146. Lee, B.-G.; Kim, M.K.; Song, H.K. Structural Insights into the Conformational Diversity of ClpP from *Bacillus Subtilis*. *Mol. Cells* **2011**, *32*, 589–595. https://doi.org/10.1007/s10059-011-0197-1.
147. Bouchnak, I.; Wijk, K.J. van Structure, Function, and Substrates of Clp AAA+ Protease Systems in Cyanobacteria, Plastids, and Apicoplasts: A Comparative Analysis. *J. Biol. Chem.* **2021**, *296*. https://doi.org/10.1016/j.jbc.2021.100338.
148. Wolf, N.M.; Lee, H.; Zagal, D.; Nam, J.; Oh, D.; Lee, H.; Suh, J.; Pauli, G.F.; Cho, S.; Abad-Zapatero, C. Structure of the N-terminal Domain of ClpC1 in Complex with the Antituberculosis Natural Product Ecumicin Reveals Unique Binding Interactions. *Acta. Cryst.* **2020**, *76*, 458-471. https://doi.org/10.1107/s2059798320004027.
149. Wang, F.; Mei, Z.; Qi, Y.; Yan, C.; Hu, Q.; Wang, J.; Shi, Y. Structure and Mechanism of the Hexameric MecA–ClpC Molecular Machine. *Nature* **2011**, *471*, 7338.

150. Gao, W.; Kim, J.-Y.; Anderson, J.R.; Akopian, T.; Hong, S.; Jin, Y.-Y.; Kandror, O.; Kim, J.-W.; Lee, I.-A.; Lee, S.-Y.; et al. The Cyclic Peptide Ecumicin Targeting ClpC1 Is Active against *Mycobacterium Tuberculosis* In Vivo. *Antimicrob. Agents Chemother.* **2015**, *59*, 880–889. https://doi.org/10.1128/AAC.04054-14.
151. Gavrish, E.; Sit, C.S.; Cao, S.; Kandror, O.; Spoering, A.; Peoples, A.; Ling, L.; Fetterman, A.; Hughes, D.; Bissell, A.; et al. Lassomycin, a Ribosomally Synthesized Cyclic Peptide, Kills *Mycobacterium Tuberculosis* by Targeting the ATP-Dependent Protease ClpC1P1P2. *Chem. Biol.* **2014**, *21*, 509–518. https://doi.org/10.1016/j.chembiol.2014.01.014.
152. Akopian, T.; Kandror, O.; Raju, R.M.; UnniKrishnan, M.; Rubin, E.J.; Goldberg, A.L. The Active ClpP Protease from M. Tuberculosis Is a Complex Composed of a Heptameric ClpP1 and a ClpP2 Ring. *EMBO J.* **2012**, *31*, 1529–1541. https://doi.org/10.1038/emboj.2012.5.
153. Vasudevan, D.; Rao, S.P.S.; Noble, C.G. Structural Basis of Mycobacterial Inhibition by Cyclomarin A. *J. Biol. Chem.* **2013**, *288*, 30883–30891. https://doi.org/10.1074/jbc.M113.493767.
154. Trott, O.; Olson, A.J. AutoDock Vina: Improving the Speed and Accuracy of Docking with a New Scoring Function, Efficient Optimization and Multithreading. *J. Comput. Chem* **2010**, *31*, 455–461. https://doi.org/10.1002/jcc.21334.
155. Jung, I.P.; Ha, N.R.; Kim, A.R.; Kim, S.H.; Yoon, M.Y. Mutation Analysis of the Interactions between *Mycobacterium Tuberculosis* Caseinolytic Protease C1 (ClpC1) and Ecumicin. *Int. J. Biol. Macromol.* **2017**, *101*, 348–357. https://doi.org/10.1016/j.ijbiomac.2017.03.126.
156. Böttcher Thomas; Sieber Stephan, A. B-Lactones as Privileged Structures for the Active-Site Labeling of Versatile Bacterial Enzyme Classes. *Angew. Chem. Int. Ed.* **2008**, *47*, 4600–4603. https://doi.org/10.1002/anie.200705768.
157. Michel, K.H.; Kastner, R.E. A54556 Antibiotics and Process for Production Thereof. Antibiotic A54556, a Complex of 8 Individual Factors, Produced by Submerged, Aerobic Fermentation of New *Streptomyces hawaiiensis* NRRL 15010. The Complex and the Individual, Separated Factors are Active against *Staphylococcus* and *Streptococcus* which are Penicillin Resistant. U.S. Patent US-4492650-A, 8 January 1985.
158. Brötz-Oesterhelt, H.; Vorbach, A. Reprogramming of the Caseinolytic Protease by ADEP Antibiotics: Molecular Mechanism, Cellular Consequences, Therapeutic Potential. *Front. Mol. Biosci.* **2021**, *8*, 1-19.
159. Lee, B.-G.; Park, E.Y.; Lee, K.-E.; Jeon, H.; Sung, K.H.; Paulsen, H.; Rübsamen-Schaeff, H.; Brötz-Oesterhelt, H.; Song, H.K. Structures of ClpP in Complex with Acyldepsipeptide Antibiotics Reveal Its Activation Mechanism. *Nat. Struct. Mol. Biol.* **2010**, *17*, 471–478. https://doi.org/10.1038/nsmb.1787.
160. Li, D.H.S.; Chung, Y.S.; Gloyd, M.; Joseph, E.; Ghirlando, R.; Wright, G.D.; Cheng, Y.-Q.; Maurizi, M.R.; Guarné, A.; Ortega, J. Acyldepsipeptide Antibiotics Induce the Formation of a Structured Axial Channel in ClpP: A Model for the ClpX/ClpA-Bound State of ClpP. *Chem. Biol.* **2010**, *17*, 959–969. https://doi.org/10.1016/j.chembiol.2010.07.008.
161. Kim, Y.-I.; Levchenko, I.; Fraczkowska, K.; Fraczkowska, R.V.; Sauer, R.T.; Baker, T.A. Molecular Determinants of Complex Formation between Clp/Hsp100 ATPases and the ClpP Peptidase. *Nat. Struct. Biol.* **2001**, *8*, 230–233.
162. Sowole, M.A.; Alexopoulos, J.A.; Cheng, Y.-Q.; Ortega, J.; Konermann, L. Activation of ClpP Protease by ADEP Antibiotics: Insights from Hydrogen Exchange Mass Spectrometry. *J. Mol. Biol.* **2013**, *425*, 4508–4519. https://doi.org/10.1016/j.jmb.2013.08.005.
163. Gersch, M.; List, A.; Groll, M.; Sieber, S.A. Insights into Structural Network Responsible for Oligomerization and Activity of Bacterial Virulence Regulator Caseinolytic Protease P (ClpP) Protein. *J. Biol. Chem.* **2012**, *287*, 9484–9494. https://doi.org/10.1074/jbc.M111.336222.
164. Li, M.; Kandror, O.; Akopian, T.; Dharkar, P.; Wlodawer, A.; Maurizi, M.R.; Goldberg, A.L. Structure and Functional Properties of the Active Form of the Proteolytic Complex, ClpP1P2, from *Mycobacterium Tuberculosis*. *J. Biol. Chem.* **2016**, *291*, 7465–7476. https://doi.org/10.1074/jbc.M115.700344.
165. Goodreid, J.D.; Wong, K.; Leung, E.; McCaw, S.E.; Gray-Owen, S.D.; Lough, A.; Houry, W.A.; Batey, R.A. Total Synthesis and Antibacterial Testing of the A54556 Cyclic Acyldepsipeptides Isolated from *Streptomyces Hawaiiensis*. *J. Nat. Prod.* **2014**, *77*, 2170–2181. https://doi.org/10.1021/np500158q.
166. Hinzen, B.; Raddatz, S.; Paulsen, H.; Lampe, T.; Schumacher, A.; Häbich, D.; Hellwig, V.; Benet-Buchholz, J.; Endermann, R.; Labischinski, H.; et al. Medicinal Chemistry Optimization of Acyldepsipeptides of the Enopeptin Class Antibiotics. *Chem. Med. Chem.* **2006**, *1*, 689–693. https://doi.org/10.1002/cmdc.200600055.
167. Conlon, B.P.; Nakayasu, E.S.; Fleck, L.E.; LaFleur, M.D.; Isabella, V.M.; Coleman, K.; Leonard, S.N.; Smith, R.D.; Adkins, J.N.; Lewis, K. Activated ClpP Kills Persisters and Eradicates a Chronic Biofilm Infection. *Nature* **2013**, *503*, 365–370. https://doi.org/10.1038/nature12790.
168. Griffith, E.C.; Zhao, Y.; Singh, A.P.; Conlon, B.P.; Tangallapally, R.; Shadrick, W.R.; Liu, J.; Wallace, M.J.; Yang, L.; Elmore, J.M.; et al. Ureadepsipeptides as ClpP Activators. *ACS Infect. Dis.* **2019**, *5*, 1915–1925. https://doi.org/10.1021/acsinfecdis.9b00245.

169. Carney, D.W.; Schmitz, K.R.; Truong, J.V.; Sauer, R.T.; Sello, J.K. Restriction of the Conformational Dynamics of the Cyclic Acyldepsipeptide Antibiotics Improves Their Antibacterial Activity. *J. Am. Chem. Soc.* **2014**, *136*, 1922–1929. https://doi.org/10.1021/ja410385c.
170. Carney, D.W.; Compton, C.L.; Schmitz, K.R.; Stevens, J.P.; Sauer, R.T.; Sello, J.K. A Simple Fragment of the Cyclic Acyldepsipeptides Is Necessary and Sufficient for ClpP Activation and Antibacterial Activity. *ChemBioChem* **2014**, *15*, 2216–2220. https://doi.org/10.1002/cbic.201402358.
171. Raju, R.M.; Unnikrishnan, M.; Rubin, D.H.F.; Krishnamoorthy, V.; Kandror, O.; Akopian, T.N.; Goldberg, A.L.; Rubin, E.J. *Mycobacterium Tuberculosis* ClpP1 and ClpP2 Function Together in Protein Degradation and Are Required for Viability in Vitro and During Infection. *PLoS Pathog.* **2012**, *8*, e1002511. https://doi.org/10.1371/journal.ppat.1002511.
172. Schmitz, K.R.; Sauer, R.T. Substrate Delivery by the AAA+ ClpX and ClpC1 Unfoldases Activates the Mycobacterial ClpP1P2 Peptidase. *Mol. Microbiol.* **2014**, *93*, 617–628. https://doi.org/10.1111/mmi.12694.
173. Alhuwaider, A.A.H.; Dougan, D.A. AAA+ Machines of Protein Destruction in Mycobacteria. *Front. Mol. Biosci.* **2017**, *4*, 1-14.
174. Personne, Y.; Brown, A.C.; Schuessler, D.L.; Parish, T. *Mycobacterium Tuberculosis* ClpP Proteases Are Co-Transcribed but Exhibit Different Substrate Specificities. *PLoS ONE* **2013**, *8*, e60228. https://doi.org/10.1371/journal.pone.0060228.
175. Schmitz, K.R.; Carney, D.W.; Sello, J.K.; Sauer, R.T. Crystal Structure of *Mycobacterium Tuberculosis* ClpP1P2 Suggests a Model for Peptidase Activation by AAA+ Partner Binding and Substrate Delivery. *Proc. Natl. Acad. Sci. USA* **2014**, *111*. https://doi.org/10.1073/pnas.1417120111.
176. Famulla, K.; Sass, P.; Malik, I.; Akopian, T.; Kandror, O.; Alber, M.; Hinzen, B.; Ruebsamen-Schaeff, H.; Kalscheuer, R.; Goldberg, A.L.; et al. Acyldepsipeptide Antibiotics Kill Mycobacteria by Preventing the Physiological Functions of the ClpP1P2 Protease: ADEPs Target ClpP1P2 of *M. Tuberculosis*. *Mol. Microbiol.* **2016**, *101*, 194–209. https://doi.org/10.1111/mmi.13362.
177. Joshi, S.A.; Hersch, G.L.; Baker, T.A.; Sauer, R.T. Communication between ClpX and ClpP during Substrate Processing and Degradation. *Nat. Struct. Mol. Biol* **2004**, *11*, 404–411. https://doi.org/10.1038/nsmb752.
178. Leodolter, J.; Warweg, J.; Weber-Ban, E. The *Mycobacterium Tuberculosis* ClpP1P2 Protease Interacts Asymmetrically with Its ATPase Partners ClpX and ClpC1. *PLoS ONE* **2015**, *10*, e0125345. https://doi.org/10.1371/journal.pone.0125345.
179. Ollinger, J.; O'Malley, T.; Kesicki, E.A.; Odingo, J.; Parish, T. Validation of the Essential ClpP Protease in *Mycobacterium Tuberculosis* as a Novel Drug Target. *J. Bacteriol.* **2012**, *194*, 663–668. https://doi.org/10.1128/JB.06142-11.
180. Lewis, A.L.; Richard, J. Challenges in the Delivery of Peptide Drugs: An Industry Perspective. *Ther. Deliv.* **2015**, *6*, 149–163. https://doi.org/10.4155/tde.14.111.
181. Brunetti, J.; Falciani, C.; Roscia, G.; Pollini, S.; Bindi, S.; Scali, S.; Arrieta, U.C.; Gómez-Vallejo, V.; Quercini, L.; Ibba, E.; et al. In Vitro and in Vivo Efficacy, Toxicity, Bio-Distribution and Resistance Selection of a Novel Antibacterial Drug Candidate. *Sci. Rep.* **2016**, *6*, 26077. https://doi.org/10.1038/srep26077.
182. Huggins, D.J.; Sherman, W.; Tidor, B. Rational Approaches to Improving Selectivity in Drug Design. *J. Med. Chem.* **2012**, *55*, 1424–1444. https://doi.org/10.1021/jm2010332.
183. Joo, S.H. Cyclic Peptides as Therapeutic Agents and Biochemical Tools. *Biomol. Ther.***2012**, *20*, 19–26. https://doi.org/10.4062/biomolther.2012.20.1.019.
184. Su, Y.; Doherty, T.; Waring, A.J.; Ruchala, P.; Hong, M. Roles of Arginine and Lysine Residues in the Translocation of a Cell-Penetrating Peptide from 13C, 31P and 19F Solid-State NMR. *Biochemistry* **2009**, *48*, 4587–4595. https://doi.org/10.1021/bi900080d.
185. Chatterjee, J.; Gilon, C.; Hoffman, A.; Kessler, H. N-Methylation of Peptides: A New Perspective in Medicinal Chemistry. *Acc. Chem. Res.* **2008**, *41*, 1331–1342. https://doi.org/10.1021/ar8000603.
186. Buccini, D.F.; Cardoso, M.H.; Franco, O.L. Antimicrobial Peptides and Cell-Penetrating Peptides for Treating Intracellular Bacterial Infections. *Front. Cell Infect. Microbiol.* **2020**, *10*, 612931. https://doi.org/10.3389/fcimb.2020.612931.
187. Lee, H.; Lim, S.I.; Shin, S.-H.; Lim, Y.; Koh, J.W.; Yang, S. Conjugation of Cell-Penetrating Peptides to Antimicrobial Peptides Enhances Antibacterial Activity. *ACS Omega* **2019**, *4*, 15694–15701. https://doi.org/10.1021/acsomega.9b02278.
188. Vale, N.; Ferreira, A.; Matos, J.; Fresco, P.; Gouveia, M.J. Amino Acids in the Development of Prodrugs. *Molecules* **2018**, *23*, 2318. https://doi.org/10.3390/molecules23092318.
189. Renukuntla, J.; Vadlapudi, A.D.; Patel, A.; Boddu, S.HS.; Mitra, A.K. Approaches for Enhancing Oral Bioavailability of Peptides and Proteins. *Int. J. Pharm.* **2013**, *447*, 75–93. https://doi.org/10.1016/j.ijpharm.2013.02.030.

190. Chatterjee, J.; Rechenmacher, F.; Kessler, H. N-Methylation of Peptides and Proteins: An Important Element for Modulating Biological Functions. *Angew. Chem. Int. Ed. Engl.* **2013**, *52*, 254–269. https://doi.org/10.1002/anie.201205674.
191. Doedens, L.; Opperer, F.; Cai, M.; Beck, J.G.; Dedek, M.; Palmer, E.; Hruby, V.J.; Kessler, H. Multiple N-Methylation of MT-II Backbone Amide Bonds Leads to Melanocortin Receptor Subtype HMC1R Selectivity: Pharmacological and Conformational Studies. *J. Am. Chem. Soc.* **2010**, *132*, 8115–8128. https://doi.org/10.1021/ja101428m.
192. Neil, E.; Marsh, G. Towards the Nonstick Egg: Designing Fluorous Proteins. *Chem. Biol.* **2000**, *7*, R153–R157.
193. Čižinauskas, V.; Elie, N.; Brunelle, A.; Briedis, V. Fatty Acids Penetration into Human Skin Ex Vivo: A TOF-SIMS Analysis Approach. *Biointerphases* **2017**, *12*, 011003. https://doi.org/10.1116/1.4977941.
194. Irby, D.; Du, C.; Li, F. Lipid–Drug Conjugate for Enhancing Drug Delivery. *Mol. Pharm.* **2017**, *14*, 1325–1338. https://doi.org/10.1021/acs.molpharmaceut.6b01027.
195. De Jong, W.H.; Borm, P.J. Drug Delivery and Nanoparticles: Applications and Hazards. *Int. J. Nanomed.* **2008**, *3*, 133–149.
196. Guisbiers, G.; Mejía-Rosales, S.; Leonard Deepak, F. Nanomaterial Properties: Size and Shape Dependencies. Available online: https://www.hindawi.com/journals/jnm/2012/180976/ (accessed on 31 August 2018).
197. Mandal, A. Copper Nanomaterials as Drug Delivery System against Infectious Agents and Cancerous Cells. *J. Appl. Life Sci. Int.* **2017**, *15*, 1–8. https://doi.org/10.9734/JALSI/2017/38444.
198. Kawabata, Y.; Wada, K.; Nakatani, M.; Yamada, S.; Onoue, S. Formulation Design for Poorly Water-Soluble Drugs Based on Biopharmaceutics Classification System: Basic Approaches and Practical Applications. *Int. J. Pharm* **2011**, *420*, 1–10. https://doi.org/10.1016/j.ijpharm.2011.08.032.
199. Kou, L.; Bhutia, Y.D.; Yao, Q.; He, Z.; Sun, J.; Ganapathy, V. Transporter-Guided Delivery of Nanoparticles to Improve Drug Permeation across Cellular Barriers and Drug Exposure to Selective Cell Types. *Front. Pharm.* **2018**, *9*. https://doi.org/10.3389/fphar.2018.00027.
200. Martínez-Carmona, M.; Lozano, D.; Colilla, M.; Vallet-Regí, M. Selective Topotecan Delivery to Cancer Cells by Targeted PH-Sensitive Mesoporous Silica Nanoparticles. *RSC Adv.* **2016**, *6*, 50923–50932. https://doi.org/10.1039/C6RA07763C.
201. Ren, G.; Hu, D.; Cheng, E.W.C.; Vargas-Reus, M.A.; Reip, P.; Allaker, R.P. Characterisation of Copper Oxide Nanoparticles for Antimicrobial Applications. *Int. J. Antimicrob. Agents* **2009**, *33*, 587–590. https://doi.org/10.1016/j.ijantimicag.2008.12.004.
202. Pan, X.; Redding, J.E.; Wiley, P.A.; Wen, L.; McConnell, J.S.; Zhang, B. Mutagenicity Evaluation of Metal Oxide Nanoparticles by the Bacterial Reverse Mutation Assay. *Chemosphere* **2010**, *79*, 113–116. https://doi.org/10.1016/j.chemosphere.2009.12.056.
203. Quan, Q.; Xie, J.; Gao, H.; Yang, M.; Zhang, F.; Liu, G.; Lin, X.; Wang, A.; Eden, H.S.; Lee, S.; et al. HSA Coated Iron Oxide Nanoparticles as Drug Delivery Vehicles for Cancer Therapy. *Mol. Pharm.* **2011**, *8*, 1669–1676. https://doi.org/10.1021/mp200006f.
204. Jafari, A.R.; Mosavi, T.; Mosavari, N.; Majid, A.; Movahedzade, F.; Tebyaniyan, M.; Kamalzadeh, M.; Dehgan, M.; Jafari, S.; Arastoo, S. Mixed Metal Oxide Nanoparticles Inhibit Growth of *Mycobacterium Tuberculosis* into THP-1 Cells. *Int. J. Mycobacteriol.* **2016**, *5*, S181–S183. https://doi.org/10.1016/j.ijmyco.2016.09.011.

CHAPTER 3.

DESIGN OF ADEP1 PEPTIDE ANALOGUES

3.1. ADEP1 analogues

Modification and modulation of conformational dynamics of existing peptides and designing similar systems that mimic the potential therapeutic peptides is the first step towards improving the pharmacokinetic properties of drug-like compounds. The peptidomimetics and analogues reported in this study were derivatised from the structure of ADEP1 (ADEP A54556A). Figure 3.1 shows the parent structure of the ADEP1 with Pro1, Ala2, methyl-Ala3, Prol4, Ser5, Phe6, and octa-2,4,6-trienoic acid7. The main aim was to design pharmacologically active, low-cost analogues with improved membrane permeability and reduced toxicity. Several techniques were employed to improve the pharmacokinetic properties of the ADEP1, including substituting L-amino acids with D–amino acids, N-methylated amino acids, peptoids moieties and also replacing the fatty acid region with saturated and caged structured lipophilic molecules.

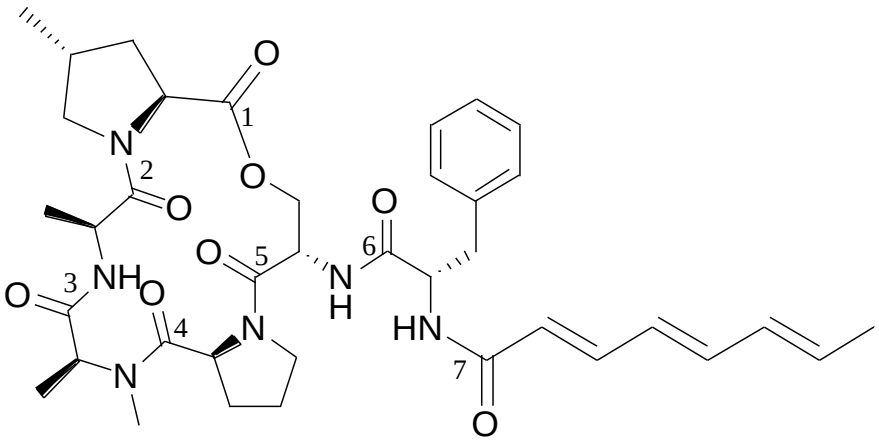


Figure 3. 1: Parent structure of ADEP1.

3.1.1. *Lipophilic molecules.*

ADEPs need to penetrate the membrane as their target protein, is intracellular. Therefore, it is neccessary to find ways to increase the membrane permeability of ADEP1. Lipophilic molecules that are conjugated to active drug compounds have been observed to enhance the transport of the drug across cell membranes.

The parent structure of ADEP1 contains an unsaturated fatty acid chain (octa-2,4,6-trienoic acid) which has been reported to possess antioxidant and anti-inflammatory properties; however, its cytotoxicity levels are high [1]. The incorporation of fatty acids such as linoleic, oleic, and Pal into the structure of pharmaceutically active moieties has been used to enhance membrane permeability [2]. Other advantages of conjugating lipids to drugs include improved oral bioavailability and decreased toxicity of the drug molecule [3]. Ada, a polycyclic cage molecule extracted from crude oil, is widely used in the design and synthesis of drug delivery systems and surface recognition studies for biomedical applications [4]. Ada is incorporated into the phospholipid structures of the lipid bilayer in the membranes, which is important for drug transfer. Ada has also been reported to enhance biological activity when conjugated with drug molecules [5].

3.1.2. *Cyclisation*

Several novel cyclic peptides, such as gramicidin and cyclosporine, use the amide bond (N-to-C or head-to-tail) as a cyclisation bridge. This strategy is the most commonly used in peptide chemistry [6]. ADEP A54556A cyclisation is due to an ester bond formed between the alcohol group (-OH) of the fifth amino acid (serine) and the carboxylic group (-COOH) of the first amino acid (proline). Cyclisation can also be achieved through chemically stable bonds such as ether, disulphide, lactone etc.

3.2. **Design of ester bond cyclised ADEP1 analogues**

The 4-methyl proline was omitted in this study, as the price is five times more than that of a natural amino acid. Therefore, the initial design of the analogues did not include the 4-methyl proline while keeping the N-methylated alanine (SC001 and SC002) (Figure 3.2). In SC003 and SC004 peptides, the N-methylated alanine found in SC001 and SC002 was replaced with an alanine peptoid known as sarcosine or N-methylated glycine. The Fmoc-N-methylated glycine and Fmoc-sarcosine were synthesised using the methods described in Chapter 4. Octa-2,4,6-trienoic acid was also replaced with Pal (SC002 and SC004) or Ada (SC001 and SC003). Not only is octa-2,4,6-trienoic acid toxic, but it is also expensive and insoluble, especially in solvents used in peptide synthesis. All these modifications (SC001-SC004) were considered while maintaining the ester bond cyclisation.

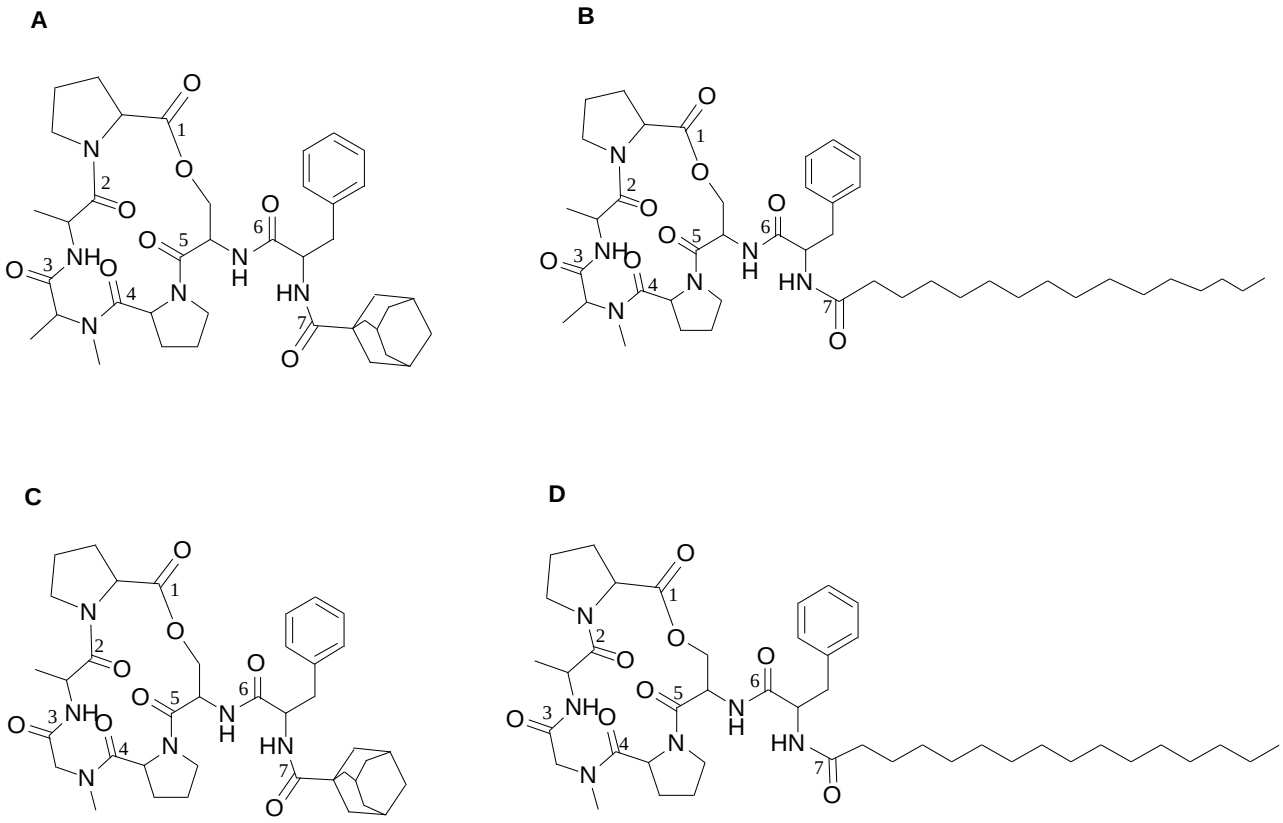


Figure 3. 2: ADEP1 ester cyclised analogues. A-SC001; B-SC002; C-SC003, D-SC004.Srtucture stereochemistry details in Table 3.1.

3.2.1. *Design and limitations encountered during the synthesis of ADEP1 analogues*

The analogues were synthesised via solid-phase peptide synthesis (SPPS). This method uses a resin as a solid support and Fmoc-protected amino acids. In this study, we chose a 2-chlorotrityl chloride resin as it yields a carboxylic group on the peptide C-terminal. The carboxylic group is necessary for the formation of an ester bond with the Ser hydroxyl group. The proline was the first amino acid to be incorporated into the 2-chlorotrityl chloride resin. The first amino acid concentration for coupling depends on the resin's loading capacity. It was assumed that the resin loads 1mmol/g of the amino acid. However, 1 equivalence of amino acid resulted in low coupling yields. The loading capacity was determined using a procedure outline in the Chapter 4. An equivalence of 2-4 of the amino acids showed better loading capacity. In this synthesis, 4 equivalence was used for maximum loading capacity. Both amino acid (4 equiv) and the activated resin (150 mg) were added into a solution of DIPEA (1 mL) prepared in 10mL dry DCM and left to shake for 2 hours. Upon filtration and washing the loading capacity was found to be 0.82 mmol/g.

During the first ADEP1 analogues synthesis attempt, 1M DIPEA, 0.2M of HBTU, and 0.2M Fmoc-amino acids were utilised as coupling reagents. All amino acids were single-coupled except for the second Ala, Phe, and Pal or ada, which were double-coupled (1 hour x 2 coupling reaction time). The information regarding which amino acids were to be double coupled was obtained from peptide synthesiser prediction software. Fmoc was removed using 20% piperidine for 30 minutes. Finally, the deprotection of the side chain protecting groups and cleavage from the resin was done using a TFA cleavage cocktail mixture of 95% TFA: 2.5% H_2O: 2.5% TIS. These peptides did not precipitate upon addition of cold diethyl ether and therefore, TFA was removed by azeotropic distillation with toluene (1:1 ratio) on a rotary evaporator set at 60-65℃. The mass spectrometry showed a mass peak (M+H), correlating to the expected linear molar mass. However, the spectrum also had peaks from masses of numerous short peptides missing some amino acids, especially Phe.

The addition of 0.4M HOBt to the same coupling method above was considered. The HOBt was added to minimise racemisation and incomplete couplings observed from the first synthesis attempt as it prevents racemisation, promotes complete amino acid coupling, and acts as a nucleophilic catalyst, which helps accelerate the rate of the coupling reaction time [7].

Optimum synthesis was obtained by decreasing the concentrations of the coupling reagents to 0.4M DIPEA, 0.19M HBTU, and 0.095M of HOBt while keeping the Fmoc-amino acids at 0.2M. The coupling reaction time was reduced from 1 hour to 45 minutes. The HOBt was used at half the equivalence of the coupling reagent. Furthermore, each amino acid was double coupled with Pal or ada triple coupled. The deprotection with 20% piperidine was also reduced to 5 minutes twice. With these conditions, there were fewer impurities and incomplete peptide sequences.

3.2.2. *Esterification techniques for cyclisation of ester ADEP1 analogues*

Unfortunately only the linear SC001 ADEP1 analogue was successfully synthesised using the developed method (Figure A.1) the other derivatives SC002-4 were obtained in very low yield with many impurities (Table 3.1). During the cyclisation of SC001 through the ester bond bridge difficulties were experience, this bottleneck has already been highlighted in previous studies [8], [9]. In cases of successful ester bond cyclisation, the yield is reported to be around 6% [10]. In this study, the cyclised peptide yield could not be determined as both the linear and cyclised peptides co eluted at the same time. As such, in the future the use of fragment

convergence synthesis will be considered since it has been reported to yield better results. The fragment convergence synthesis approach disassembles the ADEPs into three fragments, the tripeptide, linkage, and Phe-heptenamide, as described by Li *et al*., 2017 [11]. The natural ADEPs' synthesis in biological systems easily forms the ester bond linkage through bacterial depsipeptide synthases [12]. Several acylation techniques, such as the use of coupling reagents like EDC, DIC, and CDI and acids such as H_2SO_4 and TFA, were employed in this study. However, none of these approaches successfully promoted the ester bond linkage between the carboxylic end of Pro and the Ser hydroxyl side chain.

Table 3. 1: ADEP1 analogues with linear and cyclised calculated molecular mass (MM).

Code	**Peptide sequence**	**Linear MM & MF**	**Cyclised MM & MF**	**Linear found $[M+H]^+$**
SC001	$_{L-}$(PAmAPSF)-Ada	764.41 $C_{40}H_{56}N_6O_9$	746.40 $C_{40}H_{54}N_6O_8$	765.4169
SC002	$_{L-}$(PAmAPSF)-Pal	840.54 $C_{45}H_{72}N_6O_9$	822.53 $C_{45}H_{70}N_6O_8$	- NP
SC003	$_{L-}$(PApAPSF)-Ada	750.40 $C_{39}H_{54}N_6O_9$	732.38 $C_{39}H_{52}N_6O_8$	- NP
SC004	$_{L-}$(PApAPSF)-Pal	826.52 $C_{44}H_{70}N_6O_9$	808.51 $C_{44}H_{68}N_6O_8$	- NP

MM= molecular mass; MF= Molecular formular; L= L-enantiomer amino acids; NP = no product; pA= peptoid alanine; mA= methyl alanine

Investigation of different acylation techniques led to the design of SC009-12 (Figure 3.3), which are the analogues of SC001-4 with the N-methyl alanine and sarcosine replaced by L-alanine (SC009 and SC010) and D-alanine (SC011 and SC012). This was to minimise the use of N-methyl Ala and sarcosine which had to be synthesised. The N-methyl Ala and sarcosine were synthesised using a procedure outlined in the Chapter 4. The synthesis of linear SC009-12 was successful (Figure A.2-A.5).

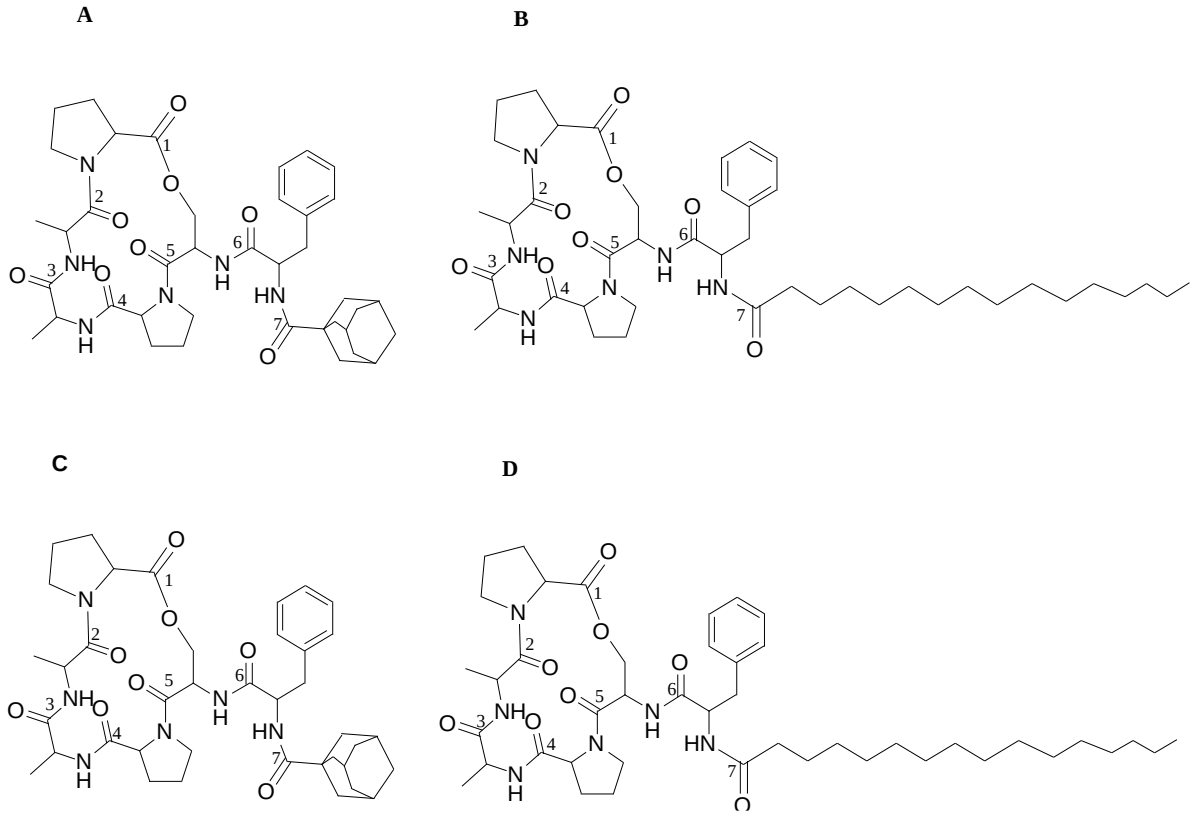


Figure 3. 3: ADEP1 ester cyclised analogues. A-SC009; B-SC010; C-SC011; D-SC012. Structure stereochemistry details in Table 3.2.

Two analogues were chosen to optimise the esterification methods (SC009 and SC010). The expected molecular weight [M+H] for linear and cyclised SC009 are 751.40 g/mol and 733.38 g/mol, respectively. Likewise, linear and cyclied M+H for SC010 is 827.06 g/mol and 809.05 g/mol, respectively. The samples were dissolved in water and acetonitrile; however, their solubility was poor. This led to the addition of 1% formic acid and 5% DMSO to aid the solubility. The Fischer esterification was the first method to be investigated using sulfuric acid [13]. When a carboxylic group is treated with an acid in the presence of alcohol, it is converted to an ester (Figure 3.4), which results in a cyclisation bridge between the proline carboxylic end and the serine R-group. Similarly, carbodiimides (DIC, EDC, and CDI) are commonly used in peptide synthesis to activate the carboxylic group (Figure 4). The use of carbodiimides to treat carboxylic groups in the presence of alcohol and DMAP result in the formation of an ester bond (Steglich esterification) [14], [15]. Steglich esterification (Figure 3.5) is a mild reaction compared to Fischer esterification and therefore the Steglich esterification is the preferred choice for further synthesis.

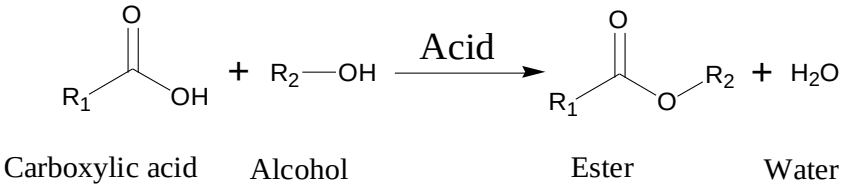


Figure 3. 4: Schematic representation of Fischer esterification.

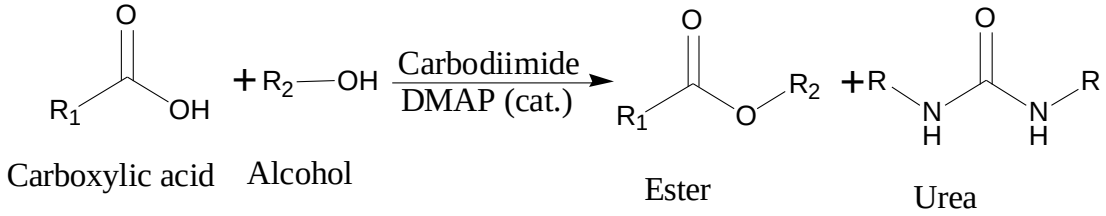
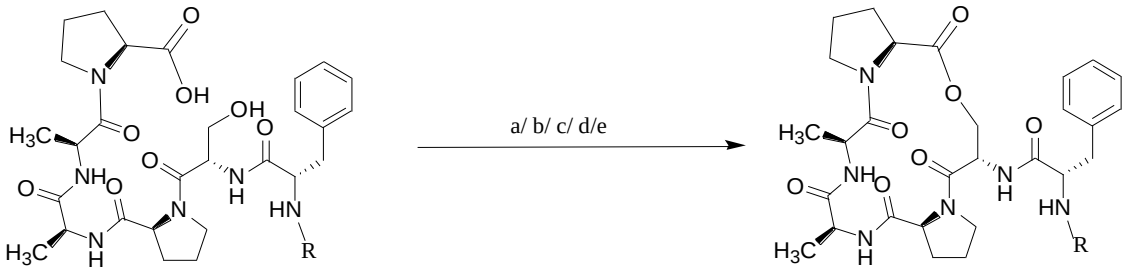


Figure 3. 5: Schematic representation of Steglich esterification.

The esterification conditions were as follows:



R= Adamantane/ Palmitic acid

Figure 3. 6: Cyclisation of the peptides through forming an ester bond. Reactions were carried on linear peptides with (**a**) 1% H_2SO_4, 3 hr, rt; (**b**) 95% TFA, 3 hr, rt; (**c**) 15 eq DIC, 0.5 eq DMAP in dry DCM: DMF on a 9:1 ratio overnight, rt; (**d**) 15 eq EDC, 0.5 eq DMAP in dry DCM: DMF on a 9:1 ratio overnight, rt; (**e**) 15 eq CDI, 0.5 eq DMAP in dry DCM: DMF on a 9:1 ratio overnight, rt.

All these reactions yielded low quantities of the cyclised Ada-containing peptide (SC009) when analysed using the MS (Table 3.2; Figure A.6-A.10). There were no traces of cyclised products from the Fischer esterification methods (Figures A.11 and A.12) of the Pal-containing analogue (SC010). However, a mass of 807.55 g/mol was observed, which lacks 2 protons from the expected cyclised M+H of 809.05 g/mol. Only the Steglich esterification methods showed a

slight cyclisation of SC010 (Figure A.13-A.15). Other researchers have observed that water production during esterification inhibits the esterification forward reaction [18]. Unfortunately, water is a by-product of esterification methods. However, to manipulate the forward reaction, the water needs to be removed during the reaction with the addition of either the carboxylic acid or alchol need to be added to the reaction. In this synthesis, it was impossible to vary the concentration of the carboxylic acid or the alcohol since they are in the same peptide sequence. In addition, we observed that water removal from the conventional cleavage mixture of 95% TFA, 2.5% H_2O, and 2.5% TIS to use 97.5% TFA and 2.5% TIS yielded better results. Therefore, the water content will be limited in the future esterification of these peptides. Nevertheless, the failure to cyclise an ester bond required an alternative cyclisation strategy that may be feasible and also improve the analogues' pharmacokinetics.

Table 3. 2: ADEP1 analogues with linear and cyclised calculated MM.

Code	**Peptide sequence**	**Linear MM & MF**	**Cyclised MM & MF**	**Linear found $[M+H]^+$**	**Cyclised found $[M+H]^+$**
SC009	$_{L-}$(PAAPSF)-Ada	750.40 $C_{39}H_{54}N_6O_9$	732.38 $C_{39}H_{52}N_6O_8$	751.4023	733.3634*
SC010	$_{L-}$(PAAPSF)-Pal	826.52 $C_{44}H_{70}N_6O_9$	808.51 $C_{44}H_{68}N_6O_8$	827.4983	809.4856#
SC011	$_{D-}$(PAAPSF)-Ada	750.40 $C_{39}H_{54}N_6O_9$	732.38 $C_{39}H_{52}N_6O_8$	751.3999	-
SC012	$_{D-}$(PAAPSF)-Pal	826.52 $C_{44}H_{70}N_6O_9$	808.51 $C_{44}H_{68}N_6O_8$	827.6740	-

L= L-enantiomer amino acids; D= D-enantiomer amino acids; *=obtained from all the studied methods; # = obtained only from the Steglich esterification methods

3.3. **Design of disulphide bond cyclised ADEP1 analogues**

The next approach to cyclise the analogs using a disulfide bridge involved the incooporation of Cys at position one of the sequences and the replacement of Ser-5 with Cys. Disulphide bonds play a major role in peptide/protein structure stability by increasing resistance to proteolysis[16]. The ester bond is susceptible to degradation by enzymes such as esterases [17]. The design and synthesis of anionic disulphide-cyclised ADEP1 analogues, SC005-8, Figure 3.7, are discussed in Chapter 5. The synthesis and characterisation were successful, with high purity and yields. However, a noticeable difference between Ada versus Pal-containing

peptides during cyclisation was observed. All four analogues were treated with 10eq of iodine in DMF: methanol (4:1 ratio) while still on the resin. The reaction was left shaking at room temperature for 40 minutes. The resin was washed with 1M of L-ascorbic acid, followed by DMF and DCM. Only the Ada-containing peptides (SC006 and SC007) were cyclised upon cleavage. The Pal-containing peptides remained linear. Formation of the intramolecular disulphide bond using DMSO is also one of the methods reported to be most effective [18]. Therefore, SC005 and SC008 were treated with a 20% DMSO solution overnight. This cleavage cocktail was also optimised for these peptides since the conventional cleavage mixture (94% TFA: 2.5% H_2O: 1% TIS: 2.5% EDT) for sulphur-containing peptides yielded linear peptides post-cyclisation. Thus, the optimised cleavage solution contained 95% TFA, 2.5% H_2O, and 2.5% TIS yielded the desired peptides listed in Table 3 below.

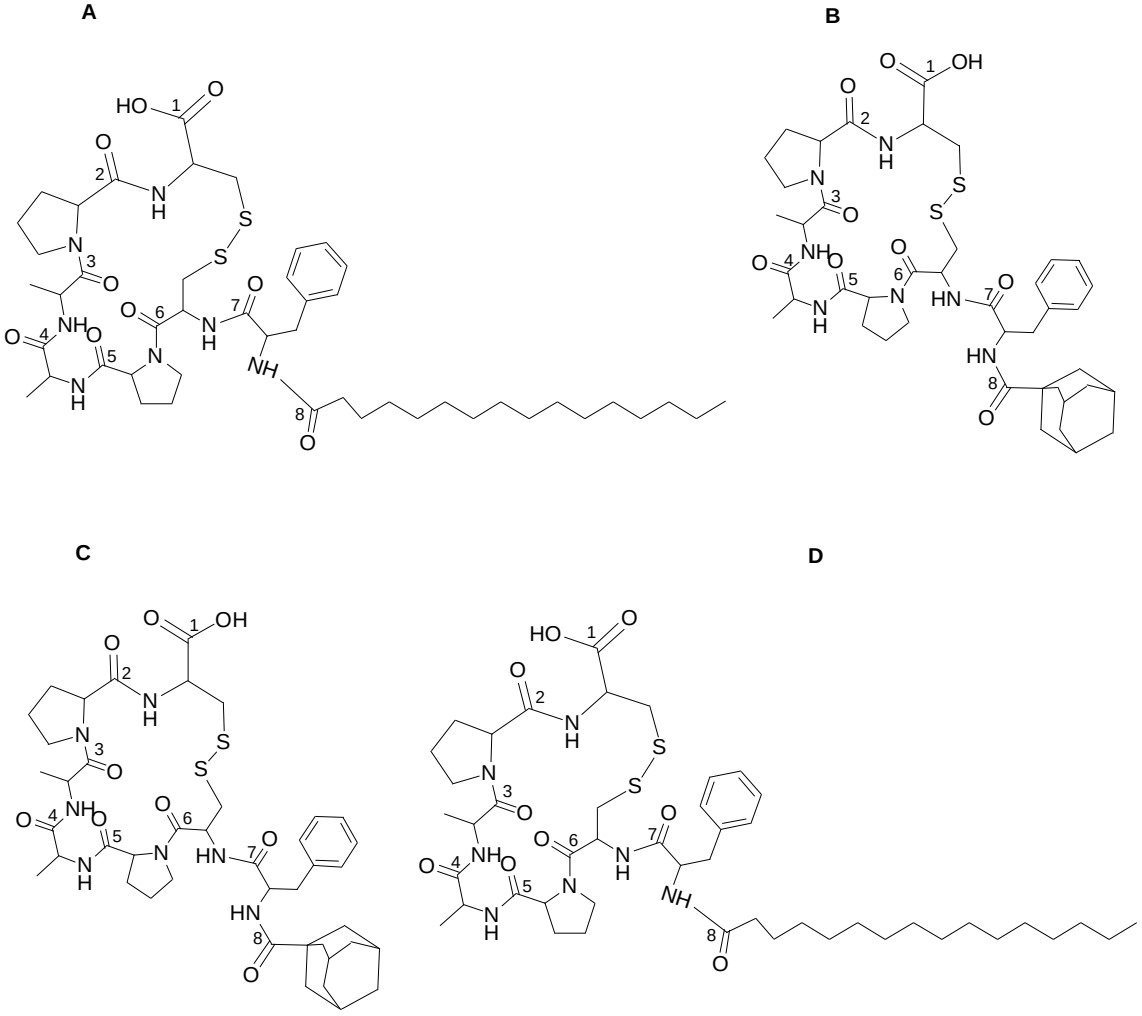


Figure 3. 7: Disulphide bond cyclised ADEP1 analogues. A-SC005; B-SC006; C-SC007, D-SC008. Structure stereochemistry details in Table 3.3.

Table 3. 3: List ADEP1 analogues with linear and cyclised calculated MM containing Cys residues.

Code	Peptide sequence	Linear MM & MF	Cyclised MM & MF	Cyclised found $[M+H]^+$	% Yield
SC005	$_{D-}$(CPAAPCF)-Pal	945.51 $C_{47}H_{75}N_7O_9S_2$	943.49 $C_{47}H_{73}N_7O_9S_2$	944.3957	46
SC006	$_{D-}$(CPAAPCF)-Ada	869.38 $C_{42}H_{59}N_7O_9S_2$	867.37 $C_{42}H_{57}N_7O_9S_2$	868.3737	37
SC007	$_{L-}$(CPAAPCF)-Ada	869.38 $C_{42}H_{59}N_7O_9S_2$	867.37 $C_{42}H_{57}N_7O_9S_2$	868.3733	39
SC008	$_{L-}$(CPAAPCF)-Pal	945.51 $C_{47}H_{75}N_7O_9S_2$	943.49 $C_{47}H_{73}N_7O_9S_2$	944.3955	45

3.4. **Design of disulphide bond cyclised ADEP1 analogues containing Lysine**

The same synthesis procedure described above (section 1.3) was employed in the synthesis of SC013-16 peptides (Figure 8) containing lysine as the first amino acid. The two-tailed Cys-cyclised peptides (SC013-16) were also designed to evaluate the role of lys which is reported to increase cell permeation, improve polarity and increase the solubility of the peptides. These cationic analogues sequences were derived from the anionic SC005-8, and lys was added as the first amino acid residue. Cationic peptides exhibit more bactericidal effects than their negative counterparts [19]. Thus adding positively charged amino acids (Lys and/or Arg) increases the positive net charge. Moreover, lys-rich peptides easily penetrate the cell and can be used to carry molecules across the cell membrane [20]. Positively charged peptides gain access to the bacterial cell by forming hydrogen bonds and electrostatic interactions with the negatively charged phosphate head group on the bacterial cell lipid bilayer [21], [22].

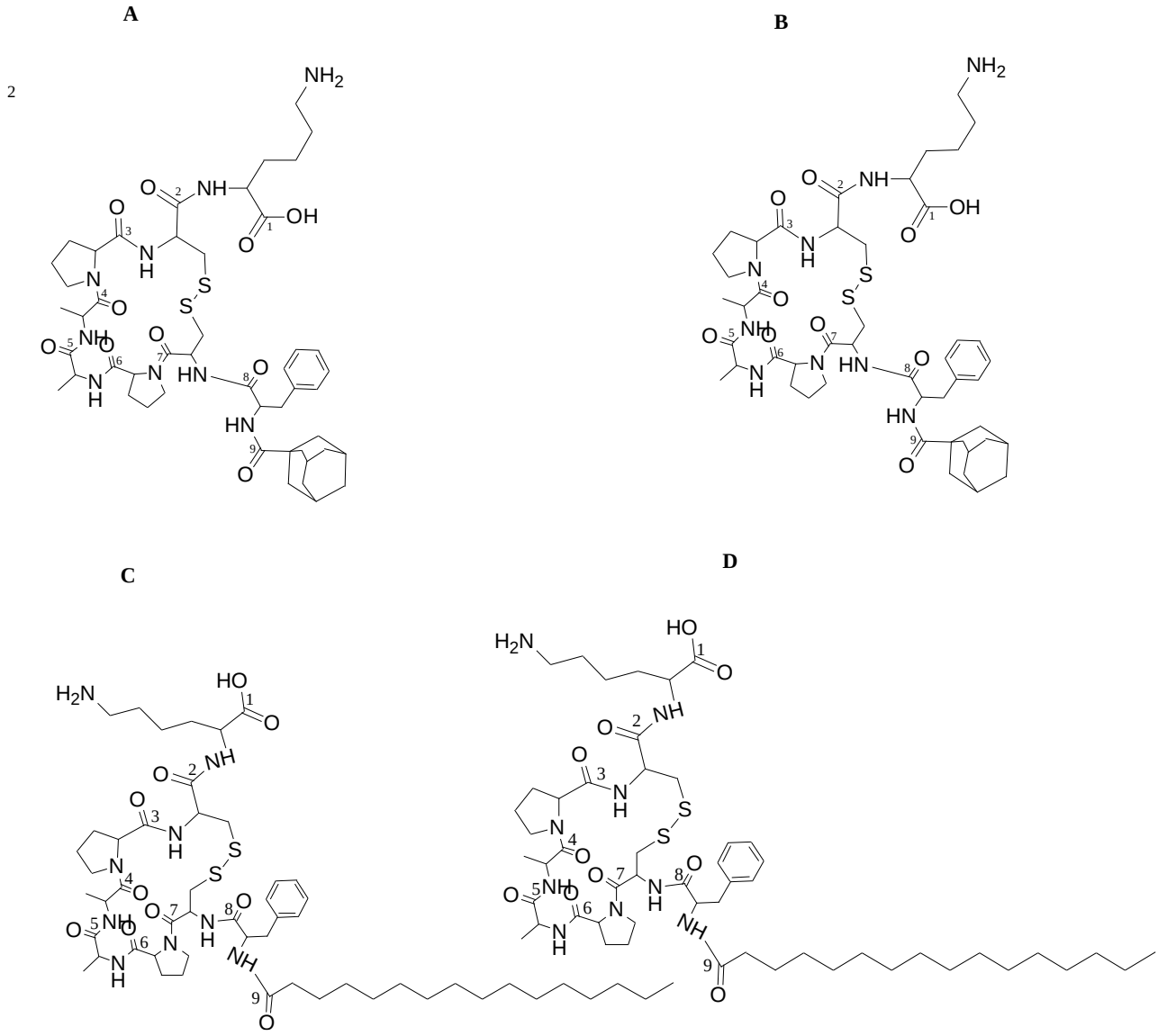


Figure 3. 8: Disulphide bond cyclised ADEP1 analogues with Lys. A-SC013; B-SC014; C-SC015, D-SC016. Structure stereochemistry details in Table 3.4.

In Table 3.4 below, the LCMS results for the four ADEP1 analogues (SC013-SC016) are presented. SC013-16 were successfully synthesised and purified (Figure A15-A19, pg). These peptides were further screened for antibacterial activity against *E. coli*, *B. subtilis*, *S. aureus*, MRSA and *P. aeruginosa*. However, none of the analogues were active against these bacterial strains. This inactivity might be linked to lys's addition at the first amino acid position. ADEPs are naturally neutral and nonpolar peptides, and adding a positive amino acid might have led to weak binding to the target site. However, the negative peptide counterparts (SC005-8) of SC013-16 were active against the bacterial strains mentioned above. The observed trend can be linked to the known ADEPs mechanism of action, which bind to the hydrophobic pocket of

the ClpP protease. Therefore, the positive charge on lys might be unfavourable for these hydrophobic pockets. The Lys might introduce electrostatic interactions with other parts of the protease, which can limit the proteolytic activation. Moreover, the bulkiness of the peptide might be restricted from tightly binding to the ClpP.

A positive zeta potential value for SC013-16 was obtained and can be credited to the positive charge of Lys. The zeta potential values of the peptides were between 0.1 and 1.3 mV, which is regarded as unstable and prone to aggregation. An mV value greater than +30 or less than -30 is generally considered stable, possessing sufficient repulsive forces to prevent aggregation [23].

Table 3. 4: List ADEP1 analogues with linear and cyclised calculated MM containing Cys residues and Lys.

Code	**Peptide sequence**	**Linear MM & MF**	**Cyclise MM & MF**	**Cyclised found $[M+H]^+$**	**% yield**	**% purity**	**Zeta potential (mV)**
SC013	$_{L-}$(KCPAAPCF)-Ada	997.48 $C_{48}H_{71}N_9O_{10}S_2$	995.48 $C_{48}H_{69}N_9O_{10}S_2$	996.6332	43	-	1.3 ±0.02
SC014	$_{D-}$(KCPAAPCF)-Ada D-	997.48 $C_{48}H_{71}N_9O_{10}S_2$	995.46 $C_{48}H_{69}N_9O_{10}S_2$	996.4676	45	-	0.9 ±0.03
SC015	$_{L-}$(KCPAAPCF)-Pal	1073.60 $C_{53}H_{87}N_9O_{10}S_2$	1071.59 $C_{53}H_{85}N_9O_{10}S_2$	1072.5477	53	99.9	0.2 ±0.02
SC016	$_{D-}$(KCPAAPCF)-Pal	1073.60 $C_{53}H_{87}N_9O_{10}S_2$	1071.59 $C_{48}H_{69}N_9O_{10}S_2$	1072.5989	56	96	0.1 ±0.03

3.5. **Design of disulphide bond cyclised ADEP1 analogues containing peptoid moieties**

Lastly, SC017-20 are analogues of SC006 and SC007 with N-methylated Ala and sarcosine. The peptides' synthesis and cyclisation were successful when using the 20% DMSO cyclisation method described above (Figure A.20-A.23). Due to time constraints, these peptides will be screened for antimicrobial activity in the future.

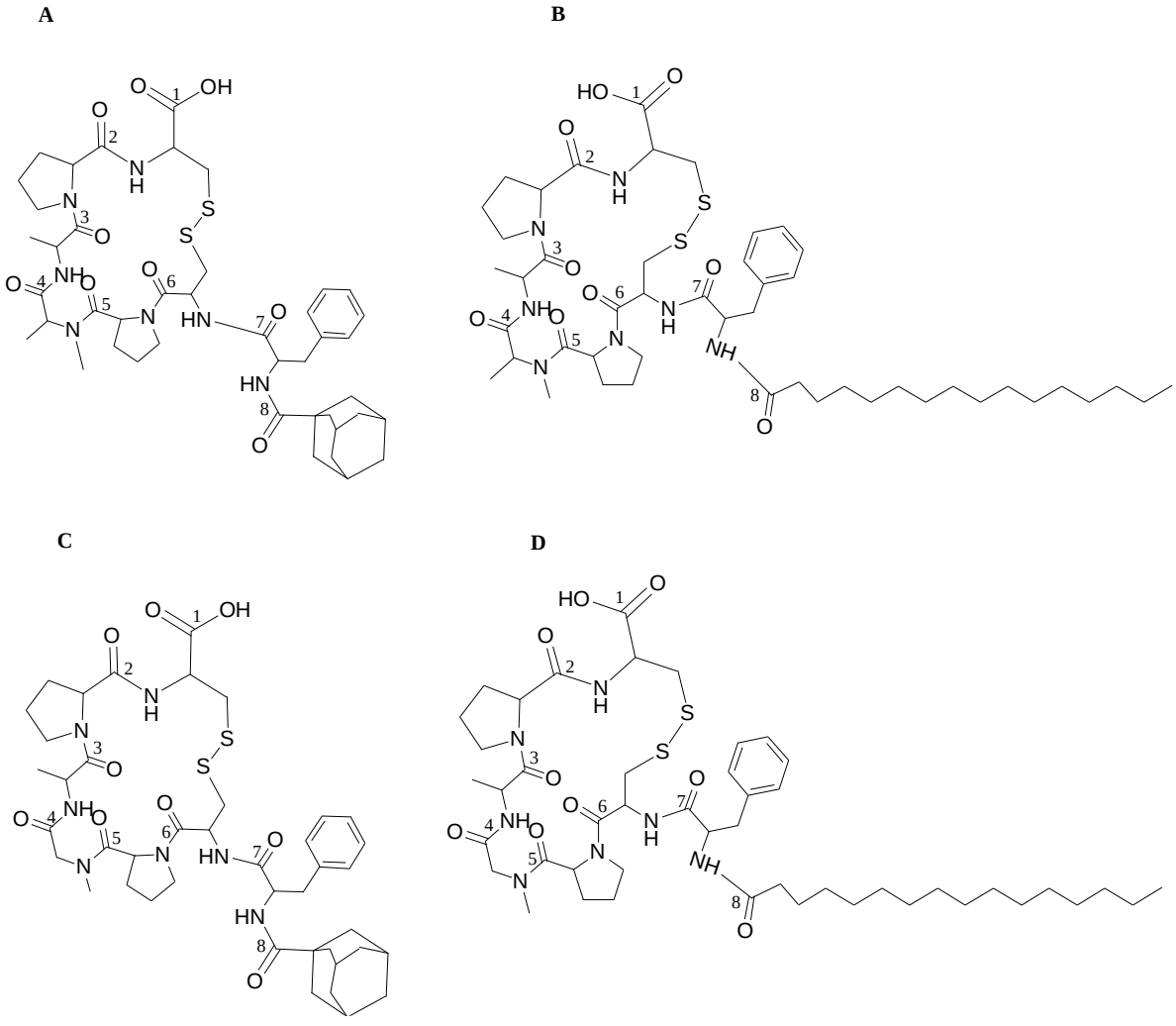


Figure 3. 9: Schematic Figure 9: Disulphide bond cyclised ADEP1 analogues with peptoid moieties. A-SC017; B-SC018; C-SC019, D-SC020. Structure stereochemistry details in Table 3.5.

Table 3. 5: List ADEP1 analogues with linear and cyclised calculated MM containing Cys residues and peptoid moieties.

Code	Peptide sequence	Linear MM	Cyclised MM	Linear found $[M+H]^+$
SC017	L-CPAmAPCF-Ada	883.40 $C_{43}H_{61}N_7O_9S_2$	881.38 $C_{43}H_{59}N_7O_9S_2$	884.4027
SC018	L-CPAmAPCF-Pal	959.52 $C_{48}H_{77}N_7O_9S_2$	957.51 $C_{48}H_{75}N_7O_9S_2$	960.5298
SC019	L-CPApAPCF-Ada	869.38 $C_{42}H_{59}N_7O_9S_2$	867.37 $C_{42}H_{57}N_7O_9S_2$	870.3874
SC020	L-CPApAPCF-Pal	945.51 $C_{47}H_{73}N_7O_9S_2$	943.49 $C_{47}H_{75}N_7O_9S_2$	946.5116

pA= peptoid alanine; mA= methyl alanine

3.6. **Summary of all designed ADEP1 analogues**

A summary of all the designed analogues is presented in the Table below, where mA is N-methyl alanine and pA is the alanine peptoid (sarcosine).

Table 3. 6: Summary of ADEP1 peptide analogues library

Code	Peptide sequence		Molecular weight L; C	Molecular formula
			L- amino acids with peptoids	
SC001	PAmAPSF-Ada		764.41	$C_{40}H_{56}N_6O_9$
			746.40	$C_{40}H_{54}N_6O_8$
SC002	PAmAPSF-Pal		840.54	$C_{45}H_{72}N_6O_9$
			822.53	$C_{45}H_{70}N_6O_8$
SC003	PApAPSF-Ada		750.40	$C_{39}H_{54}N_6O_9$
			732.38	$C_{39}H_{52}N_6O_8$
SC004	PApAPSF-Pal		826.52	$C_{44}H_{70}N_6O_9$
			808.51	$C_{44}H_{68}N_6O_8$
			Cysteine with L and D amino acids	
SC005	CPAAPCF-Pal	D-	945.51	$C_{47}H_{75}N_7O_9S_2$
			943.49	$C_{47}H_{73}N_7O_9S_2$
SC006	CPAAPCF-Ada	D-	869.38	$C_{42}H_{59}N_7O_9S_2$
			867.37	$C_{42}H_{57}N_7O_9S_2$
SC007	CPAAPCF-Ada		869.38	$C_{42}H_{59}N_7O_9S_2$
			867.37	$C_{42}H_{57}N_7O_9S_2$
SC008	CPAAPCF-pal		945.51	$C_{47}H_{75}N_7O_9S_2$
			943.49	$C_{47}H_{73}N_7O9S_2$

Code	Peptide sequence		Molecular weight L; C	Molecular formula
			L and D amino acids	
SC009	PAAPSF-Ada		750.40	$C_{39}H_{54}N_6O_9$
			732.38	$C_{39}H_{52}N_6O_8$
SC010	PAAPSF-Pal		826.52	$C_{44}H_{70}N_6O_9$
			808.51	$C_{44}H_{68}N_6O_8$
SC011	PAAPSF-Ada	D-	750.40	$C_{39}H_{54}N_6O_9$
			732.38	$C_{39}H_{52}N_6O_8$
SC012	PAAPSF-Pal	D-	826.52	$C_{44}H_{70}N_6O_9$
			808.51	$C_{44}H_{68}N_6O_8$
			L and D amino acids: two-tailed peptides	
SC013	KCPAAPCF-Ada		997.48	$C_{48}H_{71}N_9O_{10}S_2$
			995.46	$C_{48}H_{69}N_9O_{10}S_2$
SC014	KCPAAPCF-Ada	D-	997.48	$C_{48}H_{71}N_9O_{10}S_2$
			995.46	$C_{48}H_{69}N_9O_{10}S_2$
SC015	KCPAAPCF-Pal		1073.60	$C_{53}H_{87}N_9O_{10}S_2$
			1071.59	$C_{53}H_{85}N_9O_{10}S_2$
SC016	KCPAAPCF-Pal	D-	1073.60	$C_{53}H_{87}N_9O_{10}S_2$
			1071.59	$C_{53}H_{85}N_9O_{10}S_2$
			Cysteine with peptoids	
SC017	CPAmAPCF-Ada		883.40	$C_{43}H_{61}N_7O_9S_2$
			881.38	$C_{43}H_{59}N_7O_9S_2$
SC018	CPAmAPCF-pal		959.52	$C_{48}H_{77}N_7O_9S_2$
			957.51	$C_{48}H_{75}N_7O_9S_2$
SC019	CPApAPCF-Ada		869.38	$C_{42}H_{59}N_7O_9S_2$
			867.37	$C_{42}H_{57}N_7O_9S_2$
SC020	CPApAPCF-Pal		945.51	$C_{47}H_{75}N_7O_9S_2$
			943.49	$C_{47}H_{73}N_7O_9S_2$

L= Linear; C= Cyclised

3.7. **Synthesis of Bz-LL**

Bz-LL is an N-terminal blocked dipeptide agonist known to bind and activate the ClpP1P2 [24] and it was synthesised and used as a positive control for the ClpP1P2 activity assay. It is comprised of two Leu residues and a benzoic acid on the N-terminal. Leu was coupled to the activated 2-chlorotritryl resin. For the coupling of the second Leu and benzoic acid, 0.4M DIPEA, 0.19M HBTU, 0.095M of HOBt, and 0.2M Fmoc-amino acids were utilised. Fmoc was removed using 20% piperidine for 5 minutes twice. Final cleavage from the resin was done using a TFA cleavage cocktail mixture of 95% TFA: 2.5% H_2O: 2.5% TIS. The synthesis of Bz-LL was successful and confirmed by mass spectrometry. MM of Bz-LL is 348.4 g/mol, and the found M+H was 349.2471 g/mol (2M+H was 697.4836 g/mol), as seen in Figure 26.A. The tripeptide was obtained with 96% purity and a 72% yield.

3.8. **Conclusion**

The synthesis, characterisation, and structural elucidation of peptoid moieties (Fmoc-N-methyl alanine and Fmoc-sarcosine) was successful. These moieties were incorporated in the synthesis of SC001-4 and SC017-20. None of the esterification methods used in this study effectively cyclised the ADEP1 peptide analogues. However, the promising results obtained while using Steglich esterification will further be investigated to optimise the esterification of the ADEP1 analogues while still using the SPPS technique. A positive aspect however, is that disulphide bridge cyclised peptides (SC005-8, SC013-20) were successfully synthesised with high purity and yield. Of the eight peptides (SC005-8 and SC013-16) tested for antimicrobial activity, only the anionic (SC005-8) showed activity. Nevertheless, optimisation in the structural design of these peptides will still be pursued to best suit the intended use.

References

[1] R. Gandolfi *et al.*, "Synthesis and Biological Evaluation of New Natural Phenolic (2E,4E,6E)-Octa-2,4,6-trienoic Esters," *Chem. Biodivers.*, vol. 14, no. 12, Dec. 2017, doi: 10.1002/cbdv.201700294.

[2] V. Čižinauskas, N. Elie, A. Brunelle, and V. Briedis, "Fatty acids penetration into human skin ex vivo: A TOF-SIMS analysis approach," *Biointerphases*, vol. 12, no. 1, p. 011003, Mar. 2017, doi: 10.1116/1.4977941.

[3] D. Irby, C. Du, and F. Li, "Lipid–Drug Conjugate for Enhancing Drug Delivery," *Mol. Pharm.*, vol. 14, no. 5, pp. 1325–1338, May 2017, doi: 10.1021/acs.molpharmaceut.6b01027.

[4] A. Štimac, M. Šekutor, K. Mlinarić-Majerski, L. Frkanec, and R. Frkanec, "Adamantane in Drug Delivery Systems and Surface Recognition," *Mol. Basel Switz.*, vol. 22, no. 2, Feb. 2017, doi: 10.3390/molecules22020297.

[5] C. F. Chew, A. Guy, and P. C. Biggin, "Distribution and Dynamics of Adamantanes in a Lipid Bilayer," *Biophys. J.*, vol. 95, no. 12, pp. 5627–5636, Dec. 2008, doi: 10.1529/biophysj.108.139477.

[6] S. H. Joo, "Cyclic Peptides as Therapeutic Agents and Biochemical Tools," *Biomol. Ther.*, vol. 20, no. 1, pp. 19–26, Jan. 2012, doi: 10.4062/biomolther.2012.20.1.019.

[7] V. G. Ramu, E. Bardaji, and M. Heras, "pDapEer PBT as Coupling Reagent To Avoid Racemization in a Solution-Phase Synthesis of a Kyotorphin Derivative," *N. Y.*, 2014.

[8] C. J. White and A. K. Yudin, "Contemporary strategies for peptide macrocyclization," *Nat. Chem.*, vol. 3, no. 7, pp. 509–524, Jun. 2011, doi: 10.1038/nchem.1062.

[9] J. S. Davies, "The cyclization of peptides and depsipeptides," *J. Pept. Sci.*, vol. 9, no. 8, pp. 471–501, 2003, doi: 10.1002/psc.491.

[10] B. Eyermann, M. Meixner, H. Brötz-Oesterhelt, I. Antes, and S. A. Sieber, "Acyldepsipeptide Probes Facilitate Specific Detection of Caseinolytic Protease P Independent of Its Oligomeric and Activity State," *ChemBioChem*, vol. 21, no. 1–2, pp. 235–240, 2020, doi: 10.1002/cbic.201900477.

[11] Y. Li *et al.*, "Consequences of Depsipeptide Substitution on the ClpP Activation Activity of Antibacterial Acyldepsipeptides," *ACS Med. Chem. Lett.*, vol. 8, no. 11, pp. 1171–1176, Oct. 2017, doi: 10.1021/acsmedchemlett.7b00320.

[12] D. A. Alonzo and T. M. Schmeing, "Biosynthesis of depsipeptides, or Depsi: The peptides with varied generations," *Protein Sci. Publ. Protein Soc.*, vol. 29, no. 12, pp. 2316–2347, Dec. 2020, doi: 10.1002/pro.3979.

[13] J. J. Li, "Fischer–Speier esterification," in *Name Reactions: A Collection of Detailed Mechanisms and Synthetic Applications Fifth Edition*, J. J. Li, Ed. Cham: Springer International Publishing, 2014, pp. 252–252. doi: 10.1007/978-3-319-03979-4_105.

[14] M. Tsakos, E. S. Schaffert, L. L. Clement, N. L. Villadsen, and T. B. Poulsen, "Ester coupling reactions – an enduring challenge in the chemical synthesis of bioactive natural products," *Nat. Prod. Rep.*, vol. 32, no. 4, pp. 605–632, 2015, doi: 10.1039/C4NP00106K.

[15] I. Dhimitruka and J. SantaLucia, "Investigation of the Yamaguchi Esterification Mechanism. Synthesis of a Lux-S Enzyme Inhibitor Using an Improved Esterification Method," *Org. Lett.*, vol. 8, no. 1, pp. 47–50, Jan. 2006, doi: 10.1021/ol0524048.

[16] M. V. Trivedi, J. S. Laurence, and T. J. Siahaan, “The role of thiols and disulfides in protein chemical and physical stability,” *Curr. Protein Pept. Sci.*, vol. 10, no. 6, pp. 614–625, Dec. 2009.

[17] Y. Finer and J. P. Santerre, “The influence of resin chemistry on a dental composite’s biodegradation,” *J. Biomed. Mater. Res. A*, vol. 69, no. 2, pp. 233–246, May 2004, doi: 10.1002/jbm.a.30000.

[18] A. Abedini, G. Singh, and D. P. Raleigh, “Recovery and purification of highly aggregation-prone disulfide-containing peptides: Application to islet amyloid polypeptide,” *Anal. Biochem.*, vol. 351, no. 2, pp. 181–186, Apr. 2006, doi: 10.1016/j.ab.2005.11.029.

[19] B. Bechinger and S.-U. Gorr, “Antimicrobial Peptides: Mechanisms of Action and Resistance,” *J. Dent. Res.*, vol. 96, no. 3, pp. 254–260, Mar. 2017, doi: 10.1177/0022034516679973.

[20] Y. Su, T. Doherty, A. J. Waring, P. Ruchala, and M. Hong, “Roles of Arginine and Lysine Residues in the Translocation of a Cell-Penetrating Peptide from 13C, 31P and 19F Solid-State NMR,” *Biochemistry*, vol. 48, no. 21, pp. 4587–4595, Jun. 2009, doi: 10.1021/bi900080d.

[21] M. Jafari and P. Chen, “Peptide Mediated siRNA Delivery,” *Curr. Top. Med. Chem.*, vol. 9, no. 12, pp. 1088–1097.

[22] M. Hao, L. Zhang, and P. Chen, “Membrane Internalization Mechanisms and Design Strategies of Arginine-Rich Cell-Penetrating Peptides,” *Int. J. Mol. Sci.*, vol. 23, no. 16, Art. no. 16, Jan. 2022, doi: 10.3390/ijms23169038.

[23] P. J. Kadu, S. S. Kushare, D. D. Thacker, and S. G. Gattani, “Enhancement of oral bioavailability of atorvastatin calcium by self-emulsifying drug delivery systems (SEDDS),” *Pharm. Dev. Technol.*, vol. 16, no. 1, pp. 65–74, Feb. 2011, doi: 10.3109/10837450903499333.

[24] S. Vahidi *et al.*, “An allosteric switch regulates *Mycobacterium tuberculosis* ClpP1P2 protease function as established by cryo-EM and methyl-TROSY NMR,” *Proc. Natl. Acad. Sci.*, vol. 117, no. 11, pp. 5895–5906, Mar. 2020, doi: 10.1073/pnas.1921630117.

CHAPTER 4.
MATERIALS AND METHODS

4.1. Chemicals

Fmoc-protected α-amino acids, 2-chlorotrityl resin, N,N,N′,N′-Tetramethyl-O-(1H-benzotriazol-1-yl)uronium hexafluorophosphate (HBTU), Hydroxybenzotriazole (HOBt), Triisopropylsilane (TIS), N,N'-Diisopropylcarbodiimide DIC, 1-Ethyl-3-(3-dimethylaminopropyl) carbodiimide (EDC), and 1,1'-Carbonyldiimidazole (CDI) were purchased from GL Biochem (Shanghai) Ltd. Thionyl chloride, ether, thionyl chloride, bromoacetic acid, piperidine, acetic acid, 4-Dimethylaminopyridine (DMAP), trifluoroacetic acid (TFA), formic acid, Acetone, methylamine, were purchased from DLD scientific. Organic solvents such as dimethyl formamide (DMF), dichloromethane (DCM), methanol, acetonitrile, dimethyl sulfoxide and diethyl ether were supplied by Radchem. Diisopropylethylamine (DIPEA), dimethyl sulfoxide (DMSO), toluene, and acetonitrile (ACN) were also purchased from Radchem. Solvents for column chromatography (ethyl acetate, pentane, and hexanes) were purchased from Protea Chemicals (South Africa) and distilled before use to remove non-volatile components. Aluminium trichloride (AlCl3), sodium hydrogen carbonate (NaHCO3), magnesium sulphate (MgSO4), paraformaldehyde, and p-toluenesulfonic acid were purchased from Sigma Aldrich.

4.2. Instrumentation for data collection and analysis

4.2.1. *Resin loading capacity*

The resin loading capacity of the first amino acid of the sequence was determined by the Ultraviolet-visible spectroscopy (UV-Vis; Thermo-Scientific). This was then used to determine the theoretical mass.

4.2.2. *Purification*

Preparative High pressure liquid chromatography (prep-HPLC) from Shimadzu with a UV-vis detector and an automated fraction collector was used to purify the synthesised peptides on a Kinetix® 5 μm B-C18, 100 Å (250 ×230 nm) column. A two-buffer system was employed; Buffer A consisted of 0.1% formic acid in H_2O and buffer B consisted of 0.1% formic acid in

CH_3CN. A flow rate of 20 mL/min or 15 mL/min and UV wavelengths of 215 and 254 nm were utilised.

4.2.3. *Analytical analysis of the synthesised peptide*

An Ultra High Performance Liquid Chromatography (Thermo Scientific Ultimate 3000, RS diode array detectors) with a Diode Array (215 and 254 nm) coupled to a High Resolution Mass Spectrometer (Bruker Compact quadruple time of-flight) was used to obtain the molecular masses of the peptides. The system consists of a pump, autosampler, and a Diode Array detector coupled to a Mass Spectrometer (electrospray in the positive mode). A two-buffer system was employed with a flow rate of 0.3 mL/min on a C18 column (5 μm, 100 Å, 4.60 mm × 150 mm). The buffer system utilised formic acid as the ion-pairing agent, solvents-A (water with 0.1% formic acid) and solvent-B (acetonitrile with 0.1% formic acid).

4.2.4. *Structural characterisation*

Nuclear magnetic resonance spectroscopy (NMR) form Bruker, was used to determine the structures of the synthesised peptides. ^{1}H-NMR spectra were recorded on a Bruker Avance 300 MHz, Bruker Avance 400 MHz and on Bruker III 500 MHz spectrometer. The chemical shifts (δ) values are reported in parts per million (ppm) relative to deuterated chloroform ($CDCl_3$, 7.26 ppm) and dimethyl sulfoxide (DMSO-$_{d6}$, 2.49 ppm) and referenced against the internal standard, tetramethylsilane (TMS, 0.00 ppm). The spectra were analyzed as first order and the values of the coupling constant (J) are reported in Hertz (Hz). Multiplicity of signals are expressed as: s=singlet, br s=broad singlet, d=doublet, dd=double doublet, t=triplet, q=quartet, m=multiplet.

^{13}C-NMR spectra were recorded on Bruker Avance 300 MHz, Bruker Avance 400 MHz and on Bruker III 500 MHz spectrometer. The chemical shifts values are reported in (ppm) relative to deuterated chloroform ($CDCl_3$, 77.2 ppm), (DMSO-$_{d6}$, 39.52 ppm) and TMS as an internal standard.

4.2.5. *Peptoid synthesis analysis*

Analytical thin layer chromatography (TLC) plates (0.2 mm silica gel 60 with fluorescent indicator UV_{254}) were obtained from Sigma-Aldrich. Synthesis of peptoids was monitored

using TLC and further visualisation was done by staining with potassium permanganate ($KMnO_4$) solution followed by heating. The compounds were purified using column chromatography on normal silica gel (particle size 0.063-0.200 mm) and flash silica gel (particle size 0.040-0.063) purchased from Merck. Ethyl acetate and hexane were used as eluting solvents. Solvent ratios are reported as (30/70; volume-by-volume).

4.3. **General peptide synthesis**

The peptides were synthesised manually, via the solid phase peptide synthesis (SPPS) using Fmoc-amino acids [1]. The 2-chlorotrityl chloride resin was used as a solid structure.To 1 gram of chlorotrityl resin in a 50 mL tube, thionylchloride (3 mL) in dry DCM (45 mL) was added and the mixture was shaken for 2 hours. The mixture was then transferred into a glass reaction vessel fitted with a fritted filter and was washed with dry DCM (4ml x 5).

The first amino acid (4 equivalence) was loaded to the activated resin with 5 equivalence of the DIPEA. The resultant reaction mixture was gently mixed by bubbling nitrogen gas into the reaction for 45 min. After filtration the resin was washed with DMF (3×5 ml) followed by DCM (3×5 mL) to remove excess reagents and by-products. A 20% piperidine solution (10 ml) was added to the resin to remove the protecting group for ± 15 minutes. The resin was then washed with DMF (3×5 mL) followed by DCM (3×5 mL) to remove excess reagents.

The second amino acids (0.12 M) were coupled to the resin-attached amino acid using HBTU (0.519 g, 0.11 M) as a coupling reagent and DIPEA (1.26 ml, 0.6 M) as the base. The resultant reaction mixture was gently mixed by bubbling nitrogen gas into the reaction for 45 min. The resin was washed with DMF (3×5 mL) followed by DCM (3×5 mL) to remove excess reagents. The same coupling process was utilised to couple all the other amino acids however, the concentrations were changed to 0.5M for DIPEA, 0.19 M for HBTU, 0.095 M for HOBt and 0.2 M for the amino acids. Each amino acid was double coupled while Pal or 1-Adamantanecaboxylic acid were triple coupled.

4.3.1. *Resin loading test*

The resin-loading test is vital for calculating the theoretical yield of the synthesised peptides. Approximately 5-10 mg of duplicate samples of the loaded and dry resin was weighed into an Eppendorf tube. This was followed by the addition of 20% piperidine in DMF (1 mL) and the

mixture was left shaking for 20 minutes. The solution was centrifuged at 6000rpm for 5 minutes. The supernatant (100 µL) was transferred into a tube containing 10 mL of DMF and mixed well. The absorbance was read at 301 nm in triplicates, using pure DMF as a blank. The calculations were done using the equation below.

$$Loading\ capacity\ (mmol/g) = \left(\frac{101\ x\ Absorbance}{7.8\ x\ w}\right)$$

Where; A = Absorbance and w = mg of resin.

4.3.2. *Cleaving of peptides from the resin*

The cleavage solution contained 95% TFA, 2.5% H2O, and 2.5% TIS for the cleavage of SC005-8 and SC0013-20 and 97.5% TFA and 2.5% TIS for the cleavage of all other derivatives. The cleavage solution was filtered off, and the resin was washed with 5 mL of TFA and the filtrate was poured into round bottom flask. Toluene on a 10:1 ratio to TFA was added during the evaporation process to aid in the azeotropic distillation of TFA. The solvents were removed using rotary evaporator (Rotavapor R-210, Buchi Laboratory Equipment, St Gallen, Switzerland) set at 60-65°C. A complete removal of the solvents left an oily and golden brown residual on the round bottom flask which was dissolved in acetonitrile containing 5% dimethyl sulfoxide (DMSO) for further analysis.

4.4. **Cyclisation**

4.4.1. *Iodine mediated oxidation*

Cyclisation of Ada-containing peptides via disulphide bridges was performed using 10eq iodine in DMF: water in a 4:1 ratio [2]. The reaction was carried out on resin bound peptides and left shaking at room temperature for 40 minutes. The reaction was stopped using 1M L-ascorbic acid [9]. The resin was further washed thoroughly with 1M L-ascorbic acid followed by DMF and then DCM. The peptide was then cleaved using the procedure outline in section 1.3.2.

4.4.2. *DMSO mediated oxidation*

Cyclisation using DMSO was performed on cleaved Pal-containing analogues to form disulphide bridges. Peptides SC005 and SC008 were cyclised in methanol containing 20%

DMSO. The reaction was left shaking overnight at room temperature. The solvents were removed at 60-65℃ using rotary evaporator. The DMSO residues were removed by lyophilisation . The peptides were then re-suspended in acetonitrile for further analysis.

4.5. **Purification and analysis**

The peptides were purified using Preparative High-pressure liquid chromatography (prep-HPLC) (Shimadzu, South Africa (Pty) Ltd) on a prep-HPLC C-18 column (4.6 x 250 mm, 5 µm) (Phenomenex, California, United States) with the UV detector set at 215 and 245 nm wavelengths. The purification method was 20-minutes long with a flow rate of 20 mL/min. The gradient elution started from 5 % of Acetonitrile (solvent B) which was increased to 95% in 12 minutes thereafter the concentration was kept constant at 95% for another 8 minutes. (A= 0.1% FA in water; B=0.1% FA in acetonitrile). Molecular weight of peptides were confirmed using the analytical method described in section 1.2.3.

The expected peptides eluted between 13-14 minutes on the prep-HPLC. The corresponding prep-HPLC peaks were therefore collected and solvent removed using rotary evaporator at 60-65℃. The residuals were lyophilised using a freeze dryer (LyoQuest, Telstar, Terrassa, Barcelona) for further biochemical analysis.

4.6. **Synthesis of N-benzoyl-Leucyl-Leucine (Bz-LL)**

N-benzoyl-Leucyl-Leucine (Bz-LL) was also synthesised using SPPS on a 2-chlorotrityl chloride resin as described in section 1.3. Cleavage, purification and analysis were done as outline above. Structural elucidation was performed using NMR.

4.7. **Synthesis, Characterisation, and structural elucidation of Fmoc-N-methylated alanine and Fmoc-peptoid alanine (Fmoc-sarcosine)**

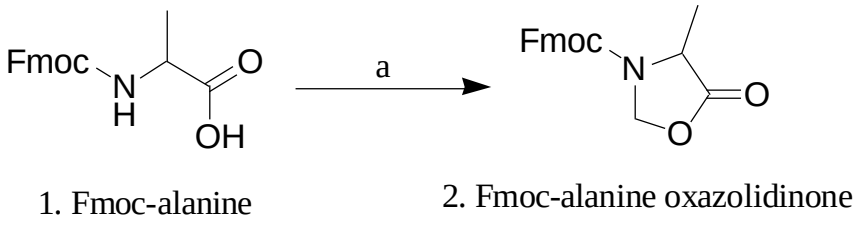
4.7.1. *General procedure for the synthesis of Fmoc-N-methylated amino acids*

Fmoc-amino acids are used as precursors for Fmoc-N-methylated amino acids. Fmoc-amino acids are easily accessible and much cheaper compared to Fmoc-N-methylated amino acids. The Freidinger synthetic route was used in the synthesis of Fmoc-N-methylated amino acids [3]. This method consists of two reaction steps: (a) the conversion of Fmoc-amino acids to

oxazolidinone precursors and (b) the conversion of the precursor to Fmoc-N-methylated amino acids.

4.7.1.1. General procedure for synthesis of oxazolidinones from Fmoc amino acids

Fmoc amino acid (Fmoc-ala, 0.05 M, 5 mmol), paraformaldehyde (0.33 M, 1 g) and p-toluenesulphonic acid (0.006 M, 100 mg) were suspended in toluene (100 mL) (Figure 1). The mixture was refluxed in a Dean-Stark apparatus until no more starting material could be detected by TLC (97.5:2:0.5 $CHCl_3$:MeOH:AcOH). The solution was cooled, washed with saturated sodium bicarbonate ($NaHCO_3$) and dried over anhydrous magnesium sulfate ($MgSO_4$). The final product was concentrated *in vacuo* at 60-65°C, and the crude product solidified upon cooling. The crude product was purified via flash chromatography on a silica gel at 3:7 ethylacetate:pentane. The HPLC-MS was used to analyse the white alanine oxazolidinone crystal/powder.



1. Fmoc-alanine 2. Fmoc-alanine oxazolidinone

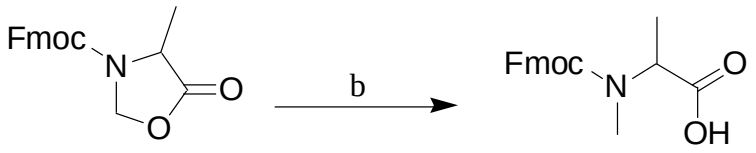
Figure 4. 1: Synthesis of the 5-oxazolidinones (2) from Fmoc alanine (1).

4.7.1.2. General procedure for synthesis of N-methylated Fmoc alanine from oxazolidinones

To a solution of the oxazolidinone (1 equiv) in dry DCM (20 mL / 1 mmol oxazolidinone), aluminium trichloride ($AlCl_3$, 2 equiv) and triethylsilane ($(C_2H_5)_3SiH$, 2 equiv) were added. The reaction in Figure 2 reaction "b" was stirred at ambient temperature until TLC (1:3 Ethylacetate:hexane) showed the absence of starting material. An additional amount of DCM was added (twice the reaction volume) and the organic phase was washed with 1M HCl. The organic phase was dried over anhydrous magnesium sulphate and concentrated *in vacuo*. The crude product was a gel-like substance, which crystallises upon cooling. Purification was achieved via column chromatography on silica gel (ethylacetate and hexane). Purification by re-crystallisation with acetonitrile was used to obtain the light yellowish crystal/powder final

product. The analysis was performed using HPLC-MS and the structure was confirmed by NMR.

For larger scale synthesis, the purification of Fmoc-protected N-methylated amino acids was achieved by extraction: The crude product was taken up in aqueous sodium carbonate solution. The aqueous layer was extracted with diethyl ether to remove non-acidic impurities, then acidified with hydrochloric acid, and the product was extracted with DCM and evaporated.



3. Fmoc-alanine oxazolidinone 4. Fmoc-N-methyl alanine

Figure 4. 2: Synthesis of Fmoc-N-methyl alanine (4) from the oxazolidinone precursors (3).

4.7.2. *Synthesis of Fmoc-Alanine peptoid*

The peptoid synthesis was perform on a 2-chlorotrityl chloride resin. The resin was activated using the same procedure outline in section 1.3. To 1 gram of activated resin in a glass reaction vessel fitted with fritted filters, 1.60 g of BAA (11.5 mmol, 1 equiv.) and 5.88 mL of DIPEA (34.5 mmol, 3 equiv.) was added and the reaction was allowed to react for 2 hours under a gentle stream of nitrogen gas. The resin was then washed three times with dry DCM. To the resin loaded with BAA an amine solution in DMF (1 M) was added and left to react under nitrogen bubbling for 1 hour. The resin was washed three times with DCM then two times with DMF (Figure 4.3).

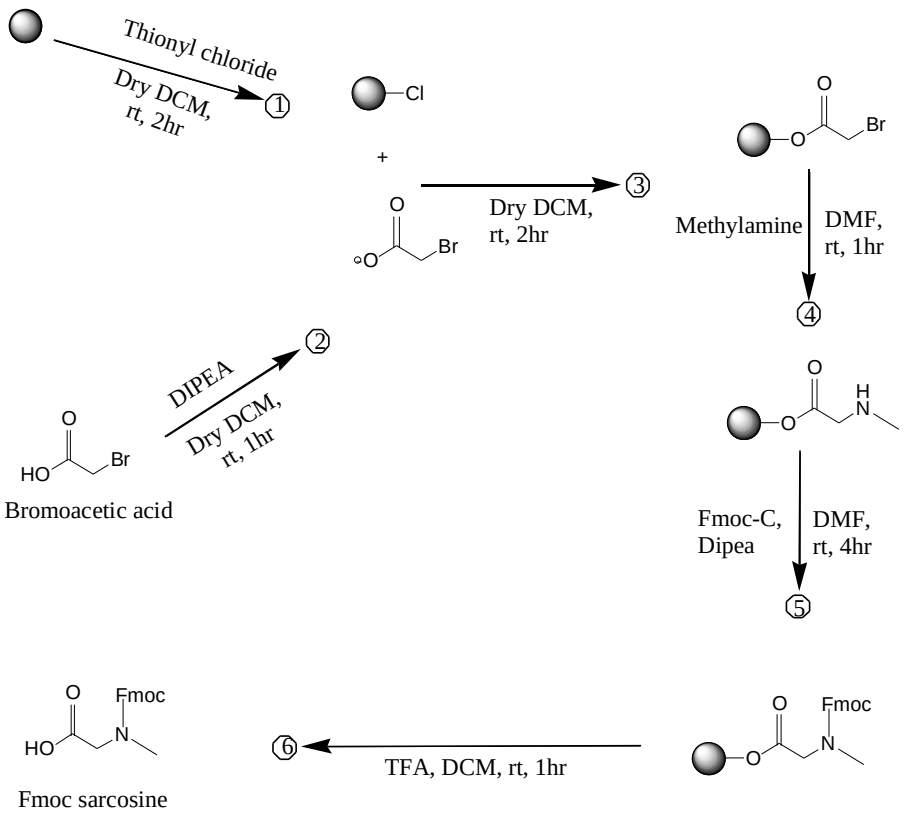


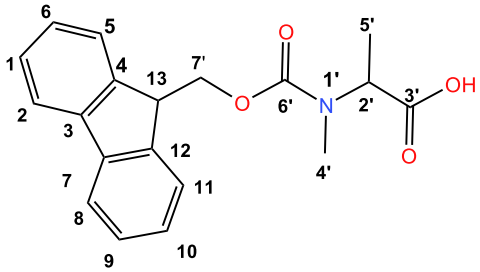
Figure 4. 3: Synthesis of Fmoc-sarcosine.

To the thoroughly washed resin, Fmoc-Cl (2.44 g, 9.43 mmol) dissolved in 1 M DIPEA (8 mL in DMF) and 9.25 mL DMF was added and allowed to react for 4 hours under nitrogen bubbling. The resin bound Fmoc-alanine peptoid was washed with (5×15 mL) DMF and (3×15 mL) DCM. The peptoid was then cleaved off the resin using a cleavage solution containing 5% TFA in DCM for 30 minutes. The TFA was removed from the filtered peptoid solution by azeotropic distillation with toluene. The evaporation was repeated several times on a rotary evaporator at 60-65°C. An additional 15 mL of DCM was added, and the organic phase was washed with 1 M HCl. The organic phase was dried over anhydrous magnesium sulphate and concentrated in *vacuo*. The crude product was purified via column chromatography on silica gel (19:1-DCM: MeOH) to give an off-white solid peptoid.

4.8. **Characterisation of peptoids and Bz-LL**

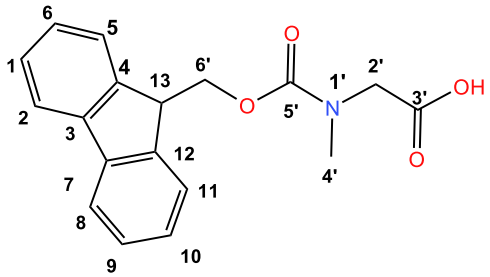
NMR spectra were recorded using a 400 MHz Bruker Avance spectrometer at 298 K and a BBI 5 mm probe. Chemical shifts are reported in ppm and calibrated using DMSO-d_6 solvent signals [2.50 for 1 H NMR and 39.52 for 13 C NMR].

4.8.1. *Fmoc-N-Methyl Alanine*



Physical characteristics: White solid; **^{1}H NMR** (400 MHz, DMSO-d_6): δ 7.85 (2H, d, J = 7.2 Hz, H-2 & H-8, ArH), 7.61 (2H, d, J = 7.6 Hz, H-5 & H-11, ArH), 7.38 – 7.58 (2H, m, H-1 & H-9, ArH), 7.30 - 7.32 (2H, m, H-6 & H-10, ArH), 4.50 - 4.54 (1H, m, H-13, CH), 4.22 – 4.32 (3H, m, H-2' & H-7', CH & CH_2), 2.73 -2.74 (3H, m, H-4', NCH_3), 1.26 (3H, d, J = 7.2 Hz, H-5', CH_3); **^{13}C NMR** (101 MHz, DMSO-d_6): δ 173.4 (O-*C*=O, C-3'), 156.0 (*C*=O, C-6'), 144.1, 141.0, 128.0, 127.5, 125.3, 120.4 (ArC), 67.1 (C-7'), 54.3 (C-2'), 46.9 (C-13), 30.7, (C-4'), 14.7 (C-5'). Specta in Figure A 29-32.

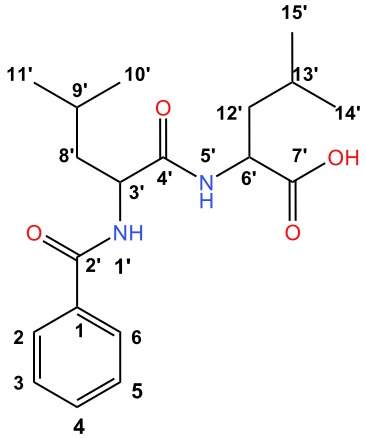
4.8.2. *Fmoc-Sarcosine*



Physical characteristics: White solid; **^{1}H NMR** (400 MHz, DMSO-d_6): δ 7.85 (2H, t, J = 6.8 Hz, H-2 & H-8, ArH), 7.57-7.65 (2H, dd, J = 7.2 Hz, H-5 & H-11, ArH), 7.40 - 7.43 (2H, m,

H-1 & H-9, ArH), 7.28 – 7.35 (2H, m, H-6 & H-10, ArH), 4.20 – 4.31 (3H, m, H-13 & H-6', CH_2 & CH), 3.89 (2H, d, *J* = 14.8 Hz, H-2', CH_2) 2.84 (3H, NCH_3, H-4'); **^{13}C NMR** (101 MHz, DMSO-d_6): δ 171.2 (*C*=O, C-3'), 155.9 (C-5'), 144.0, 141.0, 128.1, 127.5, 125.3, 120.4 (ArC), 67.2 (C-6'), 50.0 (C-2'), 46.9 (C-13), 35.2 (C-4'). Specta in Figure A 33-38.

4.8.3. *N-benzoyl-Leucyl-Leucine (Bz-LL)*



Physical characteristics: White solid; **^{1}H NMR** (400 MHz, DMSO-d_6): δ 8.39 (1H, d, *J* = 8.4 Hz, NH-1'), 8.14 (1H, d, *J* = 8.0 Hz, NH-5'), 7.41 (2H, d, *J* = 8.4 Hz, H-2 & H-6, ArH), 7.43 - 7.47 (3H, m, H-3, H-4 & H-5, ArH), 4.54 – 4.56 (1H, m, H-3', CH), 4.18 - 4.24 (1H, m, H-6', CH), 1.62 -1.69 (3H, m, H-8' & H-9', CH_2 and CH), 1.53 -1.59 (3H, m, H-12' & H-13', CH_2 and CH), 1.09 (12H, overlapping signals, H-10', H-11', H-14' & H-15', 4 x CH_3) ; **^{13}C NMR** (101 MHz, DMSO-d_6): δ 174.3, 172.7 & 166.8 (3 x *C*=O, C-7', C-4' & C-2'), 134.3.0 , 131,7, 128.6, 127.7 (ArC), 65.2 (C-8'), 51.8 (C-3'), 50.5 (C-6'), 40.7 (C-12'), 24.6 (C-9'), 24.5 (C-13), 23.4, 23.1, 21.6 & 15.4 (C-10', C-11', C-14' & C-15'). Specta in Figure A 39-43.

4.9. **References**

[1] R. B. Merrifield, "Solid Phase Peptide Synthesis. I. The Synthesis of a Tetrapeptide," *J. Am. Chem. Soc.*, vol. 85, no. 14, pp. 2149–2154, Jul. 1963, doi: 10.1021/ja00897a025.

[2] M. Pohl *et al.*, "Cyclic disulfide analogues of the complement component C3a. Synthesis and conformational investigations," *Int. J. Pept. Protein Res.*, vol. 41, no. 4, pp. 362–375, Apr. 1993, doi: 10.1111/j.1399-3011.1993.tb00452.x.

[3] S. Zhang, T. Govender, T. Norström, and P. I. Arvidsson, "An Improved Synthesis of Fmoc-N-methyl-α-amino Acids," *J. Org. Chem.*, vol. 70, no. 17, pp. 6918–6920, Aug. 2005, doi: 10.1021/jo050916u.

CHAPTER 5.

Journal Article: This article is published under the terms of the Creative Commons Attribution-NonCommercial-No Derivatives License (CC BY NC ND).

Reference: Cobongela SZZ, Makatini MM, Njengele-Tetyana Z, Sikhwivhilu LM, Sibuyi NRS. Design and synthesis of Acyldepsipeptide-1 analogues: Antibacterial activity and cytotoxicity screening. Arabian Journal of Chemistry. 2023; 16(8):105000. https://doi.org/10.1016/j.arabjc.2023.105000

Arabian Journal of Chemistry (2023) 16, 105000

King Saud University

Arabian Journal of Chemistry

www.ksu.edu.sa

ORIGINAL ARTICLE

Design and synthesis of Acyldepsipeptide-1 analogues: Antibacterial activity and cytotoxicityscreening

Sinazo Z.Z. Cobongela [a,b,c,*], Maya M. Makatini [a], Zikhona Njengele-Tetyana [b], Lucky M. Sikhwivhilu [c,e], Nicole R.S. Sibuyi [b,c,d,*]

[a] *Molecular Sciences Institute, School of Chemistry, University of the Witwatersrand, Johannesburg 2050, South Africa*
[b] *Health Platform, Advanced Materials Division, Mintek, Randburg 2194, South Africa*
[c] *Department of Science and Innovation (DSI)/Mintek Nanotechnology Innovation Centre (NIC), Advanced MaterialsDivision, Mintek, Randburg 2194, South Africa*
[d] *DSI/Mintek NIC, Biolabels Research Node, Department of Biotechnology, University of the Western Cape, Bellville 7535, South Africa*
[e] *Department of Chemistry, Faculty of Science, Engineering and Agriculture, University of Venda, Thohoyandou 0950, South Africa*

Received 20 December 2022; accepted 11 May 2023

Available online 18 May 2023

KEYWORDS

Acyldepsipeptides; Caseinolytic protease; Antimicrobial peptides; Solid phase peptide synthesis;

Palmitic acid; Adamantane

Abstract

Acyldepsipeptides (ADEPs) are receiving more attention as prospective antimicrobial agents due to their unique mode of action and chemical properties. However, their therapeutic potential is limited by their poor pharmacokinetic properties. Chemical modifications have been successful in improving the biocompatibility and bioavailability of ADEPs. In the current study, ADEP1 was modified by introducing a disulphide linkage, replacement of the octa-2,4,6-trienoic acid (OTEA) with either adamantane (Ada) or palmitic acid (Pal), and lastly, comparing the use

of D versus L amino acids. The antibacterial effects of the ADEP1 analogues were investigatedin Gram-positive and Gram-negative strains using agar well diffusion and microdilution assays. Cytotoxicity was evaluated in human embryonic kidney (HEK)-293 and colon cancer (Caco-2) cells by the MTS assay. Using solid phase peptide synthesis (SPPS), the percentage yield of the synthetic peptides was increased to > 37% with > 96% purity. The anionic ADEP1 analogues demonstrated a broad-spectrum antibacterial activity.

Abbreviations: ADEP, Acyldepsipeptide; AMP, Antimicrobial peptide; ClpP, Caseinolytic protease; MIC, Minimum inhibitory concentration; MBC, Minimum bactericidal concentration; SPPS, Solid phase peptide synthesis; OTEA, Octa-2,4,6-trienoic acid; Ada, Adamantane; Pal, Palmitate

* Corresponding authors.E-mail addresses: SinazoC@mintek.co.za (S.Z.Z. Cobongela), NicoleS@mintek.co.za (N.R.S. Sibuyi). Peer review under responsibility of King Saud University.

Production and hosting by Elsevier.

https://doi.org/10.1016/j.arabjc.2023.105000

1878-5352 © 2023 The Author(s). Published by Elsevier B.V. on behalf of King Saud University.

This is an open access article under the CC BY-NC-ND license (http://creativecommons.org/licenses/by-nc-nd/4.0/).

Although the ADEP1 analogues did not display the expected antibacterial activity in relation to the parent structure, they were not cytotoxic againstthe tested cell lines. This study proved that biocompatibility of natural ADEPs can be improvedby modifying some of its chemical groups. Further studies are required to enhance the antibacterial activity of the ADEP1 analogues either by structural modifications or through supplementation of these anionic antimicrobial peptides (AMPs) with divalent metal ions.

© 2023 The Author(s). Published by Elsevier B.V. on behalf of King Saud University. This is an open access article under the CC BY-NC-ND license (http://creativecommons.org/licenses/by-nc-nd/4.0/).

1. Introduction

The rapid increase in antimicrobial resistance remains a major concern in public health, which warrants the development of new and effective antimicrobial agents. Acyldepsipeptides (ADEPs) have gained atten- tion as potential antimicrobial agents as they have a different modeof action to current drugs and might be able to overcome drug resis- tance (Cobongela et al., 2022). ADEPs are cyclic antimicrobial pep- tides (AMPs) produced by *Streptomyces hawaiiensis* (Michel & Kastner, 1985) as part of their innate immune response against resident bacteria, and were reported to be mostly active against Gram-positive bacterial strains (Culp & Wright, 2017). ADEPs were reported to bind and deregulate the bacterial caseinolytic protease (ClpP) (Bro¨ tz- Oesterhelt et al., 2005), a cytosolic protease responsible for homeo- static degradation of misfolded and aggregated proteins and peptides (Chandu & Nandi, 2004). Under controlled homeostatic conditions, ClpP is regulated by AAA + chaperone-like ATPases, which include the ClpC1, ClpX, and ClpA. These Clp-ATPases specifically bind to the hydrophobic pockets of the ClpP, resulting in an active proteolytic conformation (Bro¨ tz-Oesterhelt et al., 2005). ADEPs act by mimickingthe binding of the Clp-ATPases to ClpP, and this inhibits the binding of Clp-ATPases while inducing uncontrollable proteolysis (Kim et al., 2001; Lee et al., 2010; Li et al., 2010). The increased proteolytic activityof ClpP rapidly degrades both essential and nonessential bacterial pro-teins leading to bacterial cell death (Cobongela et al., 2022).

There is a number of natural and synthetic ADEP analogues, which have been reported in literature. The first reported ADEP, ADEP1 also called ADEP Factor A (A54556A), was isolated from cul- tured *Streptomyces hawaiiensis*. The antibacterial activity of ADEP1 against Gram-positive bacteria (Bro¨ tz-Oesterhelt et al., 2005; Goodreid et al., 2016), Gram-negative bacteria (Goodreid et al., 2014), as well as its bactericidal action against a number of antibiotic-resistant strains (Goodreid et al., 2016) made this compoundan attractive component in antibiotic research. As a result, several synthetic derivatives of the peptide have been developed over the past fewyears. However, a major drawback associated with this class of novel antibiotics, and other therapeutic AMPs, are their unfavorable pharmacokinetic properties and cytotoxic traits (Brunetti et al., 2016; Lewis & Richard, 2015). This therefore raises a need to improve these natural peptides to drug-like molecules with minimal to no cytotoxicity, high selectivity, good solubility, increased proteolytic stability, etc.This in turn should increase the bioavailability of these peptides and consequently improve their therapeutic activity.

Several strategies, such as chemical modification and use of drug carriers, have been successful in increasing the bioavailability and efficacy of AMPs in the past (Fadaka et al., 2021). A number of synthetic AMP analogues have been modified to produce derivatives with improved physicochemical properties compared to their natural coun-terparts. A change even in a single amino acid in the peptide sequence can have significant effects on the AMP's behavior within the biolog- ical environment as well as in their bioactivity (Zai et al, 2021; Zhouet al, 2020). In the case of Temporin-PF, deletion or substitution of amino acids resulted in analogues with reduced hemolytic activity,but lesser or no antibacterial activity (Zai et al, 2021). The use of cationic and hydrophobic amino acids in Dermaseptin-PS3 (Tan et al.,2018) and AcrAP1 (Ma et al., 2019) improved their interaction with the negatively charged cellular membrane, resulting in higher potency.Some of these factors were taken into consideration when derivatizing the ADEP1 in this study. The modifications done on ADEP1 include the incorporation of D amino acids, cyclization via disulphide bond between two cysteine side chains, and ADEP1 tail replacement with lipophilic molecules. Therefore, the study was aimed to design and syn-thesize ADEP1 analogues and investigate their antibacterial activity and cytotoxicity effects.

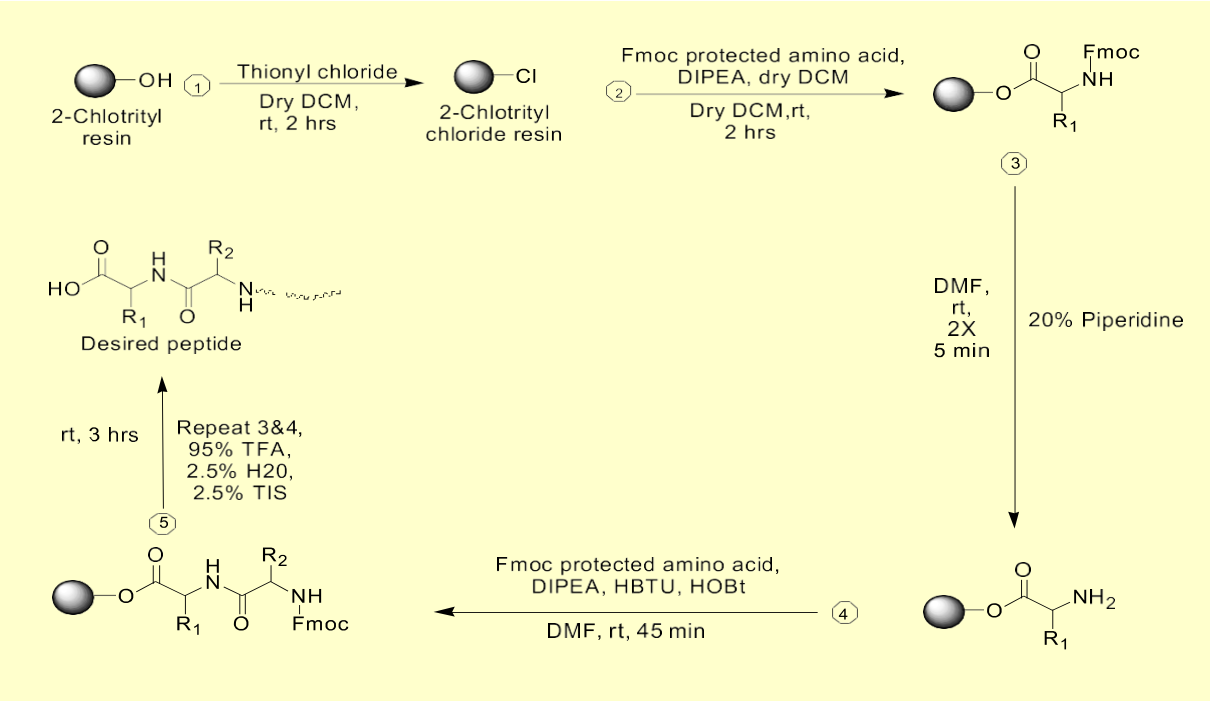
2. Materials and methods

2.1. Materials

2-Chlorotrityl chloride resin, N,N,N⁰,N⁰-Tetramethyl-O-(1H-benzotriazol-1-yl) uronium hexafluorophosphate (HBTU), Fluorenylmethyloxycarbonyl chloride (Fmoc) amino acids, Triisopropylsilane (TIS), and Hydroxybenzotriazole (HOBt) were purchased from GL Biochem Ltd., Shanghai, China. N, N' Dimethylformamide (DMF) Dichloromethane (DCM), Diisopropylethylamine (DIPEA), Acetonitrile, and Dimethyl sulfoxide (DMSO) were purchased from Radchem (PTY) LTD., Alberton, South Africa. Palmitic acid (Pal), 1-Adamantanecaboxylic acid (Ada), Trifluoroacetic acid (TFA), Thionyl chloride, Formic acid, Iodine, Dulbecco's modified Eagle Medium (DMEM), phosphate, Trypsin, Penicillin-Streptomycin, Fetal bovine serum (FBS), and trypanblue stain dye were purchased from Sigma Aldrich (St Louis, MO, USA). Human embryonic kidney (HEK)-293 and Colorectal adenocarcinoma (Caco-2) were purchased from Cellonex (Randburg, Gauteng Province, South Africa).

2.2. Solid phase synthesis of ADEP1 analogues

The ADEP1 analogues were synthesized *via* a modified solid phase peptide synthesis (SPPS) using Fmoc-amino acids, following a previously reported method as depicted in Scheme 1 (Merrifield, 1963). The 2-chlorotrityl chloride resin was used as a solid structure and activated for 2 h by 20% thionyl chloride in distilled (dry) DCM solution. The first amino acids in all ADEP1 analogues were loaded at four equivalence to the activated resin with five equivalence of the DIPEA. The concentration of reagents used during coupling cycles of the peptides were 0.5 M DIPEA, 0.19 M HBTU, 0.095 M HOBt and 0.2 M amino acids. Each amino acid was double-coupled while Pal or Ada were triple-coupled. The peptide sequence, stereochemistry and net charge are summarized in Table 1.



Scheme 1 Schematic representation of a solid phase peptide synthesis of ADEP1 analogues.

Table 1 Peptide sequences, stereochemistry, and net charge.

Peptide code	Peptide sequence	Stereochemistry	Net charge
ADEP1	OTEA-FSA(m)AA(m)P	L	(pH 7.0)
SC005	Pal-FCPAAPC	D	0
SC006	Ada-FCPAAPC	D	—1
SC007	Ada-FCPAAPC	L	—1
SC008	Pal-FCPAAPC		

Note: m denotes methyl.

2.2.1. Loading capacity and yield of ADEP1 analogues

The yield of the peptides was determined by adding duplicate samples of 5 to 10 mg into 1 mL of 20% piperidine in DMF. The reaction was left to shake for 20 min at room temperature, and then centrifuged at 6000 rpm for 10 min. This concentra- tion of piperidine cleaves off the Fmoc from the amino acids. Piperidine and Fmoc forms a dibenzofulvene-piperidine byproduct that is measurable at 301 nm. The supernatant was diluted 1:100 in DMF and read at 301 nm using Ultra- violet visual (UV-viz) spectrophotometer (SpectraMax Plus384 Microplate Reader, Molecular Devices, California, United States). The loading capacity, theoretical yield, expected yield and percentage yield were calculated using these equations(EQ):

$$L = V(A)/\varepsilon(w) \quad (1)$$

$$Y_t = L\,x\,m\,x\,MM \quad (2)$$

$$Y_e = 0.97^{mer}\,x\,Y_t \quad (3)$$

$$Y_e = 0.97^{mer}\,x\,Y_t\;\; Yield = m_p/\;Y_e$$

Where L is loading capacity, V is final volume, A is absor- bance at 301 nm, e is extinction coefficient of the dibenzofulvene-piperidine, w is mass of the loaded resin in mg, Y_t is theoretical yield, m is mass of the total resin, MMis molecular weight of the peptide, Y_e is the expected mass,m_p is mass of the peptide.

2.3. Cyclization of ADEP1 analogues

2.3.1. Iodine-mediated oxidation

Cyclization of the Ada-containing peptides (SC006 and SC007) was performed as previously described using 10 equiv-alence iodine in DMF: water in a 4:1 ratio (Pohl et al., 1993). The reaction was carried out on resin bound peptides, leftshaking at room temperature for 40 min and the reaction was stopped by adding 1 M L-ascorbic acid. The resin was washed thoroughly by 1 M L-ascorbic acid followed by DMF and then DCM. The peptides were then cleaved from the resin using a cleavage solution containing 95% TFA, 2.5% H_2O, and 2.5% TIS. The solution was filtered and sol- vents were removed using rotary evaporator (Rotavapor R- 210, Buchi Laboratory Equipment, St Gallen, Switzerland) set at 60-65 °C. Toluene:TFA solution at a 10:1 ratio was addedduring the evaporation process to aid the removal

of TFA, which usually binds on the free carboxylic end of the peptides. A complete removal of the solvents left an oily and golden brown residual on the round bottom flask which was dissolved in acetonitrile containing 5% dimethyl sulfoxide (DMSO) for further analysis.

2.3.2. DMSO-mediated oxidation

The Pal-containing peptides (SC005 and SC008) were cleaved using the TFA cleavage solution described above, and subse- quently cyclized using DMSO. Briefly, SC005 and SC008cyclization was carried out in acetonitrile containing 20% DMSO. The reaction was left shaking overnight at room tem- perature. The solvents were removed at 60-65 ℃ using rotary evaporator. The DMSO residues were removed by a lyopholy- zer (LyoQuest, Telstar, Terrassa, Barcelona). The peptides were also re-suspended in acetonitrile containing 5% DMSO for further analysis.

2.4. ADEP1 analogues purification by HPLC

The peptides were purified using Preparative High-pressure liquid chromatography (prep-HPLC) (Shimadzu, Kyoto, Japan) with a prep-HPLC c-18 column with 30 × 250 mm, 10 mm dimensions (Phenomenex, California, United States) with UV detection at 215 and 245 nm. The purification method was a 20 min running time with 20 mL/min flow rate. The gra- dient elution was 5–95% B (0.1% FA in acetonitrile) in A (0.1% FA in water) for 12 min and 95% B in A from 12 to20 min. Molecular weight of the peptides were confirmed using Thermo Scientific Ultimate 3000 (Bruker, Massachusetts, Uni-ted States). The HR-LCMS also was also performed on a c-18 column (5 µm, 100 Å, 4.60 mm x 150 mm) with a two-buffer solvent system, solvent A and B at a flow rate of 0.3 mL/min. The expected peptide molecular weight confirmed by HR-LCMS eluted between 13 and 14 min on the prep-HPLC. The corresponding prep-HPLC peaks were therefore collected and solvent removed using rotary evaporator at 60-65 ℃. The residuals were lyophilized using a freeze dryer for further bio- chemical analysis.

2.5. Antibacterial activity tests of the ADEP1 analogues

The antibacterial activity of the ADEP1 analogues was tested against three Gram-positive (*Bacillus subtilis* ATCC 11774, *Staphylococcus aureus* ATCC 25923 and Methicillin-resistant *Staphylococcus aureus* (MRSA) ATCC 43300) and two Gram-negative (*Escherichia coli* ATCC 33876 and *Pseu- domonas aeruginosa* ATCC 15442) bacterial strains using agar well diffusion and microdilution assays according to previously reported protocols (Adeyemi et al., 2018). The bacterial strains were purchased from the American Type Culture Col- lection (Manassas, Virginia, USA).

2.5.1. Agar well diffusion method

Antibacterial activity of the ADEP1 analogues were first screened using an agar well diffusion assay, a modified Kirby-Bauer disc diffusion method (Tan & Ng, 2006). The bacterial strains were cultured at 37 °C (250 rpm) for overnight, and bacterial cultures (200 mL) were then spread onLB agar plates followed by addition of 100 mL of the ADEP1 analogues at 100, 500, and 1000 mM (ADEP1 analogues stock solutions were prepared in 5% DMSO in PBS) in 8 mm agar wells. Ampicillin (11.5 mM) was used as a positive control against *E. coli*, while gentamicin (0.84 mM) was used as posi- tive control against *B. subtilis*, *S. aureus*, MRSA and *P. aerug- inosa*. Negative controls contained 2% DMSO (without the antibiotics/test compounds) in LB broth. The plates were then incubated overnight at 37 °C and the diameter of the zones of inhibition were measured using vernier caliper.

2.5.2. Minimum inhibitory concentration and minimum bactericidal concentration

The minimum inhibitory concentration (MIC) and the mini- mum bactericidal concentration (MBC) values of the ADEP1 analogues against the selected bacterial strains were deter-mined using the microdilution assay. Briefly, the tested strains were cultured at 37 °C overnight and the concentrations were adjusted to ~ 1.5×10^8 CFU/mL prior to use. Two-fold serial dilutions of the peptides, ranging from 2000 to 15,625 mM, were added to the wells at 100 mL followed by 100 mL of the diluted bacterial cultures, which yielded the following final peptide concentrations: 1000, 500, 250, 125, 62.5, 31.25, 15.625, and 7.8125 mM 3.9. The peptides were tested alongsideampicillin and gentamycin as positive controls. The plates wereincubated overnight at 37 °C. The MIC values were recordedas the lowest concentration of peptides at which there wasno visible bacterial growth. Three independent experimentswere performed for each bacterial strain.

For MBC, 1 mL of the samples from the MIC assay were transferred to fresh LB agar plates and incubated overnight at 37 °C. MBC was represented as the lowest concentrationat which there was no observed bacterial growth. The test was performed in triplicates for each ADEP1 analogue.

2.6. Cell viability studies

The cytotoxicity of the ADEP1 analogues was investigated on HEK-293 and Caco-2 cell lines using the

MTS cell prolifera- tion assay. The cells were purchased from Cellonex (South Africa) and cultured in DMEM containing 10% fetal bovine serum (FBS) and 1% penicillin–streptomycin at 37 °C in a 5% CO_2 humidified incubator. For the cell viability assay, the cells were seeded at a density of $1x10^5$ cells/mL in 96 well plates (100 mL/well). The plates were incubated at 37 °C over- night, after which the ADEP1 analogues at 15.6 mM to 2 mM were added. The plates were incubated at 37 °C for an addi- tional 48 h. Auranofin (0.78125 - 100 mM) was used as a pos- itive control and 2% DMSO was used as a negative control. The MTS dye reagent (10%) was added to the wells and incu- bated for 4 h. The absorbance was read at 490 nm wavelength using SpectraMax Plus 384 Microplate Reader. The percent- age cell viability was calculated using the equation below.

$$\%\ Cell\ viability = \left(\frac{OD\ of\ test\ sample}{OD\ of\ control}\right) x100\%$$

2.7. Statistical analysis

Differences between groups were assessed by one-way analysisof variance (ANOVA) followed by two-tailed *t*-test analysis ofvariance using the GraphPad Prism 9.510. Results with $p < 0.05$ were considered statistically significant and were expressed as the mean ± SEM of $n = 6$.

3. Results and discussion

3.1. Synthesis and characterization of ADEP1 analogues

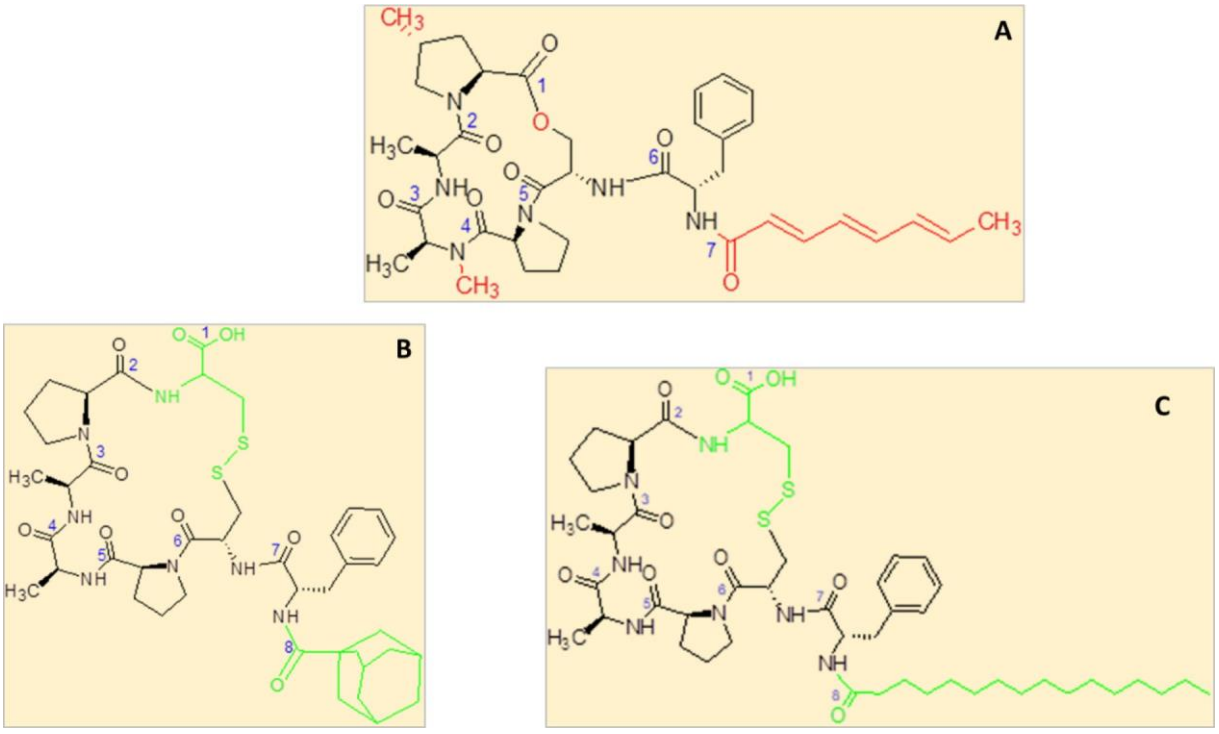
ADEPs have potential to overcome microbial resistance to antimicrobial agents as they follow a different mode of action, however, their bioactivity is limited by metabolic instability and side effects, among others. There were several strategies that were previously used to overcome these challenges. Inthe current study, the modifications introduced to the ADEP1 structure (Scheme 2A) were motivated by: 1. The need to pro- duce low cost drug candidates in high yield by developing a shorter synthetic route and use of natural peptides. Therefore, 4-methyl proline and N-methylated alanine were substituted with natural amino acids (Pro2 and Ala4) (Scheme 1B and C). 2. To improve lipophilicity and biocompatability by replac- ing OTEA with Ada in SC006 and SC007 (Scheme 2B) or Pal in SC005 and SC008 (Scheme 2C). 3. Incorporation of D- amino acids to improve metabolic stability and prevent biodegradation. SC005 and SC006 contained D-amino acids while SC007 and SC008 were made of L-amino acids.

The structure of ADEP1 is cyclized by an ester bond between the carboxylic end of Pro1 and the hydroxyl func- tional side chain of Ser5. The ester bond linkage was replaced

by a disulphide bond by adding Cys1 and substituting Ser5 with Cys6. Substitution of amino acid residues with Cys pro- duce disulphide bridges and increase stability of the peptides. For example, mutations in subtilisin E that resulted in replace- ment of Gly61 and Ser98 with Cys residues increased its activ-ity, thermal stability and shelf-life (Liu et al., 2016; Takagiet al., 1990; Zabetakis et al., 2014).

The synthesis of ADEP analogues via SPPS generally pose difficulties in cyclization with the ester bond (Wen et al., 2008;White & Yudin, 2011). The natural ADEPs synthesis in bio- logical systems easily form the ester bond linkage through bac-terial depsipeptide synthases (Alonzo & Schmeing, 2020). However, chemical synthesis make use of esterification tech- niques, which result in poor (6%) yields (Eyermann et al., 2020). Although fragment convergence synthesis have better yields, this synthesis route does not follow the normal peptide synthesis. It uses different protecting groups, prone to inter- molecular reaction, and it also comes with numerous coupling and purification steps (Goodreid et al., 2014, 2015; Li et al., 2017). This synthesis approach disassembles the ADEPs into three fragments namely tripeptide, linkage, and Phe-heptenamide (Li et al., 2017). The incorporation of disulphide cyclization allows for a simple SPPS using one protectinggroup (Fmoc), with single cleavage and purification steps.

HOBt was used as a coupling additive to suppress racem- ization. It is also a nucleophilic catalyst, which helps acceleratethe rate of the coupling reaction time (Al-Warhi et al., 2012). HOBt considerably reduced coupling reaction times from 1 h to 45 min while reducing the presence of impurities. The expected molecular mass (MM) of the analogues was con- firmed by MS. Figs. A1, A3, A5, and A7 shows MM[M + 1] of the peptides before cyclization. After cyclization with iodine or 20% DMSO, the MM observed on the MS



Scheme 2 ADEP1 analogues in relation to ADEP1 parent structure (A). The ADEP analogues were modified with either Ada (SC006and SC007) (B) or Pal (SC005 and SC008) (C).

(Figs. A4, A6, and A8) suggested the loss of the two hydrogen molecules during the formation of the disulphide bond. This confirmed the synthesis of cyclic analogues.

With the analysis on both prep-HPLC and LCMS, the pep- tides presented a higher retention time (Figs. A9-A12). This was attributed to the hydrophobic and nonpolar nature of the peptides. Out of seven amino acids in their sequence, five of those (Pro, Ala, and Phe) possess nonpolar and hydropho- bic side chains. In addition, the formation of the disulphide bond reduced the polarity and hydrophilicity of the Cys resi- dues. The peptides containing Pal were analysed with a longer LC method (16 min) compared to the Ada-containing peptides (14 min). The LCMS chromatogram and spectra of the four ADEP1 analogues are presented in Table 2. The analogues presented high purity (96%) with improved yields.

The anionic nature of all the analogues is due to the ionis- able -COOH of Cys at neutral pH range to give -COO^-. This was confirmed by their negative zeta potential values and the net charges of the ADEP1 analogues reported in Table 2. Asa consequence of using the Cys1 and Cys6 thionyl groups to cyclize the peptides, the -COO^- of Cys1 was exposed and there-fore giving the analogues a negative net charge. The additionof the two Cys also enlarged the ring, which can allow for slight conformational freedom.

3.2. Antibacterial activity of the ADEP analogues

The potential antibacterial activity of the ADEP1 analogues was screened against the benign (*B. subtilis* and *E. coli*) and the pathogenic (*P. aeruginosa, S. aureus* and MRSA) strains. Table 3 shows that the Pal-based ADEP1 analogues had higher activity compared to Ada-based ADEP1 analogues, in the order SC008 > 5 > 6 > 7. The Pal-based ADEP1 ana- logues were active against all the tested bacterial strains with SC008 showing more potency compared to its D-enantiomer, SC005. The Ada-based ADEP1 analogues showed selective activity, SC006 did not show any activity on *P. aeruginosa* while SC007 showed no activity on *S. aureus* and *E.coli*. Pal is a long chain of hydrocarbons (saturated fatty acid) that bet- ter mimics the OTEA than the Ada. Pal has been used to increase lipophilicity of drug-like compounds (Carta et al.,2017; Irby et al., 2017), and its conjugation to ADEP1 ana- logues increased their lipophilicity, which enhanced their inter- action with the bacterial cell and increased cellular uptake. Both Ada and Pal are lipophilic molecules and incorporatedin the ADEP1 analogues to increase their cell permeation abil- ity. Fatty acids (linoleic, oleic acid, Pal, and Ada) are exploited in pharmaceuticals to serve as chemical cell permeability enhancers (Cizinauskas et al., 2017). They are widely used as drug delivery systems and targeted therapies in biomedical applications (Spilovska et al., 2016; Schleyer, 1957; Stimac et al., 2017). However, agar diffusion methods have been reported to lack sensitivity

for non-polar molecules (Eloff, 2019) and highly dependent on their ability to diffuse in the agar. The microdilution assay was thus used to further evalu- ate the activity of the peptides against all the bacterial strains, their MIC and MBC values are presented in Table 4.

All the ADEP1 analogues showed a broad-spectrum antibacterial activity on the selected bacterial species at con- centration range of 125 – 500 mM (MIC) and 125 – 750 mM (MBC). The mode of action of these ADEP1 analogues has not been determined yet. However, previous reports have high- lighted the specific mechanism of ADEP by introducing ClpP mutations in *B. subtilis*, *S. aureus*, and *E. coli*. The bacterial strains with ClpP mutation showed high resistance to ADEP treatment (Brotz-Oesterhelt & Sass, 2014; Malik et al., 2020). This suggested that it is unlikely for the ADEPs to target any bacterial component than ClpP, thus making their mode of action target specific. The ADEPs binds to the ClpP, which then degrade proteins necessary for whole cell metabolism andsurvival (Frees et al., 2014; Sass et al., 2011). Therefore, the ADEP1 analogues might follow mode of action similar tothe one for ADEPs due to their structural similarities.

All the ADEP1 analogues were able to inhibit growth of theGram-positive (MIC = 63–125 mM) and Gram-negative (MIC = 250 mM) bacterial strains. The Gram-negative bacte- ria showed less susceptibility towards the ADEP1 analogues. *E. coli* presented the highest resistance with an MIC of500 mM for all the analogues while *P. aeruginosa* was inhibitedby an MIC of 250 mM for SC0006 – 8 and more susceptible to SC005 (MIC = 125 mM). This is in line with what has been reported about ADEPs or anionic AMPs which have higher potency on Gram-positive than Gram-negative bacteria (Culp & Wright, 2017). Overall, the peptides showed similar antibacterial trends despite different antimicrobial activities previously discussed between the D- and L-enantiomers. In lit- erature, D-enantiomer peptides possess higher antimicrobial activity compared to the L-enantiomer (Ye & Aparicio, 2022), this might be due to their (D-enantiomer) proteolytic stability leading to increased bioavailability *in vivo*. Natural peptides, ADEPs included, consist of L-amino acids, which are susceptible to enzymatic degradation (Vlieghe et al., 2010), while peptides composed of D-amino acids may escape protease degradation thereby increasing their bioavailability (Garton et al., 2018; Uppalapati et al., 2016). Similarly, disul-phide bonds also play a major role in peptide/protein structure stability by increasing resistance to proteolysis while also increasing activity (Siddiqui et al., 2005; Trivedi et al., 2009).

Table 2 Peptide analysis by HR-LCMS and Zetasizer.

Peptide code	Retention time (minutes)	Calculated mass (MM = g/mol)	Chemical formula	Found $[M + H]^+$ m/z[a]	% purity	% yield	Zeta potential (mV)
SC005	8.8 —3.8 ± 1.1	943.51	$C_{47}H_{73}N_7O_9S_2$	944.4973	99.9	46	—7.2 ± 1.6
SC006	9.7 —3.9 ± 0.8	867.37	$C_{42}H_{57}N_7O_9S_2$	868.3730	98	37	
SC007	10.2 —6.9 ± 1.5	867.37	$C_{42}H_{57}N_7O_9S_2$	868.3747	96	39	
SC008	8.5	943.51	$C_{47}H_{73}N_7O_9S_2$	944.4621	99.9	45	

Table 3 Diameter of zones of inhibition of CC ADEP analogues.

Microbes	[Peptide] mM	SC005 (mm)	SC006 (mm)	SC007 (mm)	SC008 (mm)	0.84 mM Gentamicin (mm)	11.5 mM Ampicilin (mm)
B. subtilis	100	6.5 ± 0.14	0	0	8.5 ± 0.14	12 ± 0.16	NT
	500	8.5 ± 0.32	6.5 ± 0.08	6.5 ± 0.16	8.5 ± 0.32		
	1000	10.5 ± 0.25	6.5 ± 0.18	8.5 ± 0.16	8.5 ± 0.25		
S. aureus	100	0	0	0	0	12 ± 0.08	NT
	500	0	0	0	0		
	1000	0	0	4.5 ± 0.180	0		
MRSA	100	0	0	0	24.5 ± 0.14	8.8 ± 0.16	NT
	500	10.5 ± 0.17	0	0	24.5 ± 0.32		
	1000	10.5 ± 0.16	6.5 ± 0.14	0	24.5 ± 0.25		
P. aeruginosa	100	0	0	0	6.5 ± 0.14	12 ± 0.16	NT
	500	0	0	4.5 ± 0.39	8.5 ± 0.32		
	1000	6.5 ± 0.31	0	10.5 ± 0.39	8.5 ± 0.25		
E. coli	100	0	6.5 ± 0.20	0	8.5 ± 0.14	NT	11.5 ± 0.16
	500	10.5 ± 0.22	6.5 ± 0.17	0	8.5 ± 0.32		
	1000	10.5 ± 0.13	6.5 ± 0.18	0	8.5 ± 0.25		

NT = Not tested.

Table 4 MIC and MBC of the ADEP analogues on bacteria.

ADEP1 analogues	*B. subtilis*		*S. aureus*		*MRSA*		*P. aeruginosa*		*E. coli*	
	MIC (mM)	MBC (mM)	MIC (mM)	MBC (mM)	MIC (mM)	MBC (mM)	MIC (mM)	MBC (mM)	MIC (mM)	MBC (mM)
SC005	125	125	63	125	125	250	125	250	500	750
SC006	250	250	63	125	250	250	125	250	500	750
SC007	125	125	63	125	250	500	125	250	500	750
SC008	125	125	63	125	250	500	125	250	500	750
Gentamicin	26.1	52.3	0.5	1.0	26.2	52.4	418.8	837.5	NT	NT
Ampicillin	NT	NT	NT	NT	NT	NT	NT	NT	2862	5724

All four ADEP1 analogues were cyclized with a disulphide bond to replace the ester bond linkage that has been reported to be susceptible to enzymatic degradation (Finer & Santerre, 2004; Yourtee et al., 2001).

The naturally occurring ester bond has not yet been reported to play a vital role in molecular conformation, inter- action with ClpP, and biological activity of the ADEPs. How- ever, a study by Li and colleagues (Li et al., 2017) made strides in comparing the effect of using different linkage motifs on the conformational behavior and bioactivity of the ADEP ana- logues. Their study showed a significant decline in *in vitro* bio- chemical activity when the ester bond was substituted with amide bond or *N*-methyl amide bond (Li et al., 2017). The same phenomenon was observed in this study, where the MIC values for ADEP1 analogues were multiple folds higher than that reported for ADEP1. Another study presented chal- lenges of incorporating 4-methylated Pro and N-methyl-Ala during synthesis of ADEPs, and removing the methyl groups in the amino acids resulted in complete loss of antibacterial activity (Hinzen et al., 2006). This then highlighted the impor- tance of methyl amino acids in the antimicrobial potency of ADEPs.

Although the ADEP1 analogues had antibacterial activity in the micromolar range, they showed great bactericidal effects. Bactericidal effects (MBC) of potential drugs are vital as they represent a concentration that completely eradicates bacteria rather than inhibiting their growth. For example, ADEPs has shown inhibition of cell division in *B. subtilis*, however, bacterial cells recover upon incubation on a fresh media (Mayer et al., 2019). This shows that even though the MICs of most ADEPs are low, they lack the bactericidal effect. In some cases, their bactericidal effect is multiple folds higher than the MIC (Sass et al., 2011). In this study, all four tested analogues had the MIC that was at the same concentration as the MBC against *B. subtilis*. Usually, the MBC of antimi- crobial drugs is greater or equals to two fold of the MIC (Levison & Levison, 2009), as observed in the other three bac-terial strains where MBC was twice the concentration of MIC.

3..3 Cytotoxicity

It is imperative that antimicrobial agents are selective in their actions to prevent or reduce off-target effects. However, the biocompatibility of natural ADEPs is challenged by their non-selectivity and toxicity to mammalian cells. Similar to microorganisms, human cells also express ClpP (hClpP) which is structurally similar to its bacterial counterparts and might respond the same way to the ADEPs. Human proteostasis is also coordinated by a network of chaperones and proteases including hClpP (Kang et al., 2005). The activity of hClpP is regulated by ClpX, an ATP-dependent protease, and dysregu- lated by ADEPs (Cole et al., 2015). Thus, the effects of ADEP1 analogues were evaluated on HEK-293 and Caco-2 cells at 2 mM using MTS assay. There was no significant reduc- tion in cell viability of HEK-293 (Fig. 1A) and Caco-2 (Fig. 1B) cells in response to increasing concentrations of ADEP1 analogues. Fig. 1C shows that Auranofin, a food and drug administration (FDA) approved antirheumatic drug (Boullosa et al., 2021), was cytotoxic to all the cells at 0. 125 mM.

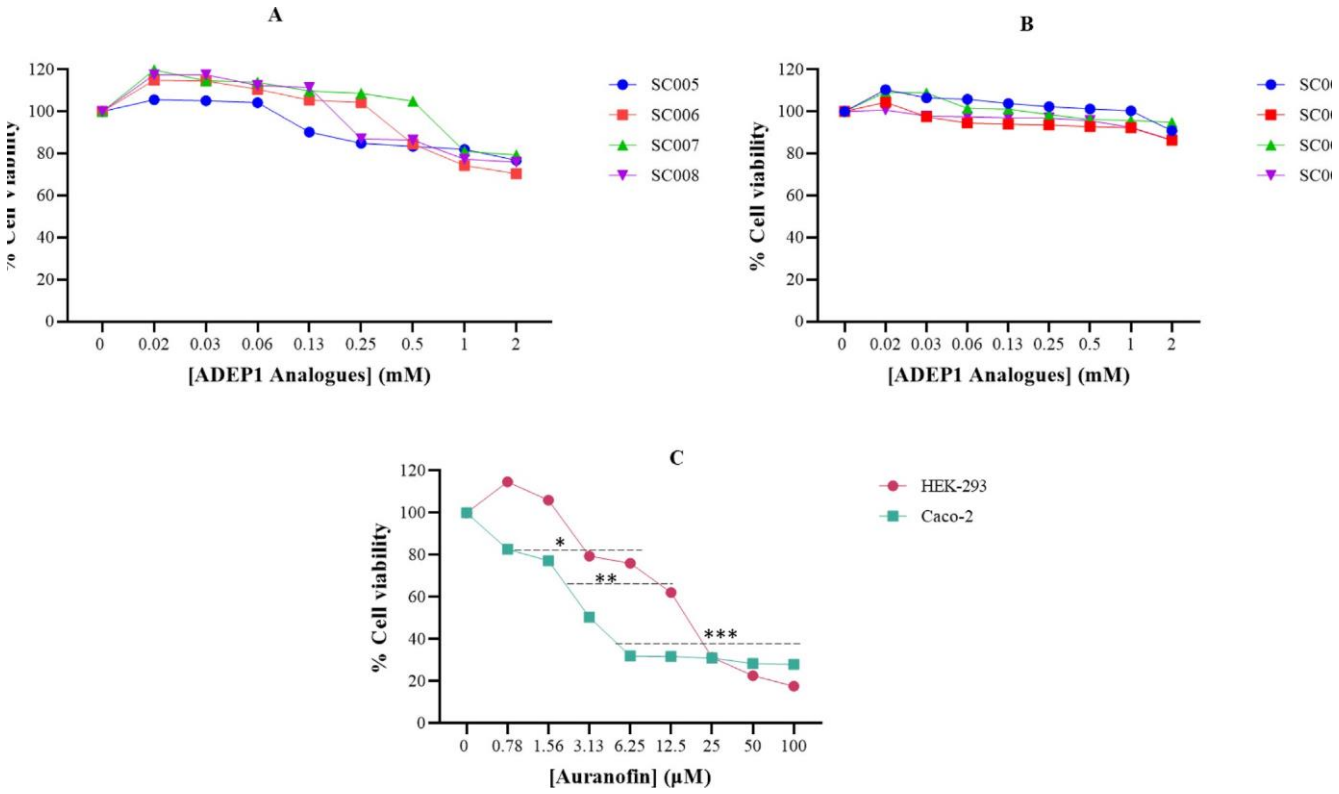


Fig. 1 Effect of ADEP analogues on the viability of HEK-293 (A) Caco-2 (B) cells, and Auranofin treatment on HEK-293 and Cac-2(C). Cell viability was assessed by MTS assay, where $p < 0.05$ was considered statistically significant. *=$p < 0.05$, **=$p < 0.01$, and***=$p < 0.001$.

The mode of action involved in the dysregulation of hClpP and the physiological consequences have not been thoroughly investigated. However, in 2018, Wong and colleagues reported that the dysregulation of hClpP by ADEPs induced cytotoxic- ity to various human cell types including HEK-293 cells (Wong et al., 2018). The concentration dependent toxicity effect of ADEPs on hClpP was demonstrated *in vitro* and *in vivo* using different ADEPs and ADEP analogues (Wonget al., 2018). Toxicity has been the major hindrance in the development of ADEPs as active pharmaceutical ingredient. The ADEP1 analogues under study showed no significant tox- icity at a dose multiple folds higher (2 mM) than their MICs. The ADEP1 analogues in this study showed an essential improvement in their biocompatibility compared to the cyto- toxicity of ADEP analogues in literature. Generally, ADEPs start showing toxicity at concentrations from 0.215 mM(Wong et al., 2018). The ADEP1 analogues showed insignifi- cant activity up to 2 mM, and implied that these synthetic pep- tides are not cytotoxic at their MICs and therefore has potential for clinical applications.

4. Conclusion

ADEPs are potent antimicrobial agents; unfortunately, they possess bystander toxicity at their bioactive concentrations. Synthetic ADEP analogues have shown potential as alternative antimicrobial agents compared to their parent structures. The analogues can be tailored to have a different characteristics, enhanced efficacy and lower cyto- toxicity. The current study demonstrated that the use of enantiomers, amino acid replacement, change in cyclization and replacement of OTEA in the parent ADEP1 structure drastically reduced cytotoxicity. Our findings also indicated that the changes made on the parent struc- ture significantly altered and compromised the antibacterial activity exhibited by ADEP1. Despite the limitations, the study has demon- strated that these peptides showed a broad spectrum antibacterial activity. This is contrary to what has been reported about anionic pep- tides and their selective activity against Gram- positive bacteria. For future studies, addition of cationic amino acids or use of a resin yield- ing a positive C-terminal to improve interaction with the negatively charged bacterial membrane would be beneficial. Structural enhance- ment would improve the potency of the ADEP1 analogues. In addi- tion, the supplementation of these anionic AMPs with divalent metal ions such as zinc may increase their antimicrobial activitie. In addition, evaluation of synergistic effects evaluation of ADEP analogues with known antibacterial drugs would be beneficial.

Declaration of conflict of interest

The authors declare no conflict of interest.

Funding

The study was financially supported by Mintek Science Vote, Project No. ADR 42304.

Appendix A. Supplementary data

Supplementary data to this article can be found online at https://doi.org/10.1016/j.arabjc.2023.105000.

References

Adeyemi, A.I., Vincent, O.I., Olujenyo, O.M., 2018. Phytochemical screening and antifungal activity of Chromolaena odorata extracts against isolate of Phytophthora megakarya using agar-well diffu- sion method. Asian Journal of Medical and Biological Research 4 (1), Article 1. https://doi.org/10.3329/ajmbr.v4i1.36815.

Alonzo, D.A., Schmeing, T.M., 2020. Biosynthesis of depsipeptides, or Depsi: The peptides with varied generations. Protein Sci.: A Publication of the Protein Society 29 (12), 2316–2347. https://doi.org/10.1002/pro.3979.

Al-Warhi, T.I., Al-Hazimi, H.M.A., El-Faham, A., 2012. Recent development in peptide coupling reagents. J. Saudi Chem. Soc. 16 (2), 97–116. https://doi.org/10.1016/j.jscs.2010.12.006.

Boullosa, L.F., Van Loenhout, J., Flieswasser, T., De Waele, J., Hermans, C., Lambrechts, H., Cuypers, B., Laukens, K., Bartho- lomeus, E., Siozopoulou, V., De Vos, W.H., Peeters, M., Smits, E. L.J., Deben, C., 2021. Auranofin reveals therapeutic anticancer potential by triggering distinct molecular cell death mechanisms and innate immunity in mutant p53 non-small cell lung cancer. Redox Biol. 42,. https://doi.org/10.1016/j.redox.2021.101949 101949.

Bro¨ tz-Oesterhelt, H., Beyer, D., Endermann, R., Ladel, C., Schroeder, W., Hinzen, B., Raddatz, S., Paulsen, H., Henninger, K., Bandow, J.E., Sahl, H.-G., Labischinski, H., 2005. Dysregulation of bacte- rial proteolytic

machinery by a new class of antibiotics. Nat. Med. 11, 1082–1087.

Bro¨ tz-Oesterhelt, H., Sass, P., 2014. Bacterial caseinolytic proteases as novel targets for antibacterial treatment. Int. J. Med. Microbiol. 304 (1), 23–30. https://doi.org/10.1016/j.ijmm.2013.09.001.

Brunetti, J., Falciani, C., Roscia, G., Pollini, S., Bindi, S., Scali, S., Arrieta, U.C., Go mez-Vallejo, V., Quercini, L., Ibba, E., Prato, M., Rossolini, G.M., Llop, J., Bracci, L., Pini, A., 2016. *In vitro* and *in vivo* efficacy, toxicity, bio-distribution and resistance selection of a novel antibacterial drug candidate. Sci. Rep. 6, 26077. https://doi.org/10.1038/srep26077.

Carta, G., Murru, E., Banni, S., Manca, C., 2017. Palmitic Acid: Physiological Role, Metabolism and Nutritional Implications. Front. Physiol. 8. https://doi.org/10.3389/fphys.2017.00902.

Chandu, D., Nandi, D., 2004. Comparative genomics and functional roles of the ATP-dependent proteases Lon and Clp during cytosolic protein degradation. Res. Microbiol. 155 (9), 710–719. https://doi.org/10.1016/j.resmic.2004.06.003.

Cˇizˇinauskas, V., Elie, N., Brunelle, A., Briedis, V., 2017. Fatty acids

penetration into human skin ex vivo: A TOF-SIMS analysis approach. Biointerphases 12, (1). https://doi.org/10.1116/1.4977941 011003.

Cobongela, S.Z.Z., Makatini, M.M., Mdluli, P.S., Sibuyi, N.R.S., 2022. Acyldepsipeptide Analogues: A Future Generation Antibi- otics for Tuberculosis Treatment. Pharmaceutics 14 (9), 1956. https://doi.org/10.3390/pharmaceutics14091956.

Cole, A., Wang, Z., Coyaud, E., Voisin, V., Gronda, M., Jitkova, Y., Mattson, R., Hurren, R., Babovic, S., Maclean, N., Restall, I., Wang, X., Jeyaraju, D.V., Sukhai, M.A., Prabha, S., Bashir, S., Ramakrishnan, A., Leung, E., Qia, Y.H., Schimmer, A.D., 2015. Inhibition of the Mitochondrial Protease ClpP as a Therapeutic Strategy for Human Acute Myeloid Leukemia. Cancer Cell 27 (6), 864–876. https://doi.org/10.1016/j.ccell.2015.05.004.

Culp, E., Wright, G.D., 2017. Bacterial proteases, untapped antimi- crobial drug targets. J. Antibiot. 70 (4), 366–377. https://doi.org/ 10.1038/ja.2016.138.

Eloff, J.N., 2019. Avoiding pitfalls in determining antimicrobial activity of plant extracts and publishing the results. BMC Com- plement. Altern. Med. 19, 106. https://doi.org/10.1186/s12906-019-2519-3.

Eyermann, B., Meixner, M., Bro¨ tz-Oesterhelt, H., Antes, I., Sieber, S. A., 2020. Acyldepsipeptide Probes Facilitate Specific Detection of Caseinolytic Protease P Independent of Its Oligomeric and Activity State. Chembiochem 21 (1–2), 235–240. https://doi.org/10.1002/cbic.201900477.

Fadaka, A.O., Sibuyi, N.R.S., Madiehe, A.M., Meyer, M., 2021. Nanotechnology-Based Delivery Systems for Antimicrobial Pep- tides. Pharmaceutics 13 (11), 1795. https://doi.org/10.3390/pharmaceutics13111795.

Finer, Y., Santerre, J.P., 2004. The influence of resin chemistry on a dental composite's biodegradation. J. Biomed. Mater. Res. A 69 (2), 233–246. https://doi.org/10.1002/jbm.a.30000.

Frees, D., Gerth, U., Ingmer, H., 2014. Clp chaperones and proteases are central in stress survival, virulence and antibiotic resistance of Staphylococcus aureus. Int. J. Med. Microbiol. 304 (2), 142–149. https://doi.org/10.1016/j.ijmm.2013.11.009.

Garton, M., Nim, S., Stone, T.A., Wang, K.E., Deber, C.M., Kim, P. M., 2018. Method to generate highly stable D-amino acid analogs of bioactive helical peptides using a mirror image of the entire PDB. Proc. Natl. Acad. Sci. 115 (7), 1505–1510. https://doi.org/10.1073/pnas.1711837115.

Goodreid, J.D., Wong, K., Leung, E., McCaw, S.E., Gray-Owen, S. D., Lough, A., Houry, W.A., Batey, R.A., 2014. Total Synthesis and Antibacterial Testing of the A54556 Cyclic Acyldepsipeptides Isolated from *Streptomyces hawaiiensis*. J. Nat. Prod. 77 (10), 2170– 2181. https://doi.org/10.1021/np500158q.

Goodreid, J.D., dos Santos, E. da S., Batey, R.A., 2015. A Lanthanide

(III) Triflate Mediated Macrolactonization/Solid-Phase

Synthesis Approach for Depsipeptide Synthesis. Org. Lett. 17 (9), 2182–2185. https://doi.org/10.1021/acs.orglett.5b00781.

Goodreid, J.D., Janetzko, J., Santa Maria, J.P., Wong, K.S., Leung, E., Eger, B.T., Bryson, S., Pai, E.F., Gray-Owen, S.D., Walker, S., Houry, W.A., Batey, R.A., 2016. Development and Characterization of Potent Cyclic Acyldepsipeptide Analogues with Increased Antimicrobial Activity. J. Med. Chem. 59 (2), 624–646. https://doi.org/10.1021/acs.jmedchem.5b01451.

Hinzen, B., Raddatz, S., Paulsen, H., Lampe, T., Schumacher, A., Ha¨ bich, D., Hellwig, V., Benet-Buchholz, J., Endermann, R., Labischinski, H., Bro¨ tz-Oesterhelt, H., 2006. Medicinal Chemistry Optimization of Acyldepsipeptides of the Enopeptin Class Antibi- otics. ChemMedChem 1 (7), 689–693. https://doi.org/10.1002/cmdc.200600055.

Irby, D., Du, C., Li, F., 2017. Lipid-Drug Conjugate for Enhancing Drug Delivery. Mol. Pharm. 14 (5), 1325–1338. https://doi.org/10.1021/acs.molpharmaceut.6b01027.

Kang, S.G., Dimitrova, M.N., Ortega, J., Ginsburg, A., Maurizi, M. R., 2005. Human mitochondrial ClpP is a stable heptamer that assembles into a tetradecamer in the presence of ClpX. J. Biol. Chem. 280 (42), 35424–35432. https://doi.org/10.1074/jbc.M507240200.

Kim, Y.-I., Levchenko, I., Fraczkowska, K., Fraczkowska, R.V., Sauer, R.T., Baker, T.A., 2001. Molecular determinants of complex formation between Clp/Hsp100 ATPases and the ClpP peptidase. Nat. Struct. Biol. 8, 230–233.

Lee, B.-G., Park, E.Y., Lee, K.-E., Jeon, H., Sung, K.H., Paulsen, H., Ru¨ bsamen-Schaeff, H., Bro¨ tz-Oesterhelt, H., Song, H.K., 2010. Structures of ClpP in complex with acyldepsipeptide antibiotics reveal its activation mechanism. Nat. Struct. Mol. Biol. 17 (4), 471– 478. https://doi.org/10.1038/nsmb.1787.

Levison, M.E., Levison, J.H., 2009. Pharmacokinetics and Pharmacodynamics of Antibacterial Agents. Infect. Dis. Clin. North Am. 23 (4), 791–vii. https://doi.org/10.1016/j.idc.2009.06.008.

Lewis, A.L., Richard, J., 2015. Challenges in the delivery of peptide drugs: An industry perspective. Ther. Deliv. 6 (2), 149–163. https://doi.org/10.4155/tde.14.111.

Li, D.H.S., Chung, Y.S., Gloyd, M., Joseph, E., Ghirlando, R.,

Wright, G.D., Cheng, Y.-Q., Maurizi, M.R., Guarne , A., Ortega, J., 2010. Acyldepsipeptide Antibiotics Induce the Formation of a Structured Axial Channel in ClpP: A Model for the ClpX/ClpA- Bound State of ClpP. Chem. Biol. 17 (9), 959–969. https://doi.org/10.1016/j.chembiol.2010.07.008.

Li, Y., Lavey, N.P., Coker, J.A., Knobbe, J.E., Truong, D.C., Yu, H., Lin, Y.-S., Nimmo, S.L., Duerfeldt, A.S., 2017. Consequences of Depsipeptide Substitution on the ClpP Activation Activity of Antibacterial Acyldepsipeptides. ACS Med. Chem. Lett. 8 (11), 1171–1176. https://doi.org/10.1021/acsmedchemlett.7b00320.

Liu, T., Wang, Y., Luo, X., Li, J., Reed, S.A., Xiao, H., Young, T.S., Schultz, P.G., 2016. Enhancing protein stability with extended disulfide bonds. Proc. Natl. Acad. Sci. 113 (21), 5910–5915. https://doi.org/10.1073/pnas.1605363113.

Ma, R., Wong, S.W., Ge, L., Shaw, C., Siu, S.W.I., Kwok, H.F., 2019.

In Vitro and MD Simulation Study to Explore Physicochemical Parameters for Antibacterial Peptide to Become Potent Anticancer Peptide. Mol Ther Oncolytics. 10 (16), 7–19. https://doi.org/10.1016/j.omto.2019.12.001.

Malik, I.T., Pereira, R., Vielberg, M., Mayer, C., Straetener, J., Thomy, D., Famulla, K., Castro, H., Sass, P., Groll, M., Bro¨ tz-Oesterhelt, H., 2020. Functional Characterisation of ClpP Muta- tions Conferring Resistance to Acyldepsipeptide Antibiotics in Firmicutes. Chembiochem 21 (14), 1997–2012. https://doi.org/10.1002/cbic.201900787.

Mayer, C., Sass, P., Bro¨ tz-Oesterhelt, H., 2019. Consequences of dosing and timing on the antibacterial effects of ADEP antibiotics. Int. J. Med. Microbiol. 309, (7). https://doi.org/10.1016/j.ijmm.2019.151329 151329.

Merrifield, R.B., 1963. Solid Phase Peptide Synthesis. I. The Synthesis of a Tetrapeptide. J. Am. Chem. Soc. 85 (14), 2149–2154. https://doi.org/10.1021/ja00897a025.

Michel, K. H., & Kastner, R. E. 1985. A54556 Antibiotics and process for production thereof. Antibiotic A54556, a Complex of 8 Individual Factors, Produced by Submerged, Aerobic Fermenta- tion of New Streptomyces Hawaiiensis NRRL 15010. The Complex and the Individual, Separated Factors Are Active against Staphy- lococcus and Streptococcus Which Are Penicillin Resistant.

Pohl, M., Ambrosius, D., Gro¨ tzinger, J., Kretzschmar, T., Saunders, D.,Wollmer, A., Brandenburg, D., Bitter-Suermann, D., Ho¨ cker, H., 1993. Cyclic disulfide analogues of the complement component C3a. Synthesis and conformational investigations. Int. J. Pept. Protein Res. 41 (4), 362–375. https://doi.org/10.1111/j.1399-3011.1993.tb00452.x.

Sass, P., Josten, M., Famulla, K., Schiffer, G., Sahl, H.-G., Hamoen, L., Brotz-Oesterhelt, H., 2011. Antibiotic acyldepsipeptides acti- vate ClpP peptidase to degrade the cell division protein FtsZ. Proc. Natl. Acad. Sci. 108 (42), 17474–17479. https://doi.org/10.1073/pnas.1110385108.

von R. Schleyer, P. 1957. A simple preparation of adamantane. Journal of the American Chemical Society, 79(12), 3292–3292. Doi:10.1021/ja01569a086.

Siddiqui, K.S., Poljak, A., Guilhaus, M., Feller, G., D'Amico, S., Gerday, C., Cavicchioli, R., 2005. Role of Disulfide Bridges in the Activity and Stability of a Cold-Active a-Amylase. J. Bacteriol. 187 (17), 6206–6212. https://doi.org/10.1128/JB.187.17.6206-6212.2005.

Spilovska, K., Zemek, F., Korabecny, J., Nepovimova, E., Soukup,O., Windisch, M., Kuca, K., 2016. Adamantane—A Lead Structure for Drugs in Clinical Practice. Curr. Med. Chem. 23 (29), 3245– 3266. https://doi.org/10.2174/0929867323666160525114026.

S˘timac, A., S˘ekutor, M., Mlinaric - Majerski, K., Frkanec, L., &

Frkanec, R. 2017. Adamantane in Drug Delivery Systems and Surface Recognition. Molecules (Basel, Switzerland), 22(2). Doi: 10.3390/molecules22020297.

Takagi, H., Takahashi, T., Momose, H., Inouye, M., Maeda, Y., Matsuzawa, H., & Ohta, T. 1990. Enhancement of the thermosta- bility of subtilisin E by introduction of a disulfide bond engineered on the basis of structural comparison with a thermophilic serine protease. The Journal of Biological Chemistry, 265(12), 6874–6878.

Tan, Y., Chen, X., Ma, C., Xi, X., Wang, L., Zhou, M., Burrows, J.F., Kwok, H.F., Chen, T., 2018. Biological Activities of Cationicity- Enhanced and Hydrophobicity-Optimized Analogues of an Antimicrobial Peptide, Dermaseptin-PS3, from the Skin Secretion of Phyllomedusa sauvagii. Toxins 10, 320. https://doi.org/ 10.3390/toxins10080320.

Tan, T.Y., Ng, L.S.Y., 2006. Comparison of three standardized disc susceptibility testing methods for colistin. J. Antimicrob. Che- mother. 58 (4), 864–867. https://doi.org/10.1093/jac/dkl330.

Trivedi, M.V., Laurence, J.S., Siahaan, T.J., 2009. The role of thiols and disulfides in protein chemical and physical stability. Curr. Protein Pept. Sci. 10 (6), 614–625.

Uppalapati, M., Lee, D.J., Mandal, K., Li, H., Miranda, L.P., Lowitz, J., Kenney, J., Adams, J.J., Ault-Riche , D., Kent, S.B.H., Sidhu, S. S., 2016. A Potent d-Protein Antagonist of VEGF-A is Nonim-munogenic, Metabolically Stable, and Longer-Circulating in Vivo. ACS Chem. Biol. 11 (4), 1058–1065. https://doi.org/10.1021/acschembio.5b01006.

Vlieghe, P., Lisowski, V., Martinez, J., Khrestchatisky, M., 2010. Synthetic therapeutic peptides: Science and market. Drug Discov. Today 15 (1), 40–56. https://doi.org/10.1016/j.drudis.2009.10.009.

Wen, S., Packham, G., Ganesan, A., 2008. Macrolactamization versus Macrolactonization: Total Synthesis of FK228, the Depsipeptide Histone Deacetylase Inhibitor. J. Org. Chem. 73 (23), 9353–9361. https://doi.org/10.1021/jo801866z.

White, C.J., Yudin, A.K., 2011. Contemporary strategies for peptide macrocyclization. Nat. Chem. 3 (7), 509–

524. https://doi.org/10.1038/nchem.1062.

Wong, K.S., Mabanglo, M.F., Seraphim, T.V., Mollica, A., Mao, Y.-Q., Rizzolo, K., Leung, E., Moutaoufik, M.T., Hoell, L., Phanse, S., Goodreid, J., Barbosa, L.R.S., Ramos, C.H.I., Babu, M., Mennella, V., Batey, R.A., Schimmer, A.D., Houry, W.A., 2018. Acyldepsipeptide Analogs Dysregulate Human Mitochondrial ClpP Protease Activity and Cause Apoptotic Cell Death. Cell Chem. Biol. 25 (8), 1017–1030.e9. https://doi.org/10.1016/j.chembiol.2018.05.014.

Ye, Z., Aparicio, C., 2022. Interactions of two enantiomers of a designer antimicrobial peptide with structural components of the bacterial cell envelope. J. Pept. Sci. 28 (1), e3299.

Yourtee, D.M., Smith, R.E., Russo, K.A., Burmaster, S., Cannon, J.M., Eick, J.D., Kostoryz, E.L., 2001. The stability of methacrylate biomaterials when enzyme challenged: Kinetic and systematic evaluations. J. Biomed. Mater. Res. 57 (4), 522–531. https://doi.org/ 10.1002/1097-4636(20011215)57:4<522::aid-jbm1198>3.0.co;2-9.

Zabetakis, D., Olson, M.A., Anderson, G.P., Legler, P.M., Goldman, E.R., 2014. Evaluation of Disulfide Bond Position to Enhance the Thermal Stability of a Highly Stable Single Domain Antibody. PLoS One 9 (12), e115405.

Zai, Y., Xi, X., Ye, Z., Ma, C., Zhou, M., Chen, X., Siu, S.W.I., Chen, T., Wang, L., Kwok, H.F., 2021. Aggregation and Its Influence on the Bioactivities of a Novel Antimicrobial Peptide, Temporin-PF, and Its Analogues. Int. J. Mol. Sci. 22, 4509. https://doi.org/10.3390/ijms22094509.

Zhou, X., Liu, Y., Gao, Y., Wang, Y., Xia, Q., Zhong, R., Ma, C., Zhou, M., Xi, X., Shaw, C., Chen, T., Wu, D., Kwok, H.F., Wang, L., 2020. Enhanced Antimicrobial Activity of N-Terminal Deriva- tives of a Novel Brevinin-1 Peptide from The Skin Secretion of Odorrana schmackeri. Toxins 12, 484. https://doi.org/ 10.3390/toxins12080484.

CHAPTER 6.

Manuscriscript: Prepared for submission

Antibacterial activity and cytotoxicity screening of Silver/Indium/Sulphide quantum dots conjugated ADEP1 analogues

Sinazo Z.Z Cobongela[1,2,3*], Bambesiwe May[3], Maya M Makatini[1], Zikhona Njengele-Tetyana[2], Nicole R.S Sibuyi[2,3,4]

[1]Molecular Sciences Institute, School of Chemistry, University of the Witwatersrand, Johannesburg 2050, South Africa

[2]Health Platform, Advanced Materials Division, Mintek, Randburg 2194, South Africa

[3]Department of Science and Innovation (DSI)/Mintek Nanotechnology Innovation Centre (NIC), Advanced Materials Division, Mintek, Randburg 2194, South Africa

[4]DSI/Mintek NIC, Biolabels Research Node, Department of Biotechnology, University of the Western Cape, Bellville 7535, South Africa

Email: SinazoC@mintek.co.za

Abstract

The continuous rise in bacterial infections and antibiotic resistance is the driving force behind the search for new antibacterial agents with novel modes of action. Antimicrobial peptides (AMPs) have recently gained attention as promising antibiotic agents with potential to treat drug-resistant infections. Several have shown a lower propensity towards developing resistance compared to conventional antibiotics. However, these peptides, especially acyldepsipeptides (ADEPs) present with unfavourable pharmacokinetic properties such as high toxicity and low bioavailability. Ways to improve these peptides to be drug-like molecules have been explored and these include using biocompatible nano-carriers. Conjugating ADEP1 analogues (SC005-8) to gelatin-capped Silver/Indium/Sulphide ($AgInS_2$) quantum dots (QD) improved the antibacterial activity against two Gram-negative bacteria, *Escherichia coli* and *Pseudomonas aeruginosa*, and three Gram-positive bacteria, *Bacillus subtilis*, *Staphylococcus aureus and* Methicillin-resistant *Staphylococcus aureus*. The unconjugated peptides exhibited minimum inhibition concentrations (MIC) between 63 – 500 µM, and MBC values between 125 – 750 µM. The conjugation of the $AgInS_2$ conjugation to the ADEP1 analogues resulted in enhanced antibacterial activity as evident from the MIC and MBC values obtained from the conjugates, i.e. 2.3 – 37.5 µM for the MIC, and 9.4 – 10 µM MBC values. These conjugates proved to be non-toxic against HEK-293 cells at the concentrations that showed antibacterial activity. The

findings reported herein could be helpful in the development of antibacterial treatment strategies.

6.1. INTRODUCTION

In recent years, nanotechnology has attracted significant interest, especially in the pharmaceutical industry. Nanomaterials have been explored as promising tools for biomedical applications such as biosensors, drug delivery and imaging, amongst others [1]. Nanomaterials are very small , usually ranging from 1 to 100nm, and yet have a large surface area that can be easily functionalized by conjugating compounds of interest [2]. Properties of nanomaterials such as size, chemical composition, shape, and surface structure can significantly influence how they interact with other molecules. For instance, surface functionalization of core nanomaterials with various ligands can lead to the use of these nanomaterials in different biological applications. Due to their small size, nanomaterials can easily diffuse through cell membrane pores and ion channels. In addition, when the nanomaterials are coated with ligands they are internalised by the cells via endocytosis [3]. Nanomaterials are therefore good drug delivery systems that can improve existing drugs to achieve desirable therapeutic efficacy. Conjugation of pharmaceutically active compounds with poor pharmacokinetic properties to nanomaterials has been shown to increase drug solubility and decrease enzyme susceptibility thus improving the bioavailability of the drugs [4] [5] [6]. Nanomaterials can reduce toxicity and adverse side effects of drug molecules by increasing selectivity and improving transfer across membranes including the blood-brain barrier [7].

Quantum dots (QDs) have gained traction in medicine as bio-imaging tools, drug delivery systems, and in sensor applications [8]. QDs used as nano-carriers of drugs have been reported to improve bioavailability, biocompatibility, and the efficacy of existing drugs [9], [10]. Conjugation of doxorubicin to ZnO QDs for treatment of lung cancer is one example that highlights the effectiveness of using nanomaterials as drug delivery systems [11]. In this study, gelatin-capped Silver/Indium/Sulphide ($AgInS_2$) QDs were utilized as nano-carriers. $AgInS_2$ QDs are known I-III-VI semiconductors that also exhibit long-term photoluminescence decay lifetime [12]. Due to their remarkable photoluminescence properties and low toxicity, they have found use in bio-imaging and cell targeting [13]–[15]. $AgInS_2$ QDs were conjugated to acyldepsipeptides 1 (ADEP1) analogues (Figure 6.1) to improve their antibacterial efficacy. ADEPs are a class of antibacterial peptides (AMPs) that target the bacterial ClpP protease and

have great potential as antibiotics. However, they lack the basic pharmacokinetic properties such as bioavailability and biocompatibility.

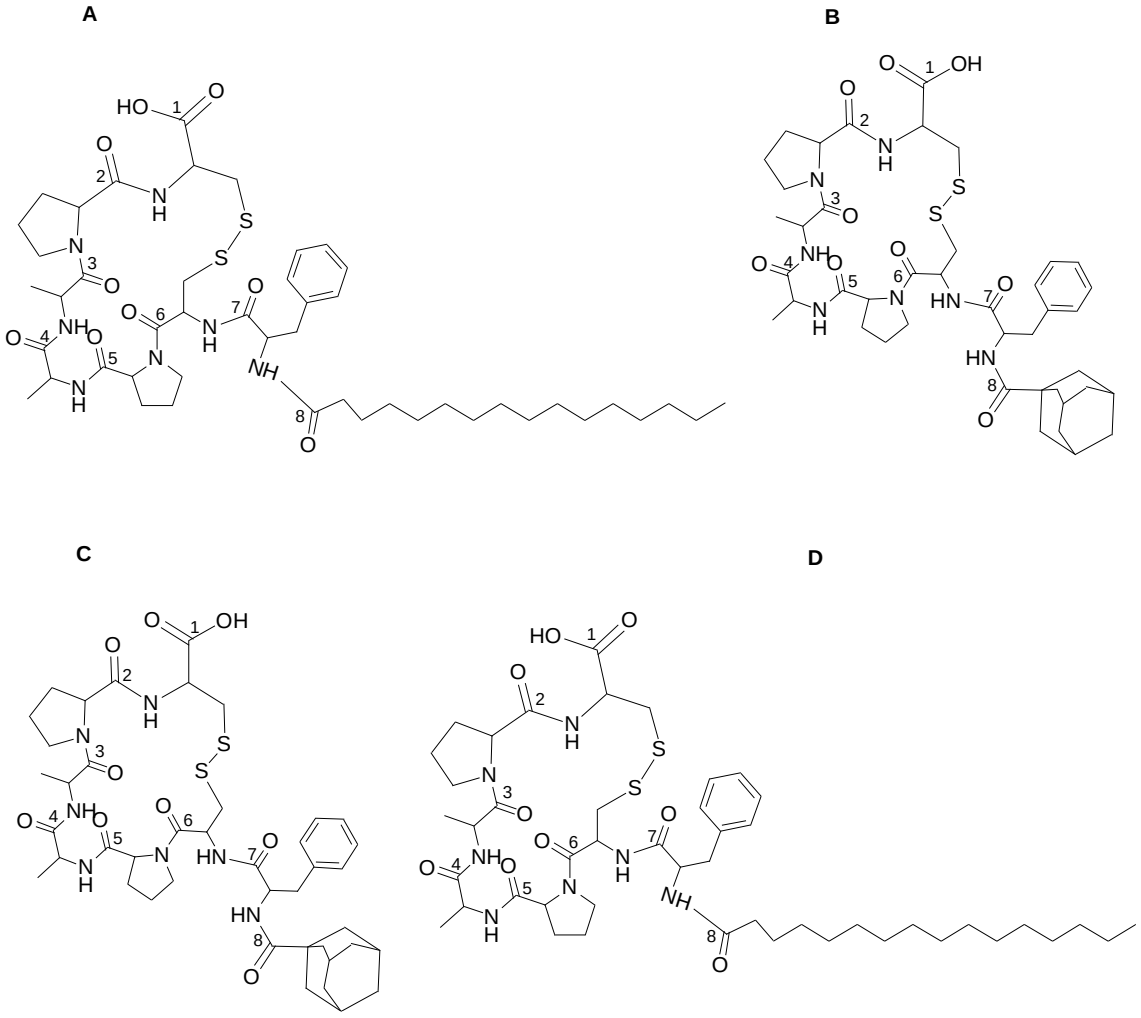


Figure 6. 1: Disulphide bond cyclized ADEP1 analogues. A-SC005 (D-form, Pal); B-SC006 (D-form, Ada); C-SC007 (L-form, Ada), D-SC008 (L-form, Pal).

6.2. **Materials and methods**

6.2.1. *Material*

ADEP1 analogues (SC005-8) were synthesized in-house (Chapter 5, Section 5.2.1-4)). 1-Ethyl-3-(3-dimethylaminopropyl) carbodiimide (EDC), dimethyl formamide (DMF) N-hydroxysuccinimide (sulfo-NHS), Dimethyl sulfoxide (DMSO), thioglycolic acid (TGA), Silver nitrate ($AgNO_3$), sodium sulfide ($Na_2S{\cdot}xH_2O$), gelatin, Dulbecco's Modified Eagle Medium (DMEM), phosphate, Trypsin, Penicillin-Streptomycin, Fetal bovine serum (FBS), 3-(4,5-dimethylthiazol-2-yl)-5-(3-carboxymethoxyphenyl)-2-(4-sulfophenyl)-2H-tetrazolium (MTS dye), and trypan blue stain dye were all purchased from Sigma. *Bacillus subtilis* ATCC

11774, *Staphylococcus aureus* ATCC 25923 and Methicillin-resistant *Staphylococcus aureus* (MRSA) ATCC 43300) and two Gram negative (*Escherichia coli* ATCC 33876 and *Pseudomonas aeruginosa* ATCC 15442. Human embryonic kidney 293 (HEK-293) cells were purchased from Cellonex (Randburg, Gauteng Province, South Africa).

6.2.2. *Synthesis of QD*

The QDs were synthesized using a procedure reported by May *et al*. 2019 [16] with some modifications [16]. In a typical synthesis, 0.25 mmol (0.0753g) of In $(NO_3)_3$, 0.438 mmol TGA, 0.0625 mmol of silver nitrate, 0.2941g of gelatin and 0.406 mmol of $Na_2S.9H_20$ were added to 100 mL of deionized water with stirring (Ag: In: S: gelatin: TGA mole ratio of 1: 4: 6.5: 16: 7). The pH was adjusted to 6. The mixture was refluxed at 95 ˚C for 1 hour to produce the gelatin-capped $AGInS_2$ QDs. The QDs were precipitated with ethanol and dried in air.

6.2.3. *Conjugation of $AgInS_2$ quantum dots to ADEP1 analogues*

The ADEP1 analogues were synthesized using the Fmoc solid peptide synthesis strategy as described in Chapter 4. EDC/sulfoNHS coupling chemistry was used to conjugate the ADEP1 analogues to the QD. ADEP1 analogues (600 µM) were treated with EDC (0.75 µM) and sulfo-NHS (0.3 µM) in DMF and the reaction was left shaking for 3 hours at room temperature. Concurrently, 8mg/mL of the QDs was dissolved in 10 mL of boiling water. Upon cooling down, the QDs were added to the ADEP1 analogues solution and the reaction was left shaking for 3 hours at room temperature. The conjugates were precipitated with ethanol and lyophilised (LyoQuest, Telstar, Terrassa, Barcelona). The powder was re-suspended in phosphate buffered saline (PBS; 137 mM NaCl, 2.7 mM KCl, 8 mM Na_2HPO_4, 2 mM KH_2PO_4, pH 7.4) to make a final concentration of 4 mg/mL QD-peptide conjugate with 300 µM ADEP1 analogues.

6.2.4. *Characterization of QD, QD-peptide conjugates and peptides*

Spectro Xepos05 energy-dispersive X-ray fluorescence (ED-XRF) instrument was used to determine the Ag, In, S and concentrations in the gelatin-capped $AgInS_2$ QD powder. QDs and QDs ADEP1 analogues conjugates particle sizes were analysed by the High-resolution transmission electron microscope (HR-TEM, JEOL, USA). The Hitachi F-2700FL spectrofluorophotometer (4J1-0004, Japan) was used for the fluorescence measurements. Dynamic Light Scattering (DLS) was used to determine the surface potential of the

nanomaterial and conjugates. The net charge of peptides, nanoparticles, and conjugates were determined by zetasizer (DLS, Malvern system 4700, Malvern, United Kingdom).

6.2.5. *Minimum inhibitory concentration and minimum bactericidal concentration*

The minimum inhibitory concentration (MIC) of the QD-peptide conjugates against *B. subtilis*, *S. aureus*, MRSA, *P. aeruginosa* and *E. coli* was determined using the broth microdilution susceptibility assay in 96-well microtiter plates. Overnight-grown bacterial cultures were adjusted to approximately 1.5×10^8 CFU/mL in a sterile Luria-Bertani broth. QD-peptide conjugates were diluted *via* 2-fold serial dilution with broth containing 5% DMSO to a final concentration range of 150-1.12 µM (150, 75, 37.5, 18.75, 9.38, 4.69, 2.34, and 1.12 µM) for peptides and 2-0.016 mg/mL (2, 1, 0.5, 0.25, 0.13, 0.06, 0.03, and 0.016 mg/mL) for QDs, respectively. The diluted culture (100 µL/well) was treated with the different concentrations of test compounds to get a final volume of 200 µL/well. Gentamicin was used as a positive control for *B. subtilis*, *S. aureus*, MRSA, and *P. aeruginosa* while ampicillin was used as a positive control for *E. coli* and 5% DMSO was used as a negative control. The 96-well plates were then incubated overnight at 37°C. The lowest concentration of the QD-peptide conjugates and controls that resulted in clear wells with no turbidity (i.e. no visible bacterial growth) was recorded as the MIC. The bacterial culture from the MIC wells and the QD-conjugates at concentrations above the MIC were inoculated into fresh Luria-Bertani agar plates and incubated overnight at 37°C. The minimum bactericidal concentration (MBC) was determined as the lowest concentration resulting in complete bacterial growth inhibition.

6.2.6. *Cytotoxicity assay*

The cytotoxicity of the QD-peptide conjugates was assessed on HEK-293 cells using the MTS cell proliferation assay. Aliquots of 100 µL/well containing $1x10^5$ cells/mL in Dulbecco's Modified Eagle Medium (DMEM) consisting of 10% fetal bovine serum (FBS), 2% DMSO, and 1% penicillin-streptomycin were seeded into a 96 well plate and cultured at 37 °C overnight in a humidified incubator at 5% CO_2. The cells were then treated by adding 100 µL/well of QD-peptide conjugates to attain a final concentration range of 4 – 0.03 mg/mL. Auranofin (concentration range = 100, 50, 25, 12.5, 6.25, 3.125, 1.5625, and 0.78125 - 100 µM) was used as a positive control and 2% DMSO was used as a negative control. The 96-well plate was prepared and incubated with the compounds for 48 hours at 37 °C. The metabolic activity of

viable cells was determined by adding 10% of MTS dye into the wells and incubating for 4 hours. Viable cells converted the yellow tetrazolium salt to a purple formazan, which was read at 490 nm wavelength using a UV-vis spectrophotometer (SpectraMax Plus 384 Microplate Reader, Molecular Devices, California, United States). The percentage cell viability was calculated using the equation below.

$$\%\ cell\ viability = \left(\frac{OD\ of\ test\ sample}{OD\ of\ control}\right) x\ 100$$

6.3. **Results and discussion**

ED-XRF was used to analyse the gelatin-capped $AgInS_2$ QDs. The ED-XRF confirmed the presence of Ag, In, and S with percentage and ratio shown in Table 6.1. The gelatin on the surface of the QD therefore accounts for majority of QD. The HR-TEM also confirmed a successful synthesis of gelatin-capped $AgInS_2$ QDs. The micrograph show that the QD are evenly dispersed and spherical in shape with a size of 6 ±2 nm (Figure 6.2).

Table 6. 1: Elemental analysis of gelatin-capped $AgInS_2$ QDs

Elements	**Ag**	**In**	**S**
%	0.8	1.6	14.4
Ratio	1	2	18

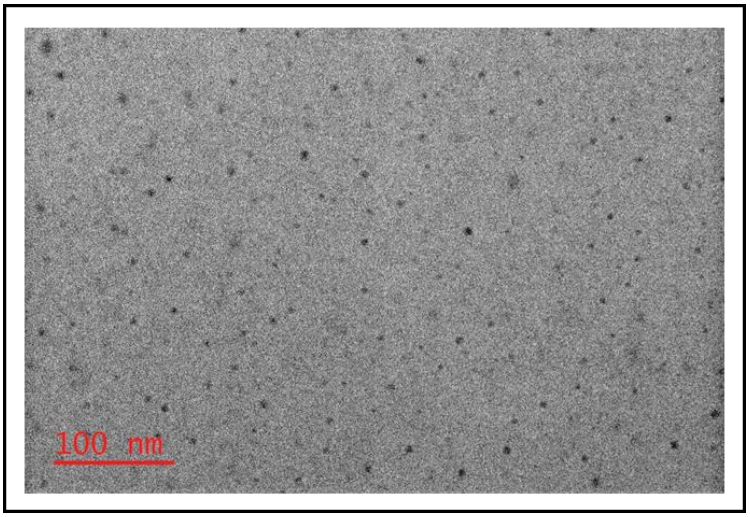


Figure 6. 2: TEM images gelatin-capped $AgInS_2$ QDs.

Gelatin-capped $AgInS_2$ QDs were functionalized with ADEP1 analogues *via* EDC/sulfo-NHS coupling-chemistry. The carboxylic groups of the ADEP1 analogues were activated in the absence of the QDs. Treatment of the ADEP1 analogues with EDC/sulfo-NHS in the presence of gelatin capped QDs could potentially result in intramolecular coupling between the carboxylic groups and amidine groups on the gelatin (Figure 6.3). The conjugation utilized the amidine group of the gelatin on the surface of the QDs and the carboxylic group on the C-terminal of the ADEP1 analogues to form an amide bond (Figure 6.4).

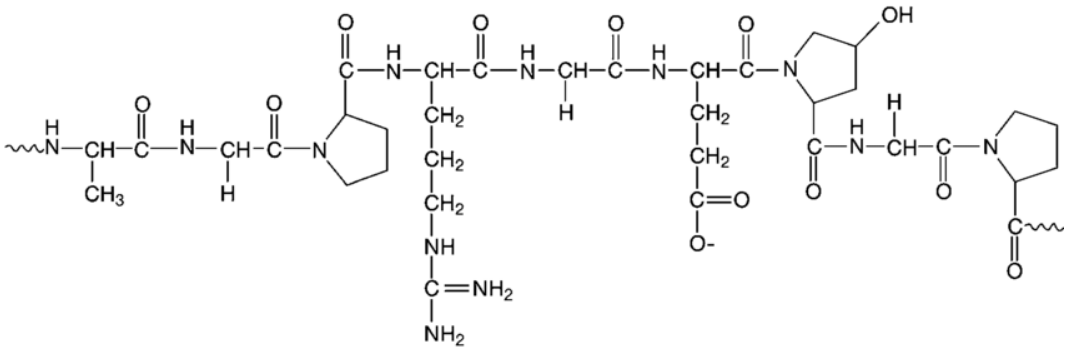


Figure 6. 3: Chemical structure of gelatin.

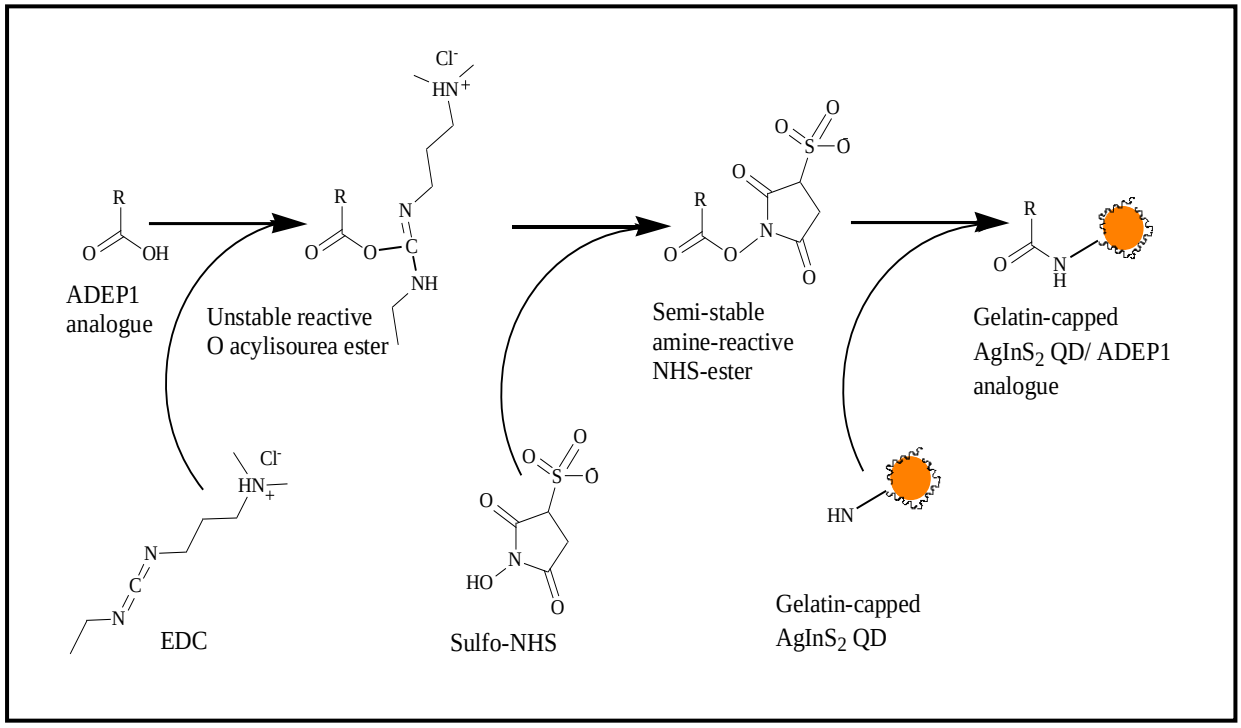


Figure 6. 4: Conjugation of ADEP1 analogues to gelatin-capped $AgInS_2$ QDs *via* EDC/sulfo-NHS coupling-chemistry. R= peptide sequence

The conjugation of SC005-8 peptides increased the size of the QDs to 13 ±5 nm (Figure 6.5 A-D). Other studies have also noted an increase in nanomaterial and QD size upon conjugation with functionalizing molecules such as peptides [17]–[19]. Optical properties were measured using photoluminescence spectroscopy with emission wavelengths between 400-700 nm. Luminescent QDs, such as $AgInS_2$ QDs, have long-lived excited states therefore, the excitation wavelength was marginalized [20]. The Gelatin-capped $AgInS_2$ QDs had an emission peak at 603 nm while the conjugates shifted the emission to lower wavelengths. QDs conjugated to the Pal-containing ADEP1 analogues (i.e. SC005 and SC008) absorbed at 595 nm while Ada-containing ADEP1 analogues (i.e. SC006 and SC007) absorbed at 599 nm (Figure 6.6). Conjugation adds a coating on the surface of the QDs, this in turn shields the surface of the QD. In addition, the shift in emission wavelength might be a result of increased size and the change in surface properties of QDs post conjugation.

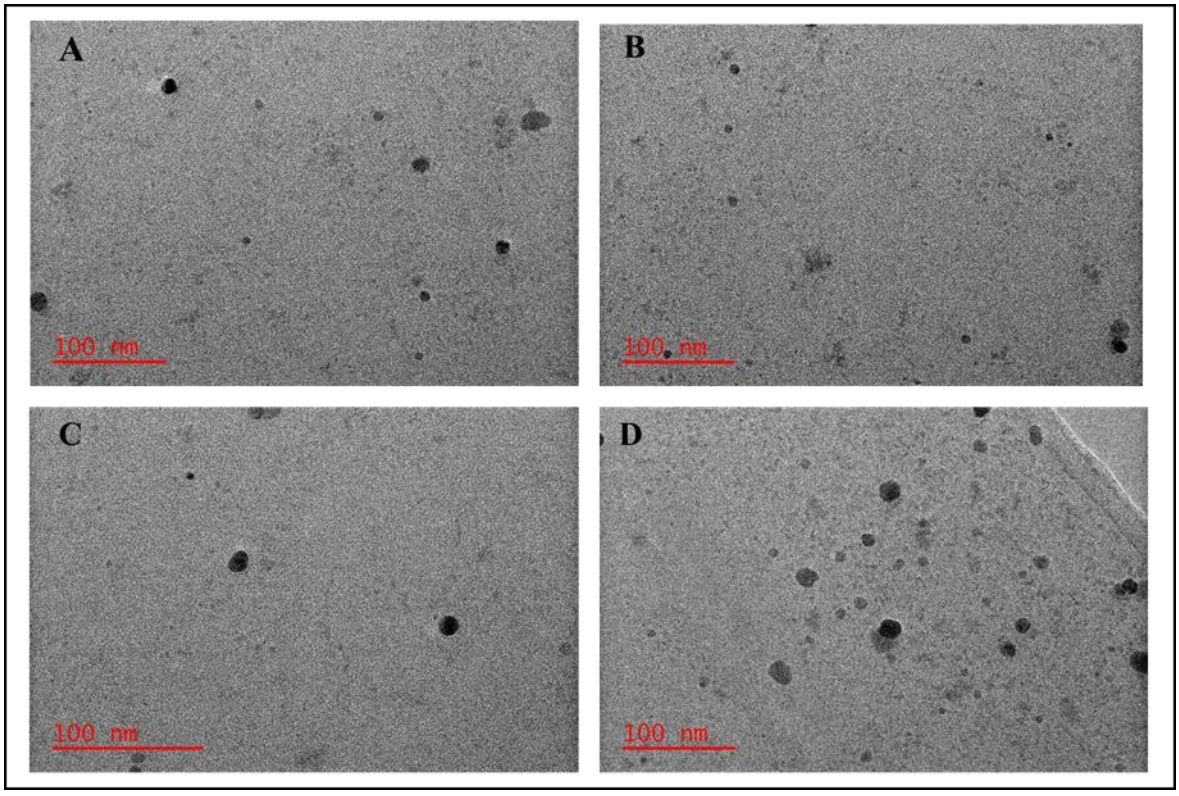


Figure 6. 5: TEM images gelatin-capped $AgInS_2$ QDs/ ADEP1 analogues conjugates. A: QD-SC005; B: QD-SC006; C: QD-SC007; D: QD-SC008.

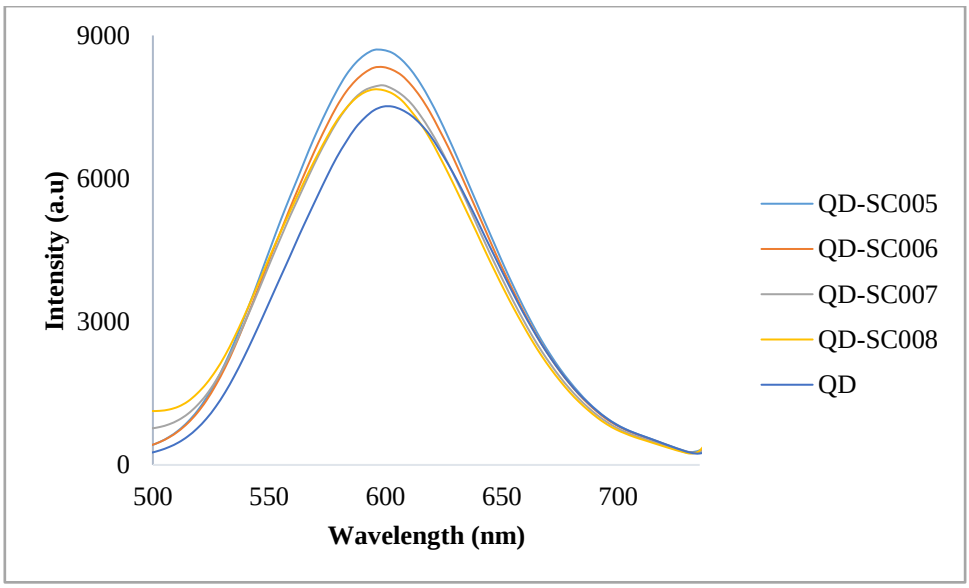


Figure 6. 6: Photoluminescence properties of gelatin-capped $AgInS_2$ QDs and ADEP1 analogues conjugates.

The QDs conjugates were further characterised using the zeta potential analyser to determine the surface charge of the material. Table 1 shows the zeta potential values of the peptides before and after conjugation. The unconjugated QDs had a zeta potential value of -3.69 ± 2.02 mV. As shown in Table 6.2, the peptides also had negative net charges ranging between -7.2 to -3.8 mV prior to conjugation. This confirmed the anionic state of the peptides, which is a result of the carboxylic anion (COO^-) at physiological pH. Anionic peptides have a disadvantage in penetrating bacterial cells as they are made up of negative polysaccharides, while cationic peptides have been commended for their cell permeability characteristics. ADEP1 analogues lack the cationic advantage, which may lead to poor cell permeability and bioavailability. Therefore, to mitigate the challenges of poor pharmacokinetic properties associated with ADEPs, the analogues were conjugated to $AgInS_2$ QDs. Table 1 shows that conjugation of the ADEP1 analogues to $AgInS_2$ QDs resulted in a positive net charge, which could enhance the cell permeability properties of the peptides.

Table 6. 2: Zeta potential values of the ADEP1 analogues before and after conjugation the gelatin-capped $AgInS_2$ QDs

ADEP1 analogue	**Zeta potential (mV) before conjugation**	**Zeta potential (mV) after conjugation**
SC005	-7.2 ±1.6	1.46 ±0.02
SC006	-3.8 ±1.1	1.38 ±0.06
SC007	-3.9 ±0.8	1.00 ±0.15
SC008	-6.9 ±1.5	1.39 ±0.09

Following the successful synthesis of the gelatin-capped $AgInS_2$ QDs and their subsequent conjugation to the ADEP1 analogues, the antibacterial activity of the conjugates was tested against three Gram-positive (*B. subtilis, S. aureus and* Methicillin-resistant *S. aureus*) and two Gram-negative (*E. coli* and *P. aeruginosa*) bacterial strains. Both MICs and MBCs of these conjugates were evaluated. On their own, the gelatin-capped $AgInS_2$ QDs did not show any antibacterial activity at the tested concentrations (0.06 – 8 mg/mL) against the tested bacterial strains. However, upon conjugation to the ADEP1 analogues, antibacterial activity was observed with MIC values ranging between 0.03 – 0.5 mg/mL (Table 6.4). The unconjugated ADEP1 analogues, as reported in Chapter 4, Table 4 had MIC and MBC values that were

between 63 – 500 µM and 125 – 750 µM, respectively. Table 6.3 shows that conjugating the ADEP1 analogues to the QDs greatly improved their antibacterial activity. The MIC and MBC values of the QD-peptide conjugates on the tested strains ranged from 2.3 – 37.5 µM and 9.38 – 150 µM, respectively.

According to Table 6.3, the most susceptible bacterium to the QD-ADEP1 analogue conjugates was *E. coli* with an MIC of 2.34 µM, followed by *B. subtilis* and *S. aureus* with MIC values of 9.38 µM, MRSA at 18.75 µM and lastly, *P. aeruginosa* at 37.5 µM. These results show that the conjugates were effective against both Gram-positive and Gram-negative bacteria. In chapter 5, the Gram-negative bacterial strains (*E. coli* and *P. aeruginosa*) showed resistance against the unconjugated peptides with MIC and MBC values of 500 and 750 µM, respectively. These observations were in line with previous studies which reported higher ADEP1 activity against Gram-positive bacteria compared to Gram-negative bacteria [25]. These new findings show that conjugating the ADEP1 analogues to the QDs helped overcome the resistance that was exhibited by *E. coli* against these peptides. Previous studies have discovered that peptides conjugated to nanomaterials show increased activity due to a re-binding mechanism to the target which then increases the retention time of the peptide with the target [22]. The re-binding or re-association mechanisms of nano-conjugates is enhanced by the slow dissociation rate of conjugates compared to free drug molecules. In addition, the increased density of the conjugate compared to either the nanomaterial or peptide alone exhibits increased binding affinity due to steric hindrance introduced upon binding to the target [23], [24].

Table 6. 3: MIC and MBC values of the QD-ADEP1 analogue conjugates focusing on peptide concentration

QD-Peptides conjugates	*B. subtilis*		*S. aureus*		*MRSA*		*P. aeruginosa*		*E. coli*	
	MIC µM	MBC µM	MIC µM	MBC µM	MIC µM	MBC µM	MIC µM	MBC µM	MIC µM	MBC µM
SC005	9.38	37.5	9.38	37.5	18.75	75	37.5	150	2.34	9.38
SC006	9.38	37.5	9.38	37.5	18.75	75	37.5	150	2.34	9.38
SC007	9.38	37.5	9.38	37.5	18.75	75	37.5	150	2.34	9.38
SC008	9.38	37.5	9.38	37.5	18.75	75	37.5	150	2.34	9.38
Gentamicin	26.1	52.3	0.5	1.0	26.2	52.4	418.8	837.5	NT	NT
Ampicillin	NT	NT	NT	NT	NT	NT	NT	NT	2862	5724

Table 6. 4: MIC and MBC values of the QD-ADEP1 analogue conjugates focusing on QD concentration.

QD	*B. subtilis*		*S. aureus*		*MRSA*		*P. aeruginosa*		*E. coli*	
	MIC mg/mL	MBC mg/mL	MIC mg/mL	MBC mg/mL	MIC mg/mL	MBC mg/mL	MIC mg/mL	MBC mg/mL	MIC mg/mL	MBC mg/mL
SC005	0.125	0.5	0.125	0.5	0.25	1	0.5	2	0.03	0.125
SC006	0.125	0.5	0.125	0.5	0.25	1	0.5	2	0.03	0.125
SC007	0.125	0.5	0.125	0.5	0.25	1	0.5	2	0.03	0.125
SC008	0.125	0.5	0.125	0.5	0.25	1	0.5	2	0.03	0.125
Gentamicin	26.1	52.3	0.5	1.0	26.2	52.4	418.8	837.5	NT	NT
Ampicillin	NT	NT	NT	NT	NT	NT	NT	NT	2862	5724

The cytotoxicity of the $AgInS_2$ QDs-ADEP1 conjugates was evaluated using HEK-293 cells and the MTS dye. Evaluating cytotoxicity is of utmost importance, especially if the materials are to be used in biological applications. For this assay, the HEK-293 cells were incubated with 2-fold serial dilutions of the conjugates (ranging from 4 – 0.03 mg/mL), incubated with the test samples for 72 hours, and the viability of the cells was quantified. The results presented in Figure 6.7 show cell viability greater than 80% for all the tested concentrations of the QD and QD-peptide conjugates. In a study by Oluwafemu *et al.* 2019 [14], a similar trend in cell viability was observed when similar QD material, AgInS2/ZnS core/shell, were tested against similar cell lines (i.e. baby hamster kidney cells). The $AgInS_2$ QDs used in this study are regarded environmentally friendly as they are capped with gelatin, an animal product that is also used in food.

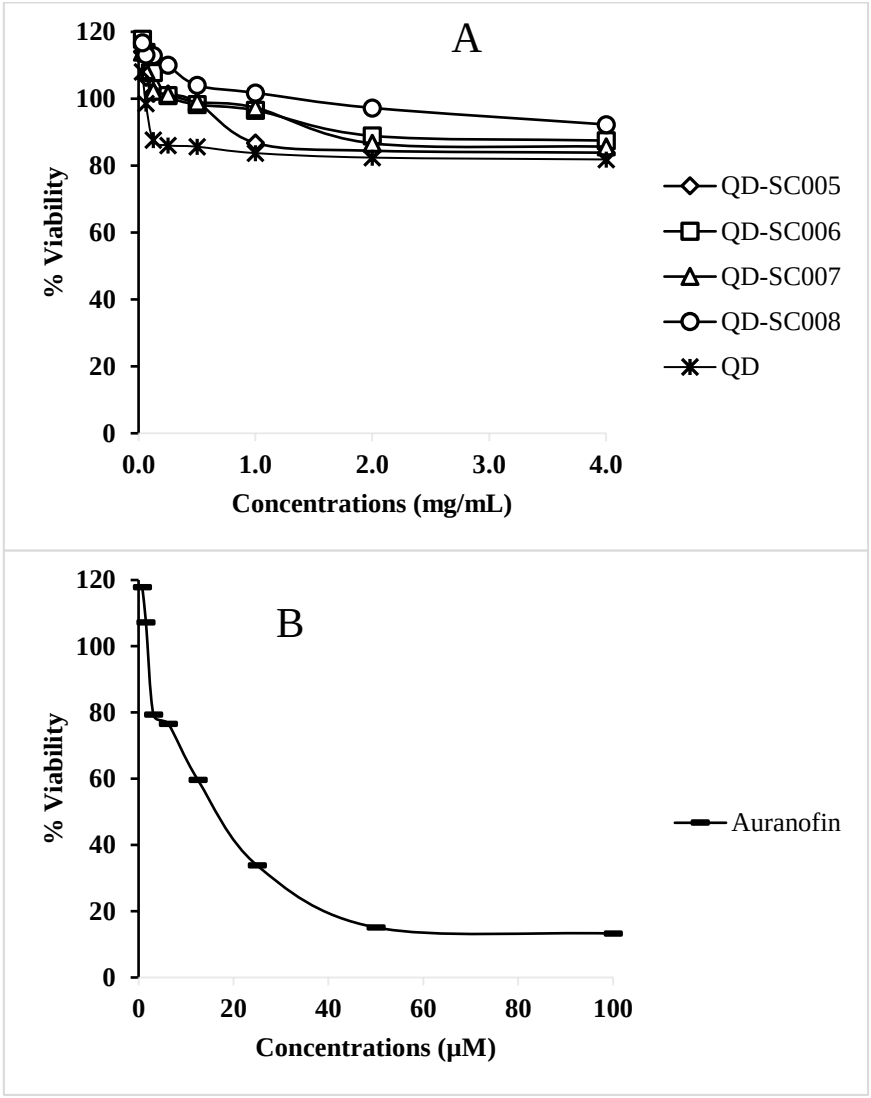


Figure 6. 7: Cell viability assay of QD-ADEP1 analogues and auranofin on HEK-293.

6.4. **conclusion and future perspectives**

In this study, gelatin-capped AgInS2 QDs were synthesised and conjugated to novel ADEP1 analogue peptides, with the aim of improving the antibacterial efficacy of these peptides. The conjugation of the QDs to the peptides was confirmed using multiple techniques, namely, zeta potential, PL, ED-XRF, and HR-TEM. The synthesis of gelatin-capped AgInS2 QDs yielded negatively charged spherical QDs with a diameter of ~6 nm. Upon conjugation to the peptides, an increase in particle size to ~13 nm was observed. Compared to the bare QDs, which did not show any appreciable antibacterial activity, and the ADEP1 analogues, which presented moderate activity, the AgInS2 QD-ADEP1 conjugates exhibited excellent antibacterial activity. The MIC values obtained for the AgInS2 QD-ADEP1 conjugates were between ~3 and ~200 folds lower than those obtained for the bare peptides, while the MBC values were between ~5 and ~13 folds lower than same. The obtained MIC and MBC values show that the conjugates were mostly potent against *E. coli*, followed by *B. subtilis* and *S. aureus*. Evaluation of the cytotoxicity of the conjugates showed that the AgInS2 QD-ADEP1 conjugates are biocompatible. The findings from this study suggest that the AgInS2 QD-ADEP1 analogue conjugates could potentially be used as antimicrobial agents without eliciting toxicity against mammalian cells.

6.5. References

[1] W. H. De Jong and P. J. Borm, "Drug delivery and nanoparticles: Applications and hazards," *Int. J. Nanomedicine*, vol. 3, no. 2, pp. 133–149, Jun. 2008.

[2] G. Guisbiers, S. Mejía-Rosales, and F. Leonard Deepak, "Nanomaterial Properties: Size and Shape Dependencies," *J. Nanomaterials*, 2012. https://www.hindawi.com/journals/jnm/2012/180976/ (accessed Aug. 31, 2018).

[3] A. Mandal, "Copper Nanomaterials as Drug Delivery System against Infectious Agents and Cancerous Cells," *J. Appl. Life Sci. Int.*, vol. 15, no. 4, pp. 1–8, Dec. 2017, doi: 10.9734/JALSI/2017/38444.

[4] Y. Kawabata, K. Wada, M. Nakatani, S. Yamada, and S. Onoue, "Formulation design for poorly water-soluble drugs based on biopharmaceutics classification system: basic approaches and practical applications," *Int. J. Pharm.*, vol. 420, no. 1, pp. 1–10, Nov. 2011, doi: 10.1016/j.ijpharm.2011.08.032.

[5] M. Martínez-Carmona, D. Lozano, M. Colilla, and M. Vallet-Regí, "Selective topotecan delivery to cancer cells by targeted pH-sensitive mesoporous silica nanoparticles," *RSC Adv.*, vol. 6, no. 56, pp. 50923–50932, May 2016, doi: 10.1039/C6RA07763C.

[6] R. H. Müller, C. Jacobs, and O. Kayser, "Nanosuspensions as particulate drug formulations in therapy. Rationale for development and what we can expect for the future," *Adv. Drug Deliv. Rev.*, vol. 47, no. 1, pp. 3–19, Mar. 2001, doi: 10.1016/s0169-409x(00)00118-6.

[7] L. Kou, Y. D. Bhutia, Q. Yao, Z. He, J. Sun, and V. Ganapathy, "Transporter-Guided Delivery of Nanoparticles to Improve Drug Permeation across Cellular Barriers and Drug Exposure to Selective Cell Types," *Front. Pharmacol.*, vol. 9, Jan. 2018, doi: 10.3389/fphar.2018.00027.

[8] C. T. Matea *et al.*, "Quantum dots in imaging, drug delivery and sensor applications," *Int. J. Nanomedicine*, vol. 12, pp. 5421–5431, Jul. 2017, doi: 10.2147/IJN.S138624.

[9] C. E. Probst, P. Zrazhevskiy, V. Bagalkot, and X. Gao, "Quantum dots as a platform for nanoparticle drug delivery vehicle design," *Adv. Drug Deliv. Rev.*, vol. 65, no. 5, pp. 703–718, May 2013, doi: 10.1016/j.addr.2012.09.036.

[10] M.-X. Zhao and B.-J. Zhu, "The Research and Applications of Quantum Dots as Nano-Carriers for Targeted Drug Delivery and Cancer Therapy," *Nanoscale Res. Lett.*, vol. 11, no. 1, p. 207, Apr. 2016, doi: 10.1186/s11671-016-1394-9.

[11] X. Cai, Y. Luo, W. Zhang, D. Du, and Y. Lin, "pH-Sensitive ZnO Quantum Dots-Doxorubicin Nanoparticles for Lung Cancer Targeted Drug Delivery," *ACS Appl. Mater. Interfaces*, vol. 8, no. 34, pp. 22442–22450, Aug. 2016, doi: 10.1021/acsami.6b04933.

[12] M. Jiao *et al.*, "Strongly emitting and long-lived silver indium sulfide quantum dots for bioimaging: Insight into co-ligand effect on enhanced photoluminescence," *J. Colloid Interface Sci.*, vol. 565, pp. 35–42, Apr. 2020, doi: 10.1016/j.jcis.2020.01.006.

[13] M. Z. Fahmi and J.-Y. Chang, "Forming double layer-encapsulated quantum dots for bio-imaging and cell targeting," *Nanoscale*, vol. 5, no. 4, pp. 1517–1528, Feb. 2013, doi: 10.1039/C2NR33429A.

[14] O. S. Oluwafemi, B. M. M. May, S. Parani, and J. V. Rajendran, "Cell viability assessments of green synthesized water-soluble AgInS2/ZnS core/shell quantum dots against different cancer cell lines," *J. Mater. Res.*, vol. 34, no. 24, pp. 4037–4044, Dec. 2019, doi: 10.1557/jmr.2019.362.

[15] X. Kang, Y. Yang, L. Wang, S. Wei, and D. Pan, "Warm White Light Emitting Diodes with Gelatin-Coated AgInS2/ZnS Core/Shell Quantum Dots," *ACS Appl. Mater. Interfaces*, vol. 7, no. 50, pp. 27713–27719, Dec. 2015, doi: 10.1021/acsami.5b10870.

[16] B. M. M. May, S. Parani, and O. S. Oluwafemi, “Detection of ascorbic acid using green synthesized AgInS2 quantum dots,” *Mater. Lett.*, vol. 236, pp. 432–435, 2019, doi: 10.1016/j.matlet.2018.10.155.
[17] M. Esfandyari-Manesh *et al.*, “Improved anticancer delivery of paclitaxel by albumin surface modification of PLGA nanoparticles,” *Daru J. Fac. Pharm. Tehran Univ. Med. Sci.*, vol. 23, no. 1, p. 28, Apr. 2015, doi: 10.1186/s40199-015-0107-8.
[18] A. E. Jablonski, W. H. Humphries, and C. K. Payne, “Pyrenebutyrate-mediated delivery of quantum dots across the plasma membrane of living cells,” *J. Phys. Chem. B*, vol. 113, no. 2, pp. 405–408, Jan. 2009, doi: 10.1021/jp809956w.
[19] H. Katas, N. N. S. Nik Dzulkefli, and S. Sahudin, “Synthesis of a New Potential Conjugated TAT-Peptide-Chitosan Nanoparticles Carrier via Disulphide Linkage,” *J. Nanomater.*, vol. 2012, p. e134607, Jun. 2012, doi: 10.1155/2012/134607.
[20] H. S. Qian, H. C. Guo, P. C.-L. Ho, R. Mahendran, and Y. Zhang, “Mesoporous-Silica-Coated Up-Conversion Fluorescent Nanoparticles for Photodynamic Therapy,” *Small*, vol. 5, no. 20, pp. 2285–2290, 2009, doi: 10.1002/smll.200900692.
[21] J. K. Jaiswal, H. Mattoussi, J. M. Mauro, and S. M. Simon, “Long-term multiple color imaging of live cells using quantum dot bioconjugates,” *Nat. Biotechnol.*, vol. 21, no. 1, pp. 47–51, Jan. 2003, doi: 10.1038/nbt767.
[22] G. Vauquelin and S. J. Charlton, “Long-lasting target binding and rebinding as mechanisms to prolong in vivo drug action,” *Br. J. Pharmacol.*, vol. 161, no. 3, pp. 488–508, Oct. 2010, doi: 10.1111/j.1476-5381.2010.00936.x.
[23] M. Mammen, S.-K. Choi, and G. M. Whitesides, “Polyvalent Interactions in Biological Systems: Implications for Design and Use of Multivalent Ligands and Inhibitors,” *Angew. Chem. Int. Ed Engl.*, vol. 37, no. 20, pp. 2754–2794, Nov. 1998, doi: 10.1002/(SICI)1521-3773(19981102)37:20<2754::AID-ANIE2754>3.0.CO;2-3.
[24] B. S. Mesquita *et al.*, “The Impact of Nanobody Density on the Targeting Efficiency of PEGylated Liposomes,” *Int. J. Mol. Sci.*, vol. 23, no. 23, p. 14974, Nov. 2022, doi: 10.3390/ijms232314974.
[25] H. Brötz-Oesterhelt *et al.*, “Dysregulation of bacterial proteolytic machinery by a new class of antibiotics,” *Nat Med*, vol. 11, pp. 1082–1087, 2005.

CHAPTER 7.

DESIGN OF ADEP1 PEPTIDE ANALOGUES

Characterization of the recombinant *M. tb* ClpP1/P2 domains, peptidase activity and pharmacokinetics of ADEP1 analogues

7.1. Introduction

Most biological processes that occur in living cells are controlled by proteins, often acting in association with other protein partners through protein–protein interactions. These include fundamental processes such as cell growth, intracellular communication, apoptosis, cell cycle control and signalling cascades to name a few. As such, a number of human diseases are a result of abnormal proteins or disruptions of protein–protein interactions either through a mutation that results in loss of an essential interaction or through formation of a protein complex at an inappropriate time or location [1]. Consequently, the drug discovery and development field typically aim to identify novel compounds that can influence the activity of disease-associated proteins [2]. This is mostly done through the use of *in silico* molecular modelling platforms followed by *in vitro* screening assays which often require large amounts of the target protein.

It is almost impossible to obtain adequate amounts of the target proteins from native organic sources, and as a result, recombinant DNA technology has become the method of choice in biotechnology industry for expression of proteins of interest [3]. Recombinant DNA technology make use of a wide range of organisms such as bacteria, yeast, mammalian cells, insect cells and transgenic plants as production systems [4], [5]. Each of these production platforms has their own advantages and limitations, and selection is usually done based on the characteristics of the target protein as well as the intended application [1]. *E. coli* is the most popular recombinant protein expression host due to its inexpensive maintenance, fast growth kinetics [6], high cell density cultures [7], and rapid plasmid transformation time [8], which translates to rapid production of recombinant proteins in large quantities. Recombinant proteins are not only useful for research purposes, but also as therapeutic drugs. Human insulin, approved by the United States Food and Drug Administration (FDA) in 1982, was the first recombinant protein to be approved as a therapeutic drug. Since then, over 130 recombinant protein drugs have been approved [1].

However, for any lead compound to be considered as a potential drug candidate, the absorption, distribution, metabolism and excretion (ADME) properties of the compound should be known, despite its activity against the target [9]. ADME addresses how the drug enters the body, how it moves, what changes it encounters, and finally how it leaves the body [10]. Analysis of clinical trial data showed that 10 – 15% of drug failures were attributed to poor pharmacokinetic properties [11]. It is therefore important to screen any newly identified lead compounds for their pharmacokinetic properties early to identify poor candidates as soon as possible.

In this study, recombinant DNA technology was used to produce the ClpP1 and ClpP2 domains of the *M. tb* ClpP1P2 protease in *E. coli*. These domains were expressed, purified and characterised with the aim of evaluating the binding affinity of the ADEP1 analogues to the respective ClpP1 and ClpP2 domains. The ability of the ADEP1 analogues to enhance the peptidase activity of the *M. tb* ClpP1P2 protease was evaluated. In addition, the solubility and membrane permeability of new ADEP1 analogues were investigated.

7.2. **Materials and Methods**

7.2.1. *Recombinant expression of ClpP1 and ClpP2 in E. coli*

The genes encoding the ClpP1 and ClpP2 subunits of the H37Rv *M. tb* strain (GenBank accession numbers YP_177883 and CCP45253.1, respectively) were synthesised and individually cloned into pET15b vectors, in-frame with the vector encoded polyhistidine tag (GenScript, USA). The pET15b-ClpP1 and pET15b-ClpP2 recombinant plasmids were separately transformed into *E. coli* T7 express competent cells (New England Biolabs) according to the manufacturer's instructions and selected on Luria-Bertani (LB) agar plates containing 100 µg/mL ampicillin at 37 °C overnight. Single colonies of successfully transformed bacterial cells were picked, inoculated in LB-ampicillin broth, and grown at 37 °C overnight under vigorous shaking (250 rpm). The overnight cultures were diluted into fresh LB-ampicillin broth at a ratio of 1:100 and grown under the same conditions until the optical density at 600 nm (OD_{600}) reached 0.6. The cultures were induced with varying concentrations of isopropyl-β–D-1-thiogalactopyranoside (IPTG; 0, 0.2, 0.4, 0.6, 0.8 and 1mM), and allowed to grow for an additional 4 hours. The cells were analysed for the over-expression of the recombinant ClpP1 and ClpP2 proteins *via* (Sodium Dodecyl-Sulfate Polyacrylamide Gel Electrophoresis) SDS-PAGE.

In addition to the inducer (IPTG) concentration, post-induction incubation time was also tested to optimise the expression yields for each protein. For this, the bacterial cultures were induced using the optimised IPTG concentrations for each protein, and the cultures were grown at 37 °C for 4 hours. Samples were collected every hour for analysis for the presence of the respective proteins by SDS-PAGE.

7.2.2. *Solubilisation of the ClpP1 and ClpP2 recombinant proteins*

Following the over-expression of the two recombinant proteins using the optimised conditions for each, i.e. 0.2 mM IPTG at 37 °C for 2 hours for ClpP1, and 0.2 mM IPTG at 37 °C for 4 hours for ClpP2, the cells were pelleted by centrifugation at 3220 xg for 30 minutes at 4 °C. The supernatants were discarded and the pellets resuspended in ice-cold phosphate buffered saline (PBS; 137 mM NaCl, 2.7 mM KCl, 8 mM Na_2HPO_4, 2 mM KH_2PO_4, pH 7.4). The cells were sonicated for 5 minutes using the Labsonic® M ultrasonic processor (Sartorius stedim, Germany), after which DNase I was added to the final concentration of 5 µg/mL and the lysates incubated on ice for 30 minutes. The lysates were centrifuged at 3220 xg for 30 minutes and the respective pellets and supernatants were analysed for the presence of the ClpP1 and ClpP2 proteins, respectively, *via* SDS-PAGE. Both recombinant proteins were associated with the insoluble fractions and were recovered from the insoluble inclusion bodies using buffer A (0.1% (w/v) N-Lauroylsarcosine sodium salt (Sarkosyl) in PBS, pH 7.4). The samples were incubated at room temperature for 2 hours, followed by centrifugation at 3220 xg and subsequent analysis by SDS-PAGE.

7.2.3. *Purification of ClpP1 and ClpP2*

The Sarkosyl solubilised ClpP1 and ClpP2 recombinant proteins were purified by immobilised-metal affinity chromatography (IMAC) using 5 mL HisTrap nickel-nitrilotriacetic (Ni-NTA) columns (Cytiva, Marlborough, United States) coupled to a NGC medium-pressure chromatography system (Bio-Rad, California, United States). The lysates were separately loaded onto Ni-NTA columns pre-equilibrated with buffer A, following which the columns were extensively washed with buffer B (PBS, 0.1% Sarkosyl (w/v), 20 mM Imidazole) to remove any non-specifically bound proteins. The recombinant proteins were then eluted from the columns using a 10-column volume linear gradient of 20 – 300 mM Imidazole in buffer A. The elution of the proteins from the columns were monitored at 280 nm, and fractions

containing protein were collected and analysed for the presence of ClpP1 and ClpP2 using 12% SDS-PAGE. Fractions containing the proteins of interest were pooled and glycerol, to a final concentration of 10% (v/v), was added to the samples. The samples were concentrated using the Amicon ultra spin concentrators with a 10-kDa molecular weight cut-off membrane (Millipore, Burlington, United States). The samples were snap-frozen in liquid nitrogen and subsequently stored at -80 °C. The purified recombinant proteins were quantified using the NanoDrop 2000 spectrophotometer (ThermoFisher, Waltham, United Sates) and the obtained absorbance values (A_{280nm}) were converted into concentration using the Beer-Lambert law:

$$A = \varepsilon cl$$

Where A is the measured absorbance value for each protein at 280 nm, ε is the molar extinction coefficient of each protein (i.e. 14 565 M^{-1} cm^{-1} for ClpP1 and 10 430 M^{-1} cm^{-1} for ClpP2) and l is the length of light path.

7.2.4. *Characterisation of the purified recombinant proteins*

7.2.4.1. Qualitative analysis of ClpP1 and ClpP2

Enzyme-linked immunosorbent assay (ELISA) was used to assess the reactivity of the purified recombinant proteins with a horseradish (HRP)-conjugated anti-His antibody (Abbkine, Wuhan, China) recognising the N-terminal polyhistidine tags on the proteins. For this assay, two-fold serial dilutions of the purified recombinant proteins (i.e. 100, 50, 25, 12.5, 6.25, 3.13 and 1.56 μg/mL) in coating buffer (15 mM Na_2CO_3 and 35 mM $NaHCO_3$, pH 9.6) were individually coated onto 96-well microtiter plates (ThermoFisher, Waltham, United Sates). The plates were incubated at 4 °C overnight, followed by washes with wash buffer (Tris-buffered saline (TBS) containing 0.1% Tween-20). The plates were blocked for non-specific binding using blocking buffer (5% casein peptone in TBS) at 37 °C for 2 hours. Following another washing step, the plates were incubated with the HRP-conjugated anti-His antibody at a dilution of 1:1000 in blocking buffer and incubated at 37 °C for 2 hours. The plates were thoroughly washed with the washing buffer before 3,3',5,5'-Tetramethylbenzidine (TMB), an HRP, substrate was added. The plates were incubated at 37 °C until sufficient colour development was observed (~20 minutes), and the HRP-TMB reaction was terminated using 2 M sulphuric acid. The absorbance of the wells was measured at 450 nm using a spectrophotometer (SpectraMax Plus 384 Microplate Reader, Molecular Devices, California, United States)

1.1.1. Structural characterisation of the purified recombinant proteins

The secondary structures of the ClpP1 and ClpP2 recombinant proteins were analysed using circular dichroism (CD) spectroscopy in the far-UV region (190 – 250 nm). For the analysis, CD spectra of 10 µM of the ClpP1 and ClpP2 proteins were measured at 20 °C using 0.1 cm path length quartz cuvettes in a Chirascan CD spectrometer. An average of 5 scans were taken for each protein, and buffer controls were also measured and subtracted from the protein measurement. The measured ellipticity values were converted to mean residue ellipticity (MRE) [θ] (mdeg.cm^2.dmol^{-1}) using the equation:

$$[\theta] = \frac{100\ x\ \theta}{Cnl}$$

Where θ is the measured ellipticity in millidegrees (m.deg), C is the concentration of the protein in millimolar (mM), n is the number of amino acid residues in the protein and l is the path length of the cuvette in centimetres.

7.2.5. *M. tb ClpP1P2 Peptidase activity assay*

The effect of the in-house produced ADEP1 analogues on the peptidase activity of the complete ClpP1P2 enzyme was investigated using the *M. tb* ClpP protease assay kit (Profoldin, United States). The assay is based on the cleavage of an amide bond between a short peptide substrate and the highly fluorescent fluorophore, 7-amino-4-methylcoumarin (AMC), by the ClpP1P2 enzyme. The amide bond between the peptide and AMC results in quenching of the fluorescence signal, however, upon cleavage of this bond by peptidases, the AMC gets released and produces a fluorescent signal. The AMC can be excited between 302-412 nm, and has an emission range of 441±100 nm [12].

The assay was performed in black-wall/clear-bottom 384-well plates with a final reaction volume of 30 µL. The assay buffer, *M. tb* ClpP1P2, test samples and the substrate were all mixed according to the manufacturer's specifications. DMSO was used as a negative control, while N-benzoyl-Leucyl-Leucine (Bz-LL, synthesized in-house) was used as a positive control. The test samples were initially incubated with the ClpP1P2 enzyme diluted in assay buffer at 37 °C for 20 minutes, after which the substrate was added, and the plate incubated for an additional 60 minutes. Fluorescence measurements were taken at 15 minute intervals during

the 60 minute incubation time using the Glomax explorer multimode microplate reader (Promega, United States). The emission was read at a range of 415-445nm and excitation at 365nm. After the 60 minute incubation, the reaction was stopped using the kit stop solution and the fluorescent readings were used to calculate the percentage activity (% Activity) of the ADEP1 analogues.

$$\%\ Activity = \left(\frac{Sample - negative\ control}{negative\ control}\right) x100$$

7.2.6. *Aqueous solubility test of the ADEP1 analogues*

Aqueous solubility test of SC005-8 (Figure 7.1) was performed using a MultiScreen Solubility Filter Plate (Millipore). This method uses a 96-well plate comprising of donor wells separated from acceptor with a filter. The peptide standards for calibration curves were prepared according to the assay protocol and read on a UV spectrophotometer (SpectraMax Plus 384 Microplate Reader, Molecular Devices, California, United States) at 240 nm with concentrations ranging from 0-500 μM (0, 3.13, 12.5, 50, 200, 500 μM). Acceptable standard curves should generate linear curves with correlation coefficients (r^2) greater than 0.85 and the obtained correlation coefficients were 0.91-0.99. The tests were performed in triplicates with a final concentration of 500 μM of each peptide in 5% DMSO solution in each donor well. The plate was left shaking at 250 rpm for 90 minutes at room temperature. The samples were then filtered from the donor well into an acceptor well. UV spectrum of the filtered compounds was read at 240 nm UV spectrophotometer and extrapolated using the standard calibration curve. Aqueous solubility was calculated using the formula below.

$$Aqueous\ solubility = \left(\frac{Absorbance\ (filtrate)}{slope}\right)$$

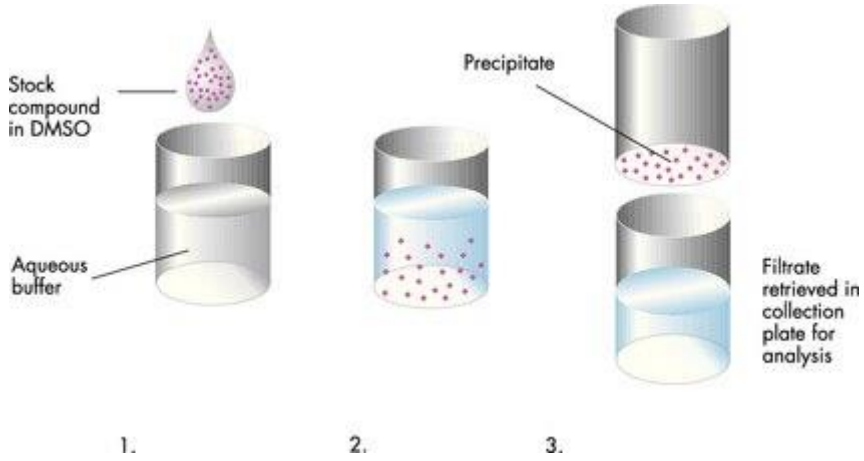


Figure 7. 1: Three steps in solubility assay protocol.

Membrane permeability potential of SC005-8 (Figure 7.2) through the blood-brain barrier and gastrointestinal membrane was measured using the Parallel Artificial Membrane Permeability Assay (PAMPA) kits (BioAssay Systems, California). The PAMPA kits were embedded with free fatty acids, cholesterol and sugars mimicking the barriers in the body. PAMPA was performed on a 96-well plate with separate donor and acceptor wells. The donor well plate contains a solution with the compounds while the acceptor well plate contains PBS (137 mM NaCl, 2.7 mM KCl, 8 mM Na_2HPO_4, 2 mM KH_2PO_4, pH 7.4). The two solutions in the wells were separated by an artificial membrane. The donor-acceptor wells were incubated at 37°C overnight. After incubation the acceptor well was analysed using UV-Vis at wavelengths ranging from 190-270 nm. Percentage permeability for each compound was calculated using the absorbance of the stock solution in the donor well (500 μM) and the absorbance of penetrated compounds using the formula below.

$$\%\ Permeability = \left(\frac{Absorbance\ penetrated\ compounds}{Absorbance\ of\ compounds\ before}\right) x\ 100$$

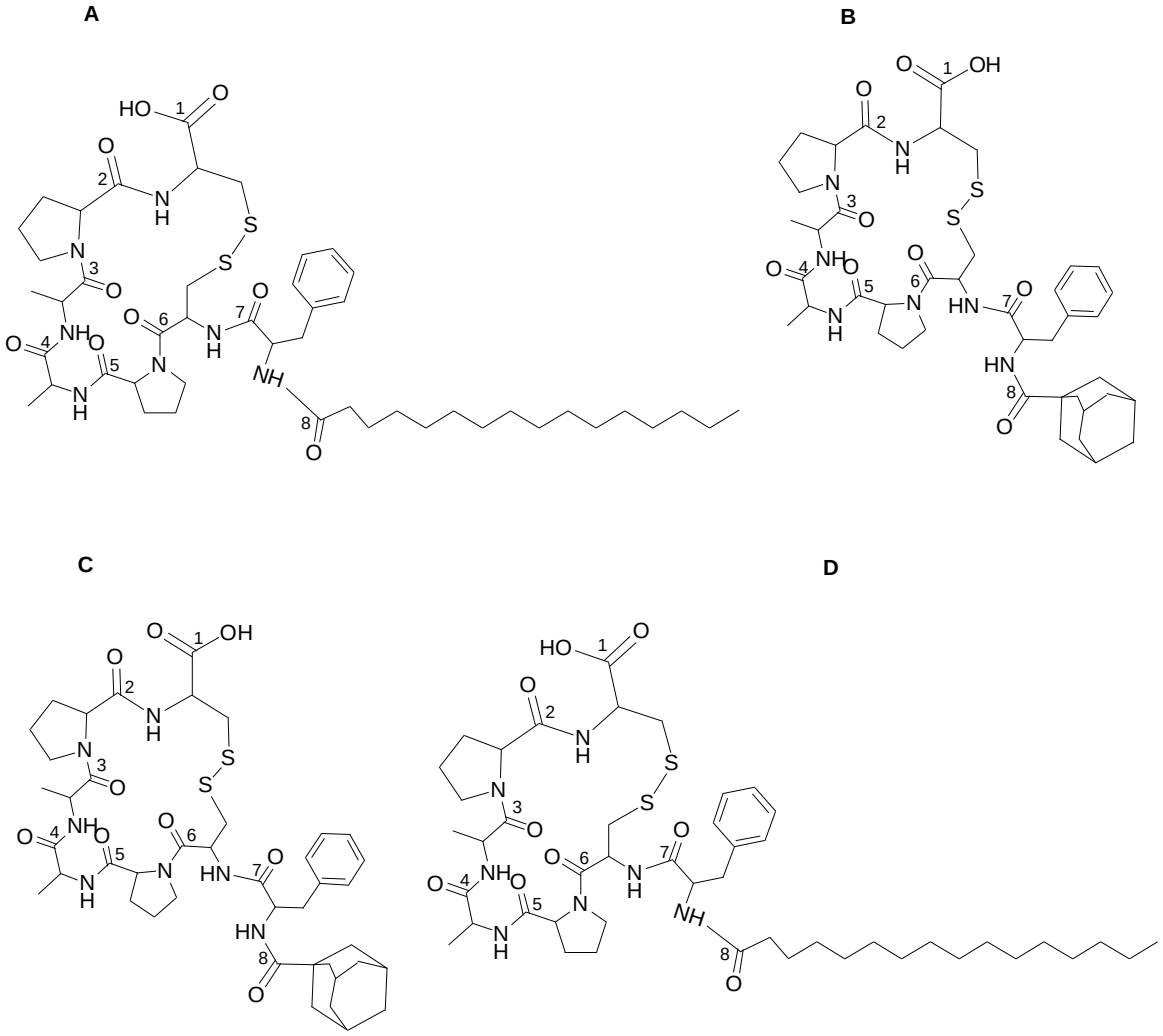


Figure 7. 2: Disulphide bond cyclised ADEP1 analogues. A-SC005 (D-form); B-SC006 (D-form); C-SC007 (L-form), D-SC008 (L-form).

7.3. **Results and Discussion**

7.3.1. *ClpP1 and ClpP2 expression, solubilisation and purification*

E. coli T7 express cells were used to heterologously express the ClpP1 and ClpP2 subunits that make up the *M. tb* ClpP1P2 protease using the shake-flask cultivation method and IPTG as an inducer. Induction trials were conducted to determine the optimum conditions for the expression of the respective recombinant proteins, where factors such as IPTG concentration, post-induction temperature and post-induction incubation time were varied. For the optimisation of the IPTG concentration, the cultures were induced with varying concentrations of IPTG (0, 0.2, 0.4, 0.6, 0.8 and 1 mM) and grown at 37 °C for 4 hours. Figure 7.3 A shows that there was no major difference in the expression levels of both ClpP1 and ClpP2 when the concentration of IPTG was increased from 0.2 to 1 mM. The lowest concentration of IPTG

tested in this study, i.e. 0.2 mM, was therefore used in the subsequent expressions of both proteins. Figure 7.3 A also shows that no expression of ClpP1 and ClpP2 was observed in the uninduced *E. coli* T7 express cells.

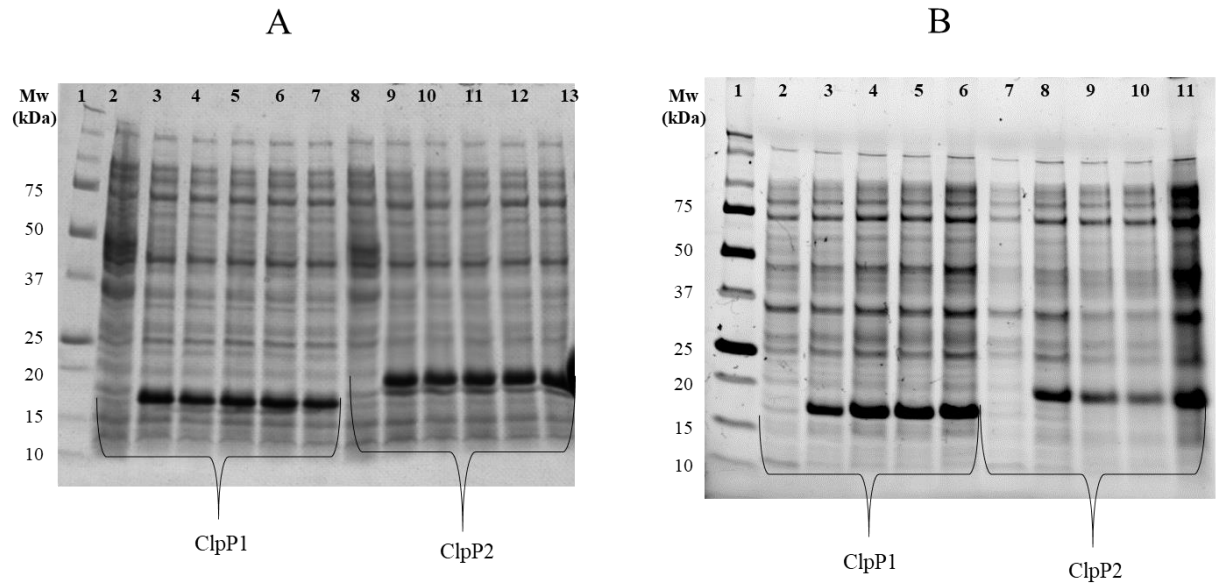


Figure 7. 3: SDS-PAGE analysis of recombinant ClpP1 and ClpP2 proteins expressed in *E. coli* T7. Lane 1 on both A and B gels contain protein molecular weight markers. A- Lane 2-7 and lane 8-13 contain ClpP1 and ClpP2 cultures, respectively, induced with varying concentrations of IPTG concentrations of 0, 0.2, 0.4, 0.6, 0.8 and 1mM for 2 and 4 hours, respectively. B- Lane 2-6 and lane 7-11 contain ClpP1 and ClpP2 cultures, respectively, with time intervals from 0-4 hours post induction with 1 mM IPTG.

To optimise the post-induction incubation time, the adjusted IPTG concentration of 0.2 mM was used and the bacterial cultures were grown at 37 °C. The cultures were grown for 4 hours, with samples taken at hourly intervals for analysis. Figure 7.3. B (lane 4) shows that the highest expression level of ClpP1 was observed at 2 hours post-induction, while that of ClpP2 was observed 4 hours post-induction (Figure 7.3 B, lane 11). The expected molecular weights of the ClpP1 and ClpP2 domains as predicted by the ProtParam tool (http://www.expasy.ch/tools/protparam.html) were ~22 and ~24 kDa, respectively; however, Figures 7.3.A and 7.3 B show that these proteins migrated at ~17 and 19 kDa. Similar observations were reported by Akopian *et al*. 2012 [13]. This is a common phenomenon in the gel migration of proteins with a high hydrophobic percentage. ClpP1 contains 46.77% hydrophobic amino acid content while ClpP2 has 43.93%. Hydrophobic proteins tend to

migrate faster in SDS-PAGE gels thus showing an observed molecular weight lower than theoretical molecular weight [14].

Following successful overexpression of the recombinant ClpP1 and ClpP2 domains, the bacterial cells were lysed and the solubility of the proteins was assessed *via* SDS-PAGE. Majority of both ClpP1 and ClpP2 proteins was observed in the insoluble fractions. Several attempts were made to enhance the solubility of the protein. These included decreasing the expression temperature to 30, 20 and 16 °C, as well as using different detergents in the extraction buffer (data not shown). The use of 0.1% Sarkosyl in the extraction buffer was found to get most of the recombinant proteins into the soluble fraction.

The solubilised protein samples were individually purified by IMAC using Ni-NTA columns and subsequently eluted using a linear gradient of imidazole from 20 to 300 mM. The elution of the proteins was monitored at 280 nm, and the elution profiles for ClpP1 and ClpP2 are shown in Figures 7.4 A and 7.4 B, respectively. Elution fractions were analysed for the presence of ClpP1 and ClpP2 using SDS-PAGE (Figures 7.4 C and 7.4 D, respectively), and fractions corresponding to the subunits were pooled and concentrated.

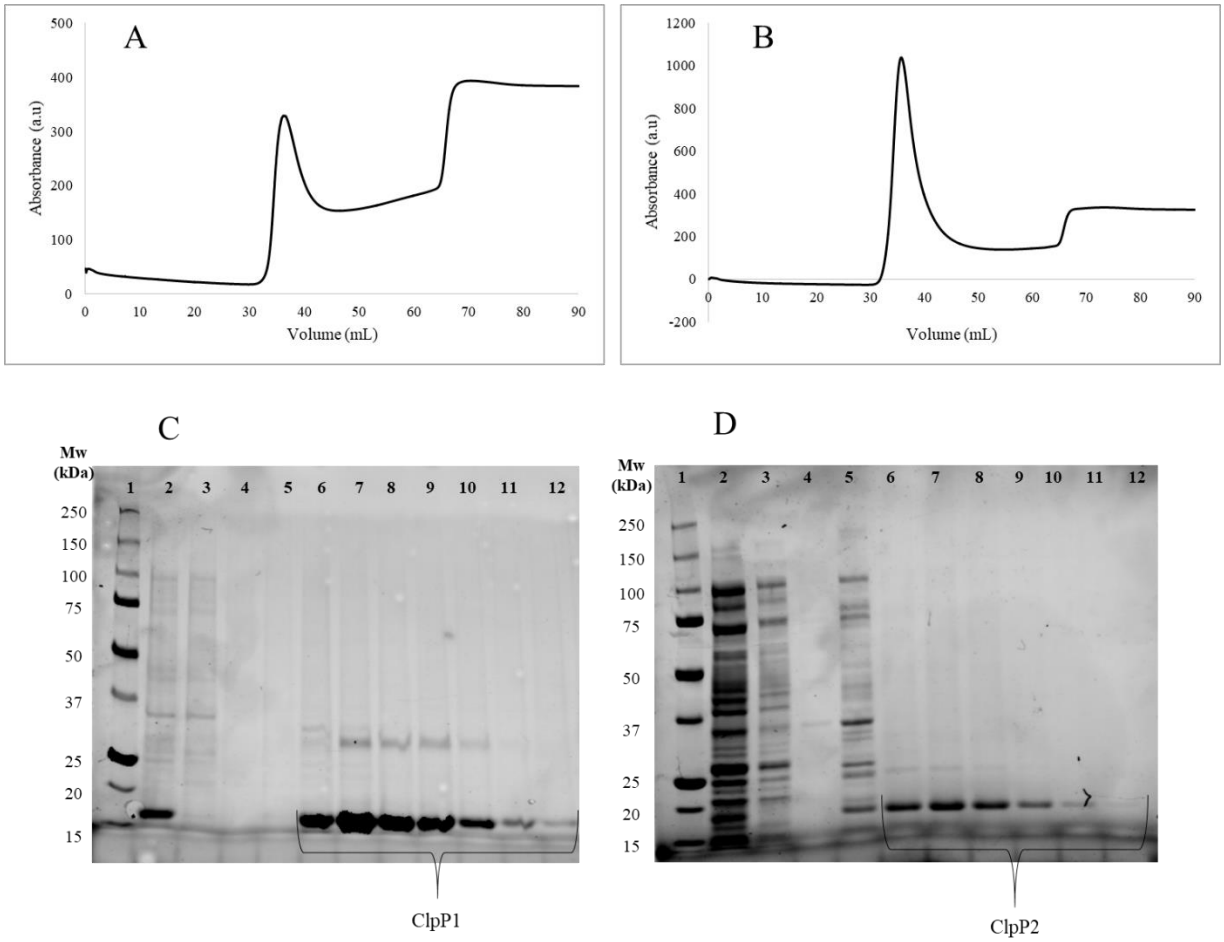


Figure 7. 4: Elution profiles ClpP1 (A) and ClpP (B) from the Ni-NTA columns. The first peaks, marked with asterisks, contained ClpP1 and ClpP2, respectively (C and D). SDS-PAGE gels of sarkosyl solubilised proteins, and purification fractions eluted from the columns. Lane 1 on both C and D gels contain protein molecular weight markers. Lane 2 and 3 in both gel C and D contain lysate and flow through, respectively. Lane 4-11 contain the eluted protein fractions.

7.3.2. *Characterisation of the purified recombinant proteins*

7.3.2.1. Qualitative analysis of ClpP1 and ClpP2 using ELISA

The His-tag that was exploited for the affinity purification of the ClpP subunits was also used in the qualitative analysis of the proteins. In the absence of antibodies specific to ClpP1 and ClpP2 domains, ELISA was conducted using HRP-conjugated anti-His antibodies to confirm the presence of the His-tagged recombinant proteins. Microtiter plates were coated with varying concentrations of the purified recombinant proteins (0-100 µg/mL) while the concentration of the antibody probe was kept constant. The absorbance values obtained show

correlation with the protein concentrations (Figure 7.5). These results can therefore be used to confirm a successful expression and purification of the His-tagged ClpP1 and ClpP2 domains.

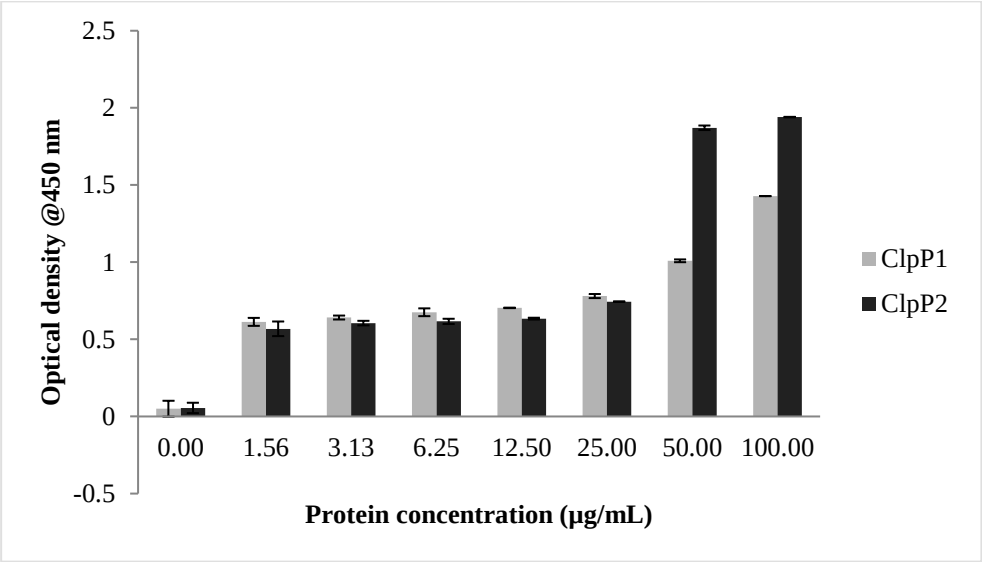


Figure 7. 5: Qualitative ELISA analysis of the purified recombinant proteins using anti-His antibodies. The responses indicate binding of HRP-conjugated anti-His antibody on ClpP1/P2 concentrations. The results are presented in average absorbance measurements at 450 nm ± standard deviation.

7.3.2.2. Structural characterisation of the purified recombinant proteins

The *M. tb* ClpP1 and ClpP2 share a sequence identity of about 48% and a common structure consisting of seven α-helices and two central β-sheets [15]–[17]. CD spectrometry was used to investigate the secondary structure of the purified recombinant ClpP1 and ClpP2 proteins. The CD spectrum obtained for both these proteins pointed to predominantly α-helical structures of the proteins that is represented by the negative bands at 208 and 220 nm (Figures 7.6 and 7.7). The subunit domains alone do no not possess peptidase or protease activity. However, they can be combined to form a ClpP1P2 active complex using Bz-LL [13], [18], [19].

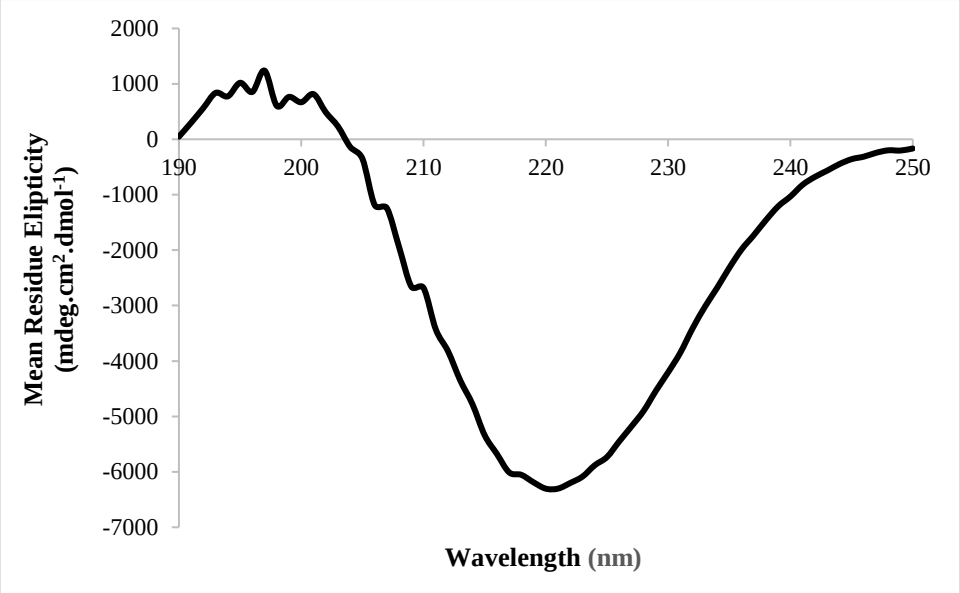


Figure 7. 6: Far-UV (190 – 250 nm) CD spectrum of the purified recombinant ClpP1 subunit at 10 µM.

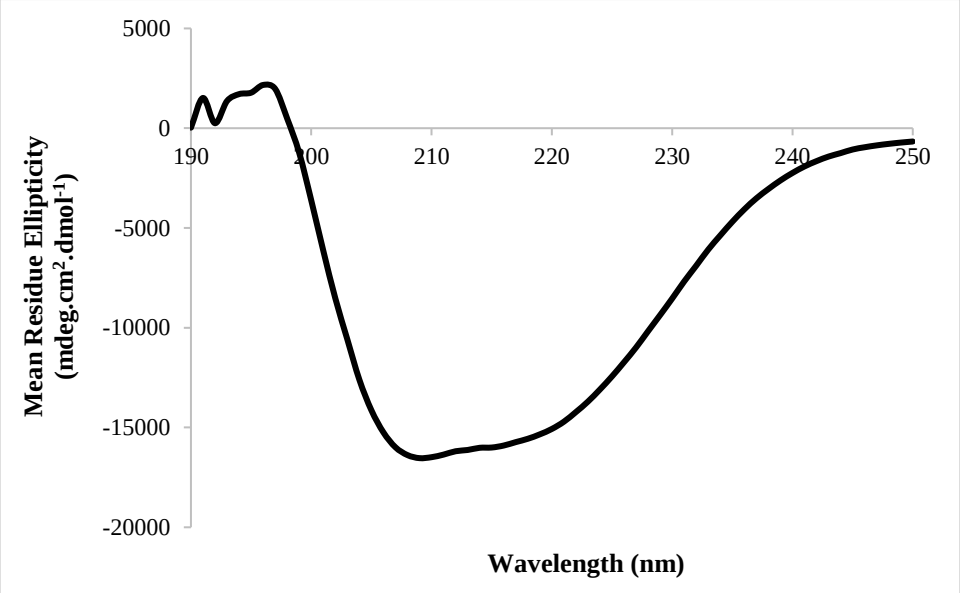


Figure 7. 7: Far-UV (190 – 250 nm) CD spectrum of the purified recombinant ClpP2 subunit at 10 µM.

7.3.2.3. *M. tb* ClpP1P2 peptidase activity assay

The *M. tb* ClpP1P2 protease assay kit was used to assess the effect of the novel ADEP1 analogues (SC005-8) on the peptidase activity of the ClpP1P2 protease. Dysregulation of ClpP1P2 by either inhibiting or enhancing the activity has been identified as potential drug target for *M. tb* [20]. Figure 7.8 showed that an increase in the detection fluorophore was

observed with the increase in incubation time. Also notable from Figure 7.8 and Table 7.1 is that SC008 showed highest activation of the *M. tb* ClpP1P2 peptidase activity with an estimated activation percentage of ~72% relative to the negative control which was treated with DMSO only. SC005 was the second most potent of the ADEP1 analogues and had an activation percentage of ~54%. These two peptides were even more effective in inducing the ClpP1P2 activity than the Bz-LL that was used as a positive control. Bz-LL is an N-terminal blocked dipeptide agonist that is known to bind and activate ClpP1P2 [13], [19]. SC006 and SC007 had similar activity trends and their activity was comparative to that of Bz-LL.

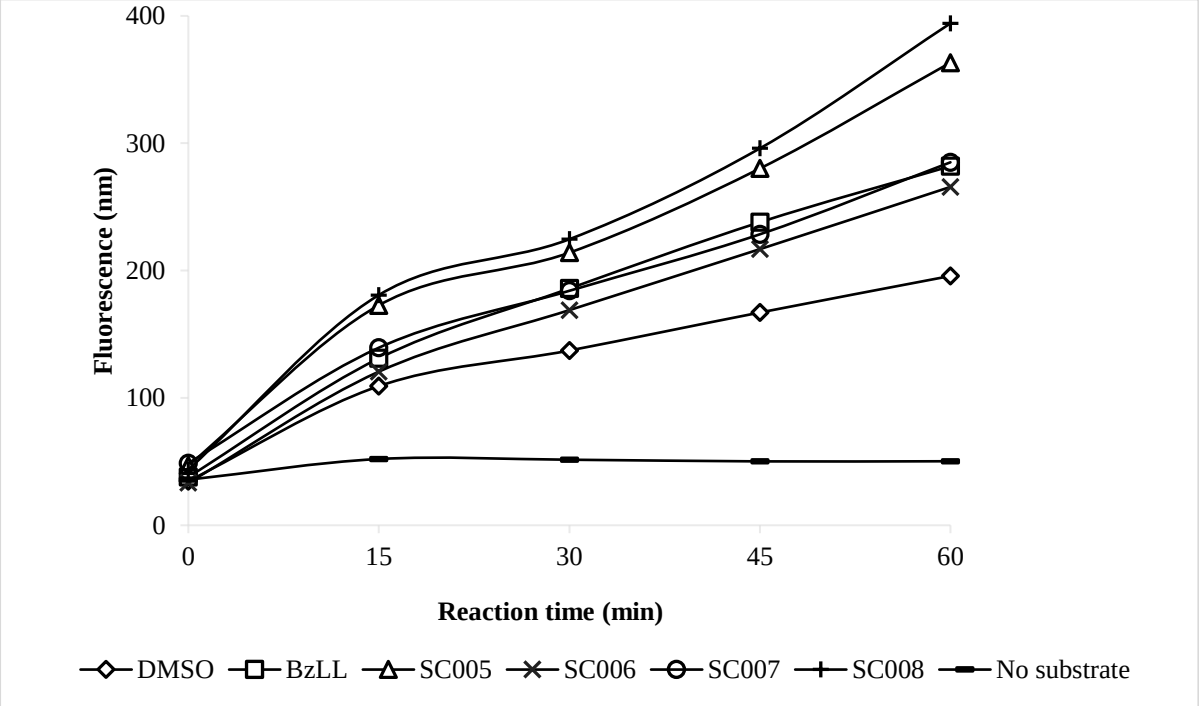


Figure 7. 8: M.*tb* ClpP1P2 peptidase activity response determined by the presence of free AMC measured by fluorescence spectrophotometer. DMSO and Bz-LL were used as negative and positive control, respectively. The emission was read at a range of 415-445 nm and excitation at 365 nm.

Table 7. 1: *M.tb* ClpP1P2 peptidase activity percentage

ADEPs	**Bz-LL**	**SC005**	**SC006**	**SC007**	**SC008**
%Activity	40	54	32	34	72

7.3.2.4. Clinical pharmacokinetic properties of ADEP1 analogues

There is a number of *in vitro* techniques and assays that screen new potential drug candidates for their pharmacokinetic properties such as membrane permeability, aqueous solubility, metabolic stability, blood partitioning, plasma protein binding, cytotoxicity, etc [21], [22]. The cytotoxicity of SC005-8 is discussed in Section 5.3.3, herein; the focus was on the aqueous solubility and membrane permeability of the analogues. Solubility of drugs is an important factor as it helps achieve the desired systemic circulation drug concentration required for a pharmacological response [23]. This is particularly important for orally administered drug, as they have to go through different conditions before they are absorbed and distributed to their targets. The parent ADEP1 peptide has been reported to possess poor aqueous solubility accompanied by high efflux [24]. Aqueous solubility results of the ADEP1 analogues are shown in Figure 7.9. A compound with aqueous solubility 500 µM is considered to be highly soluble; 00 µM < aqueous solubility > 500 µM is moderately soluble, while those with ≤ 100 µM are considered to be poorly soluble.

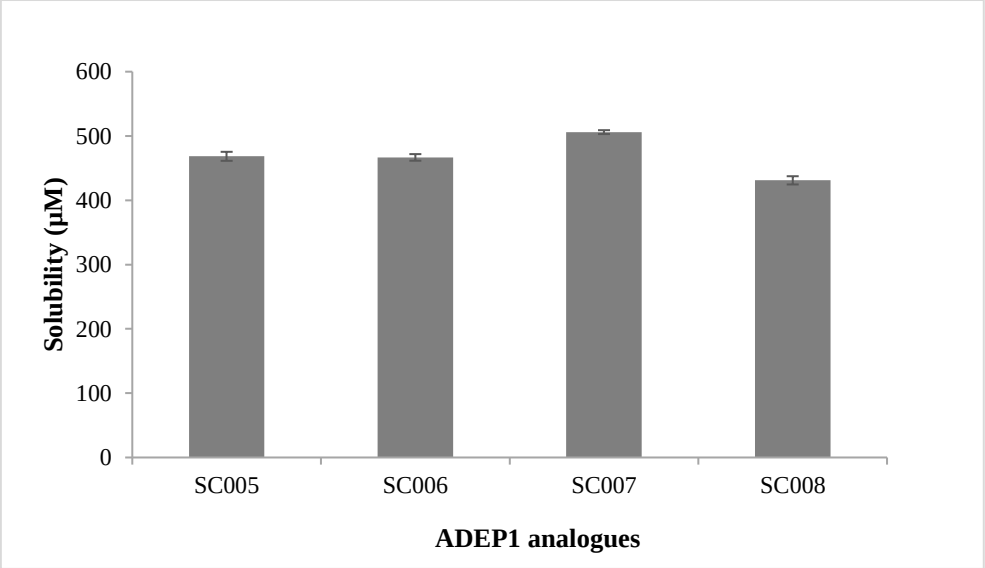


Figure 7. 9: Solubility test of ADEP1 analogues - SC005 (D-form); SC006 (D-form); SC007 (L-form), SC008 (L-form).

The structural changes and amino acid composition in the ADEP1 analogues resulted in improved solubility (the changes are described in Section 5.2.2). The amino acid composition of ADEPs is mainly hydrophobic containing Pro, Ala, and Phe with only Ser as a hydrophilic residue. This contributed to the poor solubility of ADEPs. ADEPs target intracellular

hydrophobic pockets of ClpP; therefore, it is assumed that their strength as antibacterial lies in their hydrophobic nature. Thus, designed active ADEP analogues should maintain the hydrophobicity. ADEP1 analogues contain two Cys residues, which are also hydrophobic amino acids adding to the hydrophobicity of the analogues [25]. The resultant disulphide bond from the two Cys is also reported to improve solubility of peptides [26]. There was no significant difference in solubility of peptides containing Pal compared to the Ada peptides. Also, no significant difference between the L- and D-form peptide analogues. Solubility also has a positive correlation to membrane permeability of pharmaceutical compounds. Increased solubility directly increases the membrane permeability of the oral drugs.

PAMPA assay is an *in vitro* high throughput technique used to measure the passive transcellular permeability ability of compounds. It is based on simple permeation without the complexities of active transmembrane transport [27]. PAMPA also gives an idea on how compounds absorb in different membranes such as the gastrointestinal tract, blood-brain barrier, and other body barriers.

Figure 7.10 shows the results the blood-brain barrier PAMPA (PAMPA-BBB) and gastrointestinal tract (PAMPA-GI) assays for the ADEP1 analogues. Blood-brain barrier is an endothelium membrane that creates a strong diffusional restriction between the brain and blood [28]. This barrier maintains a tight limit, which protects the brain from unwanted substances in the circulatory system. Thus, an increase in blood-brain barrier permeability can be damaging to the central nervous system's homeostasis [29]. Ideally, drugs that are targeting other body sites should have limited brain-blood barrier permeation or no permeation at all. However, anti-TB drugs should be able to cross the BBB in cases of TB meningitis. Compounds with a molecular weight larger than 600 g/mol or peptides with more than six amino acid residues usually have poor BBB permeability [30], [31]. The ADEP1 analogues are all greater than 600 g/mol, hence they were coupled to lipophilic permeability enhancers such as Pal and Ada. Both Pal and Ada have been used to enhance drug membrane permeability including the BBB [32]–[34].

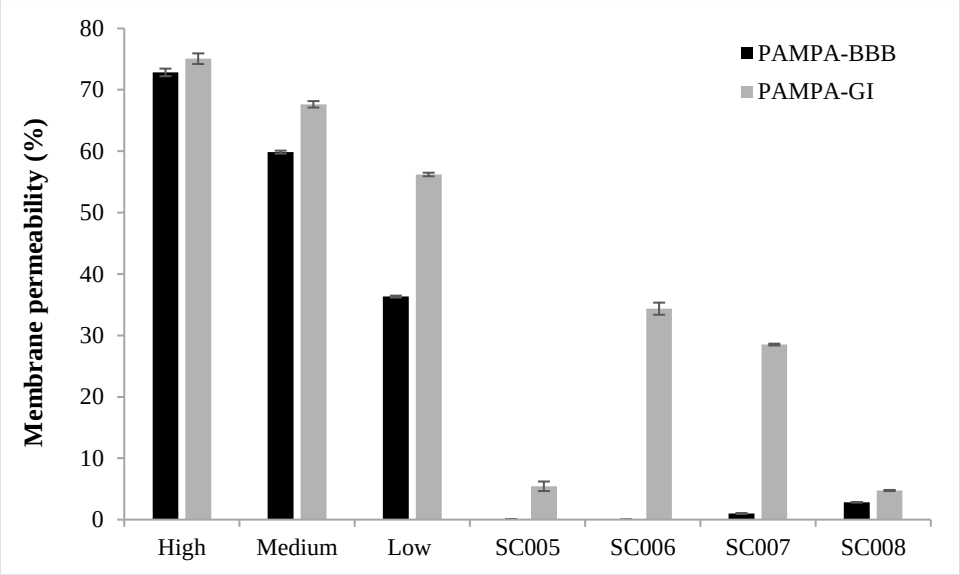


Figure 7. 10: PAMPA assay performed in blood-brain barriers and gastrointestinal tract simulated membranes. SC005 (D-form, Pal); SC006 (D-form, Ada); SC007 (L-form, Ada), SC008 (L-form Pal).

The results obtained did not suggest any significant difference in the permeability of compounds containing either Pal and Ada. A slight difference of 1% and 2% was also observed between the Pal and Ada-containing L-form ADEP1 analogues, respectively. However, a difference was noticed between D-form and L-form peptides. The D-form peptides, SC005 and SC006, struggled to go through the blood-brain barrier artificial membrane while SC007 and SC008 both had less than 3% permeability (Figure 7.10). This may be due to the BBB L-type amino acid carrier which favours L-form amino acids [35]. The L-type amino acid carrier also favours BBB permeability of peptides containing large neutral amino acids such as Phe, which is present on the ADEP1 analogues.

It is also vital for drug candidates to pass through the gastrointestinal tract to the circulatory system where they are transported to the targeted site. Analogues with Ada (SC006 and SC007) had a better permeability on gastrointestinal PAMPA than the Pal peptides (SC005 and SC008). Pal containing analogues had less than 10% membrane permeability while Ada analogues SC006 and SC007 had 29% and 34% gastrointestinal membrane permeability, respectively. This was in line with the reports in literature where lipophilic molecules are used to enhance drug permeability thus increasing oral bioavailability [36], [37]. Pal has been reported to increase membrane permeability in human intestinal epithelial Caco-2 cell line [38]. It has been used as a drug carrier through various membranes to improve drug pharmacokinetic properties [39]. Likewise, Ada uses its unique structure and hydrophobicity to transport drugs through

membrane [40]. In this study, Ada was more efficient in enhancing the membrane permeability of ADEP1 analogues.

7.4. Conclusion and future perspectives

The *M. tb* ClpP1 and ClpP2 domains were successfully expressed in *E. coli* T7 express cells. Both purified proteins showed minor impurities that will be purified further using size exclusion and/or ion exchange chromatography. In accordance with the previous reports on ADEPs activating the ClpP1P2 complex, the ADEP1 analogues tested herein also showed ability to enhance the peptidase activity of the *M. tb* ClpP1P2 protease. These findings suggested that even though the ADEP1 analogues were not yet tested for antibacterial activity on the *M. tb* strain(s), they could have potential to inhibit *M. tb* bacterial growth by inducing non-selective proteolysis of the ClpP1P2. Future studies will combine the recombinant ClpP1 and ClpP2 domains produced in this study using the in-house synthesised N-terminal blocked dipeptide (Bz-LL) to form a catalytically active ClpP1P2 complex using the method described by Akopian *et al.* 2012 [13]. Isothermal titration calorimetry (ITC) will also be conducted to measure thermodynamic parameters of the interaction between the recombinant ClpP1 and ClpP2 domains and the ClpP1P2 complex with the ADEP1 analogues. ITC is regarded as the gold standard for characterising binding energies between proteins and ligands as parameters such as standard Gibbs free energy change (ΔG), the binding constant (Ka), the enthalpy change (ΔH), the entropy change (ΔS) and the stoichiometry (N) of the binding interaction can be obtained from a single experiment.

The poor solubility of ADEPs is well documented; however, the ADEP1 analogues presented moderate aqueous solubility. The replacement of the OTEA chain with Pal or Ada and the presence of the disulphide bond formed between the added Cys residues might be responsible for the improved aqueous solubility coefficient. All the analogues had a poor blood-brain barrier permeability coefficient. However, Ada containing ADEP1 analogues had better gastrointestinal tract membrane permeability. These two factors contribute to the bioavailability of drugs, especially orally administered drugs. Oral ingestion is the most common route of drug administration over invasive drug administration such as injectables. About 84% of pharmaceutical products are administered orally [41]. This is due to advantages such as cost-effectiveness, patient compliance, least sterility requirements, etc. [42]. The major challenge for oral drugs is poor bioavailability, which is attributed to low solubility and low

membrane permeability. In Chapter 5, both Ada and Pal had lower cytotoxicity. Since Ada-containing analogues had an easier synthesis route compared to Pal-containing peptides (Chapter 3), Ada will be used as a lipophilic molecule of choice in the future studies.

7.5. References

[1] B. Leader, Q. J. Baca, and D. E. Golan, "Protein therapeutics: a summary and pharmacological classification," *Nat. Rev. Drug Discov.*, vol. 7, no. 1, Art. no. 1, Jan. 2008, doi: 10.1038/nrd2399.

[2] T. Sugiki, T. Fujiwara, and C. Kojima, "Latest approaches for efficient protein production in drug discovery," *Expert Opin. Drug Discov.*, vol. 9, no. 10, pp. 1189–1204, Oct. 2014, doi: 10.1517/17460441.2014.941801.

[3] T. W. Overton, "Recombinant protein production in bacterial hosts," *Drug Discov. Today*, vol. 19, no. 5, pp. 590–601, May 2014, doi: 10.1016/j.drudis.2013.11.008.

[4] H. S. Mason, H. Warzecha, T. Mor, and C. J. Arntzen, "Edible plant vaccines: applications for prophylactic and therapeutic molecular medicine," *Trends Mol. Med.*, vol. 8, no. 7, pp. 324–329, Jul. 2002, doi: 10.1016/s1471-4914(02)02360-2.

[5] J. A. Brannigan and A. J. Wilkinson, "Protein engineering 20 years on," *Nat. Rev. Mol. Cell Biol.*, vol. 3, no. 12, pp. 964–970, Dec. 2002, doi: 10.1038/nrm975.

[6] G. Sezonov, D. Joseleau-Petit, and R. D'Ari, "Escherichia coli physiology in Luria-Bertani broth," *J. Bacteriol.*, vol. 189, no. 23, pp. 8746–8749, Dec. 2007, doi: 10.1128/JB.01368-07.

[7] J. Shiloach and R. Fass, "Growing E. coli to high cell density--a historical perspective on method development," *Biotechnol. Adv.*, vol. 23, no. 5, pp. 345–357, Jul. 2005, doi: 10.1016/j.biotechadv.2005.04.004.

[8] B. Pope and H. M. Kent, "High efficiency 5 min transformation of Escherichia coli.," *Nucleic Acids Res.*, vol. 24, no. 3, pp. 536–537, Feb. 1996.

[9] T. Wunberg *et al.*, "Improving the hit-to-lead process: data-driven assessment of drug-like and lead-like screening hits," *Drug Discov. Today*, vol. 11, no. 3–4, pp. 175–180, Feb. 2006, doi: 10.1016/S1359-6446(05)03700-1.

[10] T. Teorell, "Kinetics of distribution of substances administered to the body, II : The intravascular modes of administration," *Arch. Int. Pharmacodyn. Ther.*, vol. 57, pp. 226–240, 1937.

[11] H. Dowden and J. Munro, "Trends in clinical success rates and therapeutic focus," *Nat. Rev. Drug Discov.*, vol. 18, no. 7, pp. 495–496, Jul. 2019, doi: 10.1038/d41573-019-00074-z.

[12] Andrew. M. Pickering and Kelvin. J. A. Davies, "A simple fluorescent labeling method for studies of protein oxidation, protein modification, and proteolysis," *Free Radic. Biol. Med.*, vol. 52, no. 2, pp. 239–246, Jan. 2012, doi: 10.1016/j.freeradbiomed.2011.08.018.

[13] T. Akopian, O. Kandror, R. M. Raju, M. UnniKrishnan, E. J. Rubin, and A. L. Goldberg, "The active ClpP protease from M. tuberculosis is a complex composed of a heptameric ClpP1 and a ClpP2 ring," *Embo J.*, vol. 31, no. 6, pp. 1529–1541, Mar. 2012, doi: 10.1038/emboj.2012.5.

[14] A. Shirai *et al.*, "Global Analysis of Gel Mobility of Proteins and Its Use in Target Identification*," *J. Biol. Chem.*, vol. 283, no. 16, pp. 10745–10752, Apr. 2008, doi: 10.1074/jbc.M709211200.

[15] Y. Yang *et al.*, "Inhibiting Mycobacterium tuberculosis ClpP1P2 by addressing the equatorial handle domain of ClpP1 subunit." bioRxiv, p. 713214, Jul. 24, 2019. doi: 10.1101/713214.

[16] N. Benaroudj, B. Raynal, M. Miot, and M. Ortiz-Lombardia, "Assembly and proteolytic processing of mycobacterial ClpP1 and ClpP2," *BMC Biochem.*, vol. 12, no. 1, p. 61, Dec. 2011, doi: 10.1186/1471-2091-12-61.

[17] H. Ingvarsson *et al.*, "Insights into the inter-ring plasticity of caseinolytic proteases from the X-ray structure of Mycobacterium tuberculosis ClpP1," *Acta Crystallogr. D Biol.*

Crystallogr., vol. 63, no. Pt 2, pp. 249–259, Feb. 2007, doi: 10.1107/S0907444906050530.
[18] M. Li *et al.*, "Structure and Functional Properties of the Active Form of the Proteolytic Complex, ClpP1P2, from *Mycobacterium tuberculosis*," *J. Biol. Chem.*, vol. 291, no. 14, pp. 7465–7476, Apr. 2016, doi: 10.1074/jbc.M115.700344.
[19] S. Vahidi *et al.*, "An allosteric switch regulates *Mycobacterium tuberculosis* ClpP1P2 protease function as established by cryo-EM and methyl-TROSY NMR," *Proc. Natl. Acad. Sci.*, vol. 117, no. 11, pp. 5895–5906, Mar. 2020, doi: 10.1073/pnas.1921630117.
[20] H. Brötz-Oesterhelt *et al.*, "Dysregulation of bacterial proteolytic machinery by a new class of antibiotics.," *Nat Med*, vol. 11, pp. 1082–1087, 2005.
[21] L. Tanner, R. K. Haynes, and L. Wiesner, "An in vitro ADME and in vivo Pharmacokinetic Study of Novel TB-Active Decoquinate Derivatives," *Front. Pharmacol.*, vol. 10, 2019, Accessed: Mar. 05, 2023. [Online]. Available: https://www.frontiersin.org/articles/10.3389/fphar.2019.00120
[22] A. MacGowan, C. Rogers, and K. Bowker, "In Vitro Models, In Vivo Models, and Pharmacokinetics: What Can We Learn from In Vitro Models?," *Clin. Infect. Dis.*, vol. 33, no. Supplement_3, pp. S214–S220, Sep. 2001, doi: 10.1086/321850.
[23] S. Kumar and P. Singh, "Various techniques for solubility enhancement: An overview".
[24] B. Hinzen *et al.*, "Medicinal Chemistry Optimization of Acyldepsipeptides of the Enopeptin Class Antibiotics," *ChemMedChem*, vol. 1, no. 7, pp. 689–693, 2006, doi: 10.1002/cmdc.200600055.
[25] M. J. Betts and R. B. Russell, "Amino Acid Properties and Consequences of Substitutions," in *Bioinformatics for Geneticists*, M. R. Barnes and I. C. Gray, Eds. Chichester, UK: John Wiley & Sons, Ltd, 2003, pp. 289–316. doi: 10.1002/0470867302.ch14.
[26] A. Abedini, G. Singh, and D. P. Raleigh, "Recovery and purification of highly aggregation-prone disulfide-containing peptides: Application to islet amyloid polypeptide," *Anal. Biochem.*, vol. 351, no. 2, pp. 181–186, Apr. 2006, doi: 10.1016/j.ab.2005.11.029.
[27] M. Fujikawa, K. Nakao, R. Shimizu, and M. Akamatsu, "QSAR study on permeability of hydrophobic compounds with artificial membranes," *Bioorg. Med. Chem.*, vol. 15, no. 11, pp. 3756–3767, Jun. 2007, doi: 10.1016/j.bmc.2007.03.040.
[28] W. G. Mayhan, "Regulation of Blood–Brain Barrier Permeability," *Microcirculation*, vol. 8, no. 2, pp. 89–104, Jan. 2001, doi: 10.1080/mic.8.2.89.104.
[29] N. R. Saunders *et al.*, "The rights and wrongs of blood-brain barrier permeability studies: a walk through 100 years of history," *Front. Neurosci.*, vol. 8, 2014, Accessed: Feb. 27, 2023, https://www.frontiersin.org/articles/10.3389/fnins.2014.00404
[30] Q. He *et al.*, "Towards Improvements for Penetrating the Blood–Brain Barrier—Recent Progress from a Material and Pharmaceutical Perspective," *Cells*, vol. 7, no. 4, p. 24, Mar. 2018, doi: 10.3390/cells7040024.
[31] C. M. Bellettato and M. Scarpa, "Possible strategies to cross the blood–brain barrier," *Ital. J. Pediatr.*, vol. 44, no. 2, p. 131, Nov. 2018, doi: 10.1186/s13052-018-0563-0.
[32] N. Tsuzuki, T. Hama, T. Hibi, R. Konishi, S. Futaki, and K. Kitagawa, "Adamantane as a brain-directed drug carrier for poorly absorbed drug: Antinociceptive effects of [D-Ala2] Leu-enkephalin derivatives conjugated with the 1-adamantane moiety," *Biochem. Pharmacol.*, vol. 41, no. 4, pp. R5–R8, Feb. 1991, doi: 10.1016/0006-2952(91)90616-D.
[33] W. M. Pardridge and L. J. Mietus, "Palmitate and Cholesterol Transport Through the Blood-Brain Barrier," *J. Neurochem.*, vol. 34, no. 2, pp. 463–466, 1980, doi: 10.1111/j.1471-4159.1980.tb06621.x.

[34] J. Strosznajder, M. Chalimoniuk, R. P. Strosznajder, V. Albanese, and M. Alberghina, “Arachidonate transport through the blood-retina and blood-brain barrier of the rat during aging,” *Neurosci. Lett.*, vol. 209, no. 3, pp. 145–148, May 1996, doi: 10.1016/0304-3940(96)12624-0.
[35] J. Pietz *et al.*, “Large neutral amino acids block phenylalanine transport into brain tissue in patients with phenylketonuria,” *J. Clin. Invest.*, vol. 103, no. 8, pp. 1169–1178, Apr. 1999.
[36] V. Čižinauskas, N. Elie, A. Brunelle, and V. Briedis, “Fatty acids penetration into human skin ex vivo: A TOF-SIMS analysis approach,” *Biointerphases*, vol. 12, no. 1, p. 011003, Mar. 2017, doi: 10.1116/1.4977941.
[37] A. Mandal, “Copper Nanomaterials as Drug Delivery System against Infectious Agents and Cancerous Cells,” *J. Appl. Life Sci. Int.*, vol. 15, no. 4, pp. 1–8, Dec. 2017, doi: 10.9734/JALSI/2017/38444.
[38] M. Gori *et al.*, “Palmitic Acid Affects Intestinal Epithelial Barrier Integrity and Permeability In Vitro,” *Antioxidants*, vol. 9, no. 5, Art. no. 5, May 2020, doi: 10.3390/antiox9050417.
[39] N. Thotakura *et al.*, “Chitosan-palmitic acid based polymeric micelles as promising carrier for circumventing pharmacokinetic and drug delivery concerns of tamoxifen,” *Int. J. Biol. Macromol.*, vol. 102, pp. 1220–1225, Sep. 2017, doi: 10.1016/j.ijbiomac.2017.05.016.
[40] G. Lamoureux and G. Artavia, “Use of the Adamantane Structure in Medicinal Chemistry,” *Curr. Med. Chem.*, vol. 17, no. 26, pp. 2967–2978.
[41] M. S. Alqahtani, M. Kazi, M. A. Alsenaidy, and M. Z. Ahmad, “Advances in Oral Drug Delivery,” *Front. Pharmacol.*, vol. 12, 2021, Accessed: Feb. 22, 2023. [Online]. Available: https://www.frontiersin.org/articles/10.3389/fphar.2021.618411
[42] Y. S. R. Krishnaiah, “Pharmaceutical Technologies for Enhancing Oral Bioavailability of Poorly Soluble Drugs,” *J. Bioequivalence Bioavailab.*, vol. 02, no. 02, 2010, doi: 10.4172/jbb.1000027.

CHAPTER 8.

8.1. Concluding remarks and future work

ADEP1 analogues were successfully synthesised through SPPS with a >96% purity and 37 – 46% yield. The ADEP1 analogues had MIC values of 125 and 500 µM against two Gram-negative (*E. coli* and *P. aeruginosa*, respectively) and MIC values of 125, 63, and 250 against Gram-positive (*B. subtilis* and *S. aureus,* and Methicillin-resistant *S. aureus*, respectively) bacteria. Most of the ADEP1 analogues had MBC values twice the MIC values of the tested bacterial strains while some had MBCs were equal to their MIC.

The modifications which include the replacement of L amino acids with D amino acids, the substitution of the OTEA with either Ada or Pal, and the cyclization through disulphide bridges instead of ester bonds; significantly impacted on the activity of the analogues. Compared to the reported activity of the natural ADEP1, the ADEP1 analogues had reduced antibacterial activity that was accompanied by enhanced biocompatibility. The fact that the analogues did not show any cytotoxic effects on the test (HEK-293 and Caco-2) cell lines, presented the peptides as lead drug candidates. To further test this theory, the gelatin-capped $AgInS_2$ QDs were used as drug delivery systems for ADEP1 analogues to help improve their uptake and internalization by test bacterial strains. Evidently, the $AgInS_2$ QDs-ADEP1 analogue conjugates had drastically enhanced antibacterial potency. The MICs of the $AgInS_2$ QDs-ADEP1 conjugates were multiple folds lower compared to those of the unconjugated ADEP1 analogues. The biocompatibility of the ADEPs after conjugation to the QDs was retained, as they exhibited no cytotoxicity to both Caco-2 and HEK-293 cells at concentrations that was multiple folds higher than their MIC.

The ADEP1 analogues on their own showed moderate aqueous solubility and gastrointestinal membrane permeability potential. Moreover, the ADEP1 analogues activated peptidase activity of *M. tb* ClpP1P2. These analogues enhanced the peptidase activity by 34-72% that was relatively similar and in others superior to the positive control (40%). These results showed an anti-mycobacterium potential of the ADEP1 analogues and their subsequent nano-conjugates by activating the *M. tb* ClpP1P2. This study further expressed, purified, and characterised the ClpP1 and ClpP2 domains that will be used in the future studies to determine the thermodynamic parameters of interactions between the domains and the ADEP1 analogues. The domains will also be combined to produce a catalytic active *M. tb* ClpP1P2 complex. This

active complex will then be used to screen ADEP analogues and other potential anti-TB drug candidates on their potential to dysregulate *M. tb* ClpP1P2. Structural modification of the AMPs in combination with naocarriers maybe used towards developments of effective antibacterial agents which can help fight against existing and emerging antimicrobial resistance challenges faced by the globe. The ADEP1 analogues together with the $AgInS_2$ QDs-ADEP1 analogue conjugates will be further tested *in vitro* and *in vivo* for their potential anti-TB activity. *In vitro* studies will be conducted on various *M. tb* strains to evaluate the MICs and MBCs of the ADEP1 analogue and $AgInS_2$ QDs-ADEP1 analogue conjugates. The molecular mechanisms of the most active ADEP1 analogue and its $AgInS_2$ QDs-conjugate will be validated in *M. tb* strains.

APPENDIX

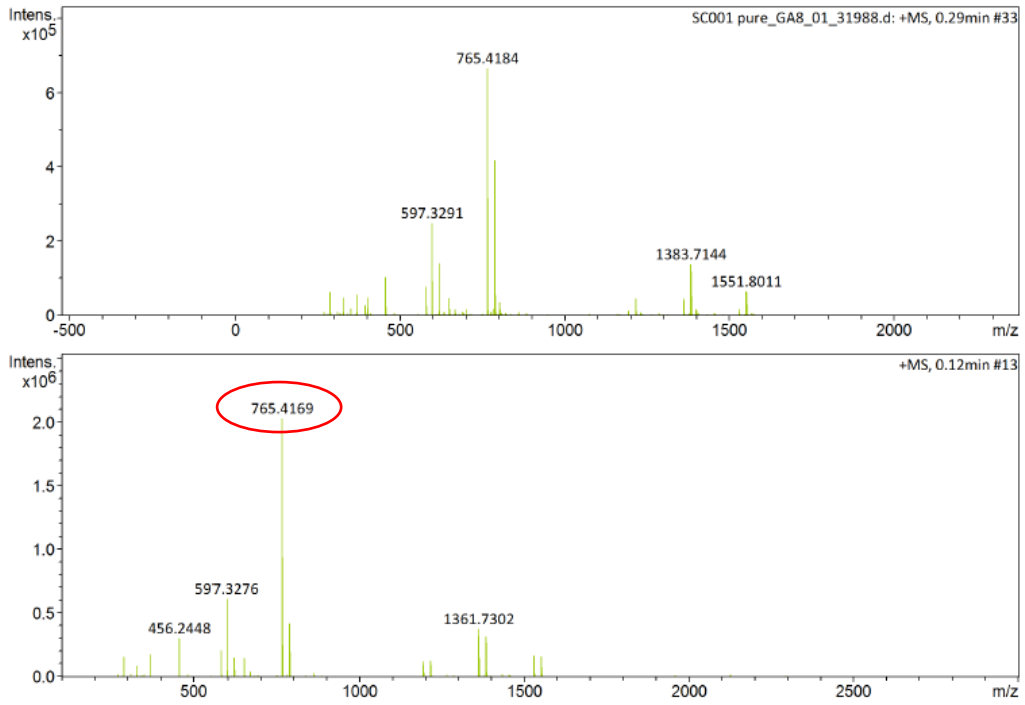


Figure A. 1: Results of linear SC001 obtained from MS.

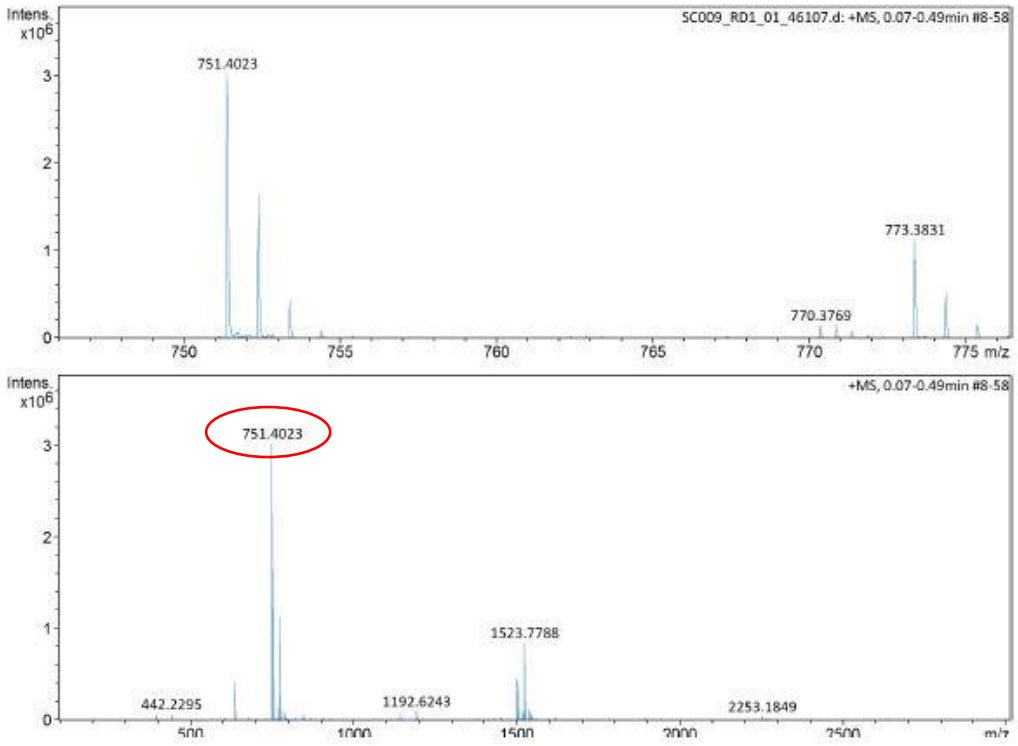


Figure A. 2: Results of linear SC009 obtained from MS.

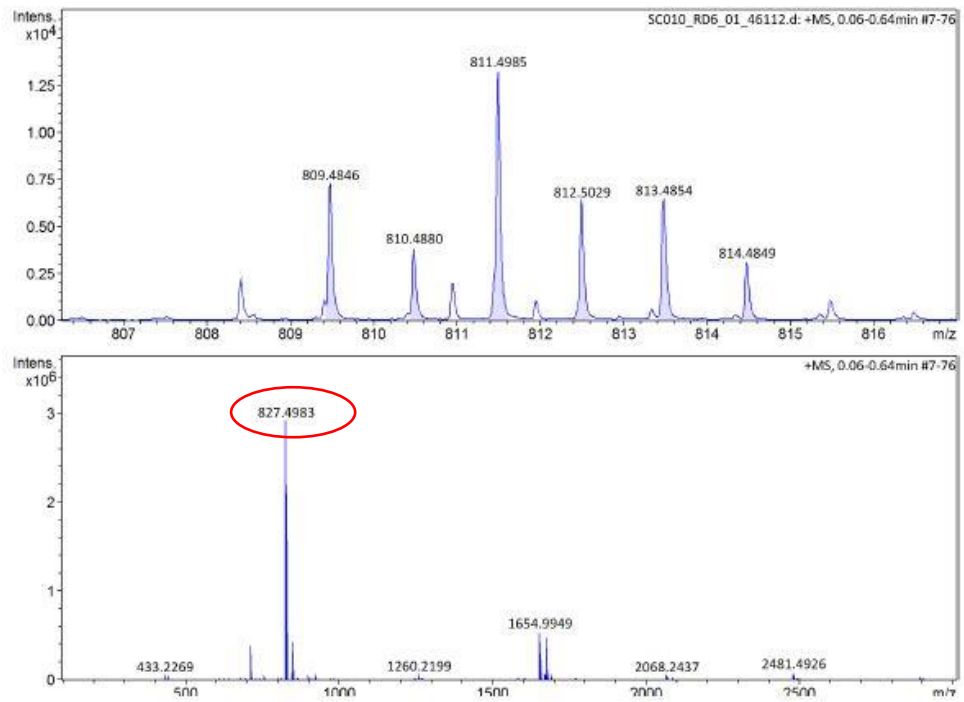


Figure A. 3: Results of linear SC0010 obtained from MS.

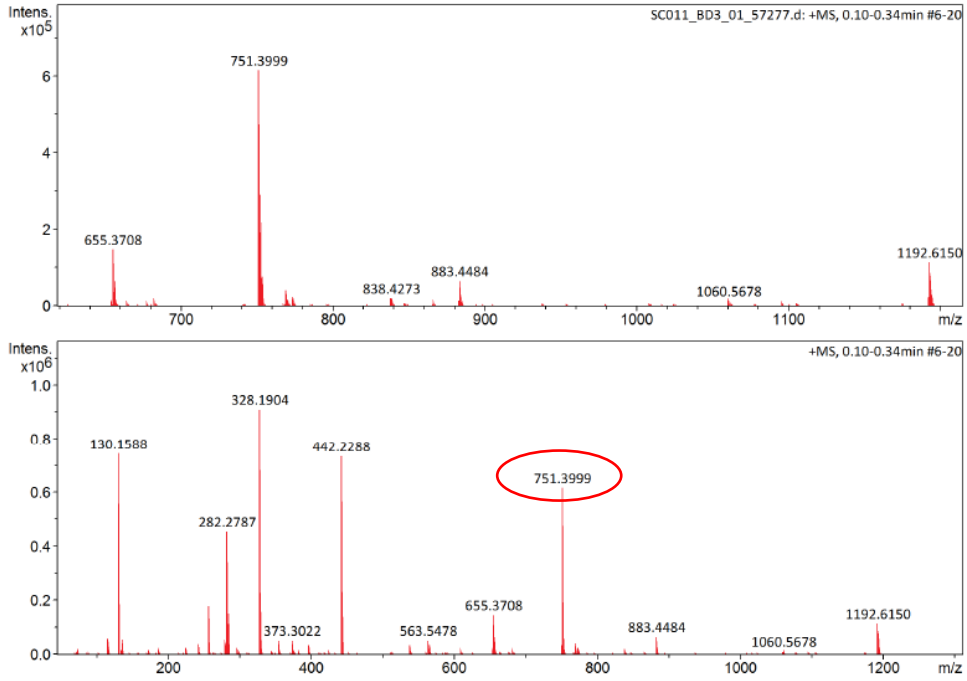


Figure A. 4: Results of linear SC011 obtained from MS.

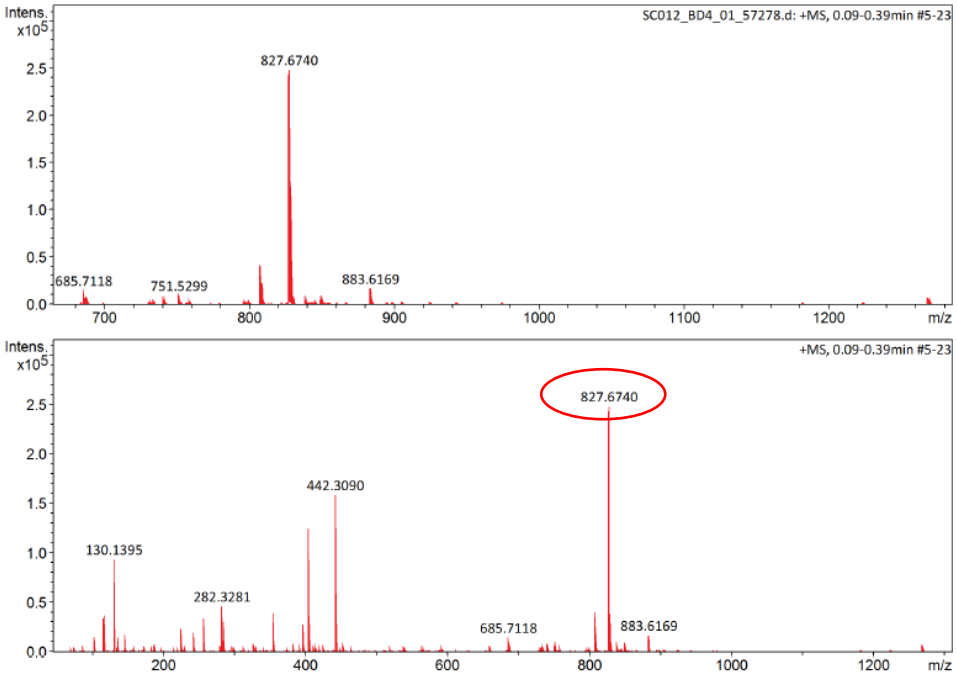


Figure A. 5: Results of linear SC0012 obtained from MS.

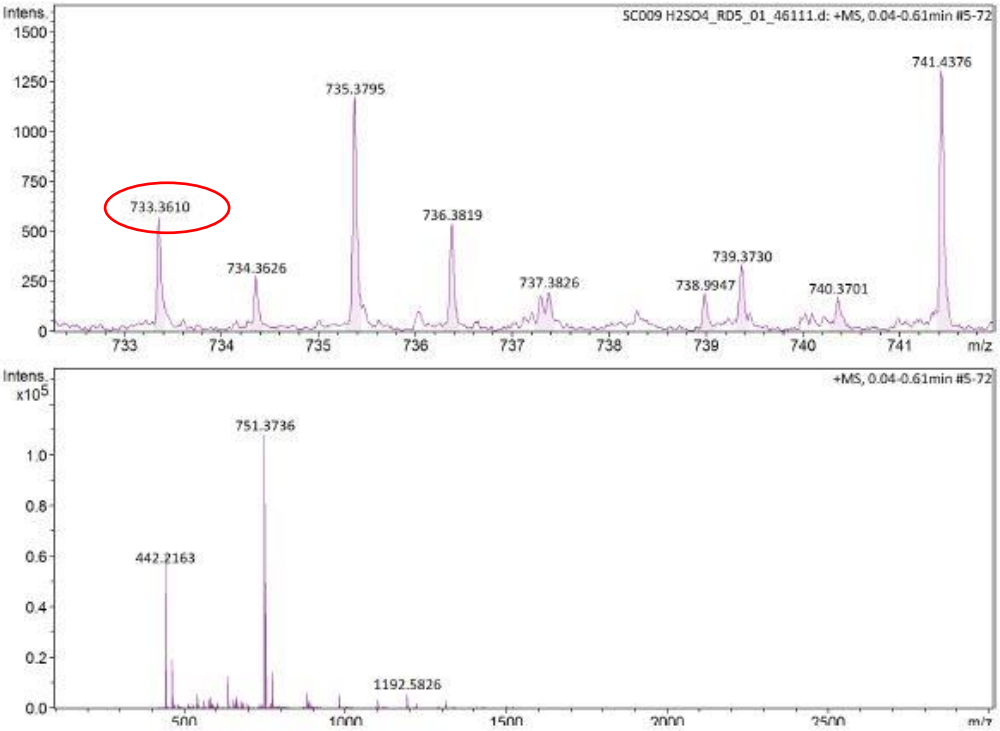


Figure A. 6: Results of SC009 treated with 1% H_2SO_4 obtained from MS.

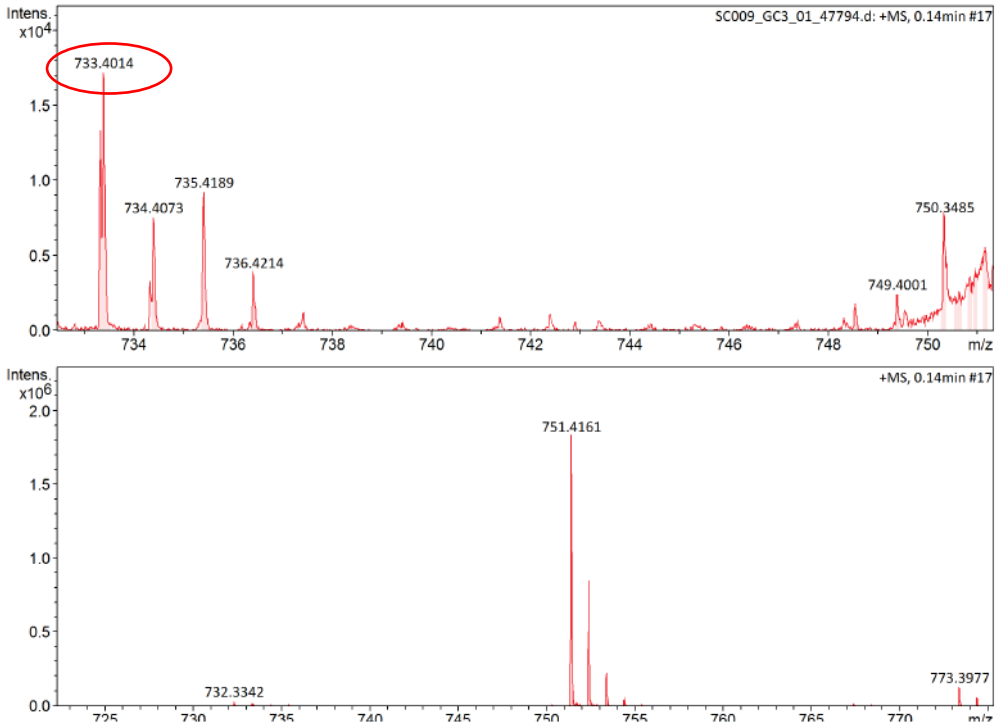


Figure A. 7: Results of SC009 treated with 95% TFA obtained from MS.

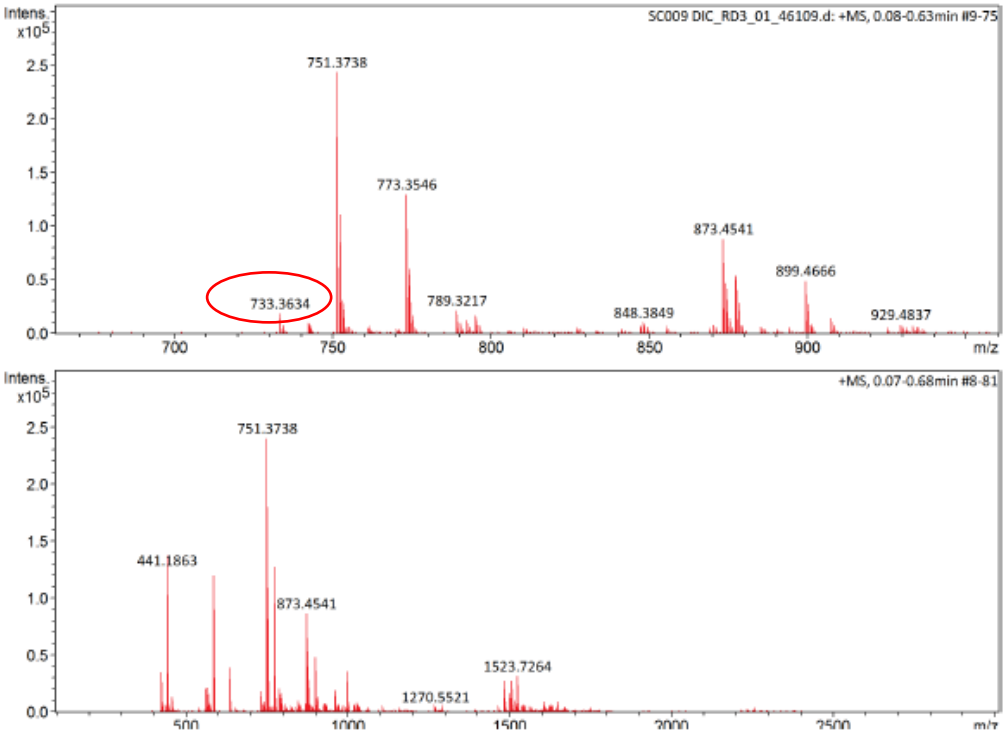


Figure A. 8: Results of SC009 treated with DIC and DMAP obtained from MS.

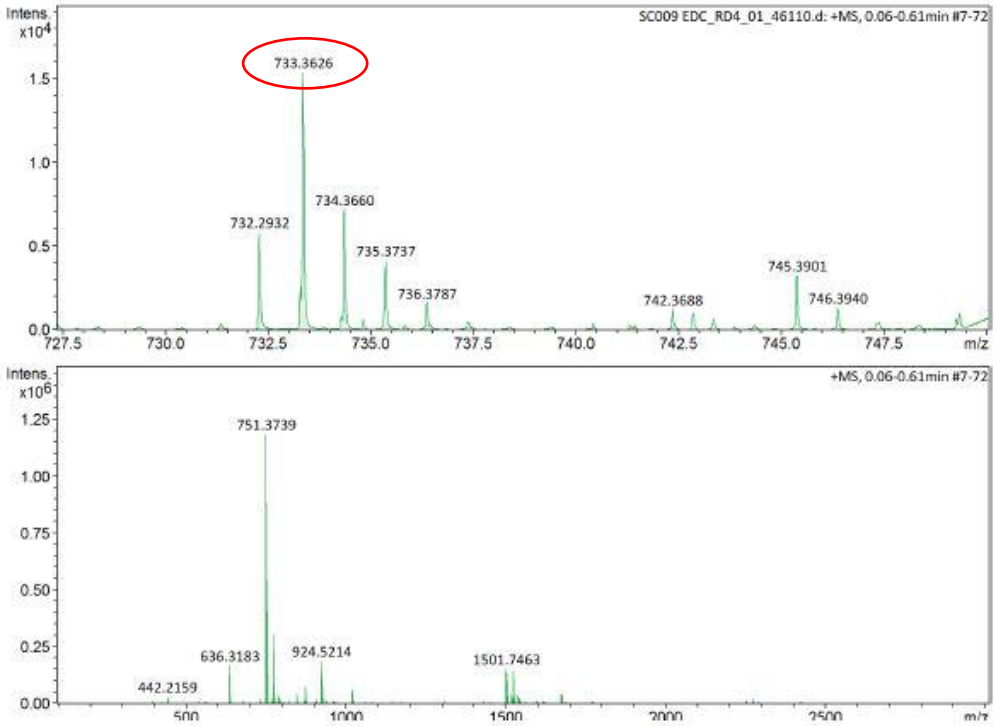


Figure A. 9: Results of SC009 treated with EDC and DMAP obtained from MS.

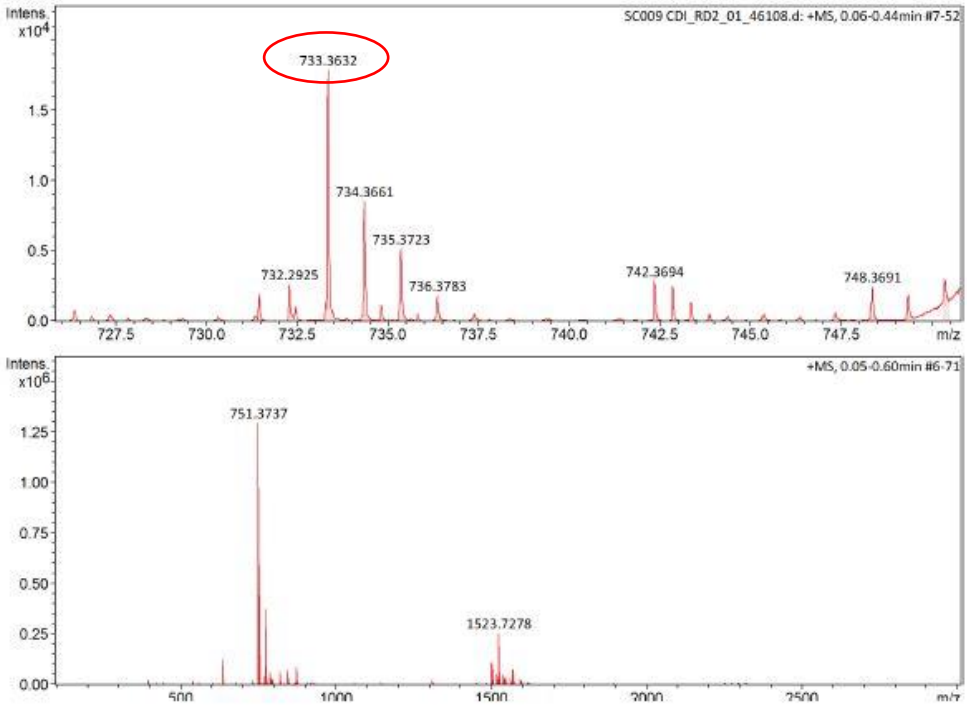


Figure A. 10: Results of SC009 treated with CDI and DMAP obtained from MS.

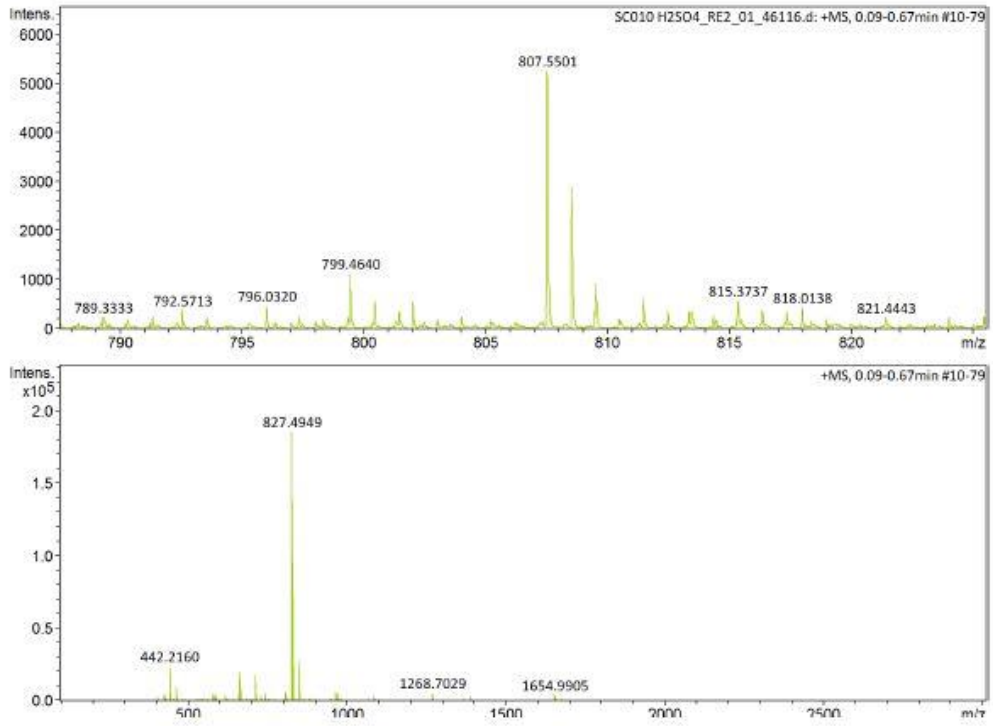


Figure A. 11: Results of SC010 treated with 1% H_2SO_4 obtained from MS.

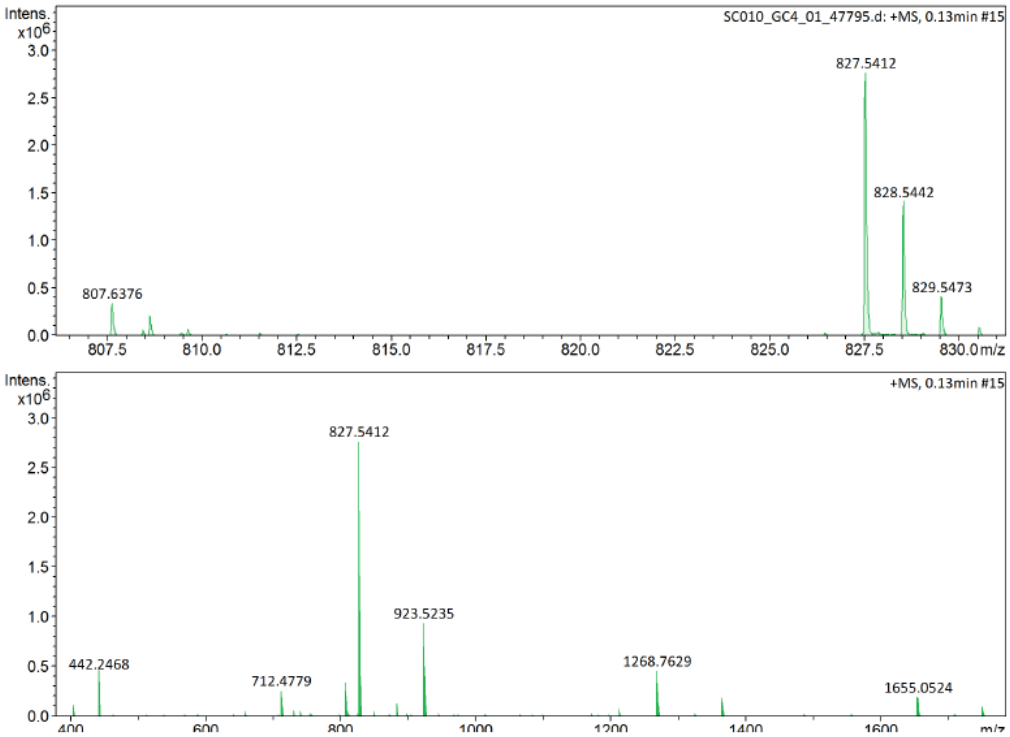


Figure A. 12: Results of SC010 treated with 95% TFA obtained from MS.

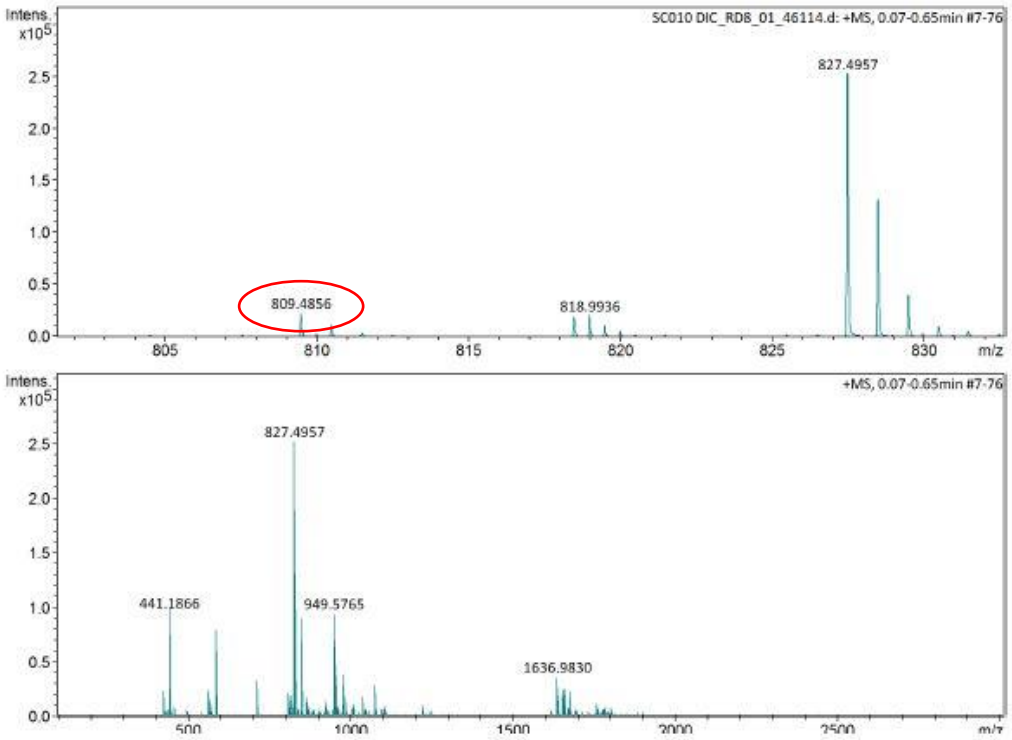


Figure A. 13: Results of SC010 treated with DIC and DMAP obtained from MS.

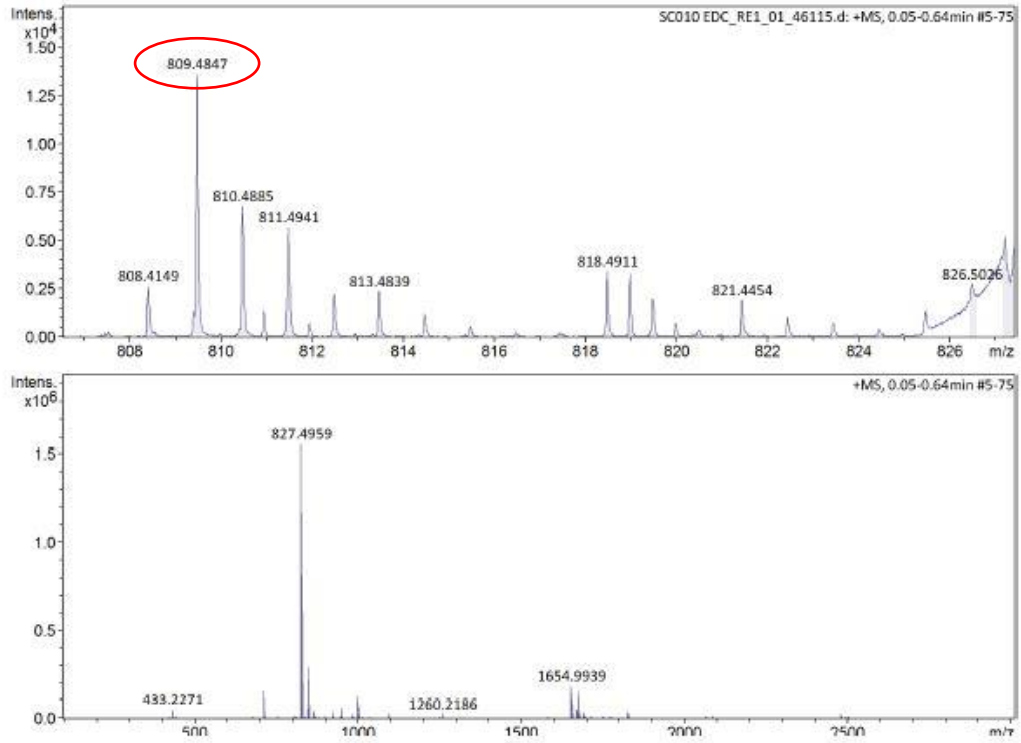


Figure A. 14:Results of SC010 treated with EDC and DMAP obtained from MS.

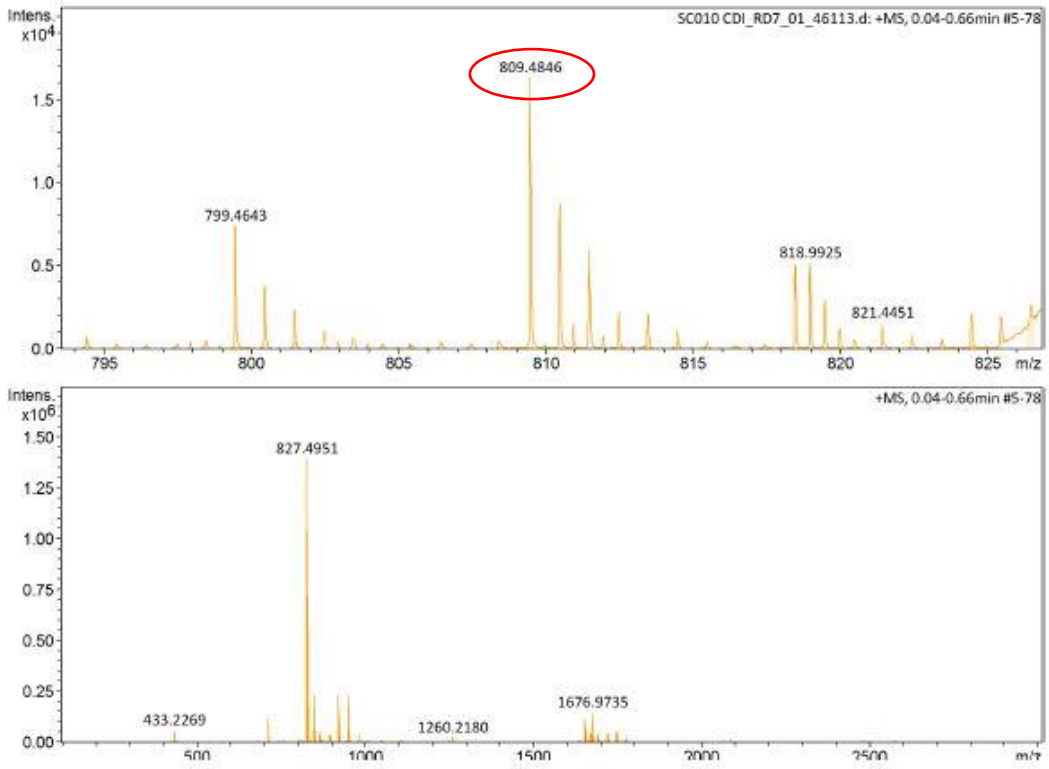


Figure A. 15: Results of SC010 treated with CDI and DMAP obtained from MS.

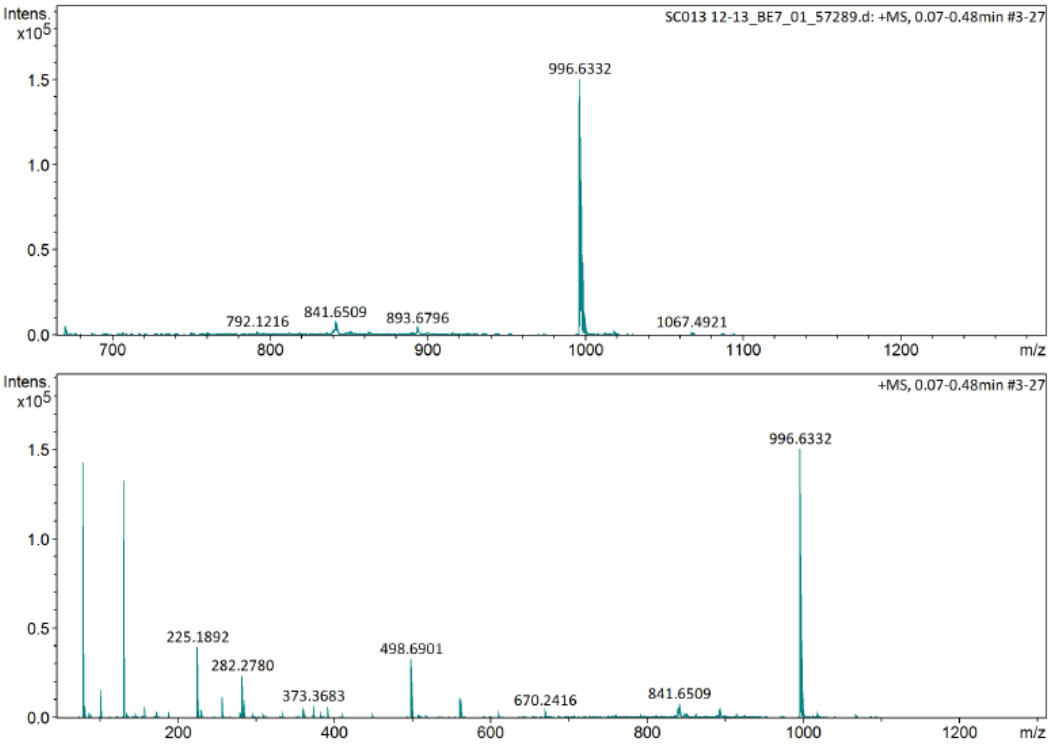


Figure A. 16: MS results of linear SC013.

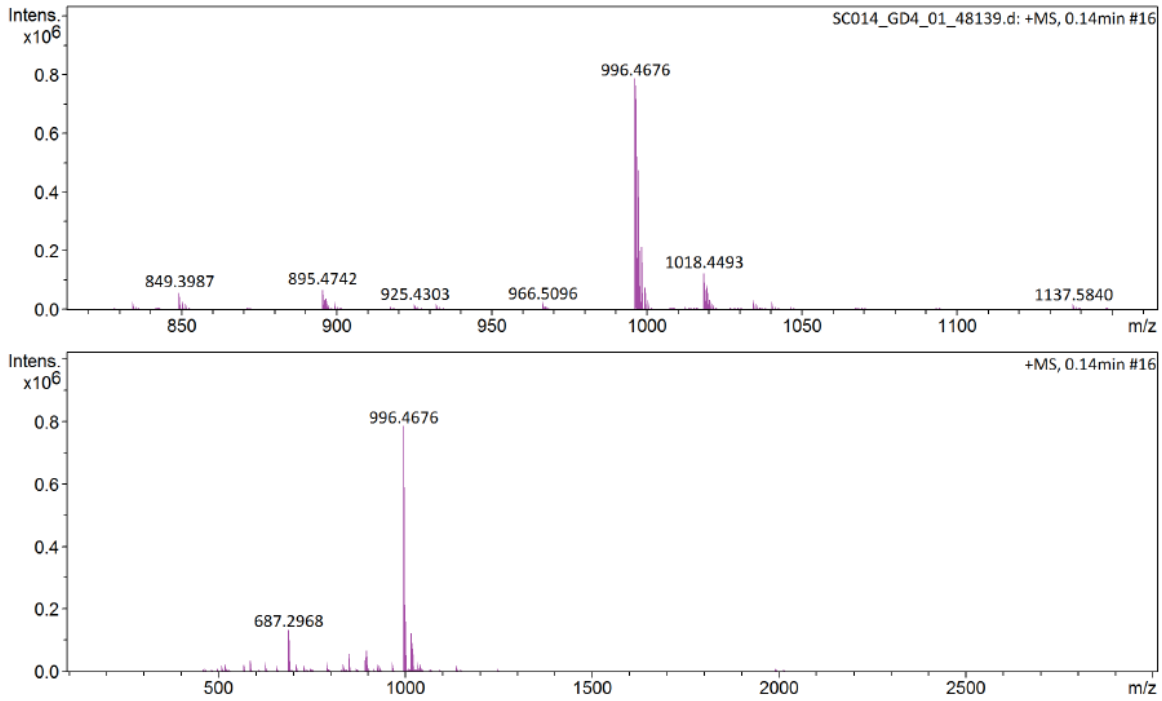


Figure A. 17: MS results of linear SC014.

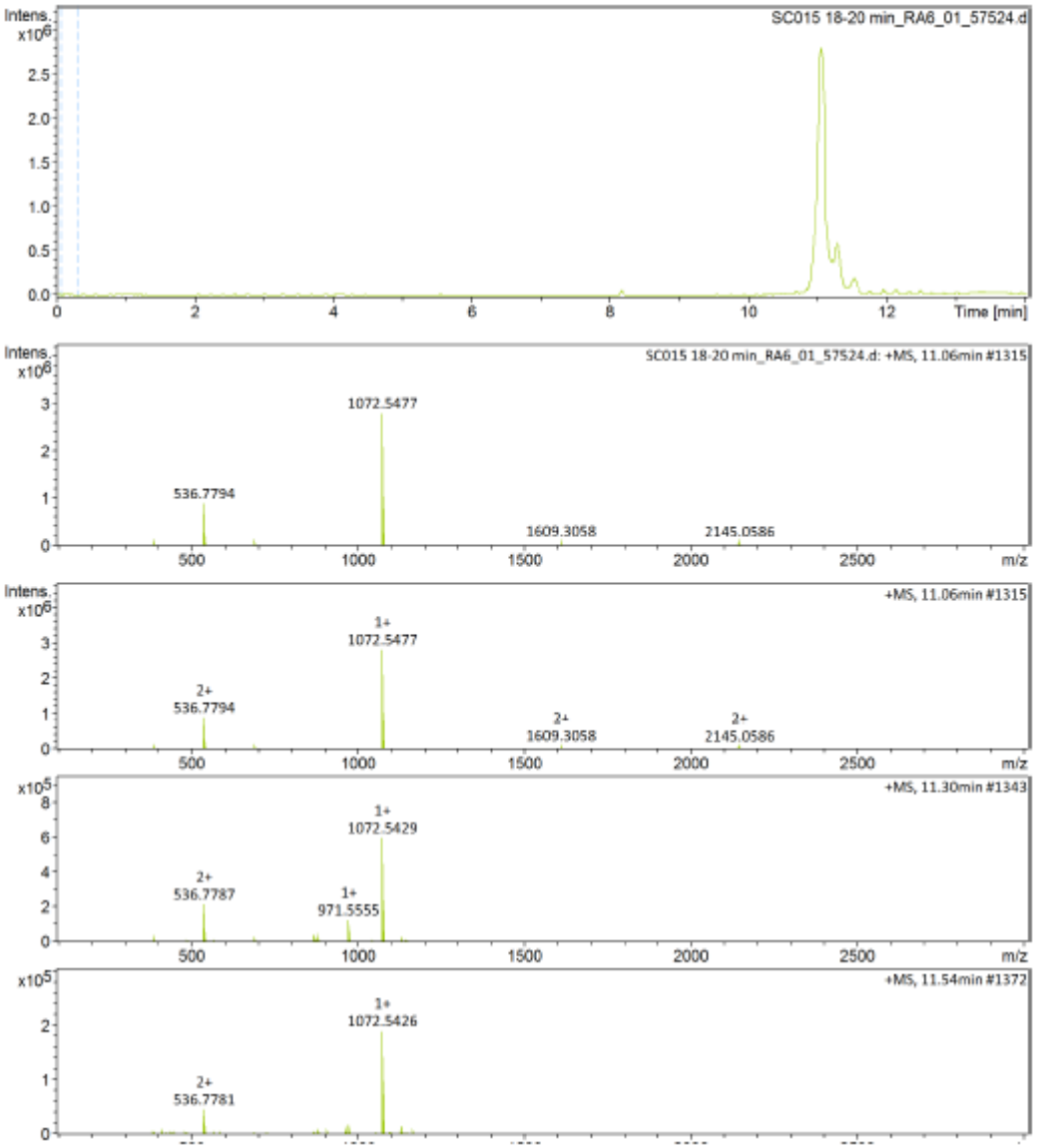


Figure A. 18: LCMS results of cyclized and purified SC016.

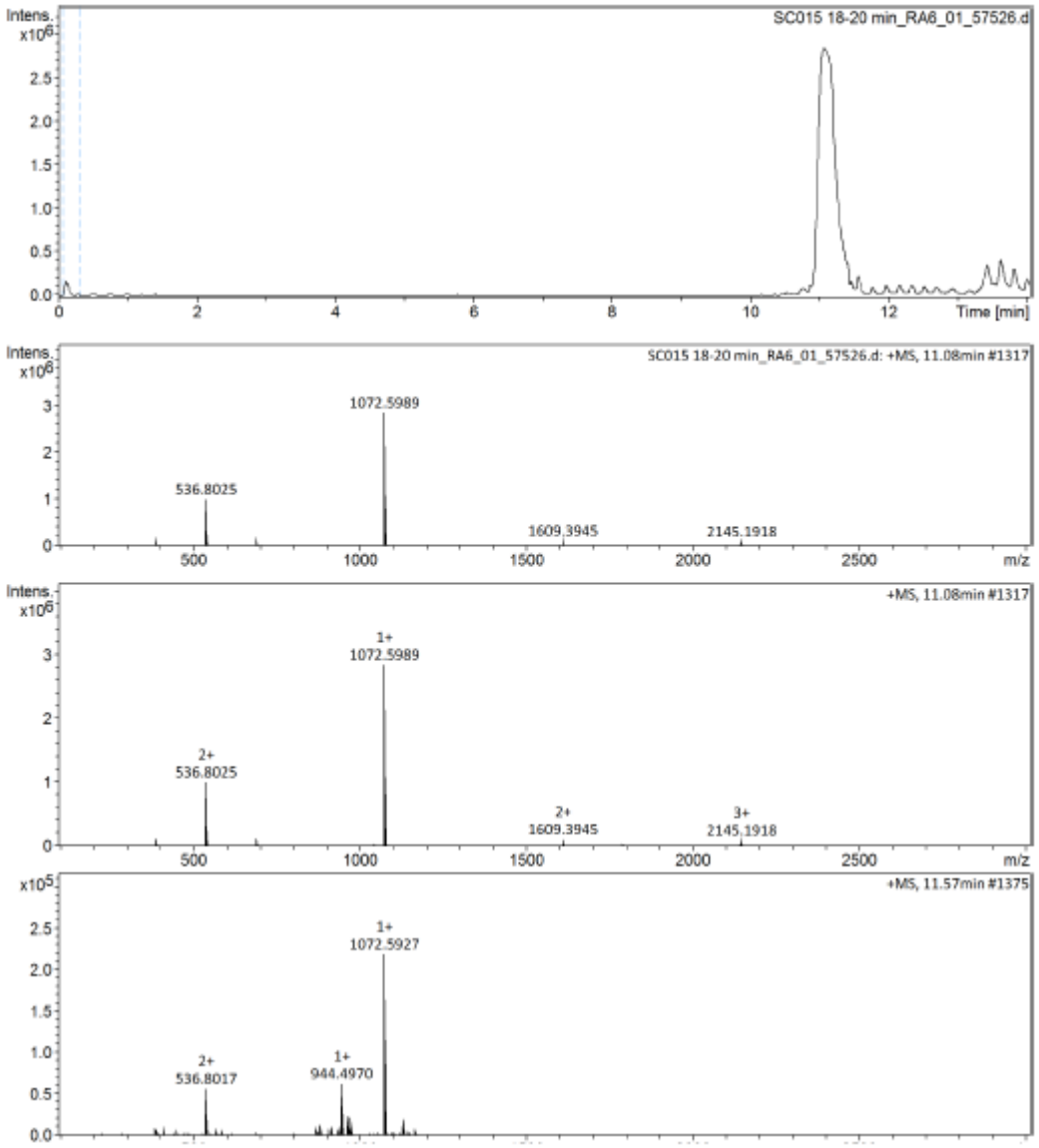


Figure A. 19: LCMS results of cyclized and purified SC016.

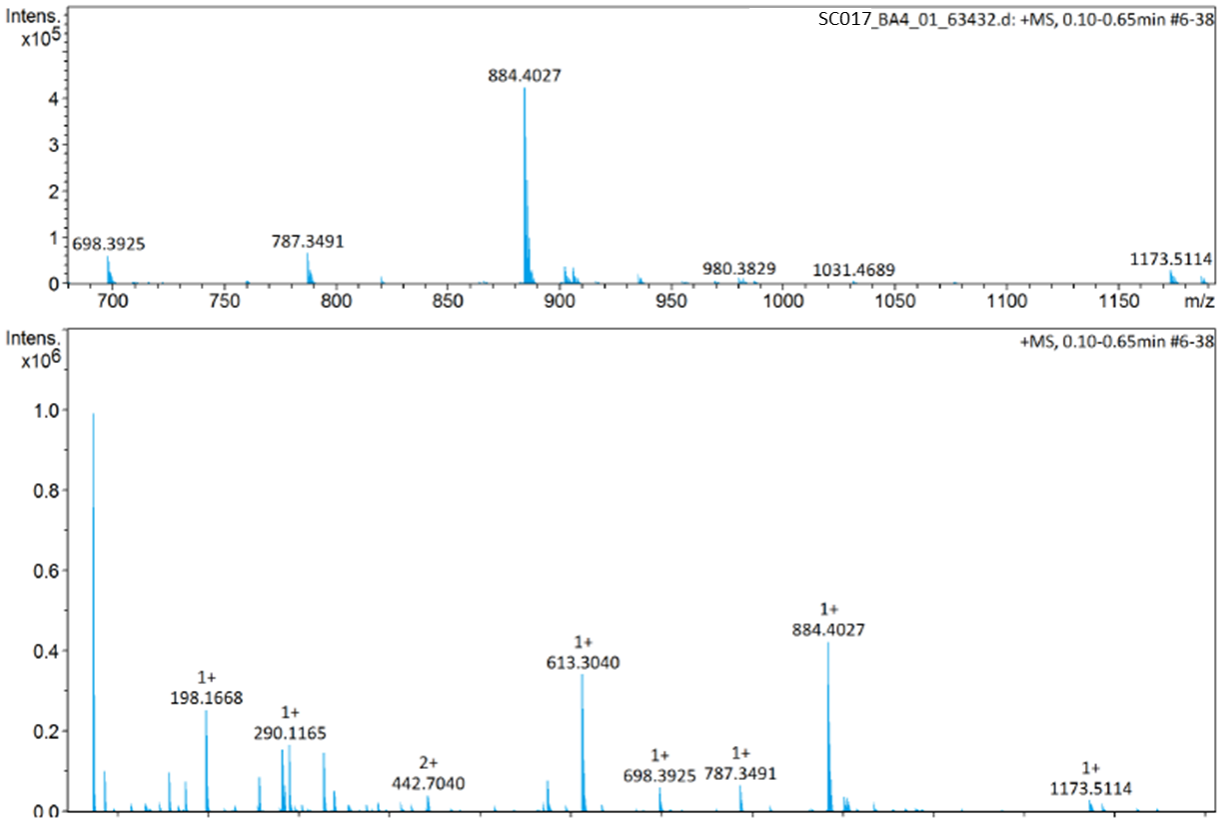


Figure A. 20: Linear SC017.

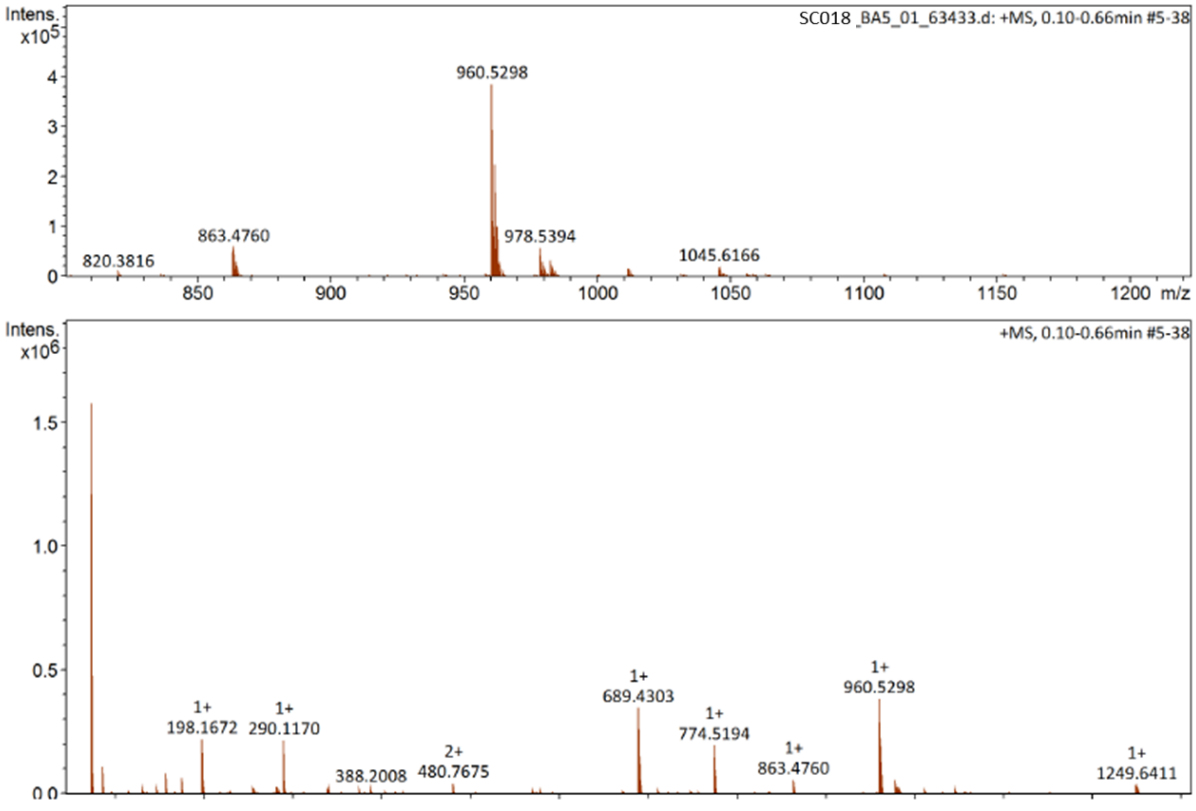


Figure A. 21: Linear SC018.

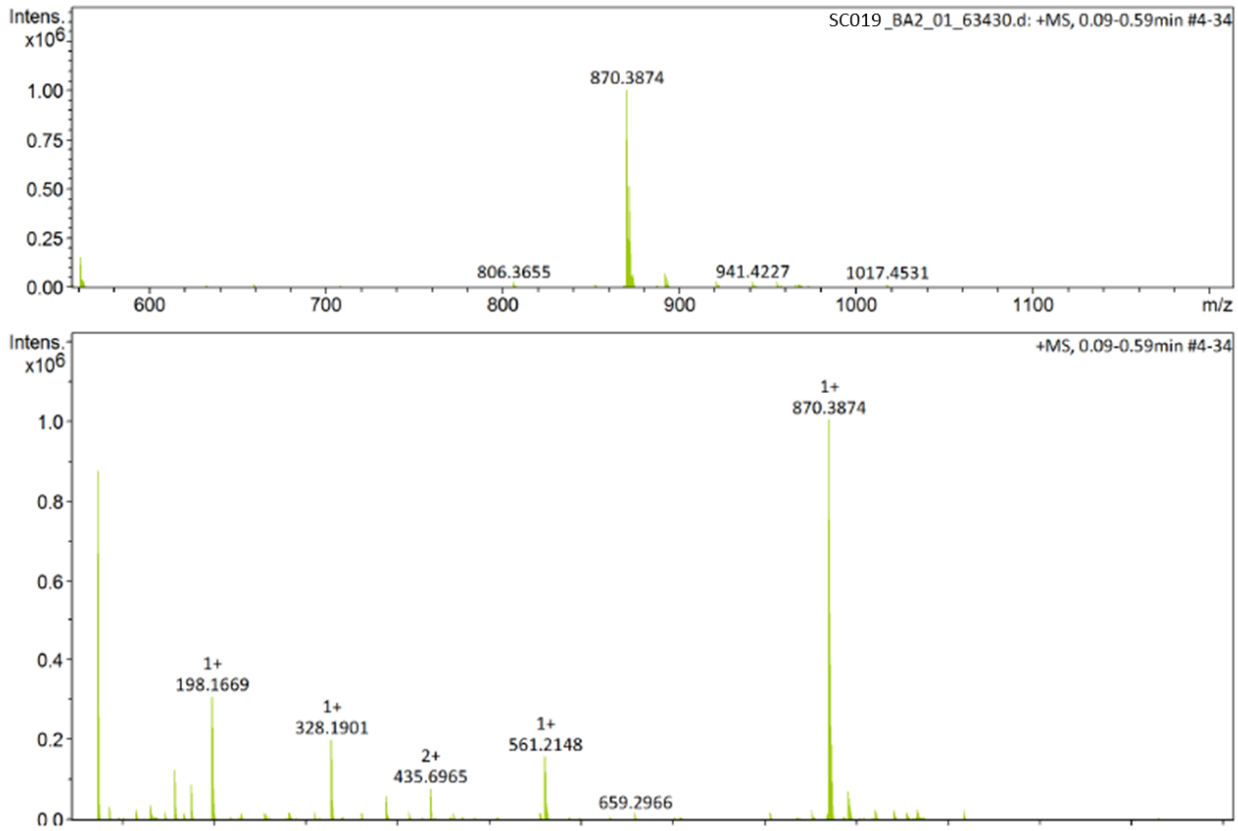


Figure A. 22: Linear SC019.

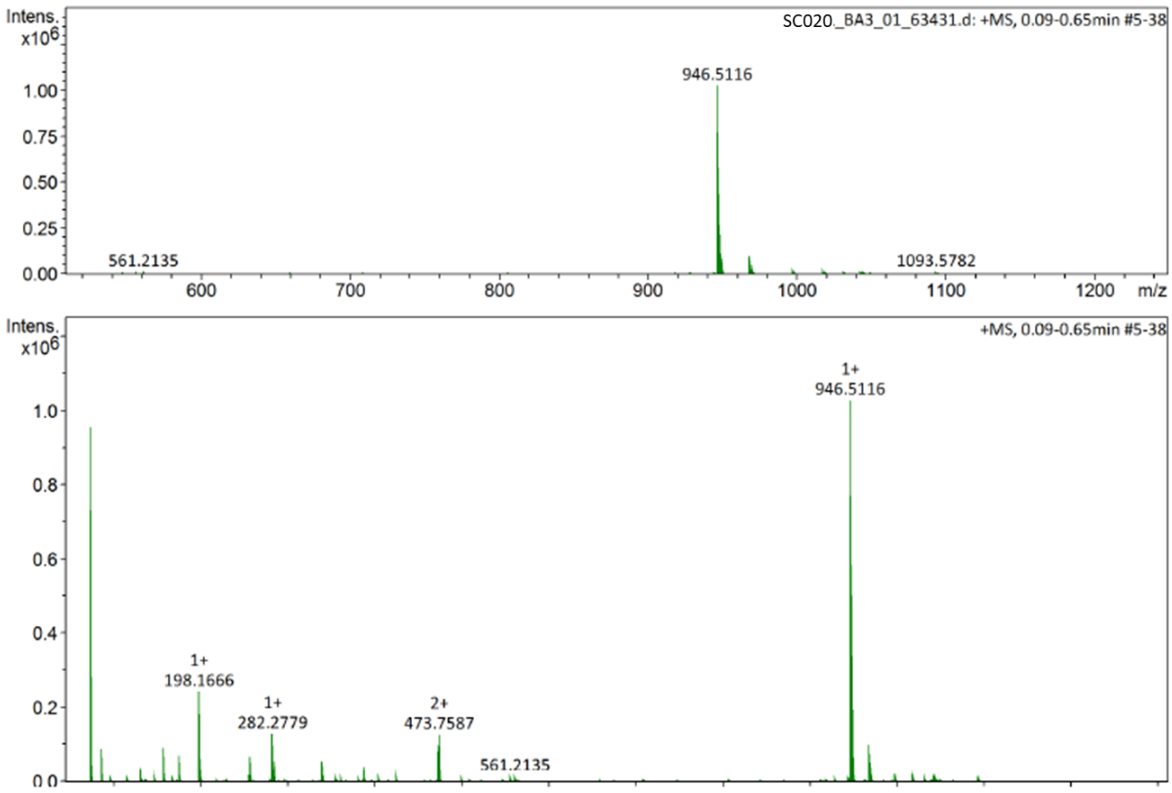


Figure A. 23: Linear SC020.

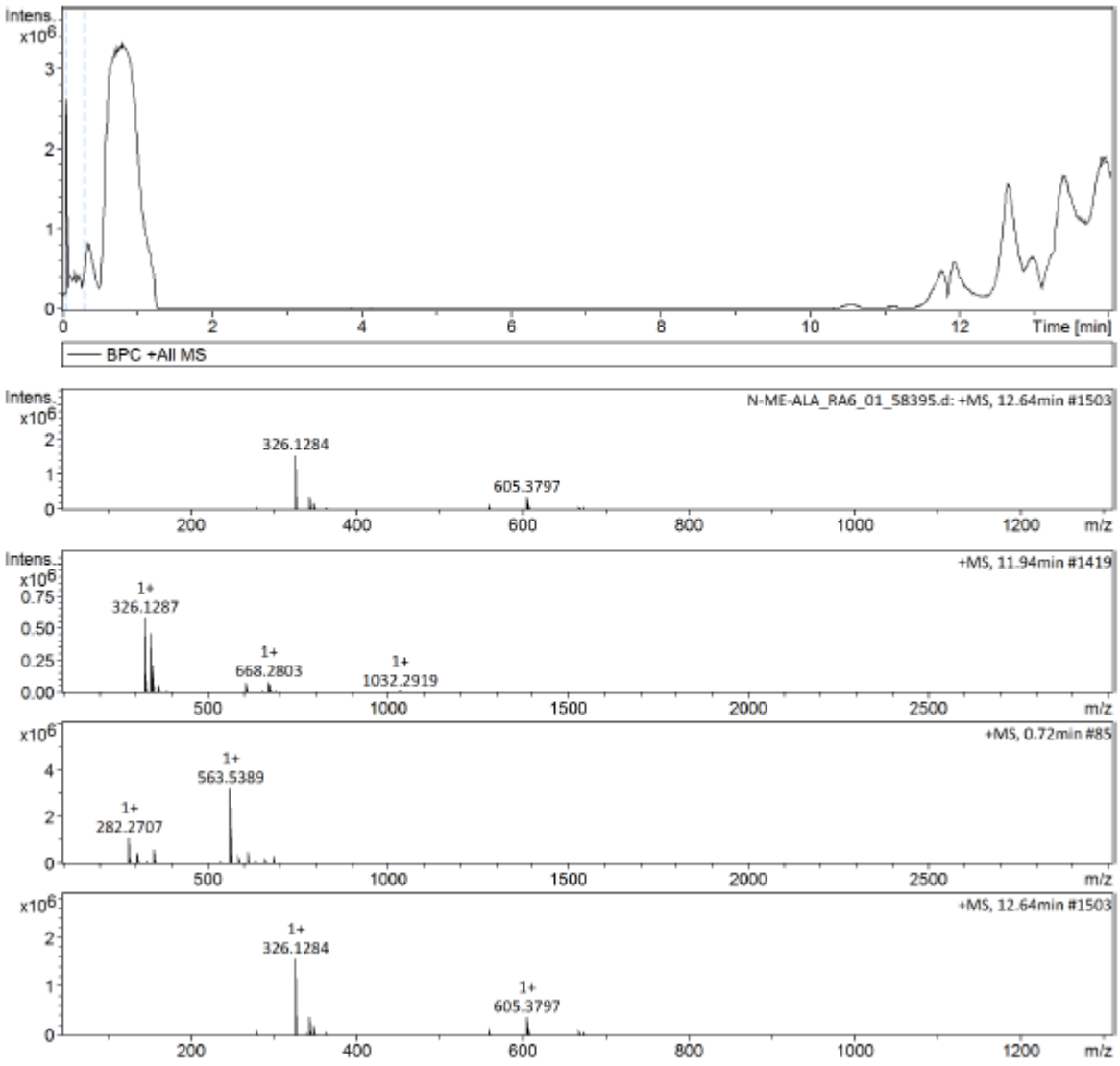


Figure A. 24: LCMS spectrum of Fmoc-N-Methyl Alanine.

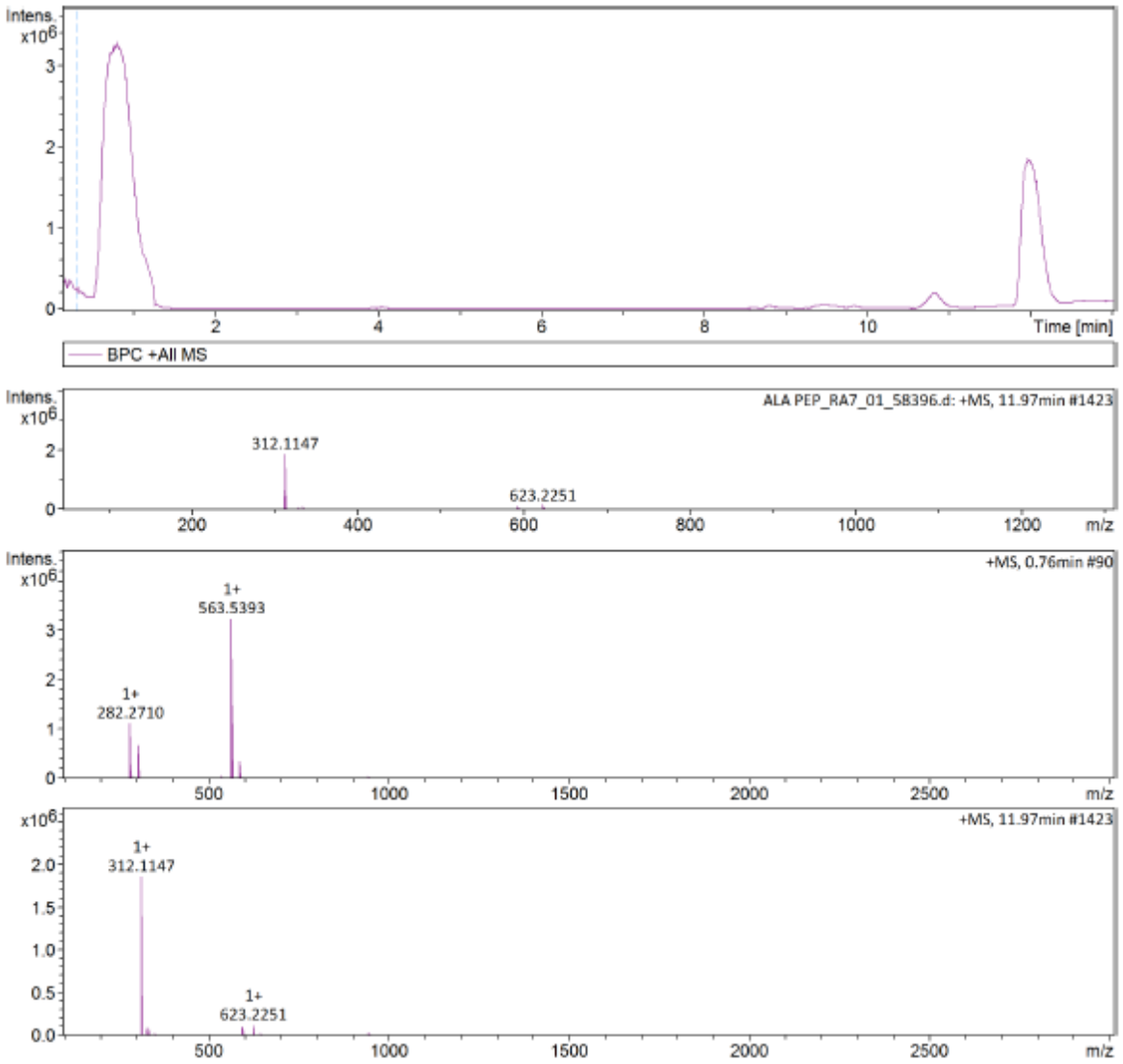


Figure A. 25: LCMS spectrum of Fmoc-Alanine peptoid.

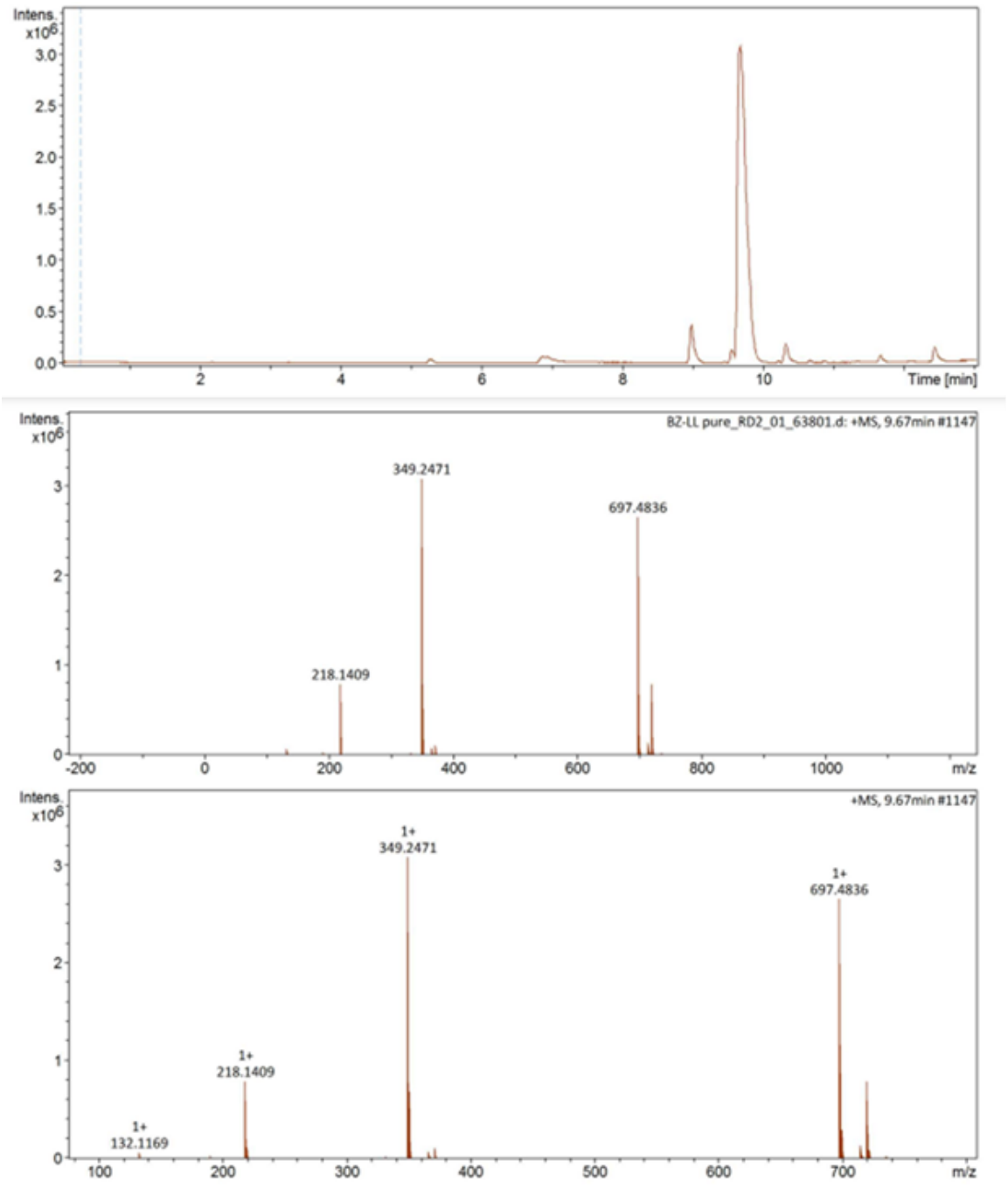


Figure A. 26: LCMS spectra of Bz-LL, N-terminal blocked dipeptide agonist comprised of two Leu residues and benzoic acid on the N-terminal.

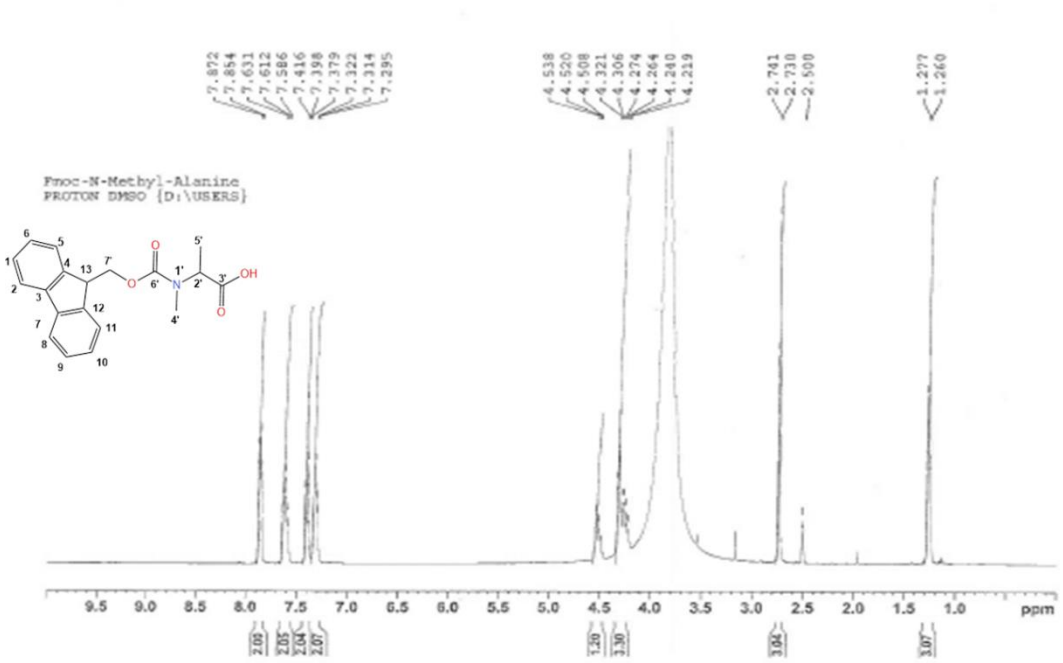


Figure A. 27: ^{1}H NMR spectrum of Fmoc-N-Methyl Alanine in DMSO-d_6.

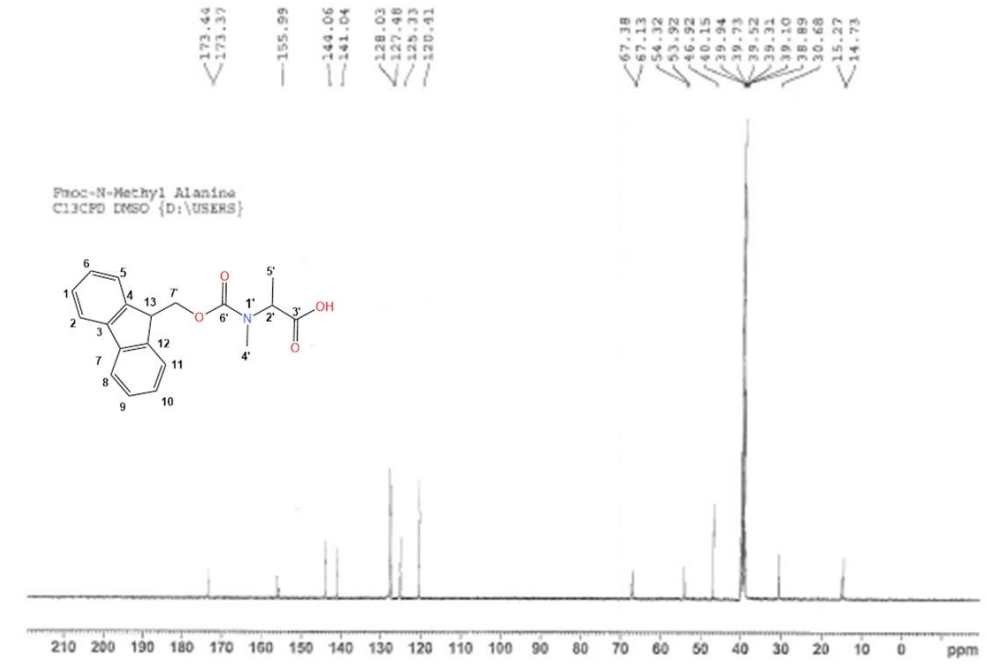


Figure A. 28: ^{13}C NMR spectrum of Fmoc-N-Methyl Alanine in DMSO-d_6.

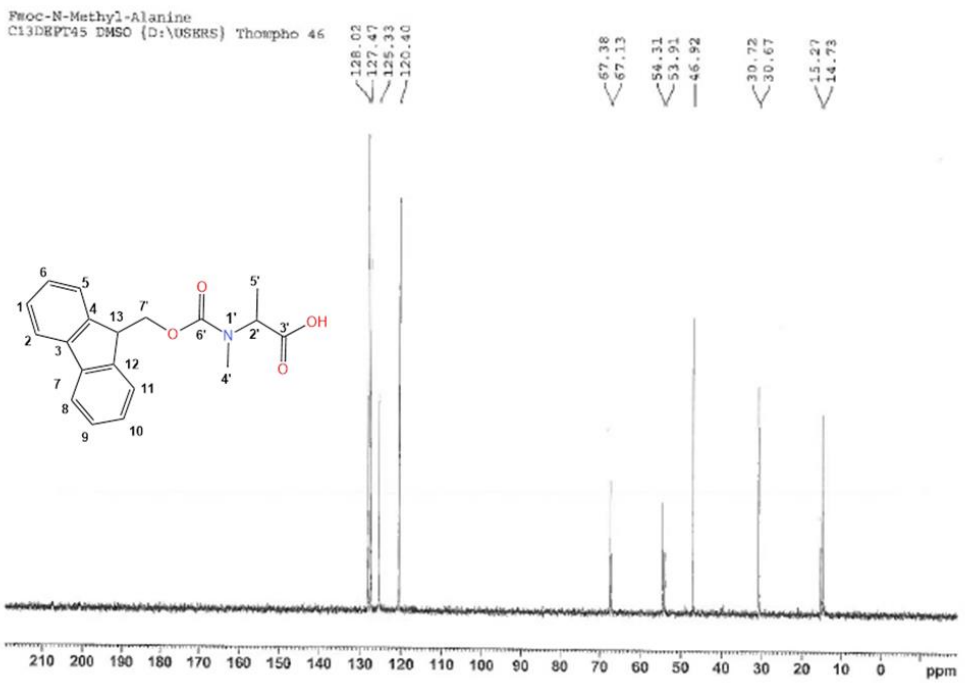


Figure A. 29: DEPT45 spectrum of Fmoc-N-Methyl Alanine in DMSO-d_6.

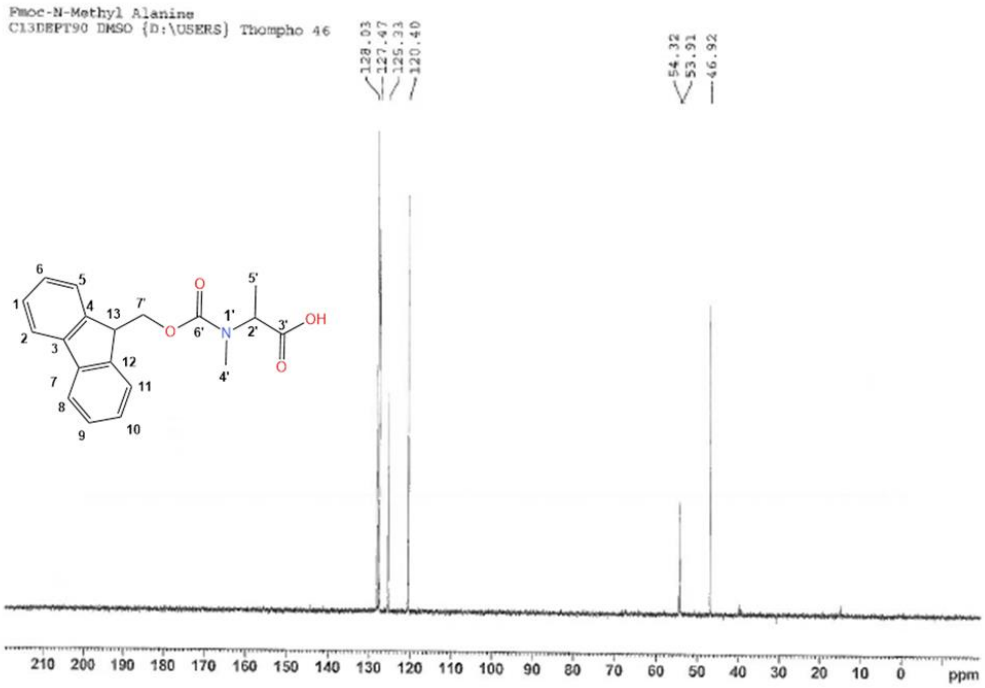


Figure A. 30: DEPT90 spectrum of Fmoc-N-Methyl Alanine in DMSO-d_6.

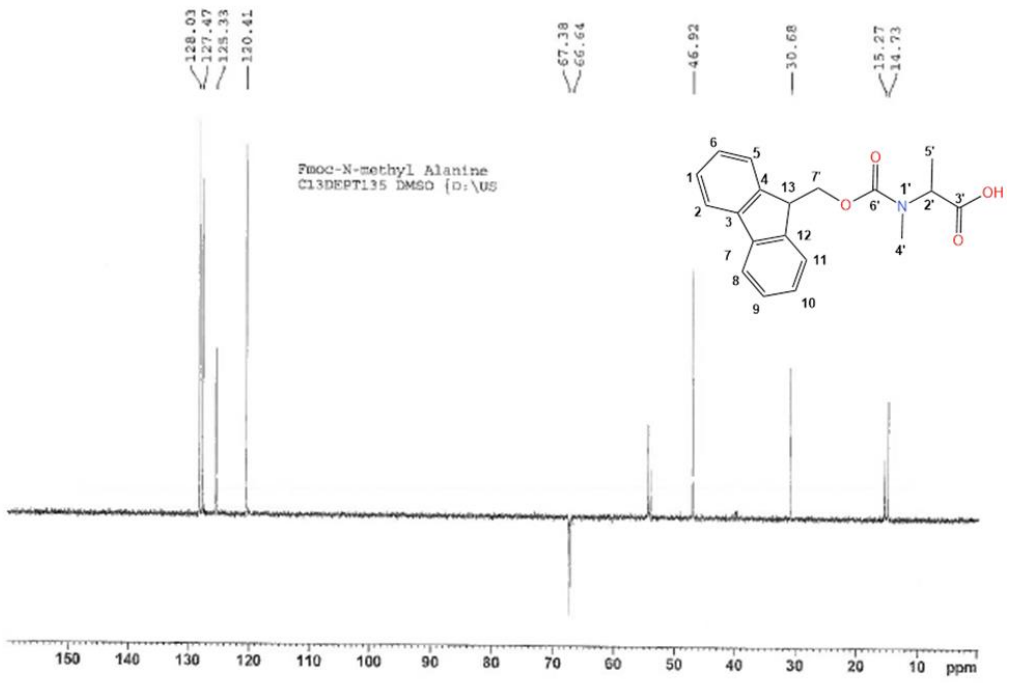


Figure A. 31: DEPT135 sepctrum of Fmoc-N-Methyl Alanine in DMSO-d_6 .

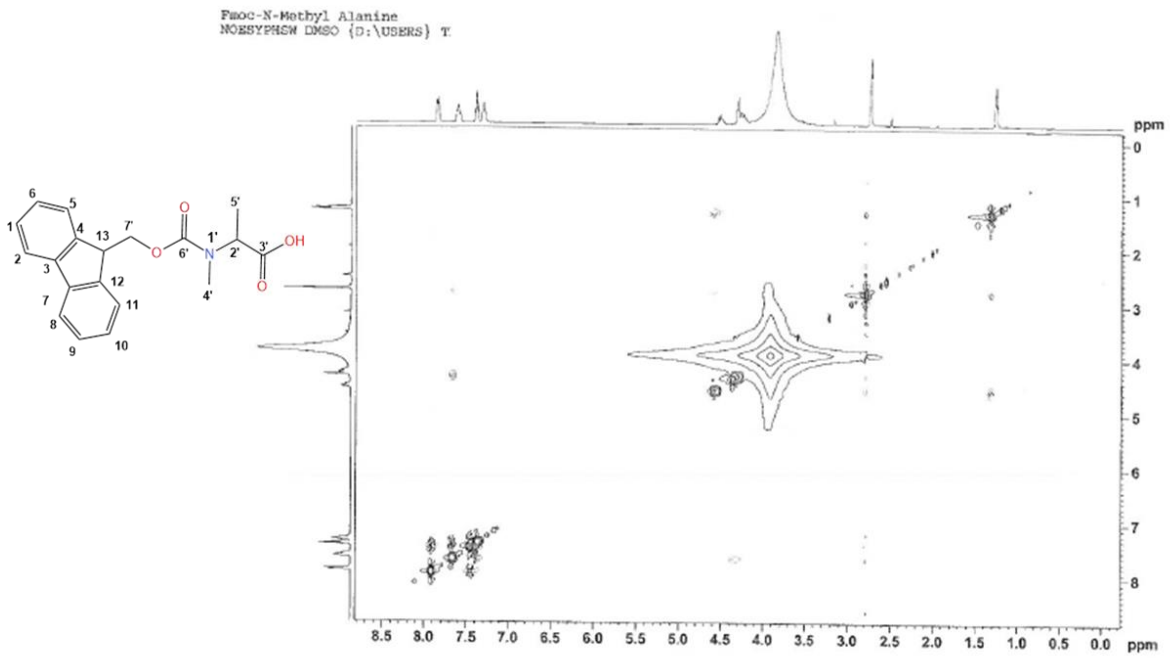


Figure A. 32: NOESYPHSW spectrum of Fmoc-N-Methyl Alanine in DMSO-d_6.

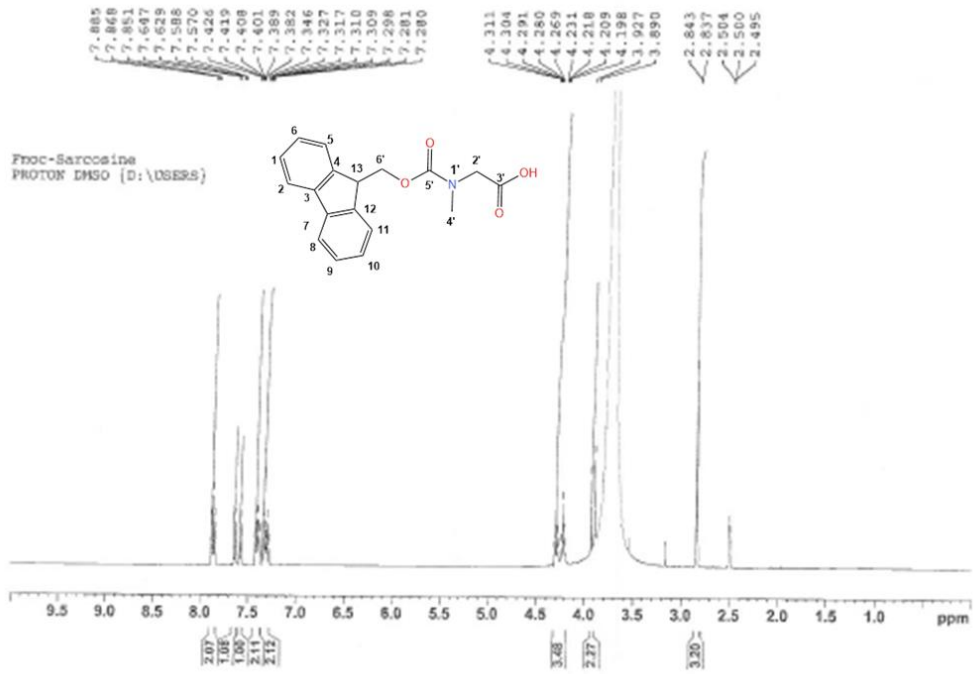


Figure A. 33: ^{1}H NMR spectrum of Fmoc-Sarcosine in DMSO-d_6.

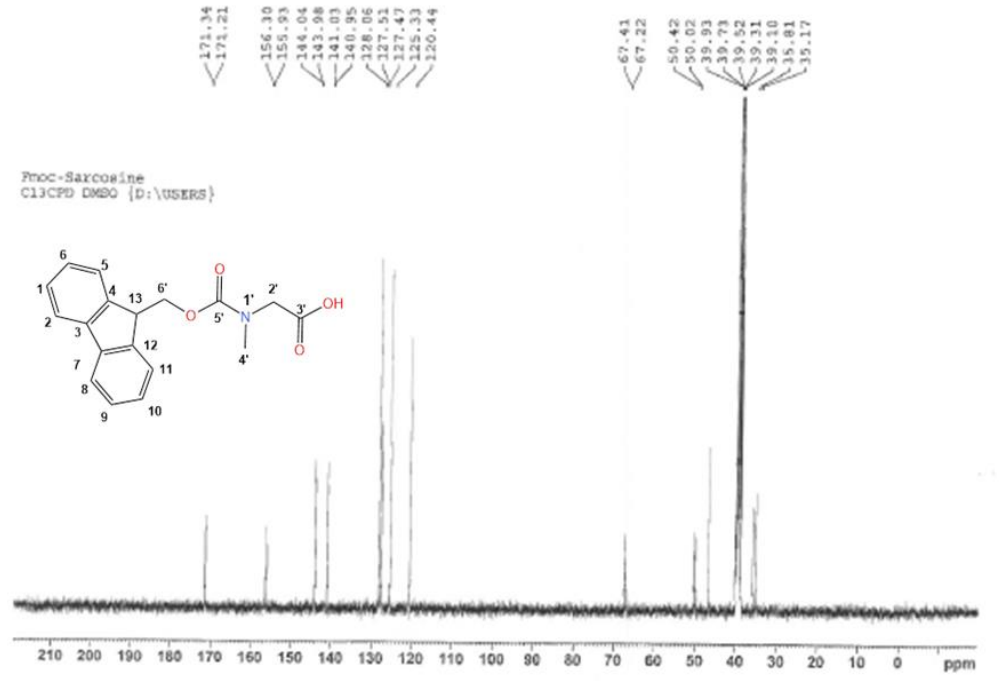


Figure A. 34: ^{13}C NMR spectrum of Fmoc-Sarcosine in DMSO-d_6..

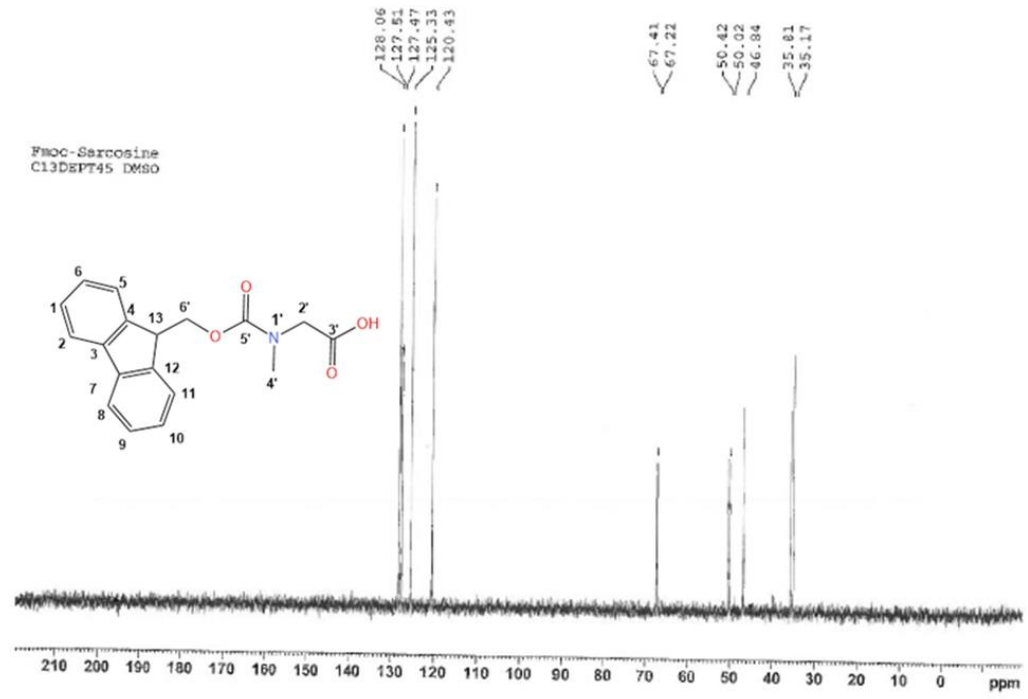


Figure A. 35: DEPT45 spectrum of Fmoc-Sarcosine in DMSO-d_6.

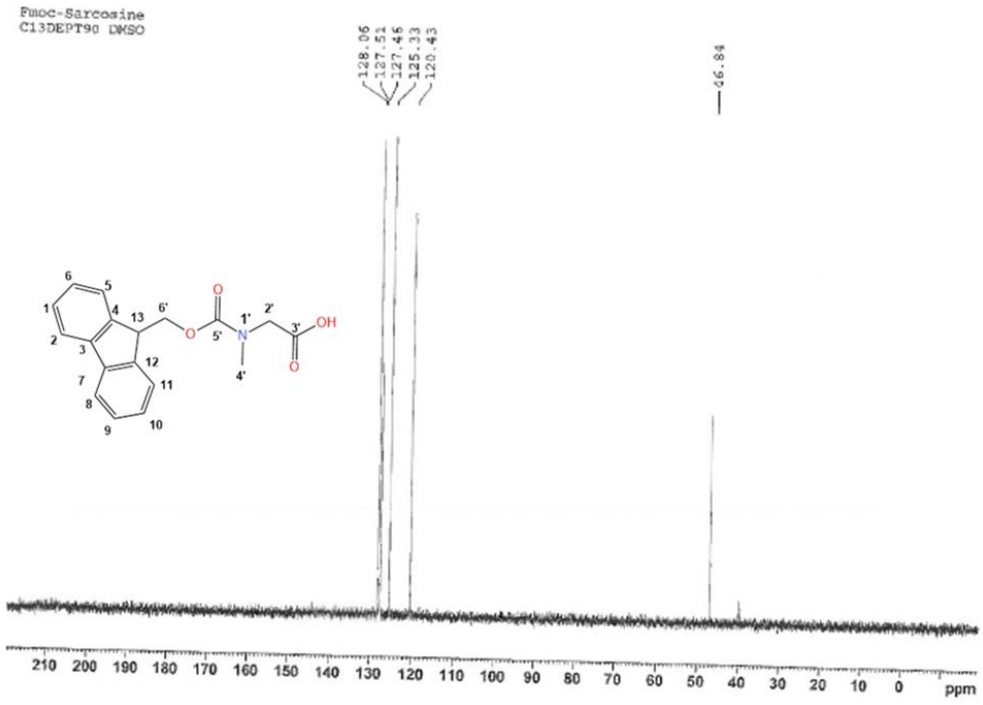


Figure A. 36: DEPT90 spectrum of Fmoc-Sarcosine in DMSO-d_6.

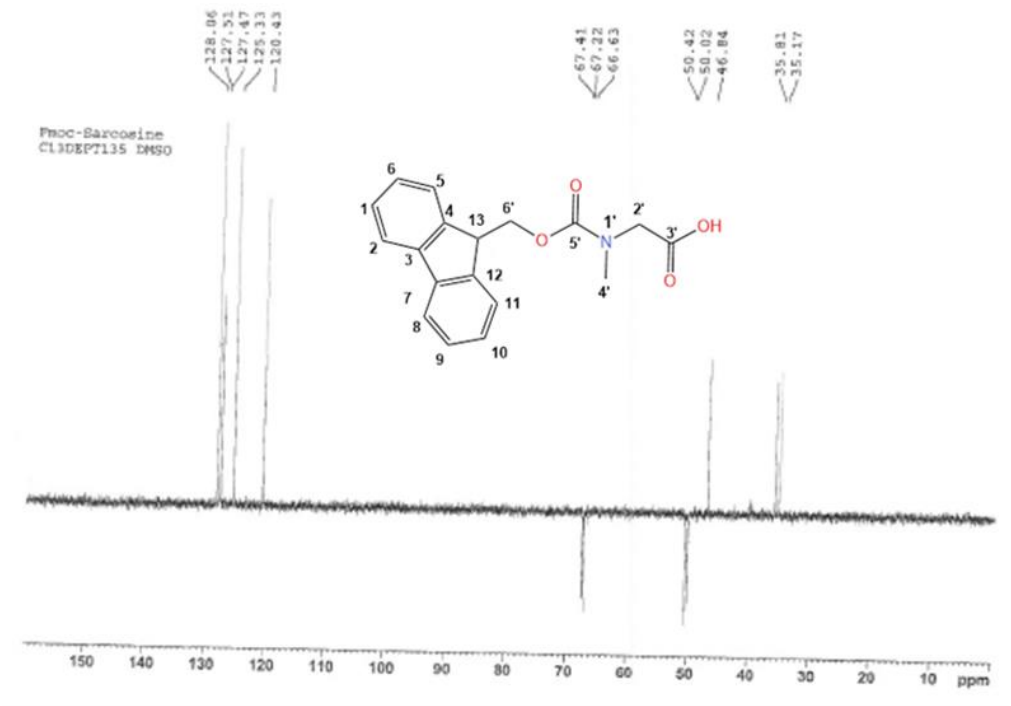


Figure A. 37: DEPT135 spectrum of Fmoc-Sarcosine in DMSO-d_6.

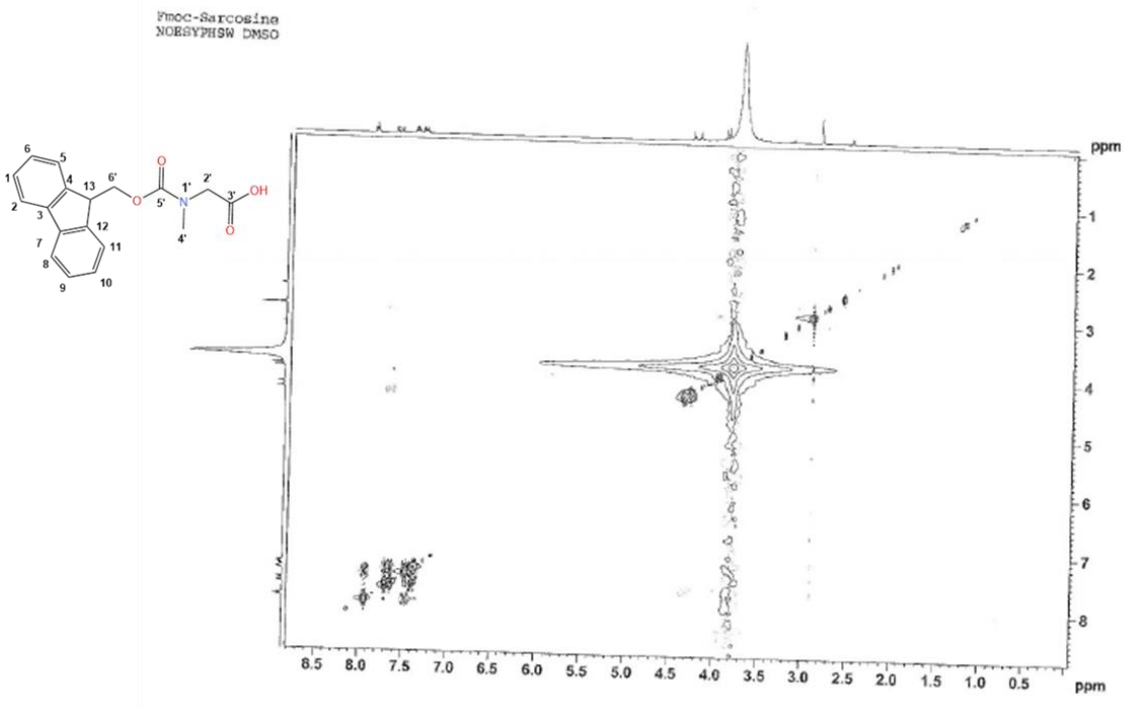


Figure A. 38: NOESYPHSW spectrum of Fmoc-Sarcosine in DMSO-d_6.

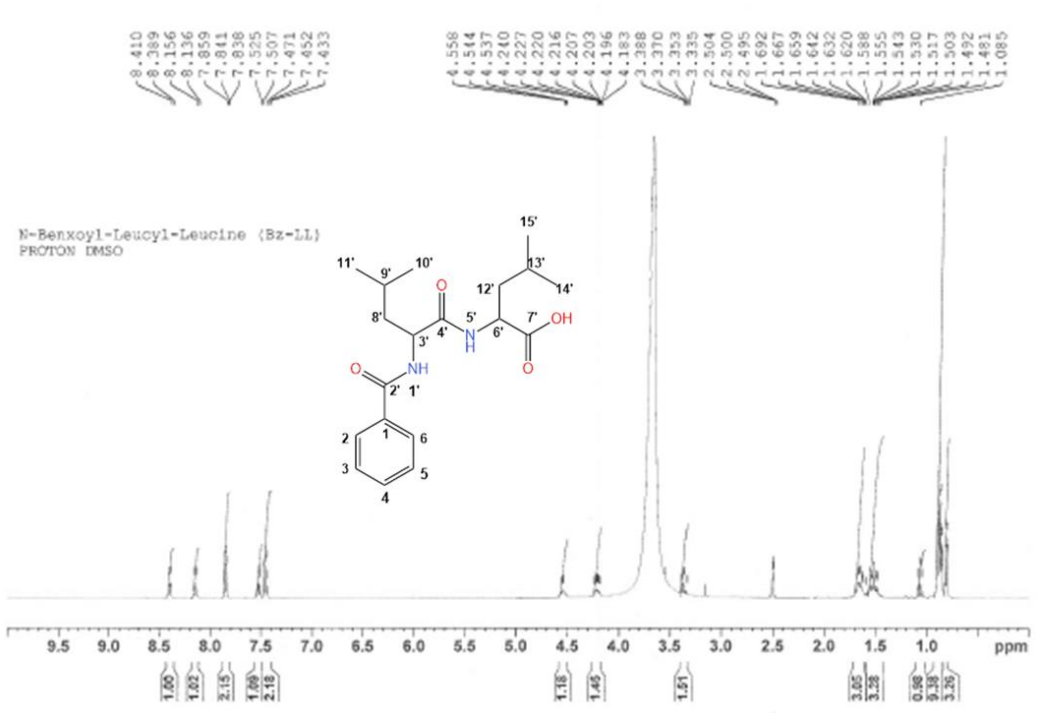


Figure A. 39: ^{1}H NMR spectrum of Bz-LL in DMSO-d_6.

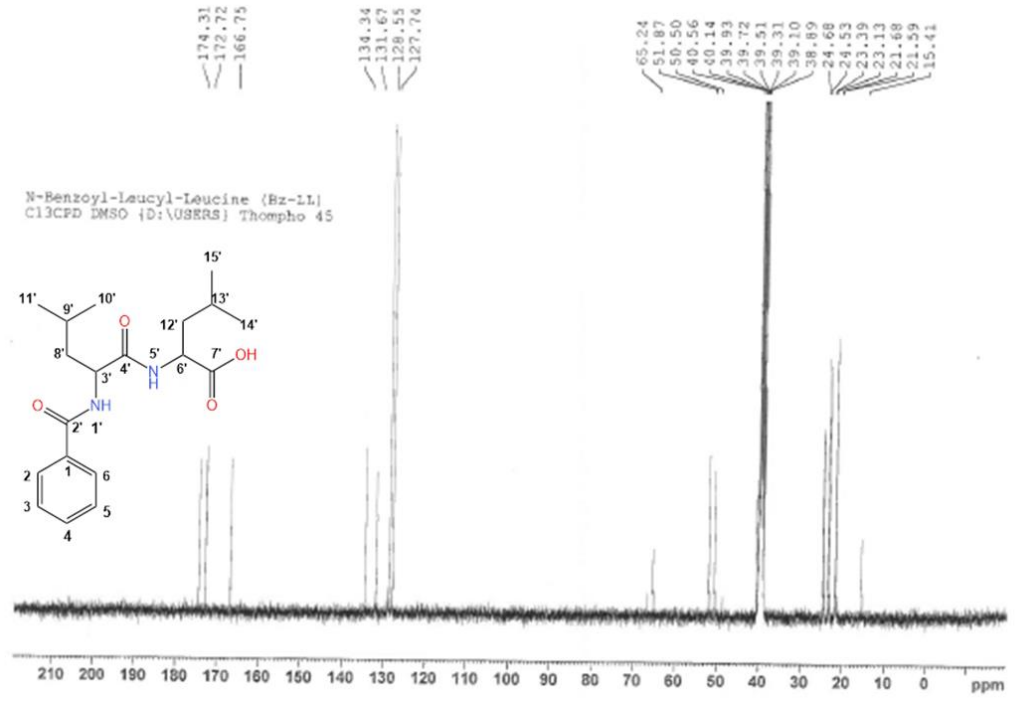


Figure A. 40: ^{13}C NMR spectrum of Bz-LL in DMSO-d_6.

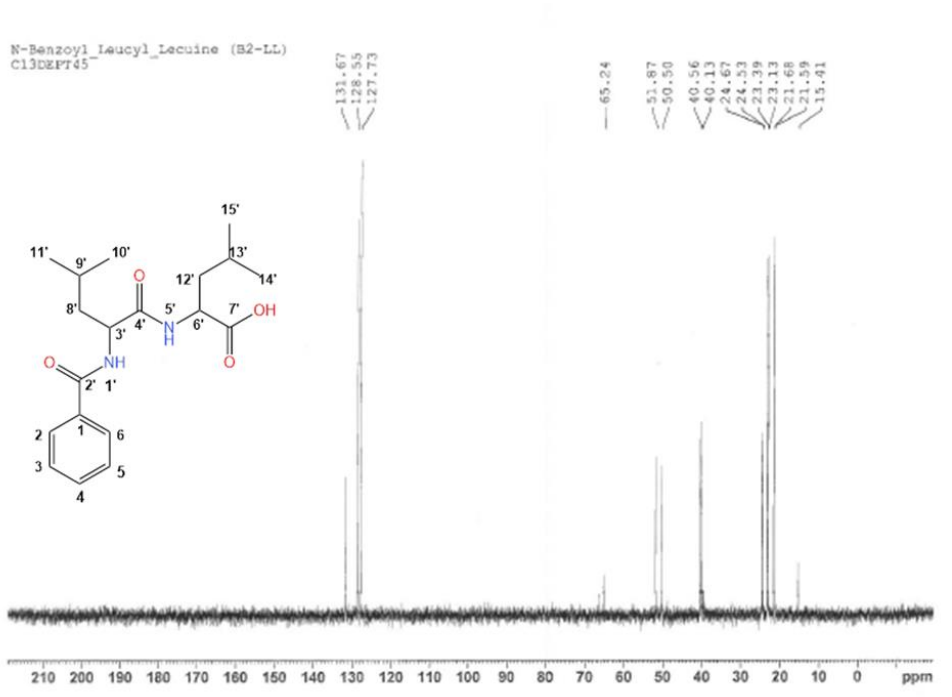


Figure A. 41: DEPT45 spectrum of Bz-LL in DMSO-d_6.

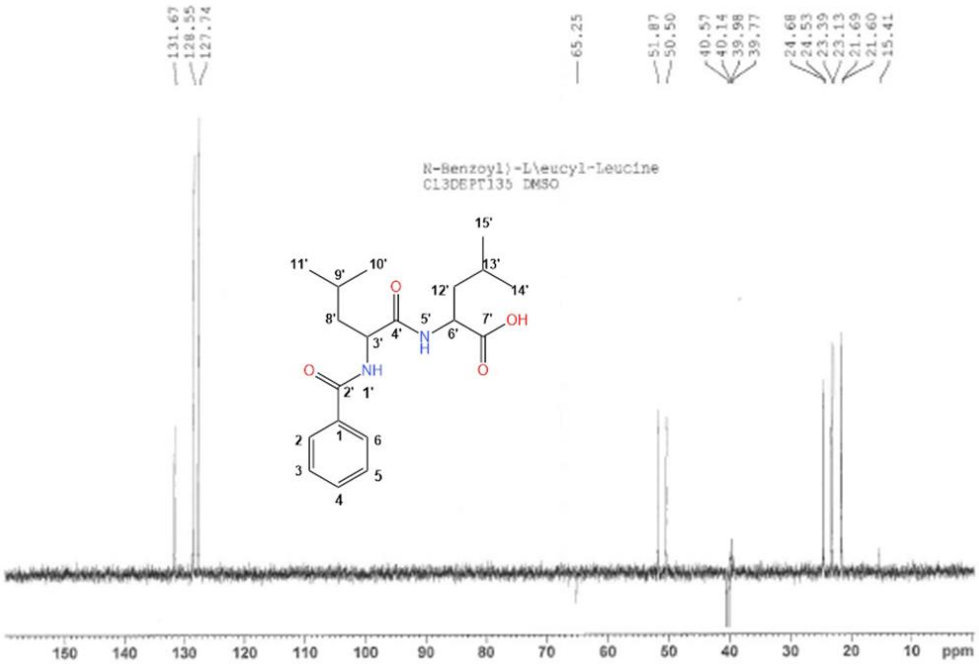


Figure A. 42: DEPT135 spectrum of Bz-LL in DMSO-d_6.

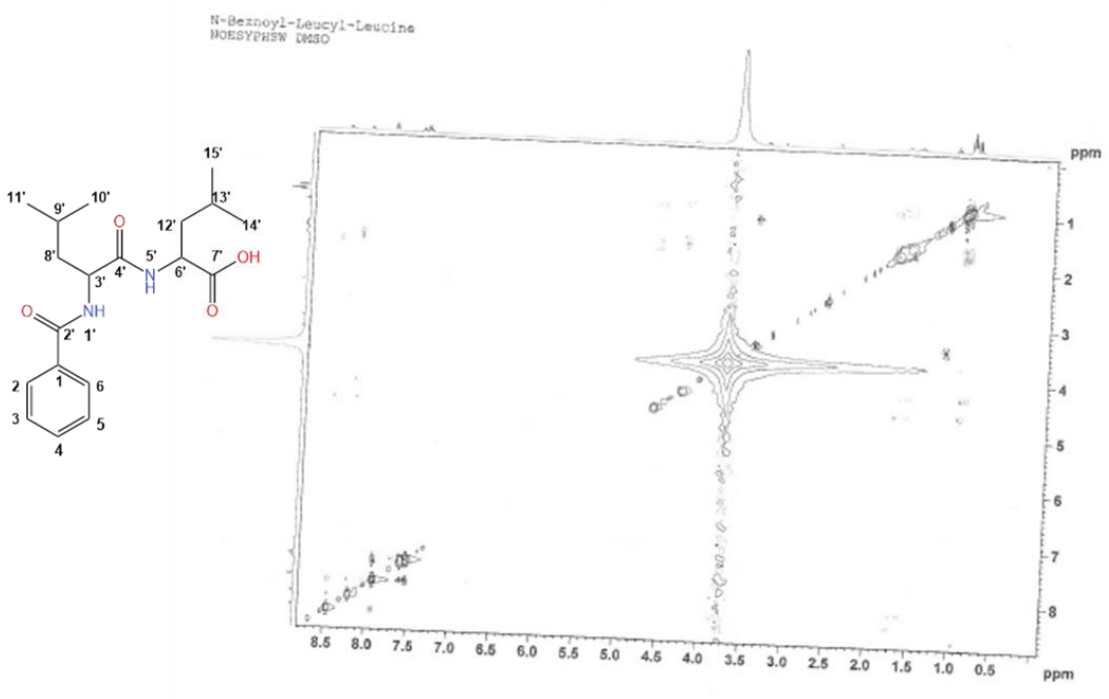


Figure A. 43: NOESYPHSW spectrum of Bz-LL in DMSO-d_6.